Physics Reports 468 (2008) 1–99

Contents lists available at ScienceDirect

Physics Reports

journal homepage: www.elsevier.com/locate/physrep

Maximizing information exchange between complex networks

Bruce J. West [a,b,*], Elvis L. Geneston [c,d], Paolo Grigolini [c,e,f]

[a] Mathematical and Information Science, Army Research Office, Research Triangle Park, NC 27708, USA
[b] Physics Department, Duke University, Durham, NC 27709, USA
[c] Center for Nonlinear Science, University of North Texas, P.O. Box 311427, Denton, TX 76203-1427, USA
[d] Physics Department, La Sierra University, 4500 Riverwalk Parkway, Riverside, CA 92515, USA
[e] Istituto di Processi Chimico Fisici del CNR, Area della Ricerca di Pisa, Via G. Moruzzi, 56124, Pisa, Italy
[f] Dipartimento di Fisica "E. Fermi" Universita' di Pisa, Largo Pontecorvo 3, 56127 Pisa, Italy

ARTICLE INFO

Article history:
Accepted 7 June 2008
Available online 9 July 2008
editor: I. Procaccia

PACS:
05.10.-a

Keywords:
Complexity matching
Information propagation
Renewal
Ergodic
Non-ergodic
$1/f$-noise
Global warming

ABSTRACT

Science is not merely the smooth progressive interaction of hypothesis, experiment and theory, although it sometimes has that form. More realistically the scientific study of any given complex phenomenon generates a number of explanations, from a variety of perspectives, that eventually requires synthesis to achieve a deep level of insight and understanding. One such synthesis has created the field of out-of-equilibrium statistical physics as applied to the understanding of complex dynamic networks. Over the past forty years the concept of complexity has undergone a metamorphosis. Complexity was originally seen as a consequence of memory in individual particle trajectories, in full agreement with a Hamiltonian picture of microscopic dynamics and, in principle, macroscopic dynamics could be derived from the microscopic Hamiltonian picture. The main difficulty in deriving macroscopic dynamics from microscopic dynamics is the need to take into account the actions of a very large number of components. The existence of events such as abrupt jumps, considered by the conventional continuous time random walk approach to describing complexity was never perceived as conflicting with the Hamiltonian view. Herein we review many of the reasons why this traditional Hamiltonian view of complexity is unsatisfactory. We show that as a result of technological advances, which make the observation of single elementary events possible, the definition of complexity has shifted from the conventional memory concept towards the action of non-Poisson renewal events. We show that the observation of crucial processes, such as the intermittent fluorescence of blinking quantum dots as well as the brain's response to music, as monitored by a set of electrodes attached to the scalp, has forced investigators to go beyond the traditional concept of complexity and to establish closer contact with the nascent field of complex networks. Complex networks form one of the most challenging areas of modern research overarching all of the traditional scientific disciplines. The transportation networks of planes, highways and railroads; the economic networks of global finance and stock markets; the social networks of terrorism, governments, businesses and churches; the physical networks of telephones, the Internet, earthquakes and global warming and the biological networks of gene regulation, the human body, clusters of neurons and food webs, share a number of apparently universal properties as the networks become increasingly complex. Ubiquitous aspects of such complex networks are the appearance of non-stationary and non-ergodic statistical processes and inverse power-law statistical distributions. Herein we review the traditional dynamical and phase–space methods for

* Corresponding author at: Mathematical and Information Science, Army Research Office, Research Triangle Park, NC 27708, USA. Tel.: +1 919 549 4257.
E-mail address: bwest@nc.rr.com (B.J. West).

0370-1573/$ – see front matter. Published by Elsevier B.V.
doi:10.1016/j.physrep.2008.06.003

modeling such networks as their complexity increases and focus on the limitations of these procedures in explaining complex networks. Of course we will not be able to review the entire nascent field of network science, so we limit ourselves to a review of how certain complexity barriers have been surmounted using newly applied theoretical concepts such as aging, renewal, non-ergodic statistics and the fractional calculus. One emphasis of this review is information transport between complex networks, which requires a fundamental change in perception that we express as a transition from the familiar stochastic resonance to the new concept of complexity matching.

Published by Elsevier B.V.

Contents

1. Introduction

One of the perennial problems in the physics of communication is matching information flow to the physical structure of the channel supporting that flow in such a way as to maximize efficiency, that is, maximize the information transferred in the channel. Of course, in order to make the problem well defined requires a rigorous definition of information, as well as, a notion of channel capacity, that being, how much information transfer can a channel support under ideal conditions. Wiener (1948) and Shannon (1948) among others defined these things over half a century ago and science is now extending their ideas to the broader context of complex networks, in which, Shannon's notion of a channel is stretched to include networks from the social and life sciences. For the perspective of this Report it is useful to replace the notion of channel with that of network in order to avoid unnecessary confusion.

Complex networks form one of the most challenging areas of modern research overarching all of the traditional scientific disciplines. The transportation networks of planes, highways and railroads; the economic networks of global finance and stock markets; the social networks of terrorism, governments, businesses and churches; the physical networks of telephones, the Internet, earthquakes and global warming as well as the biological networks of gene regulation, the human body, clusters of neurons and food webs, share a number of apparently universal properties as the networks become increasingly complex, see, e.g., Network Science (2005). Over the last century a substantial number of books have been written addressing the complexity of networks: books on biological networks, focusing on the macroscopic level as did Lotka (1924), or the explicit consideration of scaling in organisms by MacDonald (1983) and Calder (1984), or the broad study of the phenomenon of synchronization carried out by Strogatz (2003); tomes on social networks, focusing on the interaction among groups of people as did Scott (2000), and on the citations to scientific papers forming the invisible

college studied by de Sola Price (1963); monographs on networks of natural phenomena, including Mandelbrot's now classic book (1977) introducing the concept of fractals, the growth of river basins by Rodríguez-Iturbe and Rinaldo (1997) and the morphogenesis of physiologic organs by Weibel (2000); tracts on information networks, exploring the interface between man and machine as did Wiener (1948), initiating the modern theory of communication by Shannon and Weaver (1959), and quantifying complexity using information measures by Li and Vitányi (1997).

Each of these complex networks and others are generated by mechanisms specific to the phenomenon being considered, the psychology of human interaction in the social domain, the scaling across scale in the natural sciences and the explosive growth of information in nonlinear dynamical networks. On the other hand, there are properties common to all that enables us to identify them as networks. Here we focus on the fact that to understand the dynamics of these complex networks the traditional analysis of information flow and channel traffic, involving exponential distributions of messages and consequently Poisson statistics of traffic volume, must be abandoned and replaced with less familiar statistical techniques. The techniques reviewed have appeared in the diaspora of the physical sciences literature on networks and complexity.

There have been a significant number of excellent review articles on complex network published recently, each with its own philosophical slant. Albert and Barabási (2002) review complex networks from the perspective of nonequilibrium statistical physics, whereas Newman (2003) organized his review around the various applications that have been made, including social, information, technological and biological networks and the mathematical rendition of the common properties that are observed among them. The most recent survey by Costa et al. (2007) views complex network research as being at the intersection of graph theory and statistical physics and focuses on existing measurements that support the principal models found in the literature. Our approach is a hybrid of these views. We take nonequilibrium statistical physics and its techniques as our starting point, use recent experiments done on complex networks to highlight the inadequacies of the traditional approaches, but more importantly, we use these data to motivate the development of new mathematical modeling techniques necessary to understand the underlying network structure.

Apparently ubiquitous aspects of complex networks are the appearance of non-stationary, non-ergodic, non-Poisson, renewal, statistical processes. These properties are manifest through inverse power-law statistical distributions that not only challenge traditional understanding of complexity in physical networks, but require new strategies for understanding how information is exchanged between such networks. Our purpose herein is to review how the traditional methods of statistical physics used to characterize the dynamics of complex phenomena have been extended in the analysis of such physical phenomena as spin glasses and intermittent fluorescence, called blinking quantum dots (BQD); in such life phenomena as networks of neurons, biofeedback techniques and the brain's response to music, and in such geophysical phenomena as global warming. Moreover, we review how these extensions apply to the problem of information exchange between complex networks independently of the specific interactions among the elements within a network.

Resonant phenomena have been among the most useful mechanisms for extracting weak signals from noisy backgrounds. A linear dynamic process responds strongly to a harmonic perturbation with matching frequency and this linear resonance has been used in a variety of detectors, such as magnetic resonance imaging (MRI), see, e.g., Weishaupt et al. (2003). Effective two-state stochastic phenomena respond strongly when the period of a harmonic perturbation matches the transition rate of the stochastic process. This resonance (SR), see, e.g. Benzi et al. (1981), is one strategy for modeling the transmission of information through random (Poisson statistics) media that can enhance the signal-to-noise ratio, see, e.g. Gammaitoni et al. (1998).

As we review herein, if the perturbed network is a Poisson process, using ordinary linear response theory (LRT), see Kubo (1957), it is straightforward to go beyond the aperiodic SR as discussed by Collins et al. (1995) and Collins et al. (1996a,b), which is confined to the case of slow perturbation, and to derive the phenomenon of rate matching, which has been overlooked in the SR literature. Allegrini et al. (2007a) and Aquino et al. (2007) address the challenging situation where the network being perturbed is neither Poisson nor ergodic, so as to meet the conditions emerging from complex networks. Goychuck and Hänggi (2003) studied the case where the network to be perturbed is not Poisson but is still ergodic. The non-ergodic condition, studied by Bel and Barkai (2006a,b) and Margolin and Barkai (2005, 2006), violates the conditions for the Kubo (1957) form of LRT, and has been studied by Barbi et al. (2005), who conclude that a complex network described by intermittent fluctuations with non-Poisson statistics does not respond asymptotically to external periodic perturbations. Sokolov and Metzler (2003) reached the same conclusion. Herein we show that this property of violating LRT can be explained by adopting a proper definition of complexity, which, more importantly, leads us to discover a method for information transport bypassing the limitations pointed out by Barbi et al. (2005) and Sokolov and Metzler (2003).

A number of complex phenomena have been shown to have non-Poisson statistical properties, including collections of BQDs, see, for example, Nirmal et al. (1996), Kuno et al. (2001, 2003) and Shimizu et al. (2001), and aggregations of neurons in the human brain by Bianco et al. (2007a). The non-Poisson character of the distribution of sojourn times in the "on" and "off" states in BQDs is well known, see, for example, Nirmal et al. (1996), Kuno et al. (2001, 2003) and Shimizu et al. (2001), however the renewal character of the statistics has only recently been established by Bianco et al. (2005) and Brokmann et al. (2003). Moreover, Bianco et al. (2007b) have shown using a network of coupled two-state stochastic clocks that with the onset of phase synchronization at a critical value of the coupling coefficient the dynamics of the network becomes that of a non-Poisson renewal process operating in the non-ergodic regime. The breakdown of the collective phase structures occur with no memory of previous state changes, consequently yielding a non-Poisson renewal process (NPR). NPRs are characterized by a waiting-time distribution density between events, indicated by $\psi(\tau)$. The regression to equilibrium of an ensemble of NPRs is given by the survival probability $\Psi(t) = \int_0^\tau \psi(\tau)\mathrm{d}\tau$. Herein we focus most of our attention on

inverse power-law distributions $\Psi(t) \approx t^{-\alpha}$ with index $\alpha < 1$, thereby corresponding to processes that violates the finite time-scale assumption so often made in statistical physics.

One way a non-exponential decay, such as the inverse power law, can be expressed is as the sum of infinitely many Poisson components, but if these components are independent, as are the single dynamic elements in the absence of cooperation, no NPR events are generated as shown by Allegrini et al. (2006). The production of NPR events is a sign of close cooperation among distinct dynamical elements, thereby offering a rationale as to why the NPR processes do not respond to harmonic perturbations, see, for example, Barbi et al. (2005) and Sokolov and Metzler (2003), as would single independent Poisson dynamical elements. NPR processes reflect a condition shared by the phenomenological models of glassy dynamics as shown by Bouchaud (1992), laser cooling as discussed by Bardou et al. (2002) and models of atomic transport in optical lattices given by Lutz (2004). Other NPR processes have been found at the core of the correlations in DNA sequences by Mohanty and Narayana Rao (2000), heart-beat variability by Allegrini et al. (2003a) and West (2006) and earthquake statistics by Mega et al. (2003).

Herein we review a new phenomenon of information transport, that is, the determination of how one complex network responds to an excitation by a second complex network as a function of the matching of the measures of complexity of the two networks. The complex network considered is NPR and the measure of complexity is the inverse power-law index. More precisely, we consider a NPR network, whose waiting time distribution density $\psi(\tau)$ has the power-law index $\mu \equiv \alpha + 1 < 2$, and we review, in analogy with stochastic resonance (SR) theory reviewed by Gammaitoni et al. (1998), the case where the rate of production of jumps, a kind of renewal event, is modulated by an external excitation. This leads to the new concept of complexity matching, where the exchange of information between two complex networks is maximized when their complexity is the same. The complexity matching phenomenon is a special property of non-ergodic renewal (NER) processes, which are a special class of NPR processes. For this reason we subsequently replace the NPR acronym with the NER acronym.

1.1. Section summaries

In this report we briefly review the traditional dynamical and phase space methods for modeling dynamic networks as a strategy for understanding their increasing complexity and focus on the limitations of these procedures in explaining complex networks. In Section 2 we present the Hamiltonian basis for coupling microscopic dynamics to macroscopic phenomenology leading to the Generalized Langevin Equation (GLE), see, for example, Lindenberg and West (1990). In order to better understand how information is transferred among such complex networks we review the phenomenon of simple linear resonance and briefly examine the mechanism of stochastic resonance (SR), where adding noise to a nonlinear dynamic network increases rather than decreases our ability to detect a signal. The SR effect has been proposed as a way collections of neurons can effectively use biological noise to facilitate the exchange of information as explained by Moss et al. (2004). This perspective on resonance and noise suggests that we examine the influence of memory on stochastic processes, which we follow and indicate how random phenomena with memory require a description using a certain kind of GLE. We introduce the fractional Langevin equation (FLE) or more generally fractional stochastic differential equations (FSDE) in which the memory kernel of the GLE is interpreted as a fractional operator and establish a correspondence with an increasing literature on the application and interpretation of the fractional calculus, see, for example, West et al. (2003) to the description of complex dynamic phenomena. Note that the FSDE only arise when the microscopic time scales diverge, which is for $\mu < 2$ in the present context, and consequently overlap with the macroscopic time scales.

In Section 3 we replace the dynamic equations for network variables discussed in Section 2 with phase–space equations of motion for the phase–space density function and the probability density. In this section, for completeness, we briefly go over the traditional statistical physics areas of the Fokker–Planck equation (FPE) developed in the context of Brownian motion; the Generalized Master Equation (GME) as another strategy for systematically describing the influence of complexity on the information dynamics of complex networks and finally, continuous time random walks (CTRW) as a third perspective for incorporating memory into network dynamics. This section is streamlined in its use of previously published material because the literature is so vast. Consequently, we emphasize only the most recent relations that have been determined among these formalisms, for example, GME and CTRW are only equivalent under certain very restricted conditions. Finally, we demonstrate that the recent interest in fractional diffusion equations (FDE) can be traced back to these more familiar formalisms when the complex phenomena being investigated are intermittent and have memory; the FDEs are not uniquely determined and can be independently derived from the GME, CTRW and FSDE formalisms.

The kinds of complexity introduced into network dynamics in Sections 2 and 3 through the dynamic and phase space formalisms are discussed more fully in the context of what had previously appeared as the esoteric mathematical descriptions of non-ergodic, non-stationary, non-Poisson stochastic processes. In Section 4 we review these concepts in order to arrive at a general and useful definition of complexity and this involves the concept of renewal aging, as distinct from the notion of aging recently introduced in the study of glassy materials, which we also briefly discuss.

Of course we will not be able to review the entire budding field of Network Science here, so we limit ourselves to reviewing how certain complexity barriers have been surmounted using new theoretical concepts such as aging, the fractional calculus, and complexity matching. In Section 5 we illustrate an approach to understanding complexity, inspired by recent neurophysiological results, based on the modern theory of subordination. We interpret subordination theory as corresponding to the vision of complexity advocated herein. The complex processes are characterized by the occurrence

of quakes, usually small, which can accumulate so as to generate large quakes, which may be experimentally detectable. The theory of subordination is based on the assumption that the time interval between two consecutive actions, or small quakes, is described by a distribution density, subordination function, having the inverse power-law form. However, if the success probability of these actions is small, the resulting survival probability is a Mittag–Leffler function (MLF), see, for example, Rabotnov (1980) for a physical discussion of this function. One exemplar of such a process, discussed in Section 5, is the electroencephalograph (EEG) of the human brain and how the parameters of the statistics of the EEG time series change while listening to music. This section also prepares the ground for the introduction of the complexity matching effect (CME), discussed fully in Section 6.

Section 6 presents heuristic arguments that the transport of information between complex networks attains maximum efficiency at the condition where the inverse power-law indices of the two networks are equal. The basis of the analysis is a recently developed generalization of the fluctuation–dissipation theorem (FDT) of the first kind, which is used to develop analytic expressions for the perturbation of one complex network by another. The probability density describing these complex networks is inverse power law. One exemplar of how a perturbed complex network inherits the statistics of the perturbing complex network, when the power-law index is greater than two, is the linking of the statistical fluctuations in the Earth's average temperature to the variability in solar activity. When the power-law index is less than two the underlying process is non-ergodic, see Bel and Barkai (2005) and Margolin and Barkai (2005). The ergodic hypothesis in physics can be traced to Gibbs and his assertion that ensemble averages and long time averages should yield the same result. He was never able to prove this conjecture, but most of the statistical physics of the last century is based on this hypothesis being true. In the 21st century it has become clear that more and more of the complex phenomena of interest violate this assumption and so in Section 6 we review how sensitive some of the traditional relations of statistical physics are to the ergodic hypothesis.

In Section 7 we take up another fundamental mechanism of complex networks, that being synchronization, where the properties of the individual element are lost and replaced with those of the collective. However, we caution the reader that there are many subtle aspects to synchronization and so here also we remain fairly narrowly focused. In particular, we review those aspects of synchronization that relate to the NER stochastic processes of earlier sections. We use a master equation to describe the interaction of a large number of two-state clocks, how they undergo a phase transition from incoherent dynamics to dynamically synchronized, if random, collection of elements. The description has been used to show that the MLF and, consequently, the associated subordination function discussed in Section 5, is the result of cooperation among many elements. The phenomena this model has been used to describe, which we review, include BQDs and collections of neurons.

Finally, Section 8 summarizes the crucial issues highlighted in this report, specifically the new phenomenon of complexity matching in the information transport between complex networks. This is done through a discussion of the more familiar physical phenomena of $1/f$-noise. The classic review by Dutta and Horn (1981) lays out the remarkable variety of physical networks that fluctuate with approximately $1/f$-shaped spectral densities. In the subsequent quarter century $1/f$-variability has been discovered in almost every scientific domain. It has been experimentally observed in the brain and other physiologic networks, in music, in the visual arts, in linguistics, and in sociology. The CME is related to the interaction between two such networks characterized by $1/f$-noise. Finally, we tie up some loose ends and relate CME to a generalization of SR, emphasize that the discussion is now in terms of events rather than continuous processes, and close with a recapitulation of the different kinds of memory that occur in a trajectory and a probability and how this relates to renewal processes.

2. Dynamic models of statistics

Historically the disciplines of statistical physics and thermodynamics were thought to be sufficient for describing complex physical phenomena solely with the use and modifications of analytic functions. This view was supported by the successes of such physicists as Onsager (1931), who through the use of simple physical arguments was able to relate apparently independent transport processes to one another, even though these processes are associated with quite different physical phenomena. His general arguments rested on three assumptions: (1) microscopic dynamics have time-reversal symmetry; (2) fluctuations in the environmental variables decay at the same rate as do macroscopic deviations from equilibrium and (3) physical networks are aged. We refer to assumption 2 as the Onsager Principle (OP) and Aquino et al. (2004) showed that this principle is tied up with assumption 3.

Onsager's arguments focused on a network that is in contact with a thermodynamically equilibrated environment, which is referred to as a heat bath. The bath or reservoir is perturbed by the network of interest but the two are in contact for a sufficiently long time interval that the bath has come to thermal equilibrium and consequently the bath is aged. From non-equilibrium statistical physics we know that the bath is responsible for both fluctuations and dissipation, and if the fluctuations have a white spectrum, that is, the spectrum is flat and featureless, the regression of perturbations of the bath to equilibrium is virtually instantaneous. This means that the energy the bath absorbs from the network of interest, through macroscopic dissipation, is distributed over the bath degrees of freedom on a very much shorter time scale than the relaxation time of the network. This property is summarized in the well known fluctuation–dissipation theorem (FDT), which has even been generalized to the case where the fluctuations in the bath do not regress instantaneously, see, for example, Kubo (1957) and Kubo et al. (1985).

The dynamics of the physical variables to which the OP apply are described by two different kinds of equations: (1) the Langevin equation, a stochastic differential equation for the dynamical variable, discussed in this section and (2) the phase space equation for the probability density, discussed in the next section.

In this section we show that the emergence of memory in the Generalized Langevin Equation (GLE) can be thought of as a form of higher-order complexity than is contained in the ordinary Langevin equation. Moreover, there are a number of formalisms to establish the connection between the fluctuating force driving the process and the dissipative memory kernel recording the network's dynamic history.

2.1. Generalized Langevin equation (GLE)

Lindenberg and West (1990) emphasized that there are two kinds of complex physical networks considered in statistical physics, those that are open and those that are closed; the latter being completely described by a Hamiltonian. The strategy employed in using the Hamiltonian approach is to reduce the full set of deterministic dynamic equations to a much smaller set of stochastic differential equations. The latter set corresponds to the physical observables of the network, and the eliminated degrees of freedom constitute the environment. A number of approaches have been developed to show that the influence of the eliminated degrees of freedom (environment) on the observables is to modify the interaction of the network observables among themselves, generate irreversible dissipative forces, and generate random fluctuations. Here we briefly review the direct integration technique from Lindenberg and West (1990) to establish the nomenclature for a thermodynamically closed network, that is, networks that eventually achieve thermal equilibrium with their environment.

The method of explicit integration requires that one explicitly solve the equations of motion for the environment, including the dynamic effects of the network on the environment. When this solution is substituted back into the equations of motion for the network variables one obtains evolution equations whose only explicit dependence on the environment is through the initial values of those variables. It is through these initial conditions that randomness enters into the network dynamics. To be concrete in this discussion consider the classical Hamiltonian for a network described by the displacement Q and its conjugate momentum P, and a reservoir of displacements q_n and conjugate momenta p_n, $n = 1, 2, \ldots, N$, as described by Cortes et al. (1985) or Ford et al. (1965)

$$H = H_N(Q, P) + H_B(\mathbf{q}, \mathbf{p}) + H_{NB}(Q, \mathbf{q}) \tag{1}$$

where the bath coordinate vectors are defined by $\mathbf{q} = (q_1, q_2, \ldots, q_N)$ and $\mathbf{p} = (p_1, p_2, \ldots, p_N)$.

Hamilton's equations of motion for the network, when the dynamics of the bath variables are eliminated, reduces to

$$\frac{\mathrm{d}P}{\mathrm{d}t} = -V_m'(Q) - \int_0^t K\left(t - t'\right) P(t')\mathrm{d}t' + f(t) \tag{2}$$

which, when the proper interpretation of the driving force and memory kernel are introduced, is the GLE. Lindenberg and West (1990) show that if the initial conditions of the bath variables are given by a canonical distribution

$$W(\mathbf{p}, \mathbf{q}) = Z^{-1}\mathrm{e}^{-\beta H_B^{(m)}} \tag{3}$$

where Z is the partition function, the inverse temperature is given by $\beta = 1/k_B\Theta$ and the bath has come to equilibrium in the presence of the network giving rise to a modified bath Hamiltonian $H_B^{(m)}$. In this situation the $f(t)$ obtained from solving the dynamic equations can be interpreted as a random force with Gaussian statistics.

Moreover, using the explicit form of the stochastic force and the memory kernel obtained by solving the Hamiltonian equations yields

$$\left\langle [f(t) - \langle f(t)\rangle]\left[f(t') - \left\langle f(t')\right\rangle\right]\right\rangle = k_B\Theta K(t - t') \tag{4}$$

where the brackets denote an average over the bath canonical distribution, or said differently, an average over an ensemble of realizations of the fluctuations of the bath. Eq. (4) is a fluctuation–dissipation relation of the second kind as discussed by Kubo (1957). Thus, the memory kernel is dissipative and the mean value of the stochastic force decays on a time scale much shorter than the characteristic time scale of the network dynamics. Of course, this is not the complete story. Conditions on the coupling parameters and the frequency spectrum of the bath are required to complete the identification of (2) as the GLE, see, for example, Lindenberg and West (1990) or Ford et al. (1965).

In the limit where the number of degrees of freedom in the bath becomes infinite and the bath correlation time approaches zero, the memory kernel approaches the delta function $K(t) \to 2\lambda\delta(t)$ and the GLE reduces to the ordinary Langevin equation

$$\frac{\mathrm{d}P}{\mathrm{d}t} = -V_m'(Q) - \lambda P(t) + \xi(t). \tag{5}$$

The zero-centered Gaussian random force yields the fluctuation–dissipation relation

$$\left\langle \xi(t)\xi(t')\right\rangle = 2\lambda k_B\Theta\delta(t - t'). \tag{6}$$

These equations were introduced into physics by Langevin (1908) to describe the erratic motion of a heavy particle immersed in a fluid of lighter particles, such as the pollen mote in water that the botanist Brown (1829) observed through his microscope, or the powdered charcoal suspended in alcohol that the physician Jan Ingen-Housz (1973) observed a half century earlier. Langevin reasoned that Newton's Laws could describe the motion of the "Brownian" particle through its interaction with the fluid giving rise to a dissipative force and a fluctuating force. The dissipative force arises from the effects of Stokes' Law for a particle moving through a viscous fluid, whereas the fluctuating force arises from an instantaneous imbalance in the number of fluid particles impacting the surface of the much larger Brownian particle.

Consequently, the arguments leading to (5) and (6) provide a dynamic model for the Einstein (1905) form of the FDT among the temperature, dissipation and diffusion:

$$D = \lambda k_B \Theta, \tag{7}$$

thereby making the strength of the fluctuations proportional to the temperature of the fluid. The Langevin equation is consequently exact for bilinear coupling, independently of the magnitude of the coupling coefficients.

2.1.1. From the pioneer work of Mori to the present times

It is important to stress that the time convoluted structure of (2) is a consequence of the fact that the stochastic force is correlated, thereby implying a close connection between correlation and memory: a higher-order form of complexity than that contained in the ordinary Langevin equation. To properly appreciate the time evolution of this complexity concept, it is convenient to mention the important work of Mori (1965a,b), which shows how to derive the GLE for a generic variable A, not necessarily a velocity variable,

$$\frac{\mathrm{d}A}{\mathrm{d}t} = \lambda_0 A(t) - \int_0^t \mathrm{d}s \phi(s) A(t-s) + f(t). \tag{8}$$

The starting point of the derivation is the 'rate' equation

$$\frac{\mathrm{d}A}{\mathrm{d}t} = \Gamma A(t), \tag{9}$$

where $\Gamma = L^+$ is the operator adjoint to the Liouville operator and the memory kernel is given by the autocorrelation function of the random force,

$$\phi(|t-t'|) = \frac{\langle f(t) f(t') \rangle}{\langle A^2 \rangle}. \tag{10}$$

The Hamiltonian formulation of the Mori formalism has been extended by Grigolini (1985) to the non-Hermitian case and used as a convenient algorithm for calculation to evaluate relaxation processes in condensed matter. This calculation algorithm is based on expressing the Laplace transform of the equilibrium autocorrelation function of the variable A in a continued fraction form.

Proceeding along these lines it was possible to establish a first encounter with the limitations of the Liouville approach to relaxation processes. In fact, Fronzoni et al. (1985) study relaxation processes in the case of dissipative, nonlinear and stochastic networks and proved that adopting the continued fraction approach, generated by Mori theory, becomes invalid in the limiting case of extremely weak friction. Further research work in this direction was done by Sen and Philips (1995), Sen et al. (1996) and Sen (2002, 2006) which confirmed that there exist cases yielding non-convergent continued fractions. According to Sen (2006) the convergence breakdown may be the signature of the occurrence of a phase transition. The analysis of Legoll et al. (2007) suggests a possible connection with the ergodicity breakdown of the Nosé (1985)–Hoover (1985) thermostatic Harmonic oscillator. We think that these technical problems are indicative of the inadequacy of conventional Liouville-like approaches to modeling phenomena above a certain level of complexity.

Nevertheless, the fundamental work of Lee (1982a,b, 1983a) and Balucani et al. (2003) on the GLE widely known as Mori–Lee theory, has a broad range of applications, including traffic flow as pointed out by Skagerstam and Hansen (2005). This is not surprising insofar as the GLE was originally designed to predict the deviation of the variable of interest A from exponential relaxation when its dynamics are determined by highly correlated stochastic forces. The variable of interest A then generates a diffusion process whose mean-square amplitude is given by the anomalous form $\langle A^2 \rangle \propto t^{2H}$, whose Hurst coefficient H deviates from the ordinary diffusion prediction $H = 0.5$. This non-standard diffusion is in line with the experimental observation of traffic flow by Skagerstam and Hansen (2005).

The GLE has recently been used by Min et al. (2005) to account for the photon-by-photon method of protein dynamics detection. Another reason for the increased interest in the GLE is the discovery of the violation of mixing, ergodicity and of the fluctuation–dissipation relations as shown by Costa et al. (2006), Lapas et al. (2007) and Vainstein et al. (2006). A lucid discussion of this issue is given in the work of Lee (1982a,b) and Lee (2006). Of special interest is the adoption of the GLE to prove that irreversibility does not necessarily ensure ergodicity as shown by Lee (2007). These revelations have recently been the subject of intense debate rediscovering GLE properties that were established decades earlier, but are apparently not well known, see, for example, Costa et al. (2006), Lapas et al. (2007), Bao and Zhuo (2003) and Bao et al. (2005, 2006). Ferrario and Grigolini (1979), applied the continued fraction approach to the GLE, by means of the same recursion rules that have been

made popular by the work of Lee (1982a,b), to show that the GLE can be used to represent conditions intermediate between the regular behavior of harmonic oscillators and the erratic condition depicted by the ordinary Langevin equation. The same conclusion, after nearly three decades, has been reached by other authors (see Bao et al. (2006)) as well. The originality of the most recent work rests on the fact that in the earlier work of the GLE users did not consider the action of correlated stochastic forces that may generate anomalous diffusion. This is the reason why some scientists (see, for example, Heinsalu et al. (2007) and Mokshin et al. (2005)) consider the GLE an important theoretical tool for the study of complexity. In Section 8 we revisit this issue and point out the different forms of complexity that have emerged from the research work of the intervening 40 years.

2.1.2. Nonlinear dissipation

The phenomenon of dissipation is traditionally modeled, as in the previous section, in terms of a linear transport coefficient and particle momentum. For a Brownian particle the dissipation is given by the Stokes drag on the pollen mote, in terms of the kinematic viscosity of the background fluid. Models of the linear dissipation arise from a bilinear coupling of the network of interest to the environment. A natural question concerns the form of the dissipation for a more complex interaction, say when the coupling of the network to the heat bath is not linear, that is, the interaction Hamiltonian is given by

$$H_{\rm int} = -\sum_n \Gamma_n q_n G(Q) \tag{11}$$

where q_n is the displacement of the nth bath oscillator and $G(Q)$ is an analytic function of the network displacement. Here again we can solve the equations of motion for the bath degrees of freedom in terms of an integral over the function $G(Q)$. Lindenberg and West (1990) construct a nonlinear GLE from a model Hamiltonian, but here we do not consider the details, but instead concentrate on a specific form of the coupling function.

Consider the case when the coupling function is quadratic in the network displacement

$$G(Q) = \frac{1}{2}Q^2 \tag{12}$$

and determine that the force equation becomes

$$\frac{{\rm d}P}{{\rm d}t} = -V_m'(Q) - \int_0^t K\left(t-t'\right) Q(t)Q(t')P\left(t'\right){\rm d}t' + f(t)Q \tag{13}$$

with analytic expressions for the fluctuating coefficient $f(t)$, the dissipative memory kernel $K(t)$ for a linear model of the heat bath, and a fluctuation–dissipation relation of the second kind has again been implemented to obtain (13) by Lindenberg and West (1990). Note that the 'random force' in (13) is not additive, but depends on the network displacement, making it state dependent. The influence of the random variable is therefore suppressed for small displacements and amplified for large displacements of the network. If we model the potential function in the following way

$$V_m(Q) = \frac{1}{2}\omega_0^2 Q^2 + \Delta V(Q) \tag{14}$$

where $\Delta V(Q)$ contains anharmonic contributions, then the time-dependent frequency of the network oscillator is defined by the relation

$$\omega^2(t) = \omega_0^2 - f(t). \tag{15}$$

The dissipation corresponding to this multiplicative fluctuation must consequently be nonlinear in order to insure that the network plus environment is thermodynamically closed.

A simpler form of the dynamic equation can be constructed when the fluctuations are delta correlated in time. Using the explicit form of the fluctuating coefficient obtained when the number of bath variables becomes infinite (see Lindenberg and West (1990)) the fluctuation–dissipation relation becomes

$$\left\langle f(t)f(t')\right\rangle = 2\mu k_B\Theta\delta(t-t') \tag{16}$$

when the initial state of the heat bath has a canonical distribution. In this situation the heat bath is given by white noise so that the dissipative kernel reduces to the memoryless form

$$K(t) \to 2\mu\delta(t) \tag{17}$$

and the nonlinear GLE (13) reduces to the nonlinear Langevin equation

$$\frac{{\rm d}P}{{\rm d}t} = -\omega^2(t)Q - \Delta V'(Q) - \mu Q^2 P. \tag{18}$$

It is clear that in the absence of anharmonic terms, $\Delta V(Q) = 0$, (18) reduces to a harmonic oscillator with nonlinear dissipation and a fluctuating frequency. The Gaussian distribution of fluctuations implies that $\omega^2(t)$ can sometimes be

negative; when the effect of the environment on the oscillator is to provide a harmonic force to increase rather than to decrease the oscillator displacement.

Note that the existence of such a thermodynamically closed dynamical description suggests that the usual form of the FDT is limited to linear phenomena. We subsequently show that this nonlinear FDT is only one of a number of ways in which the traditional FDT has been generalized in complex networks.

2.1.3. Information and Maxwell's demon

James Clerk Maxwell (1831–1879), considered by many to be the leading scientist of the 19th Century, recognized that the kinetic theory of gases, which he invented and along with Ludwig Boltzmann refined, could in principle, lead to a violation of the second law of thermodynamics using information about the motion of molecules to extract kinetic energy to do useful work. In his 1888 book, *Theory of Heat* Maxwell (2001), he introduces his now famous demon:

> ..a being whose faculties are so sharpened that he can follow every molecule in his course, and would be able to do what is presently impossible to us . . .. Let us suppose that a vessel is divided into two portions. A and B by a division in which there is a small hole, and that a being who can see the individual molecules opens and closes this hole, so as to allow only the swifter molecules to pass from A to B, and only the slower ones to pass from B to A. He will, thus, without expenditure of work raise the temperature of B and lower that of A, in contradiction to the second law of thermodynamics.

Brillouin (1962), in his remarkable book, *Science and Information Theory*, revealed that the paradox of Maxwell's demon is at the nexus of information theory and physics. He reviewed the many 'resolutions' to the paradox that have been proposed over the nearly hundred years between the publication of the two books. He pointed out that Szilard (1929) was the first to explain that the demon acts using information on the detailed motion of the molecules, and actually changes this information into negentropy, that is, information from the environment is used to reduce the entropy of the system. Brillouin, himself, resolved the paradox using a photon of light, against a background of blackbody radiation, that the demon must absorb to see a molecule of gas. We do not present Brillouin's discussion here, but we note his observation:

> . . . every physical measurement requires a corresponding entropy increase.

He subsequently concludes that the average entropy increase is always larger than the average amount of information obtained in any measurement.

The mathematician, Norbert Weiner, in his book that started the field of scientific inquiry, *Cybernetics* Wiener (1948), suggested that the demon must have information about the molecules in order to know which to pass through the hole and at what times. He acknowledges that this information is lost once the particle passes through the hole and puts information and entropy on an equal footing by observing that the demon's acquisition of information opens up the network. The demon-gas network has an increasing total entropy, consisting as it does of the sum of the entropy of the gas, which is decreasing, and the negentropy (information), which is increasing. Ball (1956) notes that Szilard had previously concluded that:

> . . . the second law would not be violated by the demon if a suitable value of entropy were attributed to the information which the demon used in order to reduce the entropy of the rest of the system.

The key feature in the resolution of Maxwell's demon paradox is the existence of dissipation, that is, the erasure of memory, in the information cycle. This occurs in Brillouin's argument through the requirement that the photon energy exceed that of the blackbody radiation and in Wiener's discussion, in the observation that the particle forgets its origin once it passes through the hole. Landauer (1993) indicates that these early arguments can be summarized in the statement:

> The erasure of the actual measurement information incurs enough dissipation to save the second law.

independent of any specific physical mechanism. Bennett (1982) was able to pull the threads of all the various arguments together, in the context of doing reversible computation, and in so doing obtain what is considered to be the final resolution of the Maxwell demon paradox.

Landauer (1996a,b) interpreted information to be a physical phenomenon. He argued that rather than being the abstract quantity that forms the basis of intense mathematical discussion in texts on information theory, which it certainly does, information itself is always tied to a physical representation. Whether it is a spin, a charge, a pattern of human origin, or a configuration of nature's design, information is always tied to a physical process of one kind or another. Consequently, information is physical in the same sense that entropy and energy are physical. Landauer explores the consequence of this assertion by noting that the physical nature of information makes both mathematics and computer science a part of physics. We shall not dwell on this prioritizing of the sciences here, but shall review some of the consequences of this perspective when appropriate.

Moreover, this world view suggests we adopt a perspective that focuses on the occurrence of events rather than on the dynamics of network variables. We adopt this point of view and review the changes that arise in the physical descriptions of complex networks when this is done. We also find it convenient to resurrect Maxwell's demon for some of our later discussion and to give her a more well-rounded personality. In Section 5 we shall introduce another kind of Demon whose action may depart from the ordinary Poisson prescription, as well as from the second law of thermodynamics as a result of the spontaneous emergence of the Demon's organizational skills and social life.

2.2. Linear resonance

We are interested in the phenomenon of resonance in a variety of settings and therefore we briefly review how the concept arose in the context of linear harmonic oscillations. The most ubiquitous model in theoretical physics is the harmonic oscillator. It is the basis for the understanding of every phenomena from water waves, to lattice phonons, to all the *-ons* in quantum mechanics. The stature of the lowly harmonic oscillator derives from the notion that complex phenomena have equations of motion that can be generated by means of a linear unperturbed Hamiltonian H_0 and a sequence of weak perturbations producing small deviations in the vicinity of that dominant behavior. When the conditions for a perturbation approach are realized, the harmonic oscillator is often a good lowest-order approximation to the dynamics.

The equations of motion for a unit mass linear oscillator are determined by the Hamiltonian

$$H_0 = \frac{1}{2}P^2 + \frac{1}{2}\omega_0^2 Q^2 \tag{19}$$

whose equations of motion have the simple harmonic solution

$$Q_0(t) = A\cos\left[\omega_0 t + \phi\right] \tag{20}$$

where ω_0 is the natural frequency of the oscillator and the amplitude A and phase ϕ are determined by the initial conditions. A single linear oscillator driven by a periodic perturbation of amplitude A_p is described by the Hamiltonian

$$H = \frac{1}{2}P^2 + \frac{1}{2}\omega_0^2 Q^2 - QA_p\cos\omega_p t \tag{21}$$

whose equations of motion have a solution whose amplitude diverges as the frequency of the perturbation ω_p approaches the natural frequency of the oscillator. The solution becomes

$$Q_p(t) = \frac{A_p}{\omega_0^2 - \omega_p^2}\cos\left[\omega_p t + \phi_p\right]. \tag{22}$$

This is actually the inhomogeneous part of the total solution which divergence as $\omega_p \to \omega_0$, thereby overwhelming the homogeneous part of the solution. In a real system this mathematical divergence is eventually quenched by dissipation, which is to say, the amplitude of the solution may become substantial but it must remain finite even at the resonance condition $\omega_p = \omega_0$. The enhanced amplitude eventually triggers a mechanism that violates the perturbation assumption.

There are a number of ways to quench the divergence resulting from linear resonance, for example, as we saw above every thermodynamic network has fluctuations and dissipation, and for a sufficiently large amplitude of the oscillator the influence of the environment can no longer be neglected. If we introduce a periodic perturbation into the total Hamiltonian (1) the average homogeneous solution to the unperturbed oscillator (unperturbed by the periodic driving force, but still in contact with the heat bath) is

$$\langle Q_h(t)\rangle = Ae^{-\lambda t}\cos\left[t\sqrt{\omega_0^2 - \lambda^2} + \phi\right]. \tag{23}$$

In the case of a periodically driven oscillator we again have two terms in the solution, the homogeneous and inhomogeneous. In the asymptotic limit the homogeneous term (23) vanishes due to dissipation and the inhomogeneous term has a large but finite maximum amplitude even at the resonance condition. The average of the particular solution in the driven case is

$$\left\langle Q_p(t)\right\rangle = \frac{A_p}{\sqrt{\left(\omega_0^2 - \omega_p^2\right)^2 + \lambda^2\omega_p^2}}\cos\left[\omega_p t + \phi_p\right] \tag{24}$$

with the phase

$$\tan\phi_p = \frac{\lambda\omega_p}{\omega_0^2 - \omega_p^2}. \tag{25}$$

After the transient fades away, the average steady-state response of the oscillator to the driver has the same frequency as the excitation, but it is phase shifted as indicated in (24). This is the under-damped case where the resonance line has a width determined by the magnitude of the dissipation parameter and the average resonance amplitude is a factor $\left(\lambda\omega_p\right)^{-1}$ greater than the amplitude of the driver, which can be substantial for weak dissipation.

2.2.1. The bullwhip effect

In economics, supply chain management is a major topic and concerns the optimal structure of supply and distribution networks. Helbing and Lammer (2004), using methods from statistical physics, that is, treating distribution networks as transport processes, find that most supply networks manifest damped oscillations, such as those described above, even those whose units and linear chains of units, have non-oscillatory dynamics. What is surprising about this linear analysis is that networks of damped linear oscillators can produce growing oscillations and this has been related to the 'bullwhip effect':

> It describes increasing oscillations in the delivery rates and stock levels from one supplier to the next upstream supplier delivering to him.

They find that the amplification of amplitudes in the bullwhip effect is not due to an unstable eigenvalue, but is a consequence of a resonance. The supply network is modeled as a linear damped harmonic chain coupled to its nearest neighbors in one direction only, thereby having linear frequencies, dissipation parameters, coupling coefficients and external forcing due to consumption of the commodity. The form of the analytic solution to the second-order damped linear equations of motion are straight forward extensions of (24) suitably generalized to include the important economic parameters. The resonance occurs when the oscillation frequency of the consumption rate matches one of the natural frequencies of the units in the supply network. When the resonance occurs the variations in the consumption rate are amplified upstream of the resonance, leading to the bullwhip effect (analogous to the phenomenon of convective instability in fluid dynamics, see, for example, Infeld and Rowlands (1990)).

2.2.2. Medical observables

Resonance is a key physical mechanism underlying some of the most useful measures of physiological phenomena. One example is magnetic resonance imaging (MRI) used in medical science to study normal anatomy and function of the human body, and in clinical science to uncover and diagnose pathology, see, for example, Weishaupt et al. (2003). A MRI scanner polarizes the hydrogen nuclei in water molecules in the body by means of a powerful static magnetic field. These polarized nuclei are excited by the spatial gradient of a much weaker time-varying magnetic field for encoding the local spatial structure of the body and finally a weak radio-frequency (RF) field is applied to manipulate the polarized nuclei to produce a measurable signal, which is collected through an RF antenna.

Nuclear magnetic resonance, the phenomenon on which MRI is based, is determined by the quantum mechanical magnetic properties of an atom's nucleus, that being the magnetic moment. It is the magnetic moment (nuclear spin) that is manipulated in MRI. The external magnetic field creates an energy gap between nuclei aligned and anti-aligned with it, so that if the frequency of the rf signal is matched to this energy gap a resonance is created and the population of the two states are equalized.

Although traditionally MRI scanners created a two-dimensional image of a thin "slice" of the body, modern MRI instruments are capable of producing images in the form of three-dimensional blocks. An MRI scanner images hydrogen-based objects, so bone, which is calcium based, is imaged as a void, and will not affect soft tissue views. Consequently, MRI scanners are excellent for imaging joints, the central nervous system and the brain.

2.3. Stochastic resonance (SR)

Nonlinear dynamical networks with additive fluctuations often have unexpected properties. One such unexpected property was identified over a quarter century ago and has to do with the counter-intuitive response of certain weakly periodically driven nonlinear dynamical networks to the addition of noise. Experience would suggest that the signal to noise ratio in such a network would decrease as the amplitude of the added noise increases. This is not always the case, however. Here we briefly review the phenomenon of stochastic resonance (SR), first introduced by Benzi et al. (1981), where the signal to noise ratio, in fact, is a non-monotonic function of the fluctuation strength and therefore increases as the noise amplitude increases in certain parameter domains. The original application of SR was to the problem of periodically recurring ice ages and was postulated independently by a number of scientists, see, for example, Benzi et al. (1981) and Nicolis and Nicolis (1981). The first experimental verification of the existence of SR in a laboratory was made by McNamara et al. (1988) using a bistable ring laser.

To demonstrate SR in a specific network consider one described by the quartic potential

$$V(Q) = \frac{A}{4}\left(Q^2 - a^2\right)^2 \tag{26}$$

which has the three extrema, $Q = 0, \pm a$, determined by the vanishing derivative of the potential. The vanishing second derivative reveals that the point $Q = 0$ is unstable and the points $Q = \pm a$ are stable, as shown in Fig. 1. The two minima are separated by a local maximum in the potential and this energetic barrier is required for the system to manifest SR.

We need a signal and therefore we impose a periodic forcing function on this isolated nonlinear oscillator in the same way we did the isolated linear oscillator. The driven network of interest is described by the Hamiltonian for a periodically

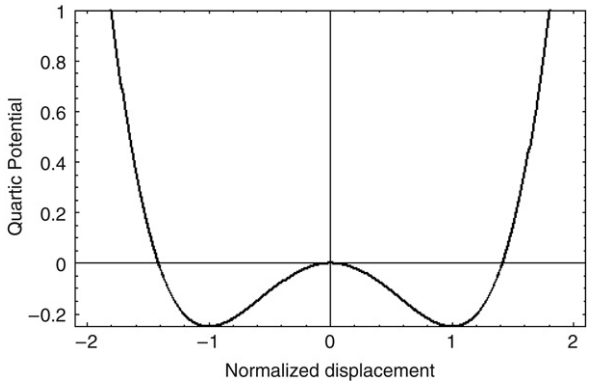

Fig. 1. The quartic or double well potential given by (26) with unit amplitude is plotted against the normalized variable, that is, $a = 1$. The height of the potential barrier is $\frac{1}{4}$ for the values of the parameters chosen.

perturbed unit mass oscillator in a double well potential is

$$H_N = \frac{1}{2}P^2 + \frac{A}{4}\left(Q^2 - a^2\right)^2 - QA_p \cos\omega_p t. \tag{27}$$

Consequently, by including the influence of the environment on the perturbed oscillator we obtain the equations of motion

$$\begin{aligned}\frac{\mathrm{d}Q}{\mathrm{d}t} &= P\\ \frac{\mathrm{d}P}{\mathrm{d}t} &= -A\left(Q^2 - a^2\right)Q + A_p\cos\omega_p t - \lambda P + \xi(t).\end{aligned} \tag{28}$$

The effective potential is obtained by grouping terms in (27) to obtain

$$V_{\mathrm{eff}}(Q) = \frac{A}{4}\left(Q^2 - a^2\right)^2 - QA_p\cos\omega_p t \tag{29}$$

in which the Brownian particle moves in the time-dependent potential depicted in Fig. 2. In this figure it is clear that when the periodic forcing has its maximum value the left-hand minimum of the potential is the absolute minimum and when the periodic forcing has its minimum value the right-hand minimum plays this role. Using the Smoluchowsky approximation on (28), we can write the equation of motion for the Brownian particle in the effective potential as

$$\frac{\mathrm{d}Q}{\mathrm{d}t} = -\Phi'(Q) + \eta(t) \tag{30}$$

where $\kappa = A_p/\lambda$, $\Phi(Q) \equiv V_{\mathrm{eff}}(Q)/\lambda$ and $\eta(t) = \xi(t)/\lambda$.

Here we can see that the Brownian particle oscillates in the vicinity of one of the minima and the potential rhythmically changes the relative position of the minima as depicted in Fig. 2. If the change in minima matches the fluctuations a particle can be propelled over the potential barrier. As observed by Gammaitoni et al. (1998) SR in such a symmetric quartic potential is essentially a synchronization of the thermally activated hopping events between the potential minima and the weak periodic forcing. Kramers (1940) calculated this rate of transition between such potential wells to be

$$r = \frac{\omega_a\omega_0}{4\pi\lambda}\exp\left[-\frac{\lambda\Delta V}{D}\right] \tag{31}$$

where the frequency of the linear oscillations in the neighborhood of the stable minima is $\omega_a = \left|V''(a)\right|^{1/2}$; the frequency at the unstable maximum is $\omega_0 = \left|V''(0)\right|^{1/2}$ and ΔV is the height of the potential barrier separating the two wells. The mean-square strength of the fluctuations is related to the temperature of the bath by the FDR.

The average long-time response of the nonlinear oscillator does not look very different from that obtained in the case of linear resonance. However here, because the potential is nonlinear we use LRT to obtain the solution for a small amplitude periodic forcing function (see Gammaitoni et al. (1998)):

$$\langle Q(t)\rangle_\xi = \frac{A_p}{D}\left\langle Q^2\right\rangle_0 \frac{2r}{\sqrt{r^2+\omega_p^2}}\cos\left[\omega_p t + \phi_p\right] \tag{32}$$

and phase shift

$$\phi_p = -\tan^{-1}\left[\frac{\omega_p}{2r}\right] \tag{33}$$

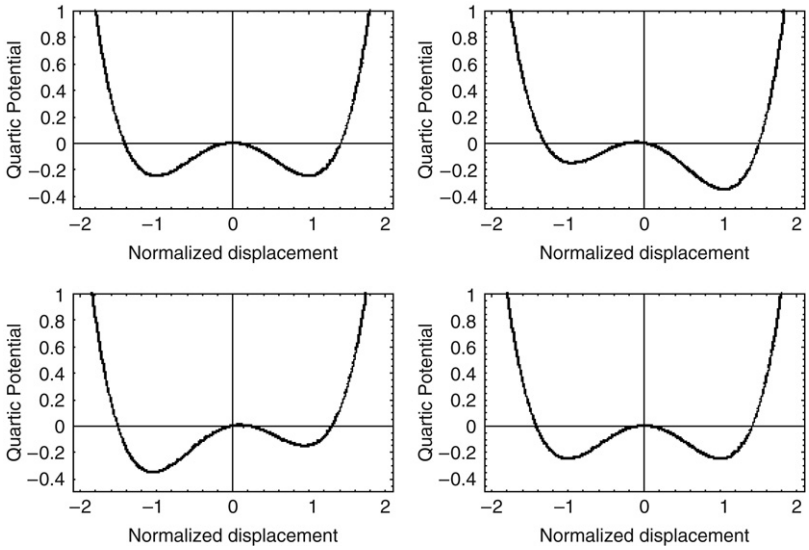

Fig. 2. Here the effective potential is plotted versus the normalized variable ($a = 1$) and the driver has amplitude $\kappa = 0.1$. Going in a circle the different graphs are separated by one half cycle of the periodic perturbation.

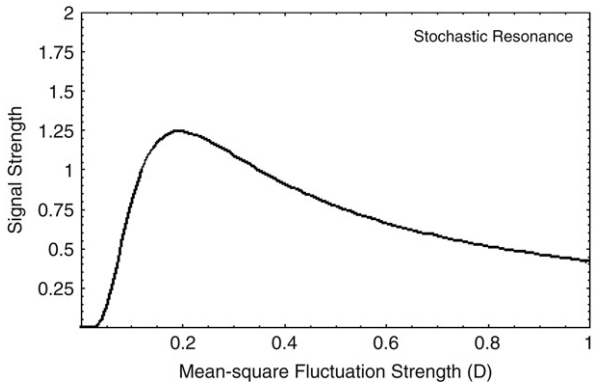

Fig. 3. The function given by (34) is graphed versus the mean-square level of the fluctuations given by the dissipation parameter D.

where Kramers' rate r replaces the frequency difference obtained in the case of linear resonance. Inserting the expression for the rate of transition (31) into the asymptotic solution for the average signal (32) allows us to express the average signal strength as a function of the intensity of the fluctuations. Extracting the D-dependence function from the resulting equation

$$G(D) = \frac{\exp\left[-\frac{\lambda\Delta V}{D}\right]}{D\sqrt{4\exp\left[-\frac{2\lambda\Delta V}{D}\right] + \omega_p^2}} \tag{34}$$

and choosing the parameters for the potential to be $A_p = a = 1$ and the frequency of the driver to be unity, we arrive at the curve shown in Fig. 3.

The average signal strength determined by the solution to the weakly periodically driven stochastic nonlinear oscillator is proportional to the curve depicted in Fig. 3. It is clear from the figure that the average signal increases with increasing D, for small fluctuations levels, which is to say; weak noise facilitates the average signal level. At some intermediate level of fluctuations, determined by the parameters of the dynamical network, the average signal reaches a maximum level. For more intense fluctuations the average signal decreases, asymptotically approaching an inverse power-law response, i.e. $G(D) \sim 1/D$. This non-monotonic response of the network to noise is characteristic of SR.

2.3.1. SR in neuronal and other networks

Stochastic resonance is a statistical mechanism whereby noise influences the transmission of information in both natural and artificial networks such that the signal-to-noise ratio is no longer monotonic. There has been an avalanche of papers on the SR concept across a landscape of applications, starting with the original paleoclimatology study of Benzi et al. (1981) and Nicolis and Nicolis (1981) all the way to the influence of noise on the information flow in sensory neurons, ion-channel

gating and visual perception shown by Moss et al. (2004). The majority of the theoretical analyses have relied on the one-dimensional bi-stable double well potential sketched above, or a reduced version given by a two-state model, both of which are now classified as dynamic SR. Another version of SR, that most commonly found in biological networks, involves the concurrence of a threshold, with a subthreshold signal and noise. The latter is called threshold SR (see Moss et al. (2004)). Here we briefly comment on how adding noise to subthreshold signals in nonlinear sensory systems can enhance sensor information processing.

Psychophysics dates back to the middle of the nineteenth century, to the work of Fechner (1860), and is concerned with the accurate detection and characterization of human perception from the physical signals of the human sensory network. Visual perception is one area in which there have been a great many experiments done to demonstrate the existence of a threshold. Moss et al. (2004) point out that through the addition of noise the SR mechanism has been found to be operative in the perception of gratings, ambiguous figures and letters and can be used to improve the observer's sensitivity to weak visual signals. The nonlinear auditory network of human hearing also manifests threshold SR behavior. The absolute threshold for the detection and discrimination of pure tones was shown by Zeng et al. (2000) to be lowered in normal hearing people by the addition of noise. They also showed the same effect for individuals with cochlear or brain-stem implants by the addition of an optimal amount of broad band noise.

The most success of SR, as pointed out by one of the leaders in the field (see Moss et al. (2004)), has been associated with modeling and simulation of networks of neurons where the effects of noise on sensory function match those of experiment. Consequently, the indications are that the threshold SR theory explains one of the fundamental neuron operation mechanisms. This does not carry over to the brain, however, since the SR mechanism cannot, in this case, be related to a specific function. One conservative conclusion is that the evidence does not support the interpretation as pointed out by Moss et al. (2004):

> . . . that naturally occurring noise actually enhances information transmission and processing, nor is it documented that neuronal systems do optimize the noise intensity for maximum information or efficacy of processing. Yet some indications that SR models may reflect mechanisms that are operative in the CNS seems to exist and justifies research . . .. SR appears to be a ubiquitous and remarkable phenomenon congruent to the available theories on brain function . . ..

2.3.2. *Information resonance*

In the previous discussion the measure of the quality of the SR mechanism was the signal-to-noise ratio (SNR). The ratio of the SNR of the input to that of the output of an SR network provides a measure of the information being transferred through the network and when maximized yields the maximum information transfer. However, Kish et al. (2001) point out that the SNR measure only provides information about the entropy of the signal versus noise and the degradation of this entropy during transfer. They also emphasize that this measure does not address the channel capacity, which is to say, it is concerned with information in bits and not in how the information changes in time in bits/s, as would be appropriate for the information transfer rate. This information transfer approach to modeling SR in neurons has been discussed as an 'information resonance' by Wallace (2000).

Kish et al. (2001) directly evaluate Shannon's formula for the channel capacity to estimate the information transfer rate of neurons in the SR region. Shannon's formula is

$$C = B_s \log_2 \left[1 + \frac{S_s}{S_n}\right]; \quad \text{bits/s} \tag{35}$$

with B_s the maximal bandwidth of the signal, S_s is the maximum mean-square signal amplitude and S_n the maximum mean-square noise amplitude. Shannon interprets the two factors of (35) to be the rate at which information is refreshed given by B_s and the potential amount of information available at each refreshing event given by the logarithm. Without going into the details of the calculation we write their result for the channel capacity, see, Kish et al. (2001),

$$C = \frac{B_{n,in}}{2\sqrt{3}} \exp\left[-\frac{U_t^2}{2B_{n,in}S_{n,in}}\right] \log_2 \left[1 + \left(\frac{2AU_t}{B_{n,in}S_{n,in}}\right)^2\right] \tag{36}$$

where $B_{n,in}$ is the bandwidth of the input noise, U_t is the excitation threshold potential of the neuron, $S_{n,in}$ is the power spectral density of the input noise and A is the root-mean-square amplitude of the input signal. To get a sense of the dependence of (36) on the mean-square level of the input noise we set all other parameters to one and graph the resulting function in Fig. 4, much like we did in Fig. 3, thereby obtaining the SNR by another measure.

In Fig. 4 we can see that the measure of the information transfer rate is non-monotonic, reaching the characteristic SR peak for an intermediate level of input noise. Consequently, the network capacity is a viable measure of the ability of a complex network to transfer information. Here again the maximum rate of information transfer is achieved when the network capacity is matched to a given level of fluctuations.

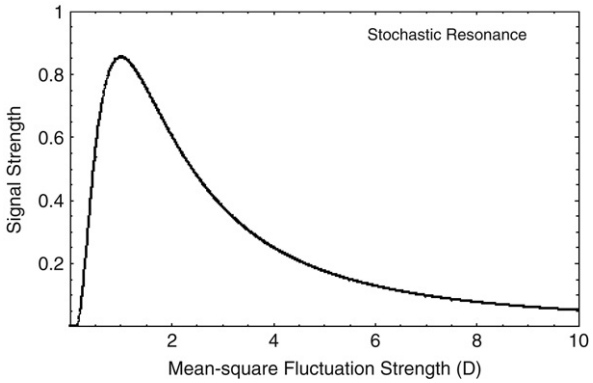

Fig. 4. The function given by (36) is graphed versus the mean-square level of the fluctuations when the other parameters of the network have been set to unity.

2.4. Fractional Langevin equation (FLE)

In this section we take note of the fact that a strictly exponential relaxation is inconsistent with a Hamiltonian description of a dynamic network. Consequently, it is not possible to establish a satisfactory connection between microscopic and macroscopic dynamics and stochastic physics. This limitation was overcome using the Van Hove method, see, Van Hove (1955) for determining the asymptotic behavior of a number of illustrative examples. This method takes the limit that the network-environment coupling is weak, along with the asymptotic time limit where the observation time is much longer than the other time scales being considered, specifically the microscopic time scale τ_c. These observations allow us to reformulate the Van Hove limit in a new way. First, we replace the asymptotic time limit with $\tau_c \to 0$. Second, we replace the weak coupling limit with the equivalent limit for the coupling constant $V \to \infty$. The quantity to be kept constant is the product $V^2\tau_c$, with $\tau_c^{-1} \gg V$ in the limit $V^2 \to \infty$.

It is well known from Mori (1965a,b) that the free-particle GLE

$$\frac{\mathrm{d}P}{\mathrm{d}t} = -\Delta_1^2 \int_0^t \Phi_1\left(t-t'\right) P(t')\mathrm{d}t' + f(t) \tag{37}$$

written explicitly in terms of the autocorrelation function of the random force $\Phi_1(t)$ and the strength of the network-bath coupling Δ_1^2, corresponds to the hierarchy of correlation functions shown by Grigolini (1985):

$$\frac{\mathrm{d}\Phi_j}{\mathrm{d}t} = -\Delta_{j+1}^2 \int_0^t \Phi_{j+1}\left(t-t'\right) \Phi_j(t')\mathrm{d}t'. \tag{38}$$

Eq. (37) is the $j = 0$ contribution to (38) relating the autocorrelation function of the network momentum to that of the random force and the general solution, in terms of continued fractions, is given by Grigolini et al. (1999).

Here we consider the solution for the momentum autocorrelation function for a random force with an inverse power-law autocorrelation function given by

$$\Phi_1(t) = \frac{T^\beta}{\left(T^2+t^2\right)^{\beta/2}}. \tag{39}$$

The situation with $\beta > 1$ has shown that the resulting GLE is consistent with traditional statistical mechanics, see, for instance, Grigolini et al. (1999), in that the Van Hove limit yields the ordinary Langevin equation. However that is not true when the power-law index is in the interval $0 < \beta < 1$ in which case the nonintegrability of the autocorrelation function (39) prevents us from adopting the traditional Van Hove approach. Grigolini et al. (1999) introduced a different procedure to go from a microscopic to a macroscopic description of the network. Their procedure can be derived in a natural way from the original Van Hove limit using the parameter

$$\Upsilon \equiv \lim_{\substack{\tau_c\to 0 \\ \Delta_1^2\to\infty}} \Delta_1^2\tau_c^\beta = \lim_{\mathrm{GVH}} \Delta_1^2 T^\beta \tag{40}$$

which we term the generalized Van Hove limit (GVH).

Inserting the autocorrelation function for the random force (39) into the integro-differential equation for the momentum autocorrelation function defined by the GLE and implementing the generalized Van Hove limiting procedure we obtain from

(38) for $j = 0$,

$$\frac{\mathrm{d}\Phi_0(t)}{\mathrm{d}t} = -\lim_{\mathrm{GVH}} \Delta_1^2 \tau_c^\beta \int_0^t \frac{\Phi_0(t')\mathrm{d}t'}{\left(\tau_c^2 + (t-t')^2\right)^{\beta/2}}$$
$$= -\Upsilon \int_0^t \frac{\Phi_0(t')\mathrm{d}t'}{(t-t')^\beta}. \tag{41}$$

Notice that in general the autocorrelation function is related to the waiting time distribution function $\psi(t)$ of the process under study by

$$\Phi_0(t) = 1 - \int_0^t \psi(t')\mathrm{d}t' \tag{42}$$

and therefore (41) can be written as

$$\psi(t) = \Upsilon \int_0^t \frac{\Phi_0\left(t'\right)\mathrm{d}t'}{(t-t')^\beta}. \tag{43}$$

Now we compare this last expression with the fractional relaxation equation obtained by Glöckle and Nonnenmacher (1993a)

$$D_t^\alpha \left[F(t;\alpha)\right] - \frac{t^{-\alpha}}{\Gamma(1-\alpha)} F(0;\alpha) = \frac{1}{\tau_c^\alpha} F(t;\alpha) \tag{44}$$

where the operator $D_t^\alpha[\cdot]$ is the Riemann–Liouville (RL) fractional derivative and $\alpha < 1$. Here we write the RL fractional integral

$$D_t^{-\alpha}\left[\Phi_0(t)\right] = \frac{1}{\Gamma(\alpha)} \int_0^t \frac{\Phi_0(t')\mathrm{d}t'}{(t-t')^{1-\alpha}} \tag{45}$$

and express (44) as

$$F(t;\alpha) - F(0;\alpha) = \frac{1}{\tau_c^\alpha} D_t^{-\alpha}\left[F(t;\alpha)\right]. \tag{46}$$

The solution to (46) is well known, see, for example, West et al. (2003) and Glöckle and Nonnenmacher (1993a), and is proportional to the Mittag–Leffler function (MLF), a generalization of the exponential function,

$$E_\alpha\left(-\left[\frac{t}{\tau_c}\right]^\alpha\right) = \sum_{n=0}^{\infty} \frac{(-1)^n}{\Gamma(n\alpha+1)} \left(\frac{t}{\tau_c}\right)^{n\alpha} \tag{47}$$

which exhibits stretched exponential behavior at short times, inverse power-law relaxation at long times and reduces to the exponential for $\alpha = 1$.

It is important to stress that the analytical function (47) has been used to fit the relaxation curves of stress experiments on glassy materials with remarkable accuracy as shown by Glöckle and Nonnenmacher (1993a,b). This success suggests that dynamic randomness without time-scale separation is manifest through time fractional derivatives and becomes experimentally detectable at the macroscopic level. Consequently, the GLE can be further extended to the fractional Langevin equation (FLE) in which the fluctuations of the heat bath contain inverse power-law memory leading to a fractional derivative in time for the network dynamics.

It is now possible to compare the solution to the fractional relaxation equation (44) with the expression for the waiting time function (43) and identify the fractional operator index as $\beta = 1 - \alpha$ to obtain

$$\psi(t) = \Upsilon \Gamma(\alpha)\, \tau_c^\alpha E_\alpha\left(-\left[\frac{t}{\tau_c}\right]^\alpha\right) \Phi_0(0,\alpha). \tag{48}$$

Consequently, if, for dimensional reasons, we write $\Upsilon \equiv V^2 \tau_c^\beta$ then the expression for the waiting time distribution function becomes

$$\psi(t) = V^2 \tau_c \Gamma(\alpha)\, E_\alpha\left(-\left[\frac{t}{\tau_c}\right]^\alpha\right) \Phi_0(0,\alpha) \tag{49}$$

which maintains the properties of the MLF, see, for instance, Grigolini et al. (1999). In particular, the asymptotic behavior of the waiting time probability density is inverse power law with index α.

The adoption of the Van Hove limit is essentially a sophisticated way of making the Markov approximation. The Markov approximation, in turn, establishes the physical condition necessary to make Hamiltonian dynamics compatible

with stochastic physics. However, when this method is applied to microscopic dynamics to derive ordinary statistical mechanics, there is no clear perception of establishing dynamic properties inconsistent with Hamiltonian dynamics. Even if the autocorrelation functions are made exponential by forcing the Markov approximation into microscopic dynamics, so as to become incompatible with both classical and quantum mechanics (see Lee (1983b)), they are still differentiable functions.

Consequently, when there is a time-scale separation between the network and bath the Van Hove method can be applied and standard exponential relaxation follows. In the absence of the condition of time-scale separation, the method of Van Hove must be generalized and this, in turn, yields a generalization of the exponential relaxation to the MLF as shown by Grigolini et al. (1999).

2.4.1. Alternative derivation

However, there is an alternate derivation of the FLE based on the Smoluchowsky approximation to the GLE, where the inertial force is neglected so that (2) becomes

$$\int_0^t K(t-t')P(t')\mathrm{d}t' = -V_m'(Q) + f(t). \tag{50}$$

Integrating by parts and using the identity

$$\begin{aligned}\frac{\partial}{\partial t}\int_0^t K(t-t')Q\left(t'\right)\mathrm{d}t' &= K(0)Q(t) + \int_0^t \frac{\partial K(t-t')}{\partial t}Q\left(t'\right)\mathrm{d}t' \\ &= K(t)Q(0) + \int_0^t K\left(t-t'\right)P(t')\mathrm{d}t'\end{aligned} \tag{51}$$

we can rewrite (50) as

$$D_t^{\alpha}\left[Q(t)\right] - \frac{t^{-\alpha}}{\Gamma(1-\alpha)}Q(0) = -V_m'\left(Q\right) + f(t) \tag{52}$$

where $\alpha = 1-\beta$ when the memory kernel in the GLE is the inverse power law with index β.

The FLE given by (52) is a generalization of Newton's force law to incorporate long-term memory into the dynamics of a network coupled to the environment, which in isolation would evolve according to the potential $V(Q)$.

2.4.2. GLE and MLF

Here we point out that the adoption of the fractional derivative method is essentially an elegant procedure to describe the memory effect of the GLE. We meet for the first time in this report, Eq. (47), the important MLF that is in fact derived by many authors using the Mori GLE, see, for example, Min et al. (2005), Vainstein et al. (2006) and Mokshin et al. (2005). It has to be pointed out that an illuminating derivation of the GLE from the interaction of an oscillator with a bath of virtually infinitely many oscillators can be found in the excellent book by Weiss (1999), which inspired the work of Pottier (2003), who, in turn, affords an attractive derivation of the MLF relaxation using the GLE. As we have seen in this section, the MLF relaxation is attracting an increasing number of investigators and therefore, deserves further discussion. We have seen that it can be introduced as a generalization of the ordinary exponential relaxation in time through (47). In the Laplace transform representation, where $\hat{E}_{\alpha}(u) \equiv \int_0^{\infty}\exp(-ut)E_{\alpha}(-(\lambda t)^{\alpha})\mathrm{d}t$, this generalization is expressed by

$$\hat{E}_{\alpha}(u) = \frac{1}{u+\lambda^{\alpha}u^{1-\alpha}}, \tag{53}$$

where $\lambda = \frac{1}{\tau_c}$. In the domain $u \to \infty$ or equivalently $t \ll 1/\lambda$ the MLF has the stretched exponential form

$$E_{\alpha} = \exp(-(\lambda t)^{\alpha}) \tag{54}$$

and in the domain $u \to 0$ or equivalently $t \gg 1/\lambda$ the MLF has the inverse power-law form

$$E_{\alpha} \propto \frac{1}{t^{\alpha}}. \tag{55}$$

Therefore, the GVH condition corresponds to making the stretched exponential regime vanish so as to fill the macroscopic time scale with an inverse power-law regime. This is in the spirit of the fractional derivative treatment of the dynamics and is equivalent to ignoring the regime of transition from microscopic to macroscopic dynamics. In Section 5 we shall see, however, that in some cases of neurophysiological and physiological interest this regime of transition is very extended and affords the only possibility to infer the cooperative nature of the process under study from experimental observation.

3. Phase space models of statistics

Another way to systematically investigate the increasing complexity of a network is by replacing the single trajectory of the Brownian particle with an ensemble of trajectories and the corresponding function that characterizes the ensemble. In Section 2 increasing complexity was accomplished by coupling the network to the environment and associating each single particle trajectory with a realization of the bath fluctuations. If we average (5) over an ensemble of such realizations of the bath fluctuations we obtain

$$\begin{aligned}\frac{\mathrm{d}\langle Q(t)\rangle_\xi}{\mathrm{d}t} &= \langle P(t)\rangle_\xi \\ \frac{\mathrm{d}\langle P(t)\rangle_\xi}{\mathrm{d}t} &= -\left\langle \frac{\partial V_m(Q)}{\partial Q}\right\rangle_\xi - \lambda\langle P(t)\rangle_\xi\end{aligned} \tag{56}$$

as the equation for the average trajectory generated by the potential $V_m(Q)$. Note that (56) is not a closed-form equation unless the potential is quadratic, that is, the rate equation is linear in the average displacement. Formally, for non-quadratic potentials we recognize that

$$\left\langle \frac{\partial V_m(Q)}{\partial Q}\right\rangle_\xi \neq \frac{\partial V_m\left(\langle Q\rangle_\xi\right)}{\partial\left\langle Q\right\rangle_\xi} \tag{57}$$

so that the equation of motion is actually equivalent to an infinite hierarchy of moment rate equations that replace the nonlinear stochastic rate equation. All but a few such equations are intractable unless the moment hierarchy is truncated in some manner, leading to an approximate set of dynamic equations which can be solved exactly. We do not pursue this approach further, but instead turn our attention to a more manageable way of characterizing the complexity of a nonlinear network coupled to a heat bath. This manageability is realized through a probability density for the network variables.

Two distinct methods have been developed to describe the phase–space evolution of the probability density: the master equation introduced by Pauli (1928) and the continuous time random walk (CTRW) approach of Montroll and Weiss (1965). The CTRW formalism describes a random walk in which a walker pauses after each jump for a sojourn specified by a waiting time distribution function. It was shown by Bedeaux et al. (1971) that the Markov master equation is equivalent to CTRW if the waiting time process is Poisson. However, when the waiting time distribution is not exponential, the case we consider in the sequel, the equivalence between the two approaches is only maintained by generalizing to the non-Markov master equation, the so-called generalized master equation (GME) derived by Kenkre et al. (1973). Recently, Metzler (2000) argued that the GME unifies the fractional calculus and CTRW. In this review we question the possibility of going beyond a formal equivalence. The reason is, as we shall see, that the CTRW rests on discrete events, while the GME, as derived from a Liouville or Liouville-like approach, relies on continuous trajectories and does not contain events.

Allegrini et al. (2003b) have shown that to create a master equation compatible with the OP requires that the network is entangled with the heat bath in such a way that the bath does not regress to equilibrium infinitely fast. The network-bath entanglement is the result of a rearrangement process that may take infinitely long to complete, leading to the GME of Kenkre et al. (1973). Allegrini et al. (2003b) were concerned with how to make the GME stationary and therefore compatible with the OP.

In order to use the probability density we must distinguish between dynamical and phase–space variables. The former are time-dependent quantities and the latter are coordinates in the phase space of the network. Here we are again considering networks that eventually achieve thermal equilibrium with their environment. Consider the universe as consisting of a network of interest and its environment described by the Hamiltonian H. The network coordinates are denoted by the collective variable $\mathbf{X}$ and those of the environment coordinates by $\mathbf{Y}$, so we can write

$$H(\mathbf{X},\mathbf{Y}) = H_N(\mathbf{X}) + H_B(\mathbf{Y}) + H_{\mathrm{int}}(\mathbf{X},\mathbf{Y}), \tag{58}$$

as we did before in a slightly different notation. Note that we are here assuming that the bath has infinitely more degrees of freedom than does the network.

The network-environment composite evolves according to the laws of classical mechanics. Let $\rho(\mathbf{x},\mathbf{y},t)$ denote the phase–space density function

$$\rho(\mathbf{x},\mathbf{y},t) = \delta\left[\mathbf{x}-\mathbf{X}(t;\mathbf{x}_0,\mathbf{y}_0)\right]\delta\left[\mathbf{y}-\mathbf{Y}(t;\mathbf{x}_0,\mathbf{y}_0)\right] \tag{59}$$

conditional on the initial values $\mathbf{x}_0$ and $\mathbf{y}_0$ of the dynamic variables $\mathbf{X}(t)$ and $\mathbf{Y}(t)$, respectively. The phase–space density evolves according to the Liouville equation

$$\frac{\partial\rho}{\partial t} = L\rho \equiv \{H,\rho\}, \tag{60}$$

where $\{\cdot,\cdot\}$ is the Poisson bracket with respect to both the $\mathbf{x}$ and $\mathbf{y}$ variables. The distribution function of interest is that for the network variables and may be obtained from the phase–space density by integrating over the bath degrees of freedom

$$W(\mathbf{x},t\mid\mathbf{x}_0) = \int \mathrm{d}\mathbf{y}\rho(\mathbf{x},\mathbf{y},t)w(\mathbf{y}), \tag{61}$$

where $w(\mathbf{y})$ is an appropriately defined weighting of the bath variables. In the discussion of the GLE we selected the canonical distribution for the initial conditions of the bath for this weighting function. As pointed out by Lindenberg and West (1990) one way to characterize the thermalization of the network with a reservoir at temperature Θ is to determine whether or not $W(\mathbf{x}, t \mid \mathbf{x}_0)$ goes to a canonical equilibrium distribution asymptotically:

$$\lim_{t\to\infty} W(\mathbf{x}, t \mid \mathbf{x}_0) = W_{\rm eq}(\mathbf{x}) = Z^{-1}(\Theta) \exp\left[-\frac{U(\mathbf{x})}{k_B\Theta}\right], \tag{62}$$

independently of the initial state. Here $Z(\Theta)$ is the canonical partition function

$$Z(\Theta) = \int \mathrm{d}\mathbf{x} \exp\left[-\frac{U(\mathbf{x})}{k_B\Theta}\right] \tag{63}$$

and $U(\mathbf{x})$ is the energy of the network in the state $\mathbf{x}$.

3.1. Fokker–Planck equation (FPE)

The phase–space equation of motion for the phase–space distribution function and subsequently that of the probability density can be determined from the dynamics of an arbitrary analytic function $F(\mathbf{X})$. Using the definition of the phase–space distribution function (59) we express this arbitrary function as the phase–space average

$$F(\mathbf{X}) = \int F(\mathbf{x})\mathrm{d}\mathbf{x}\mathrm{d}\mathbf{y}\delta\left[\mathbf{x} - \mathbf{X}(t; \mathbf{x}_0, \mathbf{y}_0)\right]\delta\left[\mathbf{y} - \mathbf{Y}(t; \mathbf{x}_0, \mathbf{y}_0)\right]. \tag{64}$$

The time derivative of this function, using integration by parts, is given by the two equivalent forms

$$\frac{\mathrm{d}F(\mathbf{X})}{\mathrm{d}t} = \int F(\mathbf{x})\mathrm{d}\mathbf{x}\mathrm{d}\mathbf{y}\frac{\partial\rho(\mathbf{x}, \mathbf{y}, t)}{\partial t}, \tag{65}$$

$$= \nabla_{\mathbf{X}} F(\mathbf{X}) \cdot \frac{\mathrm{d}\mathbf{X}}{\mathrm{d}t}. \tag{66}$$

Expressing (66) as a phase–space integral we obtain

$$\begin{aligned}\nabla_{\mathbf{X}} F(\mathbf{X}) \cdot \frac{\mathrm{d}\mathbf{X}}{\mathrm{d}t} &= \int \mathrm{d}\mathbf{x}\mathrm{d}\mathbf{y} \begin{pmatrix} \nabla_{\mathbf{q}} F(\mathbf{x}) & 0 \\ 0 & \nabla_{\mathbf{p}} F(\mathbf{x}) \end{pmatrix} \begin{pmatrix} \mathrm{d}\mathbf{q}/\mathrm{d}t \\ \mathrm{d}\mathbf{p}/\mathrm{d}t \end{pmatrix} \rho(\mathbf{x}, \mathbf{y}, t) \\ &= \int \mathrm{d}\mathbf{x}\mathrm{d}\mathbf{y} F(\mathbf{x}) \left\{-\mathbf{p} \cdot \frac{\partial}{\partial\mathbf{q}} + \nabla_{\mathbf{q}} V(\mathbf{q}) \cdot \frac{\partial}{\partial\mathbf{p}} + \frac{\partial}{\partial\mathbf{p}}\left[\boldsymbol{\lambda} \cdot \mathbf{p} - \boldsymbol{\xi}(t)\right]\right\} \rho(\mathbf{x}, \mathbf{y}, t)\end{aligned} \tag{67}$$

where we have integrated the gradient term by parts, assumed the boundary terms to vanish and substituted from Hamilton's equations of motion. Now because the function $F(\mathbf{x})$ is arbitrary we can equate terms under the integral using (65) and (67) to obtain

$$\frac{\partial\rho(\mathbf{x}, \mathbf{y}, t)}{\partial t} = \left(-\mathbf{p} \cdot \frac{\partial}{\partial\mathbf{q}} + \nabla_{\mathbf{q}} V(\mathbf{q}) \cdot \frac{\partial}{\partial\mathbf{p}} + \frac{\partial}{\partial\mathbf{p}} \cdot \left[\boldsymbol{\lambda} \cdot \mathbf{p} - \boldsymbol{\xi}(t)\right]\right) \rho(\mathbf{x}, \mathbf{y}, t), \tag{68}$$

which has the form of a stochastic Liouville equation, since one of the coefficients of the phase–space distribution is a random function of time.

Introducing the Liouville operator for the deterministic dynamics

$$L_N \rho(\mathbf{x}, \mathbf{y}, t) \equiv \left(-\mathbf{p} \cdot \frac{\partial}{\partial\mathbf{q}} + \nabla_{\mathbf{q}} V(\mathbf{q}) \cdot \frac{\partial}{\partial\mathbf{p}} + \frac{\partial}{\partial\mathbf{p}} \cdot \boldsymbol{\lambda} \cdot \mathbf{p}\right) \rho(\mathbf{x}, \mathbf{y}, t) \tag{69}$$

and for the stochastic dynamics

$$L_\xi(t)\rho(\mathbf{x}, \mathbf{y}, t) \equiv -\frac{\partial}{\partial\mathbf{p}} \cdot \boldsymbol{\xi}(t)\rho(\mathbf{x}, \mathbf{y}, t) \tag{70}$$

so that the total Liouville operator is

$$L_T = L_N + L_\xi(t), \tag{71}$$

and we change (69) into the equation of motion for the phase–space density

$$\frac{\partial\rho(\mathbf{x}, \mathbf{y}, t)}{\partial t} = L_T \rho(\mathbf{x}, \mathbf{y}, t). \tag{72}$$

The average of (72) over an ensemble of realizations of bath fluctuations as specified by (61) gives rise to

$$\frac{\partial W(\mathbf{x}, t \mid \mathbf{x}_0)}{\partial t} = L_N W(\mathbf{x}, t \mid \mathbf{x}_0) + \left\langle L_\xi(t)\rho(\mathbf{x}, \mathbf{y}, t)\right\rangle_\xi , \tag{73}$$

where we indicate that we are averaging over the bath variables by using the ξ subscript.

Evaluating the average of the product of the stochastic Liouville operator and the phase–space density is not a simple task; the references to the literature can be found elsewhere, see, for example, Lindenberg and West (1990) and are not reproduced here. We merely note that averaging over the $\boldsymbol{\xi}$ fluctuations leads to the simplified form

$$\frac{\partial W(\mathbf{x}, t \mid \mathbf{x}_0)}{\partial t} = L_N W(\mathbf{x}, t \mid \mathbf{x}_0) + \Delta L W(\mathbf{x}, t \mid \mathbf{x}_0) \tag{74}$$

where ΔL is an operator, usually in the form of an infinite series. If the ξ-fluctuations have Gaussian statistics, with mean-square cross-correlation strength given by the elements of the matrix $\mathbf{D}$, the operator series truncates at second-order and if the fluctuations are delta correlated in time reduces to

$$\Delta L = \sum_{i,j} D_{ij} \frac{\partial^2}{\partial p_i \partial p_j}, \tag{75}$$

so that (74) becomes the familiar multi-dimensional Fokker–Planck equation (FPE). In a homogeneous one-dimensional network we can write (74) as the two-variable FPE

$$\frac{\partial}{\partial t} W(q, p, t \mid q_0, p_0) = \left[-\frac{\partial}{\partial q} p + \frac{\partial}{\partial p}\left\{ V'(q) + \lambda p \right\} + D\frac{\partial^2}{\partial p^2} \right] W(q, p, t \mid q_0, p_0) . \tag{76}$$

The FPE describes the phase–space evolution of a complex network having two properties; nonlinear dynamics and an additive random force. The steady-state solution to the FPE is given by

$$W_s(q, p) = Z^{-1} \mathrm{e}^{-\beta H_N} \tag{77}$$

where we have used $V'(q) = \frac{\partial H_N}{\partial q}$ and $p = \frac{\partial H_N}{\partial p}$, the Einstein FDT

$$\beta = \frac{\lambda}{D} = \frac{1}{k_B \Theta}, \tag{78}$$

Z is the partition function and the network thermalizes to the canonical distribution with the temperature of the bath as it should.

3.1.1. Two-state distribution function

In this subsection we derive a single equation of motion for the phase–space distribution function, based on the Liouville equation of all the variables, both the diffusing variable and those responsible for the fluctuations generating the diffusion process under study. The particular method used here was developed by Allegrini et al. (1996) and is compatible with the Liouville approach, that is, imagining that the fluctuations are produced by a set of bath variables compatible with traditional statistical mechanics. We consider the simplest stochastic differential equation,

$$\frac{\mathrm{d}Q(t)}{\mathrm{d}t} = \xi_K(t) \tag{79}$$

and interpret $\xi_K(t)$ to be a two-state random process taking the values ± 1. The two-state random variable may model the right or left stepping of a random walker, the random switching between the two energy states of a dipole, the flashing light of a BQD or a firefly, or any of a number of other interesting processes. We shall have more to say about the physical and biological applications of this mathematical model subsequently.

Note that the stochastic variable $\xi_K(t)$ is not a Gaussian random process and so we introduce a projection operator formalism to study the properties of the solution to (79). The operator fluctuations have the property

$$\xi_K|0\rangle = \sum_{\mu\neq 0} k_m|\mu\rangle, \qquad \xi_K|\mu\rangle = |0\rangle \tag{80}$$

from which we shall see that it is a dichotomous variable. One that could be generated by a Hamiltonian formalism.

We adopt the Liouville formalism and write the time evolution of the total probability density $\rho(q, \xi_K, t)$ as follows

$$\frac{\partial}{\partial t}\rho(q, \xi_K, t) = L_T \rho(q, \xi_K, t) \equiv \left\{ -\xi_K \frac{\partial}{\partial q} + L_B \right\} \rho(q, \xi_K, t). \tag{81}$$

The operator L_B is responsible for the time evolution of the probability density of ξ_K, namely, it is a bath operator. Following the stochastic Liouville approach of Kubo (1969a,b) and Grigolini (1979), let us consider the density $\rho(q, \xi_K, t)$ as a state

vector and expand it in the basis set of the eigenstates of the bath operator L_B. In the stationary case the bath operator must have the eigenstate $|0\rangle$ with vanishing eigenvalue,

$$L_B|0\rangle = 0. \tag{82}$$

From within this quantum-like formalism, we have to take into account the out-of-equilibrium properties of the bath, namely the non-equilibrium eigenstates $|\mu\rangle$, with $\mu \neq 0$, defined by the eigenvalue equation

$$L_B|\mu\rangle = \mathrm{i}\omega_\mu|\mu\rangle. \tag{83}$$

With no loss of generality, we assume a symmetry of the eigenvalue and its labeling index

$$\omega_{-\mu} = -\omega_\mu. \tag{84}$$

Moreover, the components of the probability density obtained by projection onto the eigenstates are

$$P_0(q,t) \equiv \langle 0|\rho(q,\xi_K,t)\rangle. \tag{85}$$

and

$$P_\mu(q,t) \equiv \langle \mu|\rho(q,\xi_K,t)\rangle. \tag{86}$$

creating reduced densities corresponding to the bath at equilibrium (85) and to the out-of-equilibrium bath (86). By projecting (81) onto the bath equilibrium state and the bath excited states, we obtain

$$\frac{\partial}{\partial t}P_0(q,t) = -\sum_\mu \langle 0|\xi_K|\mu\rangle \frac{\partial}{\partial q}P_\mu(q,t) \tag{87}$$

and

$$\frac{\partial}{\partial t}P_\mu(q,t) = \mathrm{i}\omega_\mu P_\mu(q,t) - \langle 0|\xi_K|\mu\rangle \frac{\partial}{\partial q}P_0(q,t), \tag{88}$$

with μ running from $-\infty$ to ∞. The formal solution to (88) is given by the integral

$$P_\mu(q,t) = -\int_0^t \mathrm{d}t' \exp\left(\mathrm{i}\omega_\mu(t-t')\right) \langle \mu|\xi_K|0\rangle \frac{\partial}{\partial q}P_0(q,t'). \tag{89}$$

Inserting (89) into (87) yields the general diffusion equation (GDE)

$$\frac{\partial}{\partial t}P(q,t) = \int_0^t \mathrm{d}t' \Phi_K(t-t')\frac{\partial^2}{\partial q^2}P(q,t'), \tag{90}$$

which was derived many years ago by Kenkre and Knox (1974), who pointed out that it is exactly equivalent to the GDE generated by the adoption of the CTRW method. In (90) the memory kernel is given by

$$\Phi_K(t) \equiv \sum_\mu \mathrm{e}^{\mathrm{i}\omega_\mu t}\langle 0|\xi_K|\mu\rangle\langle \mu|\xi_K|0\rangle, \tag{91}$$

and for notational purposes we replace $P_0(q,t)$ with $P(q,t)$. Note that within the quantum-like Kubo-formalism the stochastic variable ξ_K becomes an operator. By moving from the discrete-frequency to the continuous-frequency picture, and using the symmetry (84) as well, we rewrite the memory kernel (91) in the following form

$$\Phi_K(t) = \int \mathrm{d}\omega \cos(\omega t)\Pi(\omega), \tag{92}$$

where the power spectral density for the fluctuations is given by

$$\Pi(\omega) = 2\langle 0|\xi_K|\omega\rangle\langle \omega|\xi_K|0\rangle. \tag{93}$$

Note that in this case the memory kernel $\Phi_K(t)$ is the equilibrium autocorrelation function of the stochastic variable ξ_K. According to Bologna et al. (2002) the GDE (90) is the exact equation of motion for the density $P(q,t)$ if the fourth-order correlation functions of ξ_K fulfills the factorization condition

$$\langle \xi_K(t_4)\xi_K(t_3)\xi_K(t_2)\xi_K(t_1)\rangle = \langle \xi_K(t_4)\xi_K(t_3)\rangle\langle \xi_K(t_2)\xi_K(t_1)\rangle \tag{94}$$

and the higher-order correlation functions have the analogous factorization conditions, so that at equilibrium the condition $\langle \xi^{2n}\rangle = \langle \xi^2\rangle^n$ applies. This factorization seems to be the natural property for a dichotomous variable and is referred to as dichotomous factorization (DF). It is important to point out that in the renewal and non-exponential case this condition is violated even if the stochastic variable has only two values, see, for instance, Allegrini et al. (2004). Cakir et al. (2007) show that networks with trajectory memory satisfy the DF property.

It is worth making a final remark concerning the form of $\Phi_K(t)$. We have in mind the model of the non-Ohmic bath discussed by Weiss (1999), Pottier (2003) and Cohen (1997). We select the power spectral density $\Pi(\omega) \propto \omega^{\eta-1}$, and determine, using a Tauberian theorem, that in the time asymptotic limit the autocorrelation function becomes

$$\Phi_K(t) \propto \frac{1}{t^\eta} \quad \text{for } 0 < \eta < 1 \tag{95}$$

and

$$\Phi_K(t) \propto -\frac{1}{t^\eta} \quad \text{for } 1 < \eta < 2. \tag{96}$$

The former state, called sub-Ohmic, is separated from the latter, called super-Ohmic, by the singular condition $\eta = 1$, corresponding to the rapid relaxation given by a Dirac delta function.

We distinguish between the inverse power laws for the two regimes $0 < \eta < 1$ and $1 < \eta < 2$. The super-ohmic case, (96), produces a result that is compatible with the CTRW. In fact, in this case (90) coincides with the GDE constructed by Metzler and Klafter (2000a). However, this formal equivalence does not correspond to a physical equivalence, insofar as in the CTRW case the memory kernel is not an equilibrium autocorrelation function, and depends on the time of preparation. As pointed out by Allegrini et al. (2005), this specific form corresponds to preparing the generating diffusion fluctuation when observation begins at time $t = 0$ corresponding to the occurrence of an event. They also show that if observation begins at a later time, the memory kernel attains a different form.

The case of (95), in contrast, was originally introduced to derive the Lévy walk from a Liouville approach (see Section 3.2.1). It did not produce the desired result and yielded a different scaling ($\delta = (4-\mu)/2$ rather than $\delta = 1/(\mu-1)$ (see Bologna et al. (2002)) as a consequence of the factorization condition of (94), which is incompatible with the existence of trajectories with renewal events as shown by Allegrini et al. (2004).

3.2. Generalized master equation (GME)

The *master equation* describes the temporal behavior of singlet probabilities, all multivariate one-time probabilities for *all* stochastic processes and the conditional probabilities for Markov processes (see Oppenheim et al. (1977)). The master equation was first written under that name as a differential-difference equation to describe a gain–loss process by Nordseick et al. (1940). If $P(s,t)$ is the probability that a particle is in the network state s at time t and $\varepsilon p(s,s')$ is the probability per unit time of making a transition from state s' to s, the master equation can be written

$$\frac{\mathrm{d}P(s,t)}{\mathrm{d}t} = \varepsilon \sum_{s'} \left[p(s,s')P(s',t) - p(s',s)P(s,t) \right]. \tag{97}$$

The form of the equation shows that transitions from states s' to s provide a gain to the probability, transitions out of s into s' provide a loss, and ε is the constant rate of transition from one state to another. The transition probabilities are normalized such that

$$\sum_{s'} p(s,s') = 1, \tag{98}$$

so that the master equation can also be expressed as

$$\frac{\mathrm{d}P(s,t)}{\mathrm{d}t} = -\varepsilon P(s,t) + \varepsilon \sum_{s'} p(s,s')P(s',t). \tag{99}$$

Oppenheim et al. (1977) have reviewed the properties of the master equation and have edited the reprinting of many of the basic papers in the field.

The master equation assumes that the states of the network have no structure and was consequently generalized to include state-dependent transition rates. The formal structure of the GME is (see Montroll and West (1979))

$$\frac{\mathrm{d}P(s,t)}{\mathrm{d}t} = \int_0^t \mathrm{d}\tau \sum_j \left[K_{sj}(t-\tau)P(j,\tau) - K_{js}(t-\tau)P(s,\tau) \right]. \tag{100}$$

The techniques for obtaining the GME are varied and complicated so we will not pursue them here. However we show that for certain kinds of stochastic processes described by (100) are also described by CTRWs. In particular by choosing the factorized kernel

$$K_{sj}(t) = p(s,j)\phi(t) \tag{101}$$

where the transition rate ε is replaced with a normalized function of time $\phi(t)$. Inserting (101) into (100) yields

$$\frac{\mathrm{d}P(s,t)}{\mathrm{d}t} = \int_0^t \phi(t-\tau) \left[-P(s,\tau) + \sum_j p(s,j)P(j,t-\tau) \right] \mathrm{d}\tau \tag{102}$$

where we have used the normalization condition (98).

The discrete form of the GME can be extended to the continuous version

$$\frac{\partial P(q,t)}{\partial t} = \int_0^t \mathrm{d}t' \int_{-\infty}^{\infty} \mathrm{d}q' K(q-q', t-t') P(q', t') \tag{103}$$

where the space–time memory kernel separates into two pieces

$$K(q,t) = \kappa(q,t) - \delta(q) \int_{-\infty}^{\infty} \mathrm{d}q' \kappa\left(q', t\right) \tag{104}$$

and $\kappa(q,t)$ denotes the probability for a particle to jump a distance q at time t.

Here we limit the discussion to stressing that the asymptotic regime of $P(q,t)$ as given by the GME can be studied without explicitly making the Markov approximation. In fact, noticing the property that (103) is convoluted in both the space and time variables we can solve it using the combined Fourier–Laplace transform $P(q,t) \to P^*(k,u)$ to obtain

$$P^*(k,u) = \frac{1}{u - K^*(k,u)} \tag{105}$$

where now all the information concerning the underlying process is contained in the Fourier–Laplace transform of the space–time memory kernel.

3.2.1. Lévy process

We point out here that the non-Markov nature of the GME is consistent with the notion of Lévy walks devised by Shlesinger et al. (1987). These walks were introduced in the context of turbulence where it was recognized that the relative velocity between elements of fluid separated by a given distance depends on that distance. Therefore a random walk model of such a process requires the physical assumption that steps to nearby points require different times than steps to more distant points. Usually nearby points require less time to traverse, but in the case of turbulence the relative velocity of fluid particles increases with spatial separation and so more distant points require less time to traverse.

A Lévy process is the exact solution to the chain condition for the probability density and is essential for a Markov process, see for instance, Montroll and West (1979). We show that it is possible to construct a Lévy process from the above GME even though the latter is explicitly non-Markov. We note that it is possible to make these two seemingly contradictory processes compatible if we make the non-Markov properties stemming from the inverse power-law behavior of the velocity autocorrelation function become transition probabilities with an inverse power-law dependence on the length of the jump in space (see Shlesinger et al. (1987)). Consequently, we change the time nonlocality into a space nonlocality, and show that the latter is the space nonlocality of the Lévy process expressed by a fractional diffusion equation as studied by West and Seshadri (1982). This space nonlocality cannot be eliminated by observing suitably large distances because of the inverse power-law structure of the corresponding space transition.

The connection between nonlocality in space and nonlocality in time is established by observing that, throughout the entire period of time spent by the particle within one of its two velocity states, the particle makes a jump of length $|q| = Wt$. This allows us to interpret the probability of making a jump from one site to another a distance $|q|$ from the initial site as being proportional to the waiting time distribution, obtained by integrating the transition probability over all time

$$\int_0^{\infty} \kappa(q,t)\mathrm{d}t \propto \frac{1}{(T+|q|)^{\mu}}. \tag{106}$$

Consequently, a transition of length $|q|$ takes place in time $t = |q|/W$, where the walker steps either to the right or left at the constant velocity W and the memory kernel has the factored form

$$\kappa(q,t) = \psi(t)\delta\left(|q| - Wt\right). \tag{107}$$

Trefan et al. (1994) studied the asymptotic regime of (105) incorporating the factored memory kernel (107) and yielding the following explicit form for the doubly transformed kernel:

$$K^*(k,u) = \psi^*(k,u) - \hat{\psi}(u). \tag{108}$$

To derive the Lévy distribution only one basic step remains and that is to properly incorporate the Markov condition into (108). In the asymptotic space–time limit $u \to 0$ and $k \to 0$ we obtain

$$P^*(k,u) = \frac{1}{u + b\,|k|^{\alpha}}; \tag{109}$$

$$b = \frac{(WT)^{\alpha}}{T} \alpha \Gamma(1-\alpha) \cos\left[\alpha \frac{\pi}{2}\right]; \qquad \alpha = \mu - 1. \tag{110}$$

The inverse Laplace transform of (109) yields the partial differential equation of motion for the characteristic function

$$\frac{\partial \tilde{P}(k,t)}{\partial t} = -b\,|k|^{\alpha}\,\tilde{P}(k,t). \tag{111}$$

The solution to (111) is simply

$$\tilde{P}(k,t) = \mathrm{e}^{-b|k|^{\alpha}t} \tag{112}$$

which is the characteristic function for the symmetric Lévy distribution. Note that the characteristic function is the Fourier transform of the probability density $P(q,t) \to \tilde{P}(k,t)$.

It must be remarked that the theory developed in this subsection is tailored to the region $2 < \mu < 3$. The region with $\mu < 2$ ($\alpha < 1$) is excluded by the fact that for $\mu < 2$ the first moment of the waiting time distribution diverges, thereby preventing us from defining a time scale for the process. Furthermore, even if the average sojourn time $\langle t \rangle$ were arbitrarily given a finite value, and α were still identified with $\mu - 1$, in the asymptotic limit of vanishing k and vanishing u the resulting value of b would vanish. The region $\mu > 3$ is excluded by the fact that the Markov approximation leads to the structure (109) with $\alpha > 2$, in which case the inverse transform is not positive definite and therefore cannot be interpreted as a probability density.

There is one difficulty with the solution given above and that is an apparent inconsistency in the scaling. The second moment as shown by Trefan et al. (1994) is known to scale as

$$\left\langle q(t)^2 \right\rangle \propto t^{4-\mu} \tag{113}$$

implying that the Hurst exponent is given by

$$H = 2 - \mu/2. \tag{114}$$

On the other hand, the Lévy distribution has a scaling suggesting that the Hurst exponent ought to be given by

$$H = \frac{1}{\alpha} = \frac{1}{\mu - 1} \tag{115}$$

which is different from (114). This difference in scaling is significant and warrants additional discussion. As pointed out by Allegrini et al. (1996), as well as in the earlier work of Klafter and Zumofen (1994) and Zumofen and Klafter (1994), the diffusion process described by (105) consists of a central part and a propagation front signalled by two sharp peaks. At time t a particle leaving the origin $q = 0$ at time $t = 0$ cannot be found at a distance from the origin larger than Wt. The restriction on the random walker's maximum velocity has the effect of producing an accumulation of particles at the front of the diffusion process, namely at $q = \pm Wt$. This is the origin of the two ballistic peaks of the propagation front. At earlier times the initial distribution, concentrated at $q = 0$, splits into these two ballistic peaks and the region between the two peaks is empty. Due to the effect of sporadic randomness, some trajectories leave the propagation front and the population of the central part steadily increases in time, while the peak intensity, proportional to the autocorrelation function Φ_{ξ} slowly decreases. Note that this means that the diffusion process cannot be described by a single rescaling. The peaks of the propagation front rescale with $H = 1$, a fact implying a diffusion faster than that predicted by the rescaling of (114). The rescaling of the central part is properly expressed by (115). The calculations leading to (111) refer to a physical condition where the intensity of the ballistic peaks is negligible, so that the rescaling (115) only reflects the diffusion properties of the central part of the distribution. On the contrary, the rescaling (114) is a sort of balance between the fast rescaling of the propagation front and the rescaling of the central part of the distribution, which is in fact slower than the rescaling in (115). These two rescalings reflect a conflict between the dynamic properties still present within the Lévy walk perspective and a merely probabilistic treatment.

Bologna et al. (1999) made the observation concerning the derivation of a Lévy process from the GME that the memory in the GME must be erased during the network's evolution so that asymptotically the Markov Lévy distribution is realized. Thus, in spite of the non-Markov structure of the GME, we show in the next section that an asymptotic regime appears whose statistics are determined by this process of memory erasure.

3.2.2. Fractional Lévy motion (fLm)

The properties of scaling media are often described by fractal functions and their space–time evolution. However, such functions contain hierarchies of singularities and are typically non-differentiable as shown by Mandelbrot (1977) and Meakin (1998). Thus, the understanding of such phenomena as fractional wave propagation and fractional diffusion comes about through the development and implementation of alternate modeling strategies that do not explicitly include the usual differential equations of motion. In recent years there have been a number of attempts to model the phase space evolution of the probability density for anomalous transport processes, all leading to evolution equations with fractional derivatives, see, for example, West et al. (2003) and Hennig (2002).

The first successful generalization to an anomalous diffusive process started from a Langevin equation describing a dissipative dynamical process, $Q(t)$, driven by fluctuations $\xi_{\alpha}(t)$

$$\frac{\mathrm{d}Q(t)}{\mathrm{d}t} + \lambda Q(t) = \xi_{\alpha}(t) \tag{116}$$

where the stochastic driver is a delta correlated α-stable Lévy process. The probability density for this process, $P_\alpha(q,t)$, is then described by an equation of evolution that is first order in time, but whose phase–space derivative is fractional:

$$R^\alpha\left[P_\alpha(q,t)\right]=\frac{b}{\pi}\Gamma\left(\alpha+1\right)\sin\left[\pi\alpha/2\right]\int_{-\infty}^{\infty}\frac{P_\alpha\left(q',t\right)}{|q-q'|^{\alpha+1}}\mathrm{d}q' \tag{117}$$

where $R^\alpha[\cdot]$ is a Reisz fractional derivative with $0<\alpha\leq 2$ (see Samko et al. (1993)). The solution resulting in the fractional transport equation constructed by West and Seshadri (1982) was shown to be given in terms of the centro-symmetric Lévy characteristic function

$$P_\alpha(q,t)=\int_{-\infty}^{\infty}\mathrm{e}^{\mathrm{i}qk}\exp\left[-\sigma_\alpha(t)\,|k|^\alpha\right]\frac{\mathrm{d}k}{2\pi} \tag{118}$$

where

$$\sigma_\alpha(t)=\frac{1}{\alpha\lambda}\left(1-\mathrm{e}^{-\alpha\lambda t}\right). \tag{119}$$

The characteristic function given in the integral (118) can be defined in terms of the average of the solution to the Langevin equation over the Lévy fluctuations

$$\tilde{P}_\alpha(k,t)\equiv\left\langle\mathrm{e}^{\mathrm{i}kQ(t)}\right\rangle_\alpha \tag{120}$$

which immediately yields (118). A generalization of this early work to disordered systems with external force fields has recently been given by Vlad et al. (2000). It was shown by Grigolini et al. (1999) that such a fractional transport equation could also be obtained using the inverse power-law transition probabilities in the GME. A similar approach was simultaneously considered by Metzler et al. (1999a).

A second process of interest is one in which the inhomogeneities are in time, in which case the physical observable is described by an equation of evolution that is second-order in the phase–space variable, but whose time derivative is fractional:

$$D_t^\beta\left[u(q,t)\right]=\frac{1}{\Gamma\left(n-\beta\right)}\frac{\mathrm{d}^n}{\mathrm{d}t^n}\int_0^t\frac{u\left(q,t'\right)}{|t-t'|^{1+\beta-n}}\mathrm{d}t' \tag{121}$$

where D_t^β is the Riemann–Liouville fractional derivative (see Samko et al. (1993)); where n is the smallest integer such that $\beta-n<0$ and $\beta-n+1>0$. The evolution equation with this fractional time derivative, for $0<\beta\leq 1$, was obtained using a CTRW formalism by Compte (1996) and independently using a stochastic two-state process with memory by West et al. (1997) and Allegrini et al. (1996). In this parameter domain the equation describes fractional transport. In the parameter domain $1<\beta\leq 2$ the fractional equation describes the propagation of waves in fractal media.

We include both the long-time memory effects manifest in the fractional time derivative (121) and the long-range spatial effects manifest in the fractional phase–space derivative (117) in the same fractional evolution equation. Thus, the equation of fractional evolution is given by

$$D_t^\beta\left[u(q,t)\right]-u_0(q)\frac{t^{-\beta}}{\Gamma\left(1-\beta\right)}=R^\alpha\left[u\left(q,t\right)\right] \tag{122}$$

where the initial function is given by $u_0(q)=u\left(q,t=0\right)$ and for a point source is taken as a delta function in space. The formulation of fractional equations with fractional time derivatives correspond to initial value problems where the initial values are given by certain fractional derivatives. Furthermore, (122) not only describes a more general kind of fractional diffusion, when $(0<\beta\leq 1,\,0<\alpha\leq 2)$, but also describes wave propagation in a non-dissipative fractal medium when $(1<\beta\leq 2,\;0<\alpha\leq 2)$. In addition, when $\alpha=0$ there are no spatial effects in the dynamics, and the resulting equation has been used to describe shear relaxation in viscoelastic materials, see, for example, Glöckle and Nonnenmacher (1991).

Of course (122) would be of little value if it could not be solved to reveal the physical nature of the complex phenomena being modeled. Metzler et al. (1999a,b,c) showed how to use the eigenfunction expansion technique to solve the fractional transport equation in the case $\alpha=2$ for a variety of boundary values. Glöckle and Nonnenmacher (1991) introduced another method of solution which involves taking the Laplace–Mellin transform of (122) and in the inversion process writing $u(q,t)$ in terms of Fox's H-functions. In this way the normalized solution to the fractional evolution equation can be expressed in terms of the Fourier transform of the solution

$$\tilde{P}_{\beta,\alpha}(k,t)=\sum_{n=0}^{\infty}\frac{(-1)^n}{\Gamma\left(1+\beta n\right)}\left(bt\,|k|^{\alpha/\beta}\right)^{n\beta}=E_\beta\left(-\left(bt\right)^\beta|k|^\alpha\right) \tag{123}$$

which is the MLF (see West et al. (2003) and Glöckle and Nonnenmacher (1991)). Note that (123) is the characteristic function for this transport-propagation process. The inverse Fourier transform of (123) is the solution to the fractional evolution equation

$$P\left(q,t;\alpha,\beta\right)=\int_{-\infty}^{\infty}E_\beta\left(-\left(bt\right)^\beta|k|^\alpha\right)\mathrm{e}^{\mathrm{i}kq}\frac{\mathrm{d}k}{2\pi}. \tag{124}$$

Thus, we are able to encapsulate in a single dynamical equation all the transport-propagation properties contained within a given complex phenomenon and describe its behavior with a single function.

For example, the Lévy statistics observed in heart beat dynamics by Peng et al. (1993) and reviewed and extended to a broad range of other physiological phenomena by West and Deering (1994) can be obtained from (123) using $\beta = 1$. Notice that in this limit the MLF sums to an exponential, so that (123) becomes

$$\tilde{P}_{1,\alpha}(k,t) = \exp\left[-bt\,|k|^{\alpha}\right], \tag{125}$$

which is the characteristic function for the centro-symmetric Lévy stable distribution. Thus, using (123) we see that the statistics of processes with $\beta = 1$ are Lévy stable.

Another application of (123) is given for small values of the argument of the MLF. At early times the MLF gives rise to the stretched exponential

$$\tilde{P}_{\beta,\alpha}(k,t) \approx \mathrm{e}^{-(bt)^{\beta}|k|^{\alpha}}. \tag{126}$$

If $\alpha = 2$, the inverse Fourier transform of (126) is a Gaussian distribution with a variance that increases as a power law in time, that is t^{β}, with $\beta = 2\mu$, corresponding to fractional Brownian motion for $\beta \neq 1$. Finally, the solution (126) with $\alpha \neq 2$ corresponds to a new kind of statistical process, one having Lévy statistics, but with a power-law time dependence. West and Nonnenmacher (2001) called this processes *fractional Lévy motion* (*fLm*) as a generalization of *fractional Brownian motion* (*fBm*) and Laskin et al. (2002) used a more formal argument to arrive at an exact expression of the form (126) and gave it the same name.

The motivation for combining transport and propagation into a single equation is related to the fact that the diffusion equation is unphysical in that perturbations propagate with infinite speed to all regions of space. We know however that heat consists of the propagation of phonons, and heat transport results from incoherent scatterings of phonons within a material. As the temperature of the material is lowered there are fewer and fewer scatterings so the transport of heat becomes less diffusive and more wave-like. Maxwell noted the unphysical nature of the heat equation and included a ballistic term in the kinetic theory of gases to incorporate into the description the finite propagation speed of heat. This term resulted in the heat transport equation being replaced with the telegrapher's equation (see Montroll and West (1979)). The solution to the telegrapher's equation is wave-like at early times and diffusive at late times, including as it does the finite propagation speed of heat, that is the speed of sound in the material. Thus, the transport equation is only valid asymptotically in time. An alternative argument for the telegrapher's equation can be made starting from the wave equation and considering the influence of absorption. This phenomenon is a manifestation of the resistive loses in the medium supporting the wave motion due to the inelastic scattering of waves. Like the telegrapher's equation, the fractional evolution equation, is physically realizable whereas the diffusion equation is not.

Because of the self-similar character of fractal media, the wavelength of waves propagating in such media always take on some of the hierarchial structure of the medium. Berry (1979) dubbed such waves "diffractals", a new wave regime characterized by a short-wave limit in which ever finer levels of structure are explored by the propagating waves and geometrical optics is never applicable. The physical arguments of Berry regarding the influence of fractal media on scalar waves were replaced with more formal arguments by Schneider and Wyss (1989). The latter investigators interpreted (122), in the limit $\alpha \to 2$, as a fractional diffusion equation when $0 < \beta \leq 1$ and as a fractional wave equation when $1 < \beta \leq 2$. In the limit $\alpha \to 2$ the general solution to the fractional evolution equation, the Fourier transform of (123), agrees with the Schneider–Wyss solution, their (2.33) with the initial value function indexed with $k = 0$. This is an exact solution to the propagation of a scalar wave through a fractal medium and is therefore an exact diffractal in Berry's sense.

Note that the multiple scattering of regular waves, traditionally used in describing the propagation of waves in heterogeneous media, is here replaced with a fractional time derivative. This fractional time derivative, in the wave context, models the time delay associated with multiple scattering events. In addition the value of β is a direct measure of the degree of coherence in such scattering events. Scalar waves in homogeneous media have a value $\beta = 2$ and are completely coherent. Acoustic and light waves in turbulent fluid flow, on the other hand, have a smaller value of β, becoming less and less coherent as the level of turbulence increases and the value of β becomes smaller. This is evidenced by the fact that the physical observable, the intensity of sound and light, is described by a transport equation rather than a wave equation as shown by West (1999).

In summary, we can say that complex physical processes, Newtonian mechanics notwithstanding, are non-Markovian in that they contain memory, and the above fractional time derivative incorporates that memory into the description of the evolution of the process. In a similar way the fractional spatial derivative incorporates the long-range spatial interactions into the evolution of the process. Thus, the fractional evolution equation is non-local in both space and time.

3.2.3. Network traffic models

Information traffic in communication networks, whether telephone networks, the body's central nervous system or the Internet, requires an understanding of the statistical behavior of the information in order to maximize the transfer of information metrics. The traffic theory devised in the last century to predict delay and blocking to telephone messages, relied on the Markov nature of Poisson statistics and played little role in the design of the Internet. Laskin et al. (2002) argue that this situation regarding traffic theory will change in the future as we extend traffic models to properly take into

account the observed fractal nature of data traffic, see Leland et al. (1994) and Paxson and Floyd (1995). They recognize that the broadband signals carried by such networks are significantly different from their more traditional narrowband cousins, in that the design, control and analysis of such networks are strongly dependent on their non-Markov fractal nature. For example, two models that have been proposed to approximate broadband network traffic are fractional Brownian motion (fBm) and stable Lévy motion. Mikosch et al. (2002) have shown that if the rate at which transmissions are initiated (connection rate) are low relative to heavy-tailed connection length distribution tails, then the cumulative traffic is reasonably well approximated by stable Lévy processes. If, on the other hand, the connection rate is large relative to heavy-tailed connection length distribution tails, then fBm is the better approximation. The key to distinguishing between the two models is whether or not the varying connection rates inhibit, as in the Lévy case, or induce, as the *fBm* case, long-range dependence (memory).

As another example in the queuing analysis of communication networks input processes with infinite variance, such as may arise in self-similar time series, lead to infinite moments in the queuing processes, which translates into extremely long waiting times. Consequently the *fLm* of Laskin et al. (2002) discussed in the previous subsection can be used to model traffic intensities for rates that diverge, see Leland et al. (1994). But this is not the only model to describe the self-similarity of broadband traffic, see Resnick and Rootzén (2000).

We have discussed Brownian motion, *fBm*, Poisson statistics and inverse power-law distributions. Each type of statistic was introduced to describe a well-defined physical process. In Brownian motion the fluctuating velocity variable determines the position of an erratically moving particle in time. On the other hand, in a Poisson process the focus changes from a dynamic variable to the occurrence of events. Thus, we have stochastic variables and stochastic point processes and in the case of network traffic these can be the intensity of information or the occurrence or non-occurrence of messages (see Fowler and Leland (1991)). The results of Feldmann et al. (1998) revealed that message traffic on complex networks do not have the regular statistics of Poisson, but have the kind of self-similar bursting that occurs in fractal time series. In the last decade Willinger and Paxson (1998) applied fractal modeling to broadband network traffic and more specifically to Internet traffic.

Laskin et al. (2002) use the *fLm* to construct a teletraffic model that takes into account both the Hurst exponent H and the Lévy parameter α by means of the Reimann–Liouville integral (121) with $\beta \equiv H + 1 - 1/\alpha$ and H is confined to the interval $1/\alpha < H \leq 1$. It is straightforward to show that the dynamic variable defined by the integral (121) when inserted into the definition of the characteristic function (120) yields the exact expression

$$\tilde{P}_{H,\alpha}(k,t) = \mathrm{e}^{-\sigma|k|^{\alpha}t^{\alpha H}}, \tag{127}$$

which has the same functional form as the approximate expression (126) and

$$\sigma = \frac{b}{\Gamma^{\alpha}(H+1-1/\alpha)\,\alpha H}. \tag{128}$$

This teletrafficking model is an extension of the application of *fBm* to the same problem and as Laskin et al. (2002) emphasize, it is suitable for traffic modeling in modern broadband networks. They point out that empirical data collected for a variety of communication networks exhibit self-similarity and heavy-tailed distributions, so it is reasonable to apply the *fLm* traffic model to capture these characteristics. Moreover, their preliminary results support these arguments indicating that *fLm* can describe the behavior of today's teletraffic, if not tomorrow's.

It is also important to note that the discussion of the self-similarity in the statistics literature on network traffic takes a different form than the one adopted herein. Resnick and Rootzén (2000) point out that the focus in the literature has been on heavy-tailed transmission times of sources sending data to one or more servers, assuming a cumulative distribution of transmission times $F(\tau)$ with a Pareto tail

$$1 - F(\tau) \sim \tau^{-\beta}L(\tau), \quad \tau \to \infty$$

where $L(\tau)$ is a slowly varying function. Unlike previous investigators these authors were concerned with the case $0 < \beta < 1$ in which the models are statistically unstable and the amount of ongoing traffic increases without limit. Although such models are unrealistic over asymptotically long times they do provide useful descriptions of the uncontrolled network behavior associated with high traffic that might be expected over restricted time intervals.

3.3. Continuous time random walks (CTRW)

The most useful generalization of the random walk model was made by Montroll and Weiss in 1965, where they include random intervals between successive steps in the walking process to account for local structure in the environment, such that the time interval between successive steps $\tau_n = t_{n+1} - t_n$ is a random variable. This generalization is referred to as the CTRW model since the walker is allowed to step at a continuum of times and the time between successive steps is considered to be a second random variable; the step being the first random variable. The CTRW has been used to model a number of complicated statistical phenomena, from the microscopic structure of individual lattice sites for heterogeneous media, to the stickiness of stability islands in chaotic dynamical networks.

The CTRW explicitly assumes that the sequence of time differences $\{\tau_n\}$ constitute a set of independent identically distributed random variables. The probability that the random variable τ lies in an interval $\{t, t + \mathrm{d}t\}$ is given by $\psi(t)\mathrm{d}t$,

where we again use the waiting time distribution function. The name reflects the fact that the walker waits for a given time at a lattice site before stepping to the next site. The length of the sojourn is characteristic of the structure of the medium as we discuss subsequently.

The waiting time distribution is also used to define the probability that a step has not been taken in the time interval $(0, t)$. Thus, if the function $W(\mathbf{s}, t)$ is defined as the probability that a walker is at the lattice site $\mathbf{s}$ at a time t immediately after a step has been taken, and $P(\mathbf{s}, t)$ is the probability of a walker being at $\mathbf{s}$ at time t, then

$$P(\mathbf{s}, t) = \delta_{\mathbf{s},\mathbf{0}}\Psi_0(t) + \int_0^t \Psi(t - t')W(\mathbf{s}, t')\mathrm{d}t' \tag{129}$$

that is, if a walker arrives at $\mathbf{s}$ at time t' and remains there for a time $(t - t')$, or the walker has not moved from the origin of the lattice, $P(\mathbf{s}, t)$ is the average over all arrival times with $0 < t' < t$. Note that the waiting time at the origin might be different so that $\Psi_0(t)$ can be determined from the transition probabilities. It should be pointed out that the function $P(\mathbf{s}, t)$ is a probability when $\mathbf{s}$ is a lattice site and a probability density when $\mathbf{s}$ is a point in the spatial continuum.

The probability function $W(\mathbf{s}, t)$ itself satisfies the recurrence relation

$$W(\mathbf{s}, t) = p_0(\mathbf{s}, t) + \sum_{\mathbf{s}'} \int_0^t p\left(\mathbf{s} - \mathbf{s}', t - t'\right) W(\mathbf{s}', t')\mathrm{d}t' \tag{130}$$

where $p\,(\mathbf{s}, t)\,\mathrm{d}t$ is the probability that the time between two successive steps is in the interval $(t, t + \mathrm{d}t)$, and the transition extends across $\mathbf{s}$ lattice points. The transition probability satisfies the normalization condition

$$\sum_{\mathbf{s}} p\,(\mathbf{s}, t) = \psi(t) \tag{131}$$

and the integral over time yields the overall normalization

$$\int_0^\infty \sum_{\mathbf{s}} p\,(\mathbf{s}, t)\,\mathrm{d}t = \int_0^\infty \psi(t)\mathrm{d}t = 1. \tag{132}$$

Montroll and Weiss made the specific assumption that the length of a pause and the size of a step are mutually independent, an assumption we previously relaxed in our discussion. However, using their assumption of space–time independence the time-dependent transition probability can be written

$$p\,(\mathbf{s}, t) = p\,(\mathbf{s})\,\psi(t) \tag{133}$$

in which case the random walk is said to be factorable. The Fourier–Laplace transform of the transition probability in this factorable case yields

$$p^*\,(\mathbf{k}, u) \equiv \sum_{\mathbf{s}} \mathrm{e}^{\mathrm{i}\mathbf{k}\cdot\mathbf{s}} \int_0^\infty \mathrm{e}^{-ut} p\,(\mathbf{s}, t)\,\mathrm{d}t = \tilde{p}\,(\mathbf{k})\,\hat{\psi}(u) \tag{134}$$

where $\tilde{p}\,(\mathbf{k})$ is the Fourier transform of the transition probability introduced earlier with the same notation used for both the discrete and continuous cases. Consequently, from the double convolution form of (130) we obtain

$$W^*\,(\mathbf{k}, u) = \frac{p_0^*\,(\mathbf{k}, u)}{1 - p^*\,(\mathbf{k}, u)} \tag{135}$$

and for the double transform of the probability from (129) we have using (135)

$$P^*\,(\mathbf{k}, u) = \hat{\Psi}_0\,(u) + \frac{\hat{\psi}(u)p_0^*\,(\mathbf{k}, u)}{1 - p^*\,(\mathbf{k}, u)}. \tag{136}$$

In the case where the transition from the origin does not play a special role $p_0^*\,(\mathbf{k}, \mathbf{u}) = p^*(\mathbf{k}, \mathbf{u})$, $\hat{\Psi}_0(u) = \hat{\Psi}(u)$ and (136) simplifies to

$$P^*\,(\mathbf{k}, u) = \frac{\hat{\Psi}(u)}{1 - p^*\,(\mathbf{k}, u)} \tag{137}$$

which can be further simplified when the space–time transition probability factors. We shall have need for the Laplace transform of the survival probability $\Psi(t)$ so we evaluate it here to be

$$\hat{\Psi}(u) = \frac{1 - \hat{\psi}(u)}{u} \tag{138}$$

and for a factorable network obtain

$$P^*\,(\mathbf{k}, u) = \frac{1 - \hat{\psi}(u)}{u\left[1 - \tilde{p}\,(\mathbf{k})\,\hat{\psi}(u)\right]}. \tag{139}$$

This is the Montroll–Weiss equation for the standard CTRW.

The further interpretation of (139) is accomplished by restricting the solution to the situation where the walker starts from the origin so that $P(\mathbf{q}, t = 0) = \delta(\mathbf{q})$, and consequently the probability density function is the propagator for the CTRW process. This interpretation is more apparent in the space–time form of the phase–space equation so we introduce the memory kernel in the Laplace transform representation

$$\hat{\phi}(u) = \frac{u\hat{\psi}(u)}{1 - \hat{\psi}(u)} \tag{140}$$

into (139), which after some algebra yields

$$P^*(\mathbf{k}, u) = \frac{1}{u + \hat{\phi}(u)\left[1 - \tilde{p}(\mathbf{k})\right]}. \tag{141}$$

Further algebraic manipulation of (141) yields

$$uP^*(\mathbf{k}, u) - 1 = -\hat{\phi}(u)\left[1 - \tilde{p}(\mathbf{k})\right]P^*(\mathbf{k}, u) \tag{142}$$

whose inverse Fourier–Laplace transform yields the integro-differential equation for the propagator

$$\frac{\partial P(\mathbf{q}, t)}{\partial t} = \int_0^t dt' \phi(t - t')\left\{-P(\mathbf{q}, t') + \int p(\mathbf{q} - \mathbf{q}')P(\mathbf{q}', t')\, d\mathbf{q}\right\}. \tag{143}$$

Eq. (143) is the Montroll–Kenkre–Shlesinger Master Equation (see Kenkre et al. (1973)) and is clearly non-local in both time and space. In time the nonlocality is determined by the memory kernel, which in turn is determined by the waiting time distribution function, that is the inverse Laplace transform of (140). The spatial nonlocality is determined by the transition probability which is the inverse Fourier transform of the structure function. Note that as we promised the master equation (143) is the continuous analogue of the discrete master equation (102).

3.3.1. Fractional diffusion equations (FDE)

There are a number of ways the phase–space equation of motion for the probability density can become a fractional diffusion equation (FDE) using either the GME or CTRW formalisms. Consider the factorable form of the memory kernel in the CTRW whose Fourier–Laplace transform is given in one-spatial dimension by

$$p^*(k, u) = \hat{\psi}(u)\tilde{p}(k) \tag{144}$$

so that the probability density is given by (141). In the case of the fractal time random walk, reviewed by Metzler and Klafter (2000a), the average waiting time diverges but the mean-square step length remains finite. In this case the waiting time distribution is taken to be inverse power law

$$\psi(t) \sim A_\alpha \left(\frac{\tau}{t}\right)^{\alpha+1} \tag{145}$$

where the power-law index is in the interval $0 < \alpha < 1$. The corresponding Laplace transform of this waiting time function is given by

$$\hat{\psi}(u) \sim 1 - (u\tau)^\alpha \tag{146}$$

and the Fourier transform of the structure function is

$$\tilde{p}(k) \sim 1 - \sigma^2 k^2. \tag{147}$$

Consequently, the Fourier–Laplace transform of the probability density becomes

$$P^*(k, u) = \frac{1}{1 + K_\alpha u^{-\alpha} k^2} \tag{148}$$

in the diffusion limit being asymptotic in space and time, that being $u \to 0$ and $k \to 0$. Using the methods of the fractional calculus (see West et al. (2003)) to take the inverse Fourier and Laplace transform of (148) results in a FDE of the form

$$D_t^\alpha[P(q, t)] - \frac{t^{-\alpha}}{\Gamma(1 - \alpha)}P(q, 0) = K_\alpha \frac{\partial^2}{\partial q^2}P(q, t) \tag{149}$$

where $D_t^\alpha[\cdot]$ is the Riemann–Liouville fractional derivative introduced earlier and K_α is the generalized diffusion coefficient. The solutions to such FDEs, in which the process is subdiffusive, that is $\alpha < 1$, are extensively reviewed by Metzler and Klafter (2000a).

However, there are other kinds of FDEs. In fact we constructed one in our discussion of the Lévy distribution in the context of the GME. Consider the equation of motion for the characteristic function given by (111), and the inverse Fourier transform of the magnitude of the Fourier variable k is

$$\int_{-\infty}^{\infty} |k|^{\alpha} \, \mathrm{e}^{\mathrm{i}kq} \frac{\mathrm{d}k}{2\pi} = \frac{(1-\alpha)}{2\Gamma(1-\alpha)\cos[\alpha\pi/2]} \frac{1}{|q|^{\alpha+1}}, \tag{150}$$

so that the inverse Fourier transform of the equation for the characteristic function (111) yields

$$\frac{\partial P(q,t)}{\partial t} = -\frac{\alpha\,(1-\alpha)}{2T}\,(WT)^{\alpha} \int_{-\infty}^{\infty} \frac{P\left(q',t\right)\mathrm{d}q'}{|q-q'|^{\alpha+1}}. \tag{151}$$

This form of the diffusion equation coincides with the West–Seshadri equation (see West and Seshadri (1982) and Allegrini et al. (1996)) which they solved to obtain a centro-symmetric Lévy process. Eq. (151) can also be cast in the form of a fractional diffusion equation by introducing the Reisz fractional derivative operator (117) to obtain

$$\frac{\partial P(q,t)}{\partial t} = (-\mathrm{i})^{\alpha}\, bR^{\alpha}[P(q,t)]. \tag{152}$$

The Fourier transform of (152) yields the equation for the characteristic function given by (111) whose solution with the initial condition $\tilde{P}\,(k,t=0)=1$, necessary for the inverse Fourier transform to be defined as a probability density, is given by (112). This solution indeed corresponds to the definition of the characteristic function for a symmetric Lévy process, as we found earlier.

3.3.2. Connection between FDE and FLE

What is the connection between the FLE and the FDE? To establish this connection we adopt the procedure outlined in Section 3.1 for the derivation of the FPE. Consider the fractional stochastic differential equation (FSDE) given by

$$D_t^{\alpha}\,[Q(t)] = -V'(Q) - \gamma^{\alpha} Q(t) + \xi(t) \tag{153}$$

where V is the deterministic 'potential', γ is the 'dissipation' and $\xi(t)$ is the random 'force'. The dynamics in phase space are followed by the phase–space density

$$\rho\,(q,t \mid q_0) = \delta\,(q - Q\,(q_0;t)) \tag{154}$$

so that an arbitrary analytic function can be written as

$$F(Q) = \int \mathrm{d}q F(q) \rho\,(q,t \mid q_0)\,. \tag{155}$$

The difference in the function at two nearby points in time is given by

$$F\,(Q[t+\Delta t]) - F(Q[t]) = \int \mathrm{d}q F(q)\,[\rho\,(q,t+\Delta t \mid q_0) - \rho\,(q,t \mid q_0)] \tag{156}$$

from which we can construct the limits from the difference on the *lhs*. The first form is given by the fractional time derivative of the function

$$D_t^{\alpha}\,[F] = \lim_{\Delta t \to 0} \frac{F\,(Q[t+\Delta t]) - F\,(Q\,[t])}{\Delta t^{\alpha}} \tag{157}$$

the second form is given by the fractional time derivative of the dynamic variable

$$F' D_t^{\alpha}\,[Q\,] = \lim_{\substack{\Delta t \to 0 \\ \Delta Q \to 0}} \frac{F\,(Q[t+\Delta t]) - F\,(Q\,[t])}{\Delta Q} \frac{\Delta Q}{\Delta t^{\alpha}}. \tag{158}$$

The two expressions for the limits of the function can be expressed in terms of operations on the phase–space density as follows: (157) can be expressed as

$$\begin{aligned} D_t^{\alpha}\,[F] &= \int \mathrm{d}q F(q) \lim_{\Delta t \to 0} \left[\frac{\rho\,(q,t+\Delta t \mid q_0) - \rho\,(q,t \mid q_0)}{\Delta t^{\alpha}} \right] \\ &= \int \mathrm{d}q F(q) D_t^{\alpha}\,[\rho] \end{aligned} \tag{159}$$

and (158) can be expressed as

$$F' D_t^{\alpha}\,[Q\,] = \int \mathrm{d}q F'(q) D_t^{\alpha}\,[q]\,\rho\,(q,t \mid q_0) \tag{160}$$

which integrating by parts and setting the integrands at the limits to zero we have

$$F' D_t^{\alpha} [Q] = -\int dq F(q) \frac{\partial \left[D_t^{\alpha} [q] \rho (q, t \mid q_0) \right]}{\partial q}. \tag{161}$$

Consequently, since the analytic function $F(q)$ is arbitrary we can equate the coefficients within the integrand to obtain

$$D_t^{\alpha} [\rho (q, t \mid q_0)] = -\frac{\partial}{\partial q} \left[D_t^{\alpha} [q] \rho (q, t \mid q_0) \right] \tag{162}$$

and inserting the FLE (153) into (162) yields

$$D_t^{\alpha} [\rho (q, t \mid q_0)] = -\frac{\partial}{\partial q} \left[-\frac{\partial V}{\partial q} - \gamma^{\alpha} q + \xi (t) \right] \rho (q, t \mid q_0) . \tag{163}$$

Averaging over an ensemble of realizations of the fluctuations and using the operators introduced in Section 3.1 we obtain

$$\frac{\partial}{\partial t} W (q, t \mid q_0) = D_t^{1-\alpha} [L_{FP} W (q, t \mid q_0)] \tag{164}$$

which is called the fractional Fokker–Planck equation (FFPE) because the Liouville operator is the one obtained in the FDE

$$L_{FP} = \frac{\partial V}{\partial q} + \gamma^{\alpha} q + D \frac{\partial^2}{\partial q^2}. \tag{165}$$

Note that (164) is the FDE used by Metzler and Klafter (2000a) in their review article and which they obtained by a very different procedure.

4. Complexity and aging

The phenomena of complexity and aging have recently attracted significant attention as a property of spin glasses and polymers, see, for example, Struick (1978). Part of the reason for the recent interest in these phenomena has to do with the breakdown of certain fundamental assumptions made in equilibrium statistical mechanics when applied to strongly disordered systems. For example, the Onsager Principle (OP), that being the relaxation of a perturbed network back to its equilibrium state being described by an unperturbed autocorrelation function, is violated in anomalous diffusion and relaxation. Recent papers on this phenomenon are devoted to studying aging in diffusion processes occurring in d-dimensional lattices, see, for example, Monthus and Bouchaud (1996), in low-dimensional environments, see, for example, Laloux and Le Doussal (1998), in the quantum dynamics of dissipative free particles, see, for example, Pottier (2003). Most recently there has been some interest in the manifestation of aging in processes described by means of the CTRW formalism, see, for example, Allegrini et al. (2003b) and Barkai (2003).

OP is one of the basic tenets of statistical mechanics insofar as it establishes a connection between a property of equilibrium, the autocorrelation function of a given phase space variable A, and the regression to equilibrium of a macroscopic signal. For this reason, we judge the OP to be a fundamental step in establishing the connection between dynamics and thermodynamics. It is important to stress, as clearly stated by Onsager himself, see Onsager (1931), that this principle holds true for aged networks, namely networks in contact with heat reservoirs that are in thermal equilibrium. If the regression to equilibrium is very fast, it is not necessary that the bath be in equilibrium at the moment when we begin measuring the regression of the network of interest to equilibrium. In fact, in the specific case where the bath is responsible for fluctuations that can be assumed to be white, that is, to have a flat frequency spectrum, the regression to equilibrium of the bath is essentially instantaneous. OP refers to a variable of interest whose dynamics are made stochastic by the interaction with a bath. Thus, when we discuss the process of regression to equilibrium, we should specify if we are referring to the network or to its bath (environment).

If we adopt the white noise approximation to describe the fluctuations that are responsible for the erratic motion of the network variable, then the regression to equilibrium of the reservoir is virtually instantaneous and we can easily satisfy the condition for the validity of the OP. The network variable is characterized by a stationary autocorrelation function $\Phi_{AA} \left(t, t' \right) = \left\langle A(t) A(t') \right\rangle$, which only depends on the time difference $t - t'$. The stochastic behavior of the network variable is caused by the interaction between the network and bath, and this kind of process is often studied by means of the master equation method discussed earlier. However these conditions need not be met in complex networks and the autocorrelation function in general need not be stationary.

As we demonstrate, to create a master equation compatible with the OP, in the case when the bath is not infinitely fast, we need a condition of entanglement between network and bath. This is not a trivial problem, since the departure from the Poisson condition generates an infinitely extended memory, and the network-bath entanglement is the result of a rearrangement process with an indefinite time scale. In fact the traditional fluctuation–dissipation relation needs modification in such networks.

Recall that the CTRW has also been used in foundational discussions of statistical physics and the connection between the master equation formalism and the CTRW has been debated continuously starting with the pioneering work of Bedeaux et al. (1971). The focus of the discussion is often on the waiting time distribution function $\psi(t)$ and it was proven, see, Bedeaux et al. (1971), that the Markov master equation is compatible with the CTRW if the stepping process is Poisson and the waiting time distribution is exponential. This result raises the related issue of the connection between CTRW, a non-Poisson stepping process, and a non-Markov master equation. Kenkre et al. (1973) solved this problem by means of the GME, also discussed earlier, and which we demonstrate in this section can be made compatible with the OP. Recently the GME was discussed by Metzler and Klafter (2000a) who argue that it unifies the fractional calculus and CTRW. We discuss this connection subsequently, but first we focus our attention on how to make the GME stationary and thus compatible with the OP.

The OP is a property that makes it possible for us to derive the autocorrelation function from the GME. If we require the GME and CTRW to be equivalent, we find the result that the two are compatible only when the statistics are Poisson. The reason for this restriction is that a departure from Poisson statistics generates memory that makes the GME incompatible with the Markov condition. This incompatibility implies that the structure of the GME is dictated by the initial condition. If it is not stationary, the resulting GME is not a *bona fide* transport equation, as first articulated by Fox (1977). On the other hand, if the waiting time distribution $\psi(t)$ is not exponential, there are aging effects. This implies that we allow the network to age until it reaches the state where the OP is valid. In this aged situation it is possible to establish a GME that is a *bona fide* transport equation and to establish this last relation we also establish a complete equivalence between CTRW and GME as shown by Allegrini et al. (2003b).

4.1. Intermittent stochastic processes

When a physical network exceeds the domain where the linear approximation is valid, say, the elastic limit in a piece of material, then nonlinear interactions become important and the Hamiltonian must be modified to include terms beyond the quadratic. As we noted earlier, another way to model the increased complexity of a network is to put it in contact with the environment, which in the simplest physical case provides interrelated fluctuations and dissipation. In the phenomenon of Brownian motion the statistics of the fluctuations are resolved to be Gaussian delta correlated in time and the response of the Brownian particle at equilibrium to these fluctuations is determined by the canonical distribution. However, the statistics of the heat bath need not be Gaussian nor delta correlated in character, so another way complexity can enter network models is through modification of the statistical properties of the fluctuating force in the Langevin equation.

In this subsection we present a model for the generation of intermittent fluctuations, as a prototype of crucial event generators, the crucial events being the main property of the form of complexity that we illustrate in Sections 5 and 6.

Following Allegrini et al. (2003c) and Akin et al. (2006) and references therein, we use a dynamical model based on a particle moving in the positive direction along the q-axis and confined to the unit interval I defined by [0, 1]. The equation of motion is chosen to be the nonlinear rate equation

$$\frac{\mathrm{d}q(t)}{\mathrm{d}t} = aq(t)^z \tag{166}$$

where $a \ll 1$. Statistics are inserted into the deterministic equation (166) through the boundary condition; whenever the particle reaches the border $q = 1$, it is injected back into the unit interval I to a random position having uniform probability. Throughout this discussion we refer to this back injection as an event; an event that disconnects what happens in one sojourn on the interval to another.

We wish to construct the distribution function for the particle's sojourn time in the unit interval. One can construct an argument for $z = 1$ with the result that the distribution of the number of events (reinjections) is Poisson and the sojourn time distribution function is exponential. For $z \neq 1$ that is not the case and one obtains a non-Poisson distribution. The time it takes for the particle to reach the boundary $q(\tau) = 1$ is determined by quadrature to be

$$\int_{q(0)}^{1} \frac{\mathrm{d}q}{q^z} = a\tau \tag{167}$$

resulting in the relation between the random initial condition $q(0)$ and the random sojourn time τ

$$q(0) = \frac{1}{[1-(1-z)\,a\tau]^{\frac{1}{1-z}}}. \tag{168}$$

The sojourn or waiting time distribution function $\psi(\tau)$ is consequently determined by

$$\psi(\tau)\mathrm{d}\tau = p\,(q(0))\,\mathrm{d}q(0) \tag{169}$$

and since by assumption the reinjection distribution is uniform $p\,(q(0)) = 1$, we have after some algebra

$$\psi(\tau) = \left|\frac{\mathrm{d}q(0)}{\mathrm{d}\tau}\right| = \frac{(\mu-1)T^{\mu-1}}{(T+\tau)^{\mu}} \tag{170}$$

where the familiar parameters μ and T are determined to be related to those in the dynamical equation by

$$\mu = \frac{z}{z-1} \quad \text{and} \quad T = \frac{1}{(z-1)\,a}. \tag{171}$$

The inverse power-law distribution (170) is a model that we use as a prototype for any dichotomous renewal network. It depends on two parameters, μ and T, with very different interpretations. The parameter T is the time lapse necessary for the expression on the *rhs* of (170) to become identical to a strict inverse power-law. In the asymptotic region T is also a measure of the weight of the fat tail of the distribution. The second parameter μ, on the other hand, is a fractional index that marks the presence of complexity. It can, for instance, be due to a hierarchial scaling superposition of exponentials, indicating the invisible (inaccessible) exploration of structures within structures, or the effect of an Arrhenius-activated process with a fluctuating rate, subject to another local temperature. It may also be the expression of many other models with many or few degrees of freedom (returns in random walks in exotic topologies or energy landscapes). When we record a relatively rare event such as a threshold passage, or a structure change, all these networks yield a point process in time that may or may not be renewal. In many cases it is also possible to assign a sign to these rare events. It is evident that, in the renewal case, the dichotomous model can be adopted.

The sojourn time distribution (170) is normalizable

$$\int_0^\infty \psi(t)\mathrm{d}t = 1 \tag{172}$$

for $\mu > 1$. The mean sojourn time is given by

$$\langle t \rangle = \int_0^\infty t\psi(t)\mathrm{d}t = \frac{T}{\mu - 2} \tag{173}$$

for $\mu > 2$, but diverges if $\mu < 2$, so that (170) is normalizable, but with a diverging mean sojourn time for $1 < \mu < 2$. The probability that no event occurs up to time t is given by the survival probability

$$\Psi(t) \equiv \int_t^\infty \psi(t')\mathrm{d}t'. \tag{174}$$

4.1.1. Poisson distribution

It is a simple matter to substitute these expressions for the parameters (171) in terms of z back into (170) to obtain

$$\psi(\tau) = a\left[1 + (z-1)\,a\tau\right]^{-\frac{z}{z-1}} \tag{175}$$

which in the limit $z \to 1$ yields the exponential distribution

$$\psi(\tau) = a\mathrm{e}^{-a\tau}. \tag{176}$$

The waiting time probability density for n events occurring in the time t is given by the convolution

$$\psi_n(\tau) = \int_0^t \psi_{n-1}\left(t - t'\right)\psi_1(t')\mathrm{d}t' \tag{177}$$

and associating $\psi_1(t)$ with the exponential (176) this convolution equation can be solved to yield

$$\psi_n(t) = \frac{a\,(at)^{n-1}}{\Gamma\,(n)}\mathrm{e}^{-at}. \tag{178}$$

In the Renewal Theory, see, Cox (1967) and Queueing Theory, see Gross and Harris (1998), literature (178) goes by the name of the Erlang distribution which for the probability of n events occurring in a given time interval gives the Poisson distribution

$$P_n(t) = \frac{(\gamma t)^n}{n!}\mathrm{e}^{-\gamma t}. \tag{179}$$

Thus, we see that an exponential distribution of waiting times implies a Poisson distribution for the number of events occurring in a given time interval, indicating the statistics of the time intervals and the statistics of the number of time intervals are not the same, but they are related.

4.2. Inverse power-law distributions

Inverse power laws constitute one of the most familiar manifestations of complexity. Machlup (1977) discusses such laws in the context of avalanches; Willis (1922) and Yule (1924) identify them in biological speciation; Zipf (1949) connects an inverse power law to linguistics; Pareto (1897) finds it in the tails of the distribution of income; de Sola Price (1963) determines that scientific citations have such a heavy-tailed distribution; Lotka (1924, 1926) uncovers such a law for the number of scientific publications; Szeto et al. (1992) reveal it for fetal lamb breathing; West (1990), West and Deering (1994) and Vlad (1992a) discuss it in the branching of bronchial trees, and Barabási (2003) and Watts (1999) discuss such inverse power laws in small world phenomena, connections on the Internet and the World Wide Web, and the list goes on and on. We give more extensive discussions of experimental data sets at the appropriate points in our presentation of the underlying theory.

Complexity, as we have seen, can be addressed starting from the dynamical equations, by introducing more and more degrees of freedom that are allowed to interact nonlinearly with one another. With each new variable the network becomes more complex as we discussed in Section 2. Alternatively, we can start with the evolution of the probability density in a homogeneous isotropic phase space. Things become more complex as additional structure is introduced into the space, structure in the form of spatial heterogeneities or temporal memory. Historically a number of approaches have been taken to generate inverse power laws, see, e.g., Mandelbrot and van Ness (1968), Arecchi and Lisi (1982), Montroll and Shlesinger (1983), Vlad (1992b) and Lowen and Teich (1993), and in a later section we examine the experimental evidence for $1/f$-phenomena leading to such distributions, but for the moment we focus on how various complexity mechanisms fit into the random walk perspective. As discussed in Section 3 one strategy to systematically include these effects is the CTRW where after each step the random walker waits for a random time interval before taking her next step. Let us consider the inverse power-law waiting-time distribution density introduced using a dynamic argument resulting in (170). This distribution can be obtained by means of the transformation, see, Buiatti et al. (1999),

$$\tau = T\left(\frac{1}{y^{\mu-1}} - 1\right), \tag{180}$$

which changes the variable y defined to be uniformly distributed over the interval $I = [0, 1]$ into the numbers τ distributed according to (170). Note that the numbers y coincide with the initial conditions $q(0)$ used in (167). In other words, the algorithm (180) has a dynamical origin, corresponding to a slow and regular motion towards a condition of abrupt change, that is, a quake. The time interval between two consecutive quakes is generated by regular dynamics that is not linear.

Again, renewal events are defined as those events whose occurrence has the effect of erasing the memory of earlier events, and it is evident that the transformation (180) accomplishes this erasure. In the dynamic case, the lack of correlation among the waiting times τ_i, and the consequent renewal character of the process, is a consequence of deterministic chaos.

We refer to the work in Section 4.3 and Allegrini et al. (2007b) for an example of a network described by (170), but chosen to violate the renewal condition. We emphasize that the adoption of the transformation defined by (180) makes it easy to realize the renewal condition through the random selection of y. Adopting other methods, for instance fluctuating Poisson dynamics, can produce renewal events that do not have anything to do with the dynamics leading to the inverse power-law (170). As studied by Allegrini et al. (2007b), the method of fluctuating Poisson dynamics produces renewal events that are embedded in a cloud of Poisson events, thereby generating a significant departure from the genuinely renewal condition, and presents a challenge for the detection of renewal properties as well. If the fluctuations of the Poisson parameter are made infinitely slow, the renewal events are totally annihilated, and the physics of such networks, for instance the response to external excitations, may depart from the physics of the renewal events, in spite of sharing the same inverse power-law waiting-time distribution (170).

In a recent conference on the approach to complexity – see Grigolini et al. (2007) – the authors determined that there are two main complexity categories, the Renewal Approach to Complexity (RAC) and Complexity Without Renewal (CWR). We adopt the same perspective here for the reasons given below.

It is well known that $1/f$-noise is considered to be a manifestation of complexity, as described in the excellent review on $1/f$-noise in physical networks by Dutta and Horn (1981). It is not so well known that the most popular approaches to explaining $1/f$-noise are different forms of CWR. We refer the reader to the excellent book of Jensen (2000), who shows with clarity the connection between complexity and Self-Organized Criticality (SOC) proposed by Bak (1996) and Bak et al. (1987) and the superstatistics of Beck and Cohen (2003), with an approach to complexity based on the slow fluctuation of a Poisson parameter, in accordance with more recent observations by Baiesi et al. (2006). Thus, we conclude that SOC is another form of CWR and we may use Jensen's arguments that SOC is not a satisfactory approach to $1/f$-noise, to declare the issue of whether $1/f$-noise rests on the CWR or on the RAC perspective to be still open.

Here we focus our attention on the approach to $1/f$-noise proposed by Voss and Clarke (1976). This makes it possible for us to show that in the case where the ergodic condition $\mu > 2$ applies, the RAC yields results equivalent to the CWR, thus generating the mistaken impression that the two categories are physically equivalent. As discussed in Section 4.3 and by Cakir et al. (2006), it is possible to express the signal $\xi(t)$ as a sum of harmonic oscillations in such a way as to obtain for its normalized autocorrelation function the form

$$\Phi_\xi(t) = \left(\frac{T}{T+t}\right)^\beta, \tag{181}$$

with $\beta < 1$. This inverse power-law autocorrelation function is a consequence of assuming the power spectral density has the form

$$P(f) \propto \frac{1}{f^{\alpha}}, \tag{182}$$

where $\alpha = 1 - \beta$. This very simple argument yields the same conclusion as that of Voss and Clark, concerning the origin of $1/f$ noise with α slightly smaller than 1.

On the basis of these remarks one might be tempted to adopt the CWR philosophy to model complexity. In fact, the superposition of very many oscillations does not generate renewal events. However, let us use the inverse power-law distribution (170) to create a renewal time series $\{\tau_i\}$ from which the time sequence t_i can be generated according to the prescription $t_{i+1} = \tau_i + t_i$, where the subscript denotes the order in which the time interval occurs and the initial time is $t_0 = 0$. Let us imagine that the event occurring at time t_i is a coin tossing used to define the sign of the entire time region between t_i and t_{i+1}. This prescription creates a fluctuation $\xi(t)$, whose autocorrelation function is determined by renewal theory to be, see Geisel et al. (1985),

$$\Phi_{\xi}(t) = \frac{1}{\langle\tau\rangle}\int_t^{\infty} \mathrm{d}\tau(\tau - t)\psi(\tau), \tag{183}$$

where again $\psi(\tau)$ is the inverse power-law waiting time distribution (170) and $\langle\tau\rangle = T/(\mu - 2)$ is the mean waiting time. The mean waiting time diverges at the border $\mu = 2$, between $2 < \mu$, which is compatible with the existence of infinitely aged condition, see, Allegrini et al. (2003b), and the region $2 > \mu$, which is characterized by perennial aging and ergodicity breakdown studied by Bel and Barkai (2005, 2006a,b,c). It is straightforward to show that (183) yields (181) with $\beta = \mu - 2$. In the case $2 < \mu < 3$, adopting the Wiener–Kintchine theorem, see, Voss and Clarke (1976) suggests that this renewal time series is a form of $1/f$-noise.

Thus, even though we usually find references to CWR theories to explain the origin of $1/f$-noise, we cannot rule out RAC as a plausible alternative approach to complexity. In the next subsection we point out that with an approach to the inverse power-law distribution (170) based on the slow modulation of a Poisson process, see, e.g., Allegrini et al. (2007b), that is, on a form of *superstatistics* approach to complexity, the aging effect is strongly reduced, thereby allowing us to establish if a given physical process corresponds to the CWR or to the RAC perspective. Furthermore, we have to point out that the practical realization of the CWR prescription generates unexpected renewal events. The slower the modulation, the rarer are the emerging renewal events, thereby making them difficult to detect. The renewal events play the crucial role of determining the scaling of the time asymptotic limit, but this anomalous scaling may show up at times so large as to make it almost impossible to reveal the existence of these renewal events. In this case we have to consider the process as belonging to the CWR category.

In the field of single molecule spectroscopy and BQDs such as studied by Nirmal et al. (1996), Kuno et al. (2001, 2003), Shimizu et al. (2001) and Bianco et al. (2005) established that the BQD data undergo renewal aging, thereby ruling out the CWR, in the description of intermittent switching in BQD. In the field of econophysics, the work of Scalas (2007) does not take a position on the two categories being considered, thereby leaving open the possibility that econophysics may be properly described by either SOC or superstatistics. Bianco et al. (2005) and Bianco and Grigolini (2005), on the contrary, using the idea of aging, establish that the econophysics processes they study obey renewal theory, even if the critical events underlying trade action are not ostensible, and become observable only as a result of additional analysis.

It is important to note that the BQD phenomenon is related to the origin of $1/f$-noise with α slightly larger than one rather than slightly smaller than one. In fact, the BQD phenomenon is known, see, e.g., Nirmal et al. (2006), Kuno et al. (2001), Shimizu et al. (2001) and Kuno et al. (2003), to correspond to (170) with $\mu < 2$. This condition on the power-law index, in turn, is known, as shown by Margolin and Barkai (2005), to violate the ergodic condition, thereby violating the condition for the existence of stationarity. The work, as studied by Allegrini et al. (2005), affords a way to evaluate the non-stationary correlation function, and, thus to use the same dimensional arguments as those adopted by Voss and Clarke (1976), to reach the conclusion that

$$\alpha = 3 - \mu, \tag{184}$$

in accordance with the experimental observation by Pelton et al. (2004).

Thus, not only can we not rule out RAC as a possible theory for the origin of $1/f$-noise, but we are tempted to advocate RAC as an approach to $1/f$-noise as being even more attractive than earlier theories. Notice that (184) locates the ideal condition of $1/f$ at $\mu = 2$, which is the border between the ergodic ($\mu > 2$) and non-ergodic ($\mu < 2$) conditions. This interesting aspect has been overlooked by earlier investigations into the origins for $1/f$-noise and this is probably a consequence of the fact that these earlier approaches were based essentially on the CWR perspective.

4.3. Dynamic approach to modulation

In the CTRW the walker stays in a given state for a length of time determined by the waiting or sojourn time statistical distribution. Here we illustrate a strategy for constructing this sojourn time distribution function that may range from slow

modulation to the renewal condition depending on the condition adopted. We search for a distribution $\Pi(\lambda)$ of Poisson rates λ, each of them characterized by the familiar exponential distribution

$$\psi_\lambda(\tau) = \lambda e^{-\lambda\tau}, \tag{185}$$

in such a way as to produce a waiting time distribution $\psi(\tau)$

$$\psi(\tau) = \int_0^\infty d\lambda \Pi(\lambda)\psi_\lambda(\tau) \tag{186}$$

with an inverse power-law form.

The proper distribution $\Pi(\lambda)$ is given by the steady-state solution of a proper FPE. The rates λ are time dependent and so are the corresponding relaxation times

$$T_{\rm relax} = 1/\lambda. \tag{187}$$

Thus we select the FPE corresponding to the multiplicative stochastic process

$$\frac{dT_{\rm relax}}{dt} = -\nu\,(T_{\rm relax} - T_0) + T_{\rm relax}\xi(t) \tag{188}$$

where $\xi(t)$ is taken to be a delta correlated Gaussian random process and the rate ν keeps the modulation rate under control. The average over an ensemble of realizations of this random process is given by

$$\left\langle \xi(t)\xi(t')\right\rangle = 2D\delta(t - t') \tag{189}$$

and the deterministic part of the Langevin equation (188) gives a relaxation to the rate $1/T_0$ in a time $1/\nu$.

The Stratonovitch version of the FPE corresponding to the multiplicative noise Langevin equation (188), affording the probability distribution density $\sigma(T_{\rm relax}, t)$, is, see Lindenberg and West (1990),

$$\frac{\partial\sigma(T_{\rm relax}, t)}{\partial t} = \nu\frac{\partial}{\partial T_{\rm relax}}\left[(T_{\rm relax} - T_0)\,\sigma(T_{\rm relax}, t)\right] + D\frac{\partial}{\partial T_{\rm relax}}\left[T_{\rm relax}\frac{\partial}{\partial T_{\rm relax}}\left\{T_{\rm relax}\sigma(T_{\rm relax}, t)\right\}\right]. \tag{190}$$

The steady-state solution to (190) is given by the solution to

$$\frac{\partial\sigma(T_{\rm relax}, t)}{\partial t} = 0, \tag{191}$$

which for the zero flux case yields

$$\frac{1}{T_{\rm relax}\sigma(T_{\rm relax})}\frac{\partial}{\partial T_{\rm relax}}\left\{T_{\rm relax}\sigma(T_{\rm relax})\right\} = -\frac{(T_{\rm relax} - T_0)}{DT_{\rm relax}^2} \tag{192}$$

where we have been facile in our use of notation and denote the steady-state solution without subscripts. The solution to (192) is

$$\sigma(T_{\rm relax}) = \frac{N_{\rm norm}}{T_{\rm relax}^{\alpha+1}}e^{-\gamma/T_{\rm relax}} \tag{193}$$

where $N_{\rm norm}$ is the normalization constant and the parameter values are given by

$$\alpha = \frac{\nu}{D}; \qquad \gamma = \frac{\nu}{D}T_0 = \alpha T_0. \tag{194}$$

Normalizing the distribution (193) yields

$$\sigma(T_{\rm relax}) = \frac{\gamma^\alpha}{\Gamma(\alpha)\,T_{\rm relax}^{\alpha+1}}e^{-\gamma/T_{\rm relax}}. \tag{195}$$

If we substitute the steady-state solution to the FPE (195) into the integral (186), using the exponential (185) for the basic process yields

$$\begin{aligned}\psi(t) &= \frac{\gamma^\alpha}{\Gamma(\alpha)}\int_0^\infty dT_{\rm relax}\frac{e^{-\gamma/T_{\rm relax}}e^{-t/T_{\rm relax}}}{T_{\rm relax}^{\alpha+2}} = \frac{\Gamma(\alpha+1)}{\Gamma(\alpha)}\frac{\gamma^\alpha}{(\gamma+t)^{\alpha+1}}\\ &= \frac{\alpha\gamma^\alpha}{(\gamma+t)^{\alpha+1}}.\end{aligned} \tag{196}$$

Thus, we obtain an inverse power-law sojourn time distribution function from the superposition of an infinite number of exponential functions with different rates. Note that this inverse power-law behavior is a direct consequence of the multiplicative nature of the relaxation dynamics in (188).

We change notation to make the distribution (196) conform to the literature; replace the parameter γ with T and the exponent α with $\mu - 1$ so that the inverse power-law distribution becomes

$$\psi(t) = \frac{(\mu-1)T^{\mu-1}}{(T+t)^{\mu}} \tag{197}$$

which we determined previously to be normalizable. Taking note of the parameter values for the multiplicative relaxation process given in (188) we observe that $0 < \alpha < 1$ and the time scale in the inverse power law is less than τ_0, that is, $T = \alpha\tau_0$. In this case $\mu < 2$ so that the distribution is normalizable but the mean waiting time diverges.

Note that to attain the result (197) we made a change of integration variable by replacing λ with $1/T_{\rm relax}$. We now go back to the λ-representation and taking into account that

$$\Pi(\lambda) = \frac{\sigma(1/\lambda)}{\lambda^2}, \tag{198}$$

obtain

$$\Pi(\lambda) = \frac{T^{\mu-1}}{\Gamma(\mu-1)}\lambda^{\mu-2}\exp(-\lambda T). \tag{199}$$

This is the statistical weight to adopt in (186) to obtain an inverse power-law distribution of waiting times. It is a Γ-distribution of order $\mu - 1$ proposed by Beck (2001) and used in later work by Bologna et al. (2003).

It is convenient to stress that the slow modulation condition is realized by setting the relaxation rate ν very small. In this case, as we shall see, the theory illustrated here does not produce aging effects. In the opposite limit of very large ν, the dynamical approach of this subsection yields a renewal condition, but at that stage the process is again Poissonian. To realize a non-Poisson renewal condition, we must ensure that after drawing a given waiting time τ that for the next drawing we use a different λ. This is an ideal condition, difficult if not impossible to realize dynamically.

If the time scale defined by (173) exists, which is to say that $\mu > 2$, it is possible to guess the asymptotic solution of the process by using the central limit theorem. The diffusion process for time velocity u taking place at times much larger than $\langle t\rangle$ becomes indistinguishable from a sum of steps, the total number of steps being $t/\langle t\rangle$. If the variance of the distribution of step lengths is finite, the diffusion process is indistinguishable from standard Brownian motion. If the variance of the distribution of step lengths is infinite, however, then one can apply the generalized central limit theorem to predict a Lévy process, see, e.g., West et al. (2003).

4.3.1. Modulated Poisson process

For the theoretical discussion of this subsection, it is useful to turn the sequence of times $\{\tau_i\}$, generated by the inverse power-law distribution, into a diffusion generating fluctuation $\xi(t)$. Each laminar region in time is assigned either the value W or the value $-W$ through a coin tossing procedure, thus creating a dichotomous fluctuation $\xi(t)$, which is interpreted as a stochastic velocity. We study the time evolution of the coordinate $Q(t)$, obeying the dynamic prescription

$$\frac{dQ(t)}{dt} = \xi(t). \tag{200}$$

The central issue of this study of the two kinds of diffusion processes (renewal or modulation) has to do with scaling, namely the property:

$$P(q,t) = \frac{1}{t^{\delta}}F\left(\frac{q}{t^{\delta}}\right), \tag{201}$$

which is expected to hold true in the time asymptotic limit. Complexity, namely the departure from ordinary statistical mechanics, is signaled by either $\delta \neq 0.5$ or $F(y)$ departing from the Gaussian form, or by both.

The modulation approach to complexity, meant as the foundation of non-exponential waiting time distributions, is based on conventional Poisson processes whose rates sporadically change in time (non-homogenous processes). For instance, Allegrini et al. (1997) proved that a double-well potential under the influence of white noise yields the exponential distribution of the time of sojourn in the two wells. In the case of a symmetric double-well potential we have (185) where the parameter λ is determined by the Arrhenius formula $\lambda = k_B\exp[-U/k_B\Theta]$. In the case when either the barrier intensity U, see Allegrini et al. (1997), or temperature Θ, see Compiani et al. (1985), are slowly modulated, the resulting waiting-time distribution becomes a superposition of infinitely many exponentials. As shown in the last subsection a superposition of infinitely many exponentially decaying functions can generate an inverse power-law distribution, see Shlesinger and Hughes (1981).

In recent times, the term superstatistics has been coined by Cohen (2004) to denote an approach to non-canonical distributions, of any form, not only the inverse power-law form, as in the original work of Beck (2001). We note that Cohen (2004) points out explicitly that the time scale to change from one canonical distribution to another must be much larger than the time scale of each of the individual canonical processes. Thus, we can qualify superstatistics as a form of infinitely slow modulation such as we did in the discussion in Section 4.1. According to the modulation theory, we write the

waiting time distribution $\psi(\tau)$ in the form (170). This is identical to (197) which was obtained by means of the modulation procedure.

The renewal process yields a time series which is homogeneous and non-Poissonian. Since $\mu > 2$, the renewal process is ergodic, and the autocorrelation function of the fluctuation $\xi(t)$, $\langle\xi(t_1)\xi(t_2)\rangle$, with $t_2 > t_1$, can be evaluated by adopting the time average, for the time interval t_T,

$$\langle\xi(t_1)\xi(t_2)\rangle = \lim_{t_T\to\infty}\frac{1}{t_T}\int_0^{t_T} \mathrm{d}t\xi(t)\xi(t+t_2-t_1). \tag{202}$$

Using renewal theory, see Geisel et al. (1985), we have for the normalized autocorrelation function $\Phi_\xi(t)$

$$\Phi_\xi(t) \equiv \frac{\langle\xi(t_0)\xi(t_0+t)\rangle}{\langle\xi^2\rangle} = \frac{\langle\xi(0)\xi(t)\rangle}{\langle\xi^2\rangle}, \tag{203}$$

and using (183) we obtain the following analytical expression

$$\frac{\mathrm{d}^2}{\mathrm{d}t^2}\Phi_\xi(t) = \frac{\psi(t)}{\langle\tau\rangle}. \tag{204}$$

On the other hand, the distribution density $\Pi(\lambda)$ is an equilibrium distribution allowing us to evaluate the autocorrelation function through the prescription (202) even if we realize the inverse power-law distribution of (197) through modulation rather than by using the renewal prescription. We note that the time spent by the network with a given λ is inversely proportional to λ. By integrating (200), squaring $Q(t)$, averaging over an ensemble of realizations of the time intervals, and exploiting the stationary nature of the autocorrelation function $\langle\xi(t_1)\xi(t_2)\rangle = \langle\xi(0)\xi(t_2-t_1)\rangle$, we obtain

$$\langle Q^2(t)\rangle = 2\langle\xi^2\rangle\int_0^t \mathrm{d}t'\int_0^{t'}\mathrm{d}t''\Phi_\xi(t''). \tag{205}$$

We conclude that the condition $2 < \mu < 3$ allows the modulation prescription to generate the same superdiffusion statistics as does the corresponding renewal process. As a consequence, studying the second moment of the diffusing variable $Q(t)$, through the average over the distribution $W(q, t \mid q_0)$ of the diffusing process is not sufficient to discriminate between renewal and modulation.

In the next subsection we show that adopting aging techniques make it possible to distinguish modulation from renewal theory even when they produce the same autocorrelation function.

4.4. Aging effects in renewal and modulation theories

We have dealt with a number of similarities between two approaches to inverse power-law relaxation: a non-homogeneous Poisson process and a homogenous renewal process. This distinction is widely made when studying glass-forming liquids. Also the related phenomenon of *aging* has been known for a long time to be a property of spin glasses and polymers, see, e.g., Struick (1978). The most familiar manifestation of aging is given by the two-time autocorrelation function that does not depend on the difference in the two times t_1 and $t_2 > t_1$, but depends on each time separately. The relaxation of the correlation as a function of $t_2 - t_1$ becomes slower for larger t_1. Aging is thought to be determined by the fact that the network under study is out of equilibrium and that the regression to equilibrium involves times longer than the observation time, see Calabrese and Gambassi (2005).

Herein we have in mind *renewal aging*. For recent investigations into this form of aging we refer the readers to the works of Allegrini et al. (2003b), Barkai (2003) and Godréche and Luck (2001). The renewal model studied herein yields renewal aging, whose immediate manifestation is revealed by the dependence of $\psi(t)$ on the observation time. The quantity $\psi(t)\mathrm{d}t$ is the probability that a laminar region begins at $t = 0$ and ends in the small time interval $[t, t + \mathrm{d}t]$. If we have at our disposal a Gibbs ensemble of time sequences, all of which begin with the first laminar region, located at $t = 0$, to derive experimentally a $\psi(t)$, we have to observe the time at which the first laminar region of each sequence of the sample ends. This is equivalent to making the *preparation* and *observation* times coincide.

4.4.1. Exact treatment of aging

Let us imagine that after preparing the network at $t = 0$, with an event occurring at that time in any of the Gibbs networks, we postpone the beginning of the waiting process for the occurrence of a new event to time $t' > 0$. In this case, if the process is renewal, the probability of an event occurrence at time t is given by

$$\psi(t, t') = \psi(t) + \sum_{n=1}^{\infty}\int_0^{t'}\mathrm{d}t''\psi_n(t'')\psi(t-t''). \tag{206}$$

The physical meaning of this prescription is as follows. At time $t = 0$ an event occurs. However, since the observation process begins later at time $t' > 0$, the probability of observing a new event after t' depends on the last event occurring

prior to t', at time t'', $\psi(t-t'')$. The event occurring at $t''<t'$ is in general the last of a sequence of n events, occurring exactly at t'', while the earlier events can occur at any earlier time. The probability for this last event is $\psi_n(t'')$, with $n\geq 1$; the first term in the integrand of (206). Note that (206) is an exact relation and is the foundation of the new FDT of the first kind, subsequently discussed in Section 6.

The corresponding non-stationary survival probability reads

$$\Psi(t,t')=\int_t^\infty \mathrm{d}t''\psi(t'',t'). \tag{207}$$

Note that by taking the t'-derivative of (207) and using (206) we obtain

$$\frac{\mathrm{d}}{\mathrm{d}t'}\Psi(t,t')=P(t')\Psi(t-t'), \tag{208}$$

where

$$P(t)=\sum_{n=0}^{\infty}\psi_n(t). \tag{209}$$

The quantity $P(t)$ is the rate of events occurring at time t, under the condition that an event occurs at $t=0$.

In the case $\mu>2$, when the stationary condition is adopted this rate (209) is constant. Of special interest herein is the case $\mu<2$, where the Laplace transform of (197), for $u\to 0$ is

$$\hat{\psi}(u)=1-\Gamma(2-\mu)(Tu)^{\mu-1}. \tag{210}$$

On the other hand, using (209) and (210), we obtain

$$\hat{P}(u)=\frac{1}{1-\hat{\psi}(u)}\approx\frac{1}{\Gamma(2-\mu)(Tu)^{\mu-1}}, \tag{211}$$

which, using a Tauberian theorem, yields

$$P(t)\propto\frac{1}{t^{2-\mu}}. \tag{212}$$

In other words, the renewal aging, in the case $\mu<2$ is characterized by the property that the rate of event occurrence, tends to decrease as a function of time.

4.4.2. Modulation and renewal aging

Let us imagine now that preparation of the network is made at time $t=-t_a<0$. The first measured waiting time is denoted by τ_1. The first waiting time, distinct from the observation of the successive waiting times, does not necessarily correspond to the total time duration of a laminar region. The resulting histogram records time lengths that are generally smaller than those corresponding to preparing the network at time $t=0$. Nevertheless, in the case when the waiting-time distribution is exponential, both long and short time lengths are reduced by the same percent. Thus, turning the histogram into a normalized waiting-time distribution density has the effect of recovering the same exponential form. A renewal exponential process does not age. In the non-exponential case delaying the observation process has the effect of producing a percent cut of the short-time laminar regions larger than that of the long-time laminar regions. As a consequence, with the normalization of the distribution, the weight of the short-time laminar regions is reduced and the weight of the long-time laminar regions is enhanced, thereby generating a slower decay of the survival probability $\Psi(t)$.

Allegrini et al. (2007b) numerically generated the $\Pi(\lambda)$ distribution and used this approach to generate trajectories, i.e., artificial sequences of random waiting times. They compared the results for the aging analysis of trajectories characterized by the same exponent μ of the power-law, but generated from the renewal process and from modulation processes with different numbers of drawings N_d from the distribution $\lambda\exp(-\lambda t)$. After N_d drawings, they selected from $\Pi(\lambda)$ a new rate λ. It is evident that if $N_d=1$, and only one waiting time is drawn from the Poisson distribution with a given λ and immediately afterward a different λ is selected from the distribution density $\Pi(\lambda)$, the resulting sequence is renewal. Increasing N_d has the effect of realizing the prescriptions of superstatistics, see Beck and Cohen (2003), which requires a long-time sojourn in a given Poisson condition, for the network to adapt to the local thermodynamic condition.

Allegrini et al. (2007b) adopted a procedure proposed earlier by Bianco et al. (2005) referred to as *aging experiment analysis*. Following that analysis, we generate a sequence of times $\{t_i\}$, which are recorded as vertical lines on the t-axis. Then we use a mobile window of size t_a, corresponding to the age to be simulated. The beginning of the window is located on each of the times of the sequence $\{t_i\}$ and we measure the time distance between the end of the window and the first event time after it. These truncated time intervals are used to build up a t_a-aged histogram, which is then used to define the *aged* probability density distribution $\psi_{t_a}(\tau)$ and the corresponding aged survival probability

$$\Psi_{t_a}(\tau)=\int_\tau^\infty\psi_{t_a}(\tau')\mathrm{d}\tau'=1-\int_0^\tau\psi_{t_a}(\tau')\mathrm{d}\tau'. \tag{213}$$

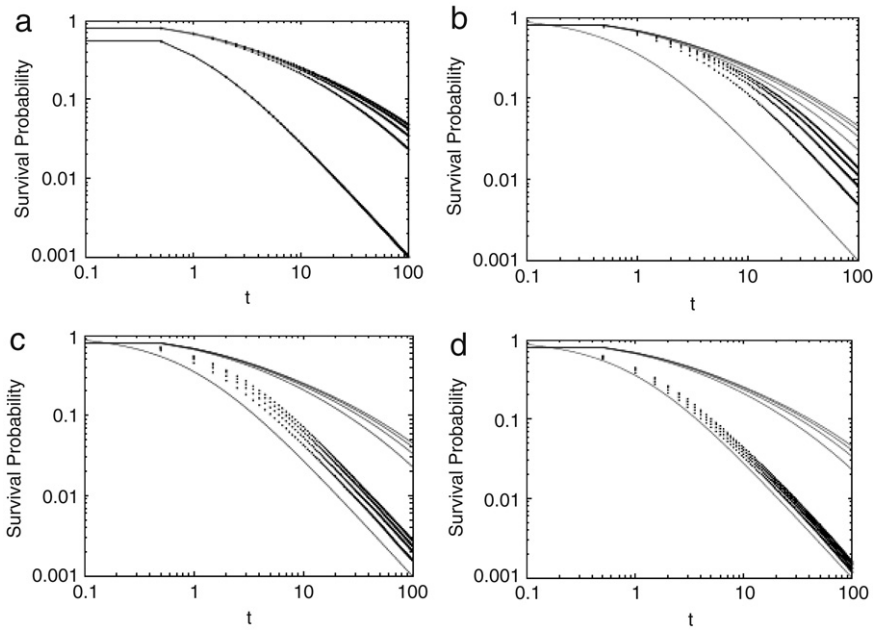

Fig. 5. Comparison between the function $\Psi_{t_a}(t)$ of a renewal process (continuous lines) and the function $\Psi_{t_a}(t)$ produced by a modulation approach with a changing value of N_d (dotted lines). The curves from bottom to top refer to the ages $t_a = 0, 50, 100, 150, 200$. (a) $N_d = 0$; (b) $N_d = 10$; (c) $N_d = 100$; (d) $N_d = 500$. Taken from Allegrini et al. (2007b).

Note that with this notation the exact prescription of (206) yields

$$\psi_{t_a}(\tau) = \psi(\tau + t_a) + \sum_{n=1}^{\infty} \int_0^{t_a} \mathrm{d}y \psi(y + \tau)\psi_n(t_a - y). \tag{214}$$

The results of this aging experiment are illustrated in Fig. 5. When we draw only one waiting time τ and then use a different $\psi_\lambda(\tau) \equiv \lambda \exp(-\lambda\tau)$ for the drawing of the next waiting time, the process is renewal. If we increase the number of waiting times drawn from the same $\psi_\lambda(\tau)$, the intensity of aging is reduced until the condition of a total lack of aging is reached when the number of waiting times drawn from the same waiting-time distribution becomes very large.

The aging experiment can be used to establish if a real sequence is renewal or not. The earlier described aging experiment is applied to a real sequence so as to determine the aged histogram and through it the corresponding survival probability, called $\Psi_{t_a}^{(\mathrm{exp})}(\tau)$. We also establish a criterion to determine the form of the survival probability produced by the renewal condition. This is not quite straightforward, due to the fact that the exact form of (206) is not a simple functional of $\psi(\tau)$. A simple functional is given by (217) that makes it possible to obtain $\psi_{t_a}(\tau)$ from $\psi(\tau)$ and thus to derive from the form that the renewal theory assigns to the aged survival probability, denoted by $\Psi_{t_a}(t)$. If these two procedures applied to the same sequence generate the condition

$$\Psi_{t_a}^{(\mathrm{exp})}(t) = \Psi_{t_a}^{(\mathrm{ren})}(t), \tag{215}$$

we consider the process to be renewal. Note that a virtually exact criterion is obtained by shuffling the time distances between two consecutive events to produce a more reliable $\Psi_{t_a}^{(\mathrm{ren})}(t)$.

4.4.3. Aging and rejuvenation

To discuss the interesting effect of a time dependent μ and of rejuvenation, let us adopt a simplified formula rather than the exact formula (214). As in the earlier subsection we set the condition that the network is prepared at $t_a < 0$ and that observation begins at $t = 0$. The exact expression for $\psi_{t_a}(t)$ of (214) can be written in the form

$$\psi_{t_a}(t) = \int_0^{t_a} \mathrm{d}y P(y)\psi(y + t), \tag{216}$$

where $P(y)$ is defined by (209) and for $\mu < 2$, this quantity is not constant and decreases as $1/t^{2-\mu}$ (see (212)). Under the simplifying assumption that $P(y)$ is constant, we obtain, see Aquino et al. (2004):

$$\psi_{t_a}(t) = \frac{\int_0^{t_a} \psi(t + y)\mathrm{d}y}{K(t_a)}, \tag{217}$$

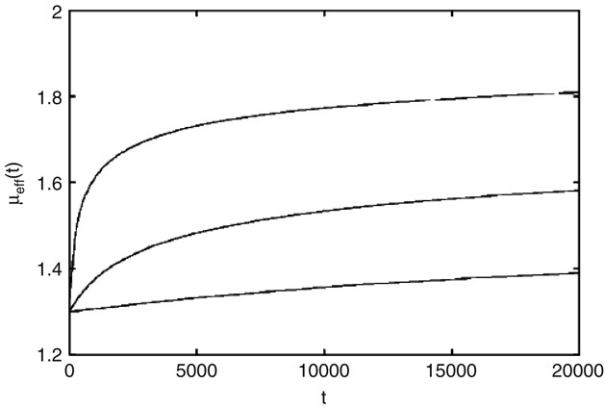

Fig. 6. The effective power index $\mu_{\rm eff}$ of Eq. (221) as a function of time. The curves refer, from top to bottom, to $t_a = 100,\ 1000,\ 10\,000$. Taken from Aquino et al. (2004).

where $K(t_a)$ is the normalization factor defined by

$$K(t_a) \equiv \int_0^{t_a} \Psi(t')\mathrm{d}t', \tag{218}$$

and $\Psi(t)$ is the probability that no event occurs throughout the time interval of length t. We then introduce the aged survival probability by means of (213). This expression can be used for the comparison of (217), even if it is not exact, insofar as it is expected to be reliable in both the short and the long-time limit. Note that in Section 5.2.5 we shall apply this formula to the case of $\mu < 2$, but very close to 2, so as to make the time dependence of $P(t)$ very slow.

Using for $\psi(t)$ the explicit form (197), it is straight forward to show that (217) reduces to

$$\psi_{t_a}(t) = (\mu - 2)\frac{(t+T)^{(1-\mu)} - (t+T+t_a)^{(1-\mu)}}{T^{(2-\mu)} - (t_a+T)^{(2-\mu)}}. \tag{219}$$

This formula establishes that for $t \ll t_a$ the index of the distribution is $\mu - 1$, whereas for $t \gg t_a$ the index becomes μ. This result for the age-dependent waiting-time distribution function agrees with the predictions of Barkai (2003) as well as that of Allegrini et al. (2005). Notice that the formula (219) is equivalent to drawing the initial condition for y from an aged distribution of this variable.

Here, we are in a position to evaluate the waiting time index at a generic time, where, we write $\psi_{t_a}(t)$, as

$$\psi_{t_a}(t) = \frac{A(T, t_a)}{(t+T)^{\mu_{\rm eff}(t)}}. \tag{220}$$

Using (219) we arrive at the following formula for the time dependence of the effective power-law index

$$\mu_{\rm eff}(t) = -\frac{\ln[(t+T)^{(1-\mu)} - (t+T+t_a)^{(1-\mu)}]}{\ln[t+T]}. \tag{221}$$

Fig. 6 illustrates the regression of the effective power-law index to μ with three different ages, and shows clearly that the regression is slower for older networks. This formula shows that it is possible to build a GME that at short times follows the prescription of the GME reviewed in Section 3 and at long times moves into the basin of attraction of the one discussed by Sokolov and Metzler (2003). This is certainly the case, if $t_a > -1$.

4.4.4. Non-stationary autocorrelation function

The aging aspect of the distribution is important and needs more extensive discussion. We note that our approach, see Allegrini et al. (2005), can be easily extended to the case where the distribution of first exit times has a finite age. In the case of a two-state system, the conventional master equation is given by

$$\frac{\mathrm{d}}{\mathrm{d}t}\mathbf{p}(t) = -\lambda \mathbf{K}\mathbf{p}(t), \tag{222}$$

where

$$\mathbf{p}(t) \equiv \begin{pmatrix} p_1(t) \\ p_2(t) \end{pmatrix} \tag{223}$$

and

$$\mathbf{K} \equiv \frac{1}{2}\begin{pmatrix} 1 & -1 \\ -1 & 1 \end{pmatrix}. \tag{224}$$

Alternatively, using the CTRW illustrated in Section 3.3, we write the probability as

$$\mathbf{p}(t) = \sum_{n=0}^{\infty} \int_0^t \mathrm{d}t' \psi_n(t') \Psi(t-t') \mathbf{M}^n \cdot \mathbf{p}(0), \tag{225}$$

where

$$\mathbf{M} \equiv \frac{1}{2}\begin{pmatrix} 1 & 1 \\ 1 & 1 \end{pmatrix}. \tag{226}$$

It is important to understand the meaning of Eq. (225). First of all, let us point out that $\mathbf{p}(0)$ denotes the initial random walker distribution. The main purpose of this treatment is to determine the distribution $\mathbf{p}(t)$ at time t as a function of the initial condition $\mathbf{p}(0)$. Eq. (225) determines $\mathbf{p}(t)$ through the occurrence of random events. A random event corresponds to the occurrence of jumps from one site to other sites, with a probability described by the matrix $\mathbf{M}$. The times of occurrence of these jumps are described by the function $\psi_n(t)$.

When we observe the network at time t, the distribution $\mathbf{p}(t)$ is the result of an arbitrary number n of these random events. The function $\psi_n(t)$ denotes the probability that at time t, and exactly at time t, the nth member of a sequence of n random events, occurs. Of course, we have also to consider the case when no event occurs, this being expressed by $\psi_0(t) = \delta(t)$. It is evident that such a renewal process satisfies the recursion relation (177). The time convoluted nature of this connection allows us to express the Laplace transform of $\psi_n(t)$, $\hat{\psi}_n(u)$, in terms of the Laplace transform of $\psi(t)$. Thus, we obtain

$$\hat{\psi}_n(u) = [\hat{\psi}(u)]^n. \tag{227}$$

Note that the last of a sequence of n random events does not necessarily occur at time t, at which time we observe the network. It might occur at an earlier time $t' < t$. Thus, for the prescription to become reliable, we set the constraint that no event occurs between time t' and time t. In general, the probability that no event occurs up to a given time t, is given by the survival function $\Psi(t)$ defined by (174). The Laplace transform of $\Psi(t)$, $\hat{\Psi}(u)$, is related to $\hat{\psi}(u)$, through (138). Note that between t', the time at which the nth member of a chain of n events occurs, and the observation time t, the distribution keeps the value $\mathbf{M}^n$, the matrix $\mathbf{M}$ being the prescription establishing the jumps that the random walker undergoes when an event occurs. Since n events occurred, this matrix is applied n times to the initial condition $\mathbf{p}(0)$.

Using (227) and (138), and the property $\sum_{n=0}^{\infty}[\hat{\psi}(u)]^n = 1/(1-\hat{\psi}(u))$, we write the Laplace transform of $\mathbf{p}(t)$ as $\hat{\mathbf{p}}(u)$, and of (225) as

$$\hat{\mathbf{p}}(u) = \frac{1}{u + \hat{\Phi}(u)(\mathbf{M}-1)}\mathbf{p}(0), \tag{228}$$

where $\hat{\Phi}(u)$, the Laplace transform of the memory kernel $\Phi(t)$, is related to the Laplace transform of $\psi(t)$, through

$$\hat{\Phi}(u) = \frac{u\hat{\psi}(u)}{1-\hat{\psi}(u)}. \tag{229}$$

Let us consider the GME given by

$$\frac{\mathrm{d}}{\mathrm{d}t}\mathbf{p}(t) = -\int_0^t \mathrm{d}t' \Phi(t-t')\mathbf{K}\cdot\mathbf{p}(t'). \tag{230}$$

We see that the Laplace transform of (230) yields

$$\hat{\mathbf{p}}(u) = \frac{1}{u + \hat{\Phi}(u)\mathbf{K}}\mathbf{p}(0), \tag{231}$$

thereby establishing that the CTRW is equivalent to the GME of (230), with the condition

$$\mathbf{M} = -\mathbf{K} + \mathbf{1}. \tag{232}$$

At this stage we make the assumption that $p_1(0) = 1$ and $p_2(0) = 0$. This is equivalent to establishing an out-of-equilibrium fluctuation at the same moment the network is prepared. We are interested in determining the regression to equilibrium of this fluctuation. Therefore we define the residual probability

$$\Pi(t) \equiv p_1(t) - p_2(t). \tag{233}$$

Using the GME of (230) and the explicit expression for $\mathbf{K}$ given by (224), we obtain

$$\frac{\mathrm{d}}{\mathrm{d}t}\Pi(t) = -\int_0^t \mathrm{d}t'\Phi(t-t')\Pi(t')\mathrm{d}t'. \tag{234}$$

It is straightforward to prove that the Laplace transform of $\Pi(t)$, as determined by (234), is identical to the Laplace transform of $\Psi(t)$ of (174). Consequently their inverse Laplace transforms are also equal

$$\Pi(t) = \Psi(t), \tag{235}$$

which identifies the regression to equilibrium with the survival probability. The survival probability $\Psi(t)$ is not the equilibrium autocorrelation function, but it can be interpreted as a non-stationary autocorrelation function of age $t_a = 0$.

This approach has been extended by Allegrini et al. (2005), to the case when the preparation of the network is done at $-t_a < 0$, while the out-of-equilibrium fluctuation is created at $t = 0$. In this case they derived an aged GME that reads

$$\frac{\mathrm{d}}{\mathrm{d}t}\mathbf{p}(t) = -\int_0^t \mathrm{d}t'\Phi_{t_a}(t-t')\mathbf{K}\cdot\mathbf{p}(t'). \tag{236}$$

The Laplace transform of the aged memory kernel $\Phi_{t_a}(t)$ is given by

$$\hat{\Phi}_{t_a}(u) = \frac{u\hat{\psi}_{t_a}(u)}{1-\hat{\psi}_{t_a}(u)}. \tag{237}$$

In direct analogy with the $t_a = 0$ case, the time evolution for $\Pi(t)$ reads

$$\frac{\mathrm{d}}{\mathrm{d}t}\Pi(t) = -\int_0^t \mathrm{d}t'\Phi_{t_a}(t-t')\Pi(t')\mathrm{d}t'. \tag{238}$$

Thus, we obtain the following generalization of the OP

$$\Pi(t) = \Phi_\xi^{(t_a)}(t). \tag{239}$$

The function $\Phi_\xi^{(t_a)}(t)$ is the aged autocorrelation function of the dichotomous fluctuation $\xi(t)$, whose Laplace transform is given by

$$\hat{\Phi}_\xi^{(t_a)}(u) = \frac{1}{u+\hat{\Phi}_{t_a}(u)}. \tag{240}$$

Using (237) we find that (240) can also be written as

$$\hat{\Phi}_\xi^{(t_a)}(u) = \frac{1}{u}(1-\hat{\psi}_{t_a}(u)), \tag{241}$$

which establishes the equivalence between the aged autocorrelation function and the aged survival probability

$$\Phi_\xi^{(t_a)}(t) = \Psi_{t_a}(t). \tag{242}$$

It is straightforward to prove that for $t_a = 0$ (237) reduces to (229) so that we recover the relation (239). It is even more important to understand why this procedure is a generalization of the OP. To realize this important fact, let us rewrite (206) in the equivalent form

$$\psi_{t_a}(t) = \int_0^{t_a} \mathrm{d}yP(y)\psi(y+t), \tag{243}$$

where $P(t)$ is the time density of event production defined in (209). In the case $2 < \mu < 3$, we have

$$\hat{\psi}(u) = 1 - \langle\tau\rangle u - \Gamma(2-\mu)(uT)^{\mu-1} + \cdots. \tag{244}$$

In this case (211) yields

$$P(t) = \frac{1}{\langle\tau\rangle}\left[1+\left(\frac{T}{t}\right)^{\mu-2}\right]. \tag{245}$$

Although $\mu > 2$ ensures the ergodic condition, as we move closer and closer to $\mu = 2$, the border with the non-ergodic condition, the relaxation towards the constant rate production becomes critically slow. Nevertheless, for $t_a \to \infty$, (243) yields

$$\psi_\infty(t) \equiv \psi_{t_a=\infty}(t) = \frac{1}{\langle\tau\rangle}\int_t^\infty \mathrm{d}t'\psi(t'). \tag{246}$$

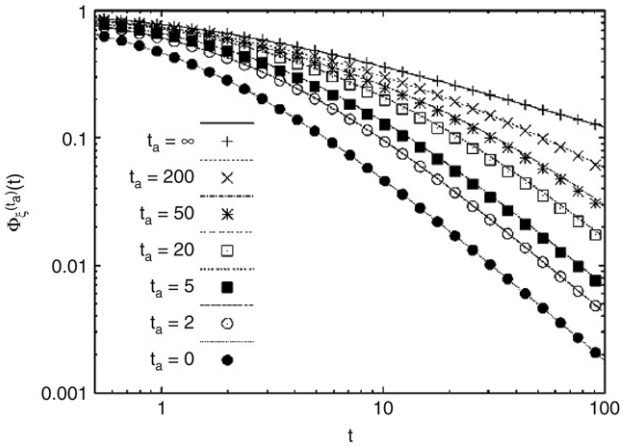

Fig. 7. The t_a-old correlation function, $\Psi_\xi^{(t_a)}(t)$, for different values of t_a. Curves represent the exact result of Eq. (241) for $\mu = 5/2$ and $T = 1.5$, obtained with the numerical procedure described by Allegrini et al. (2005). The dots correspond to the approximate formula of Eq. (247). Taken from Allegrini et al. (2005).

Then, using (237) and (240), we find that the Laplace transform of $\hat{\Phi}_\xi^{(\infty)}(t) \equiv \hat{\Phi}_\xi^{(t_a=\infty)}(t)$ coincides with the Laplace transform of (183) which is a well known expression established by renewal theory for the equilibrium autocorrelation function of $\xi(t)$, see Geisel et al. (1985). This demonstrates in an explicit way that (239) is a generalization of the OP. It is, at the same time a procedure yielding the non-stationary autocorrelation function that coincides, see Allegrini et al. (2005), with the exact prescription of Godréche and Luck (2001).

Unfortunately, the exact expression for the aged autocorrelation function does not have a simple analytical form, however, using the method of conditional probabilities the following analytical expression was constructed, see Allegrini et al. (2005),

$$\Phi_\xi^{(t_a)}(t) = \left(\frac{T}{T+t+t_a}\right)^{\mu-1} + \left[1 - \left(\frac{T}{T+t_a}\right)^{\mu-1}\right] C(t), \tag{247}$$

where

$$C(t) \equiv \frac{\left(\frac{T}{T+t}\right)^{\mu-2} + \left(\frac{T}{T+t+t_a}\right)^{\mu-2}}{1 - \left(\frac{T}{T+t_a}\right)^{\mu-2}}. \tag{248}$$

In Fig. 7 we compare this approximate expression to a numerical treatment yielding the exact autocorrelation function. Moving from the top to the bottom curves the age increases from the brand new kernel ($t_a = 0$) to the infinitely aged, or stationary kernel ($t_a = \infty$). The comparison of the approximate to the exact autocorrelation function is seen to be very good.

4.5. Aging networks

Let us review the main results established in this section. First of all, we determined that the waiting-time distribution is not, by itself, an unambiguous indicator of complexity. This confirms the conclusion of earlier work done by Allegrini et al. (2002a) from within a new perspective made attractive by the modulation, or superstatistics, approach to complexity, see, e.g., Beck (2001) and Cohen (2004). We have seen that the adoption of the aging perspective bypasses the limits of the conventional methods of analysis, since it establishes beyond any doubt the difference between the renewal and the modulation character of a sequence of event occurrence times. This is a fact of some physical importance for the physics of BQDs, see, e.g., Kuno et al. (2001). The work of Brokmann et al. (2003) has already established aging in the intermittent fluorescence of these new materials, and more recent work of Bianco et al. (2005) and Bianco and Grigolini (2005) confirms that this aging is due to the renewal character of the process. Thus, we conclude, that the dynamic process responsible for intermittent fluorescence must be built up on the basis of a renewal perspective. Of course, the fact that superstatistics is ruled out as a proper interpretation of the physics of BQDs does not mean, in any way, that there are no interesting complex processes in nature that might have their roots in this attractive perspective. This remark is related to the second important result of this section. Modulation, underlying superstatistics, corresponds to a slow physical process whose realization does not rest on a unique procedure. However, it is plausible that any realization of modulation might generate its own crucial events. These crucial events are embedded in a Poisson sea, exerting a camouflage action, which makes it extremely difficult

to confirm their existence. We have seen that these invisible events establish the anomalous scaling of the process. On the basis of earlier work done by Allegrini et al. (2002b) we think that this anomalous scaling refers to the central part of the probability density distribution, and that the resulting anomalous diffusion is multiscaling. There are good reasons to believe that with suitable developments along the lines of other work, see Allegrini et al. (2002b), that it will be possible to successfully address this challenging problem.

5. Subordination and complexity matching

This section is devoted to preparing the ground for the derivation of the new phenomenon of complexity matching (CM). The CM phenomenon is based on the dialogue between the crucial events of the perturbed and the crucial events of the perturbing network. The crucial events are not always visible as in the paradigmatic case of the subordination to the ordinary fluctuation–dissipation (SOFD) process (of the second) that will be illustrated in Section 5.2.2. Although the phenomenon of CME is illustrated in Section 6 with the help of a new FDT (of the first kind) determined by the direct action of crucial events, there are preliminary experimental results showing that the crucial events may lead to the transport of information even if the events are not visible. For this reason, before illustrating the CME we describe the subordination perspective, in a form similar to that used by Sokolov (2000), Barkai and Silbey (2000) and Metzler and Klafter (2000b).

The essential theoretical argument presented in this section is based on the CTRW, which is here freely interpreted and generalized as a way to express anomalous statistical physics in terms of ordinary Poisson and fluctuation–dissipation processes. The events occurring on the natural time scale in the continuum become the *critical events*: events that are non-Poisson and in some extreme cases are also non-ergodic. These critical events are expected to produce significant effects in the long-time limit, which may require however, suitable techniques of analysis, to be revealed. Relaxation processes described by stretched exponential functions, which are interpreted as intermediate asymptotic properties that play the important role of disclosing the true complexity of the network under study, in spite of the finite size effects that annihilate the asymptotic inverse power-law. Although the inverse power-law is correctly interpreted as a genuine form of complexity, it may be difficult to directly observe it for some phenomena. The CME rests on tuning the index of the inverse power law of the perturbation to the index of the inverse power law of the network, and the effect can occur in spite of the fact that the inverse power law may not be directly observable.

Electroencephalogram (EEG) data provide an attractive example of this latter CM phenomenon. All this is described by the process of SOFD processes through a subordination function, with the distinct aspect of an inverse power law. However, subordination generates macroscopic survival probabilities, where the inverse power-law is apparently lost, leaving its influence only on an extended stretched exponential regime that shows up in brain dynamics both at the global level of interacting signals recorded by multiple electrodes and at the single signal level of an individual electrodes.

5.0.1. Electroencephalograms (EEGs)

In this section the data to which we apply many of our ideas are taken from the electrical activity of the human brain. The mammalian brain generates a small but measurable electrical signal; first measured in small animals by Caton in 1875 and in people by Berger in 1925. The trace left on a stripchart by this amplified signal was called an electroencephalograph and the term electroencephalogram (EEG) has subsequently been used to identify the electrical signal. The power associated with the EEG signal is distributed over the frequency interval 0.5–100 Hz, with most of it concentrated in the interval 1–30 Hz. A typical EEG signal looks like a random time series with contributions from every part of the spectrum appearing with random phases. This aperiodic signal changes throughout the day and changes clinically with sleep, that is, the *alpha* (8–14 Hz) rhythm which dominate the EEG signal of an awake individual with eyes closed is almost completely absent when a person is asleep.

In over one hundred years since its discovery there have been a variety of methods used in attempts to establish the taxonomy of EEG patterns in order to delineate the correspondence between brain wave patterns and brain activity. The mathematician Norbert Wiener believed that *generalized harmonic analysis*, see Wiener (1958), would provide the mathematical tool necessary to penetrate the mysterious relations between the EEG time series and the functioning of the brain. More recently nonlinear dynamics, chaos and fractals have lead the parade of methodologies hoping to accomplish this task, see, e.g., West and Deering (1995) for a brief review. The progress along this path has been slow and the understanding and interpretation of EEG signals remain elusive. However along the way certain properties of EEG signals have revealed themselves.

The erratic behavior of the EEG signal is so robust that it persists through all but the most drastic situations including near-lethal levels of anesthesia, several minutes of asphysia and the complete surgical isolation of a slab of cortex, see, e.g., Freeman (1975). Babloyantz and Destexhe (1987) suggested that cognitive attractors exist, as demonstrated using attractor reconstruction techniques and that the observed fluctuations in EEG time series were the result of chaotic dynamics within the brain. The EEG time series of awake, alert individuals were shown to have non-stationary statistics, see Layne et al. (1986), and are of high, perhaps infinite, dimension, suggesting that the signals are not generated by strange attractors, but are random and not chaotic. However, these observations were made before the properties of intermittent chaotic maps were widely known. By way of contrast, it was shown by Babloyantz (1986) that the various stages of sleep can be

characterized by quite different fractal dimensions implying that if a cognitive attractor does exist it is not static; it and its corresponding fractal dimension varies with the level of sleep. One of the strongest arguments for this latter perspective is the explicit set of coupled nonlinear differential equations with interconnections that are specified by the anatomy of the olfactory bulb, the anterior nucleus and the prepyriform cortex of a rat, see Freeman (1987). The solution to these equations yield an attractor that is qualitatively very similar to that obtained from the observed EEG time series for an induced epileptic seizure in the rat's brain, using the attractor reconstruction method.

The brain's electrical signals originate from the interconnections of the neurons through collections of dendritic tendrils interleaving the brain mass. These collections of dendrites generate signals that are correlated in space and time near the surface of the brain, and their propagation from one region of the brain's surface to another can be followed in real time. The EEG signal is consequently the field generated partly by a superposition of spike trains from individual neurons and partly the result of such trains triggering additional neurons along their path to the network. According to some neurophysiologists the statistics of neural spike trains are renewal, see van Vreewijk (2001), and they are remarkably non-Poisson, see Baddeley et al. (1997). The mathematics of such point processes are presented in the excellent monograph of Lowen and Teich (2005). The experimental evidence of *in vitro* observations coupled with the analysis of *in vivo* spiking patterns indicate that single neurons generate non-Poisson time series, see, e.g., Stevens and Zador (1998), Sakai et al. (1999), Sakai (2001), Shinomoto and Tsubo (2001), Feng and Zhang (2001), Salinas and Seinowski (2002), Hinomoto et al. (2003) and Shadlen and Newsame (1998). The implicit assumption made in much of the neurophysiology literature is that even if the spiking activity of a single neuron is not Poisson, the activity of a network of many neurons is Poisson. The implied Poisson nature of the human brain has been proven to be invalid, see Câteau and Reyes (2006); a conclusion also reached by Bianco et al. (2007a,b). Consequently, we anticipate that brain activity can be interpreted as a non-stationary, non-Poisson, renewal process and we implement a number of techniques to support this interpretation.

5.1. Single subordination

Let us assume that at every time step we toss a coin so as to generate the fluctuations of our now standard dichotomous variable ξ_S. Let us adopt a Gibbs perspective, and assume that at any time step we locate in the state $|1\rangle$ all the N_1 networks corresponding to heads and in the state $|2\rangle$ all the N_2 networks corresponding to tails. Note that we assume $N = N_1 + N_2$ to be very large so as to identify N_1/N with the probability of finding the network in the state $|1\rangle$ and N_2/N with the probability of finding the network in the state $|2\rangle$. Let us define the vector $\mathbf{p} \equiv (p_1, p_2)$. Thus, in a discrete time representation, we have

$$\mathbf{p}(n+1) - \mathbf{p}(n) = -\mathbf{K} \cdot \mathbf{p}(n), \tag{249}$$

where $\mathbf{K}$ is given by (224). As a consequence of this coin tossing procedure, the non-equilibrium indicator function

$$\Pi(n) = p_1(n) - p_2(n), \tag{250}$$

moving from an out-of-equilibrium condition $\Pi(0)$, reaches the equilibrium value $\Pi = 0$ in one time step.

Let us imagine now that the nth coin tossing action takes place at time $t(n)$ and that the time interval between two consecutive coin tossing actions $\tau_n = t(n+1) - t(n)$ is derived from a given distribution density $\psi^{(S)}(\tau)$, called the subordination function for reasons that are explained subsequently. In this case the CTRW yields

$$\mathbf{p}(t) = \sum_{n=0}^{\infty} \int_0^t \mathrm{d}t' \psi_n^{(S)}(t') \Psi^{(S)}(t - t') \mathbf{M}^n \mathbf{p}(0), \tag{251}$$

with the relation between the matrices $\mathbf{M}$ and $\mathbf{K}$ given by (232). Note that $\psi_n^{(S)}(t)$ is the probability of drawing from the waiting-time distribution n times with the condition that the last drawing occurs exactly at time t. Thus, in the case of (251) the last of n drawings occurs at time t', thereby generating the vector $\mathbf{M}^n\mathbf{p}(0)$ whose form remains unchanged up to time t, insofar as no further drawing occurs between t' and t. This last condition is ensured by the survival probability $\Psi^{(S)}(t - t')$. In fact

$$\Psi^{(S)}(t) \equiv \int_t^{\infty} \mathrm{d}t' \psi^{(S)}(t') \tag{252}$$

is the probability that no drawing occurs up to time t.

By Laplace transforming (251) we obtain

$$\hat{\mathbf{p}}(u) = \frac{1 - \psi^{(S)}(u)}{u} \frac{1}{(1 - \mathbf{M}\hat{\psi}^{(S)}(u))} \mathbf{p}(0), \tag{253}$$

which, after simple algebra, is shown to be equivalent to

$$\hat{\mathbf{p}}(u) = \frac{1}{u - \frac{u\hat{\psi}^{(S)}(u)}{1 - \hat{\psi}^{(S)}(u)}(\mathbf{M} - 1)} \mathbf{p}(0). \tag{254}$$

Let us consider the GME given by (230)

$$\frac{\mathrm{d}}{\mathrm{d}t}\mathbf{p} = -\int_0^t \mathrm{d}t' \Phi(t-t')\mathbf{K}\cdot\mathbf{p}(t'), \tag{255}$$

whose memory kernel, $\Phi(t)$, is related to the subordination function $\psi^{(S)}(t)$, in the Laplace domain, by

$$\hat{\Phi}(u) = \frac{u\hat{\psi}^{(S)}(u)}{1-\hat{\psi}^{(S)}(u)}. \tag{256}$$

The Laplace transform of the GME (255) coincides with (254), when the Laplace transform of the memory kernel is given by (256), thereby establishing that (255) coincides with (251) and the GME coincides with the result of CTRW using the subordination function as well.

5.1.1. Physical meaning of subordination and coin tossing

The coin tossing process described by the matrix (224) can be thought of as a two-state network that at any time step can make a jump from one to the other state or remain in the same state with equal probability. We have seen that when we adopt the Gibbs perspective the quantity $\Pi(n)$ in one single step moves from the non-equilibrium value $\Pi(n) \neq 0$ to the equilibrium value $\Pi(n+1) = 0$. In other words, the network relaxes to equilibrium in one time step. Adopting (255) allows us to define the relaxation to equilibrium by (234), whose Laplace transform is

$$\hat{\Pi}(u) = \frac{1-\hat{\psi}^{(S)}(u)}{u}\Pi(0), \tag{257}$$

thereby implying

$$\frac{\Pi(t)}{\Pi(0)} = \Psi^{(S)}(t). \tag{258}$$

This is an expected result, insofar as the probability that the quantity $\Pi(t)$ does not vanish is evidently equal to the probability that no event occurs up to time t. In this case the regression to equilibrium is directly related to the critical events. In fact, the value of $\Pi(t)$ at time t is proportional to the probability that no critical event occurs up to time t.

We can also reverse this result. Any relaxation process described by the survival probability $\Psi^{(S)}(t)$ can be thought of as being subordinated to the coin tossing process described by the matrix $\mathbf{K}$ of (224) by means of the subordination function

$$\psi^{(S)}(t) = -\frac{\mathrm{d}}{\mathrm{d}t}\Psi^{(S)}(t). \tag{259}$$

Note that a significant restriction to the possibility of relating a generic relaxation to a subordination function is given by the fact that the subordination function is the distribution of waiting times between two consecutive events. Thus, it is always positive and the corresponding survival probability must correspond to a monotonic relaxation.

5.1.2. Ordinary master equation

Let us consider the case where the subordination function $\psi^{(S)}(t)$ has the exponential form

$$\psi^{(S)}(t) = g\mathrm{e}^{-gt}. \tag{260}$$

In this case the Laplace transform of the memory kernel (256) yields

$$\hat{\Phi}(u) = g, \tag{261}$$

and the memory kernel is

$$\Phi(t) = g\delta(t). \tag{262}$$

Thus the GME (255) becomes identical to the ordinary master equation

$$\frac{\mathrm{d}}{\mathrm{d}t}\mathbf{p} = -g\mathbf{K}\cdot\mathbf{p}(t). \tag{263}$$

Note that the stochastic trajectory, of which this master equation is the Gibbs representation, is described by Fig. 8(a). This is the case because we consider the stochastic dichotomous variable $\xi_S(t)$.

Let us consider the special case $g \ll 1$, where we can realize the subordination process with the help of a Demon's action sketched in Fig. 8(b). The coin tossing process is done by the Demon. However, the coin tossing corresponds to an event and the coin tossing event is realized only when the Demon draws a black ball from a box filled by a very large number of white balls, with only a few black balls. In other words

$$g = \frac{N_B}{N_B + N_W}, \tag{264}$$

where N_B and N_W denote the number of black and white balls contained in the box, respectively.

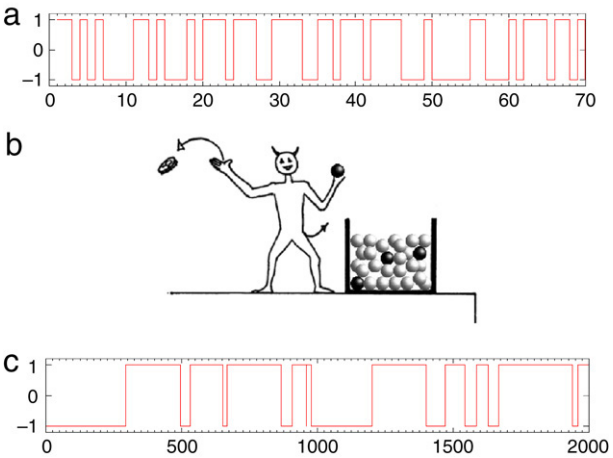

Fig. 8. Panel (a) illustrates the fluctuation generated by adopting a coin tossing procedure. Heads yields the value 1 and tails the value −1. Panel (b) sketches the Demon's action with $g = 0.001$. When the Demon draws a black ball he tosses a coin to decide whether to adopt the value of 1 or the value of −1, as illustrated by Panel (a). Panel (c) shows the fluctuations produced by the Demon by tossing a coin when he draws a black ball.

According to (259) the exponential subordination function of (260) yields the exponential survival probability

$$\Psi^{(S)}(t) = \mathrm{e}^{-gt}. \tag{265}$$

This result can be easily recovered with the model of the Demon trying to get a black ball by means of random drawings from a box filled mainly with white balls. In fact, the survival probability in one drawing is evidently $1 - g$. Consequently, the survival probability after t drawings is

$$\Psi^{(S)}(t) = (1 - g)^t, \tag{266}$$

which is, in fact, equivalent to (265), for $t \to \infty$, due to the small value of g.

In summary, a lazy Demon, who does the coin tossing only from time to time, as prescribed by the subordination function of (260), is equivalent to a Demon who never rests but has a small success rate, $g \ll 1$. In the Poisson case a very limited success rate is equivalent to a time dilatation, from 1 to $1/g$. We shall see that when the social life of the Demon is described by an inverse power-law distribution density, a limited success rate produces not only a time dilatation, but a more extended regime of transition to the inverse power-law regime in the form of a stretched exponential.

5.1.3. Non-exponential subordination

The subordination function, interpreted as the measure of the time interval between two critical events, the drawing of a black ball, is not confined to the exponential case. Let us imagine, for instance, that the Demon's box has a leak that reduces the number of black balls as a function of time so that g, rather than being constant, is time dependent:

$$g(t) = \frac{g_0}{1 + g_1 t}. \tag{267}$$

In this case the survival probability is

$$\Psi^{(S)}(t) = \prod_{t'=1}^{t} \left(1 - g(t')\right), \tag{268}$$

which, in the time continuum limit, becomes

$$\Psi^{(S)}(t) = \exp\left(-\int_0^t \mathrm{d}t' g(t')\right). \tag{269}$$

By inserting (267) into (269), after some algebra yields

$$\Psi^{(S)}(t) = \left[\frac{T_S}{T_S + t}\right]^{\mu_S - 1}, \tag{270}$$

where the time parameter is $T_S = \frac{1}{g_1}$ and the power-law index is $\mu_S - 1 = \frac{g_0}{g_1}$. The corresponding subordination function $\psi^{(S)}(t)$, according to (259), is given by

$$\psi^{(S)}(t) = (\mu_S - 1)\frac{T_S^{\mu_S - 1}}{(t + T_S)^{\mu_S}}, \tag{271}$$

which, of course, is properly normalized.

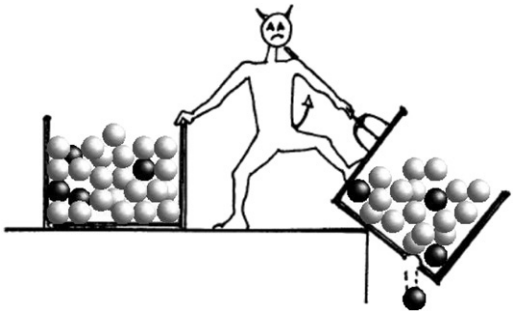

Fig. 9. The Demon immediately after drawing a black ball, throws away the leaking box and begins using a new one that at the moment when it is used begins leaking.

Note that the form of (271) is a simple way of connecting the short-time properties, where the inverse power-law form does not yet appear, to the long-time limit $t \gg T_S$, where the inverse power-law form becomes evident. The parameter T_S keeps under control the time extent through which the transition from microscopic dynamics, with no inverse power law, to macroscopic dynamics with an inverse power law, occurs. As we shall see, non-renewal aging is related to this parameter becoming larger and larger as an effect of aging. It is important to remark, however, that this regime of transition to the long-time regime bears signs of complexity in the form of the inverse power-law index μ_S. For simplicity's sake, it is convenient to assume this transition regime is as short as possible and assign to T_S the shortest possible value, $T_S = 1$, if we set the elementary time step to be $\Delta t = 1$. We shall see, however, that when the non-exponential waiting time distribution $\psi^{(S)}(t)$ is used as the subordination function, a new intermediate time regime appears, and this time regime contains information about the network's complexity.

The adoption of (259) is made possible when the renewal condition applies as pointed out by Cox (1967). This is an important property that requires further comment. Let us examine two distinct situations:

(a) When the Demon draws a black ball, after a time much longer than expected due to the leaking of the black balls, she becomes very upset, throws away the leaking box and replaces it with a brand new box. The new box is characterized by the same properties as the original one, including the leaking of black balls (see Fig. 9). The result is a homogeneous non-Poisson process.

(b) The Demon keeps using the same box. In the case where the time dependence of $g(t)$ is slow enough this process becomes virtually equivalent to the slow modulation phenomenon discussed in Section 4.3. It is evident that this condition is not renewal, thereby preventing us from using (259).

As to condition (a), the work of Daly and Porporato (2006) allows us to interpret it in terms of a neuron firing model. According to these authors the voltage x of a neuron obeys the equation of motion

$$\frac{\mathrm{d}}{\mathrm{d}t}x = k + F(x, t), \tag{272}$$

where k is a constant yielding the deterministic motion $x(t) = kt$. The voltage increases linearly from $x = 0$ and the condition for firing resets the network back to zero, once the voltage has attained a preset level. The firing process is described by the function $F(x, t)$ which we assume to have the voltage-dependent form

$$F(x) = \frac{A}{1 + x}. \tag{273}$$

The time-dependent rate is obtained by inserting the deterministic solution into (273) to yield

$$F(t) = \frac{A}{1 + kt}, \tag{274}$$

which is identical to (267), with $g_0 = A$ and $g_1 = k$.

It is important to notice that, according to the perspective emerging from the work of Barabási (2005) and Vazques et al. (2007), on e-mail users, as well as on the Einstein and Darwin correspondence, the inverse power law of the waiting time distribution is an ineluctable consequence of the social nature of human activities. Thus, it is perhaps more convenient to interpret the inverse power law distribution density $\psi^{(S)}(\tau)$ of (271) as a consequence of the Demon's social life.

Let us now focus on the renewal case. It is possible to demonstrate that the subordination function $\psi^{(S)}(t)$, of any analytical form, can be realized with the Demon model (a). In fact, for a given $\psi^{(S)}(t)$ we use (259) to derive the survival probability $\Psi^{(S)}(t)$. Then, using (269) we obtain

$$g(t) = \frac{\psi^{(S)}(t)}{\Psi^{(S)}(t)}, \tag{275}$$

which is an important relation of Renewal Theory, see, e.g., Cox (1967), allowing us to establish the time dependence of the number of black balls to realize a subordination function of any form.

It is important to point out, however, that the model of a time-dependent rate, $g(t)$, which ultimately corresponds to the well known prescriptions of renewal theory, see Cox (1967), is here used only for tutorial purposes. The reasons why the inverse power law with index μ_S emerges are rooted, in the case of neuron dynamics on the cooperation among neurons, even in the case when only the firing of a single neuron is observed, see, e.g., Beggs and Plenz (2003), Plenz and Thiagarajan (2007), Haldeman and Beggs (2005) and Kinouchi and Copelli (2006).

Note that to take into account the renewal character of case (a), it is convenient to write the time-dependent rate of event production $g(t)$ in the time region between the event occurring at time t_i and the next event, occurring at time $t_{i+1} > t_i$, in the form

$$g(t) = \frac{g_0}{1 + g_1 \Delta t}, \tag{276}$$

where $\Delta t = t_{i+1} - t_i$. The introduction of the *stochastic* time Δt is made necessary to generate a calculational algorithm that is a faithful representation of both conditions illustrated in this subsection. The first condition is the upset Demon throwing away a box and replacing it with a new one when she eventually, after many drawings, finally gets a black ball. The second condition is that of the neuron voltage recovering its initial condition immediately after firing, see Daly and Porporato (2006). We emphasize that the upset Demon throwing away a box is an intuitive representation of a critical event. Unfortunately, the critical events are not so plainly evident, and special methods must be adopted to reveal their occurrence. We show that such methods exist, and are used to reveal the occurrence of critical events in the brain's EEG time series.

5.1.4. Renewal versus non-renewal aging

The cases (a) and (b) of the last subsection makes it convenient for us to go back to the aging issue of Section 4.4 to shed further light on the difference between *renewal* and *non-renewal* aging. The non-renewal aging is easier to understand. Therefore, let us begin by discussing this case. Note that the subordination process is implemented with the subordination function $\psi^{(S)}(t)$, which corresponds to a renewal process. We do not produce subordination by means of a non-renewal process. Let us imagine that at a given time t', regardless of whether an event occurs or not, the Demon focuses her attention only on the networks in the state $|1\rangle$, and she evaluates the corresponding non-stationary survival probability:

$$\Psi(t, t') = \exp\left(-\int_{t'}^{t} \mathrm{d}t'' g(t'')\right). \tag{277}$$

In fact, this is the same condition as that examined by means of (269). The survival probability $\Psi(t) = 1$ at $t = t'$ as a consequence of the fact that at the moment when observation begins, the Demon focuses her attention only on the networks in the state $|1\rangle$. This is a way to generate out-of-equilibrium conditions, without perturbing the network's dynamics, see, e.g., Allegrini et al. (2005). In the special case when at $t = t'$ an event occurs, equilibrium would be realized. However, if this is also the beginning of the observation process, the Demon creates an out-of-equilibrium condition that is not associated with the replacement of the old box with a new one. This Demon keeps drawing balls from the same box. After some straightforward algebra in this case we obtain

$$\Psi(t, t') = \left[\frac{T_S}{T_S + t}\right]^{\mu_S - 1} \left[\frac{T_S + t'}{T_S}\right]^{\mu_S - 1} = \left[\frac{T_S + t'}{T_S + t' + (t - t')}\right]^{\mu_S - 1}. \tag{278}$$

We see that this kind of non-renewal aging corresponds to the parameter T_S becoming larger and larger as a consequence of the increasing time. If the out-of-equilibrium condition corresponding to the observation beginning is realized at time $t' > 0$, while the ball box is brand new at time $t = 0$, T_S is replaced by $T_S + t'$.

In summary, the non-renewal aging yields a survival probability characterized by the property that the emergence of the inverse power-law behavior occurs at later times with increasing t', the age of the network.

Case (a) is characterized by different properties. First of all the survival probability, this time, depends on whether or not the beginning of the observation process coincides with the occurrence of an event. Let us denote by $\Psi(t|t_i)$ the survival probability referred to the initial time t_i, under the condition that the beginning of observation process corresponds to the occurrence of an event, so that

$$\Psi^{(S)}(t|t_i) = \Psi^{(S)}(t - t_i). \tag{279}$$

This result is easily obtained by inserting (276) into (277). Thus, we see that a major difference between the renewal and non-renewal cases is that the non-renewal aging is independent of whether the observation beginning coincides with the event occurrence or not. In the renewal case we have

$$\Psi^{(S)}(t|t') \neq \Psi^{(S)}(t, t'). \tag{280}$$

We now address the delicate problem of evaluating $\Psi^{(S)}(t,t')$ in the case of renewal aging. This problem has been discussed at length in the recent literature by Allegrini et al. (2007c) and Aquino et al. (2004). From a formal point of view, the waiting time distribution density of age t' is given by (see also (206))

$$\psi^{(S)}(t,t') = \psi^{(S)}(t) + \sum_{n=1}^{\infty} \int_0^{t'} \psi_n^{(S)}(t'')\psi^{(S)}(t-t'')\mathrm{d}t''. \tag{281}$$

We refer the reader to Section 4.4.1 for the physical meaning of this exact expression.

5.2. Double subordination

Let us now address the problem of creating a process subordinated to the fluctuations $\xi_S(t)$ illustrated in Fig. 8(c). In the long-time limit, the survival probability $\Psi(t) = \exp(-gt)$ is indistinguishable from the coin-tossing survival probability itself. Thus, to create a process departing from the conditions of ordinary statistical mechanics, we adopt for the second subordination process the subordination function given by the inverse power law (271).

To shed light on the nature of the resulting process, we analytically evaluate the resulting survival probability $\Psi_{SP}(t)$ by means of the following formula

$$\Psi_{SP}(t) = \sum_{n=0}^{\infty} \int_0^t \mathrm{d}t' \psi_n^{(S)}(t')\Psi^{(S)}(t-t')\mathrm{e}^{-gn}. \tag{282}$$

This formula rests on the same arguments as those leading to (251), but with a different physical meaning. We are using the very small rate condition $g \ll 1$. Thus, we imagine that the original Poisson process rests on the unit time step $\Delta t = 1$, and assume that it refers to a natural time scale, where time is a discrete number $n = 1, 2, \ldots$. The exponential survival probability of (265) now reads

$$\Psi(n) = \mathrm{e}^{-gn}. \tag{283}$$

Let us now consider the generic time t. How many times did the Demon of Fig. 8(b) draw balls from her box filled mainly with white balls? She may have done no drawing, one drawing, two drawings, and so on. When she draws a black ball, she tosses a fair coin, and consequently, she realizes equilibrium. The survival probability becomes smaller with an increased number of drawings. This explains the exponential weight $\exp(-gn)$ on the right-hand side of (282). As in the case of (251), the probability that the last of a sequence of n drawings occurs at time t' is given by $\psi_n^{(S)}(t')$, and the probability that no drawing occurs after this last drawing up to time t is given by $\Psi^{(S)}(t-t')$.

Using the same Laplace transform method as that adopted to derive (254) we now obtain

$$\hat{\Psi}_{SP}(u) = \frac{1}{u + \frac{u\hat{\psi}^{(S)}(u)}{1-\hat{\psi}^{(S)}(u)}\,(1-\mathrm{e}^{-g})}. \tag{284}$$

Note that in accordance with the condition $g \ll 1$ we may expand the exponential and write (284) as

$$\hat{\Psi}_{SP}(u) = \frac{1}{u + \frac{u\hat{\psi}^{(S)}(u)}{1-\hat{\psi}^{(S)}(u)}g}. \tag{285}$$

At this point we stress the difference between the two cases $\mu_S > 2$ and $\mu_S < 2$. As mentioned earlier we are using the subordination function (271). The mean waiting time is therefore given by

$$\langle\tau\rangle = \frac{T_S}{\mu_S - 2} \tag{286}$$

which diverges at $\mu_S = 2$ and remains divergent in the whole range from $\mu_S = 2$ to $\mu_S = 1$. When $\mu_S > 2$, the mean waiting time is finite and we have for $u \to 0$

$$\hat{\psi}^{(S)}(u) = (1 - \langle\tau\rangle u). \tag{287}$$

Thus, in this case (285) becomes

$$\hat{\Psi}_{SP}(u) = \frac{1}{u + \frac{g}{\langle\tau\rangle}} \tag{288}$$

whose inverse Laplace transform again yields an exponential survival probability. In the latter case the exponential lifetime $1/g$ is turned into $\langle t\rangle/g$, which becomes much larger than the original lifetime in the vicinity of the border with the non-ergodic region, $\mu_S = 2$. In other words, a second subordination process, resting on an exponential subordination function is equivalent to a trivial time dilatation.

The non-ergodic condition $\mu_S < 2$ is much more interesting than the $\mu_S > 2$ situation. In this case, the Laplace transform of $\psi^{(S)}(t)$ is given by (210). Thus, using (284), we obtain for $u \to 0$

$$\hat{\Psi}_{SP}(u) \to e^{g}\hat{E}_{\alpha}(u), \tag{289}$$

where

$$\hat{E}_{\alpha}(u) = \frac{1}{u + \lambda^{\alpha}u^{1-\alpha}}, \tag{290}$$

with $\alpha \equiv \mu_S - 1$ and

$$\lambda = \left(\frac{e^{g} - 1}{\Gamma(2-\mu_S)(T_S)^{\alpha}}\right)^{1/\alpha}. \tag{291}$$

When $\mu_S = 2$ we have $\alpha = 1$ and (290) becomes the Laplace transform of an exponential. The exponential is expected, because $\mu_S = 2$ is the border with the region where, as shown earlier, the mean waiting time $\langle\tau\rangle$ is finite, and consequently the non-exponential subordination is not sufficiently substantial to establish a significant departure from the mere time dilatation produced by a second subordination resting on an exponential subordination function.

We note that the inverse Laplace transform of (290) is the MLF, which we proposed for the generalization of exponential relaxation, see, e.g. West et al. (2003). The main property of the stretched exponential invading the whole time region with $\lambda \to 0$ has already been used in Section 2.4.2. For the reader's convenience, let us adapt this property to the special condition here under study. According to Mittag–Leffler theory, the stretched exponential

$$E_{\alpha}(t) = \exp(-(\lambda t)^{\alpha}) \tag{292}$$

occurs for $t \ll 1/\lambda$, and the inverse power-law

$$E_{\alpha}(t) \propto \frac{1}{t^{\alpha}} \tag{293}$$

occurs for $t \gg 1/\lambda$. We see that decreasing g has the effect of extending the region where the stretched exponential relaxation of (292) applies. If we increase the parameter g we can significantly reduce the time over which the stretched exponential dominates even making it completely disappear. The double subordination method that we have used rests on the small rate approximation making it impossible to completely suppress the stretched exponential regime. Notice that by increasing g we come close to the condition corresponding to the direct application of the subordination procedure to the coin-tossing process, yielding

$$\Psi_{SP}(t) = \Psi^{(S)}(t), \tag{294}$$

thereby making the resulting survival probability identical to the subordination survival probability of (270).

In summary, the direct subordination to the coin-tossing process does not create any significant intermediate complexity. The transition regime does not afford any information on the network complexity. The subordination to a sufficiently slow Poisson process, or sufficiently slow fluctuation–dissipation process, as we shall see in Section 5.2.2, has, on the contrary, the significant effect of creating an extended intermediate regime with important information on the network's complexity. If there exists an extended regime of transition to the inverse power-law behavior of the survival probability, which significantly departs from the stretched exponential behavior, this may be an indication that the subordination function $\psi^{(S)}(\tau)$ of (271) has a very large T_S, or, more generally, it is characterized by its own slow transition to the inverse power-law regime. In this case we do not obtain reliable information on the complexity parameter μ_S, characterizing the Demon's social life. If, on the contrary, this extended regime of transition to the inverse power-law behavior is distinctly a stretched exponential with the stretching coefficient $\alpha < 1$, then $\mu_S = 1 + \alpha$ may afford reliable information on the Demon's social life. Note that the time series emerging from complex processes are usually of finite duration. Consequently, if the stretched exponential regime is very extended in time, it may be the only form of complexity experimentally accessible. In the opposite situation when the stretched exponential regime is significantly reduced by the adoption of large values of g, the inverse power-law part of the survival probability may become the only one experimentally observable if the finite-size induced truncation of the waiting time distribution density is not drastic (see Section 5.2.3).

As a final remark, we present support for the claim that with $\mu_S > 2$ the subordination process does not produce visible effects that depart from ordinary statistical physics, with an example drawn from Metzler and Klafter (2000a). Let us imagine that there are no truncation effects and that we can explore the asymptotic time regime, where the inverse power-law behavior distinctly appears. The quantity

$$v_t = \xi_S(t) - \xi_S(t-1) \tag{295}$$

is almost everywhere vanishing, becoming finite only when an event occurs and is equivalent to the fluctuations responsible for the sub-diffusion process studied by Metzler and Klafter (2000a). The model of sub-diffusion proposed by these authors yields for $t \to \infty$

$$\langle x^2(t)\rangle \propto t^{\beta}, \tag{296}$$

where

$$\beta \equiv \frac{\alpha}{2} = \frac{\mu_S - 1}{2}. \tag{297}$$

We come back to the scaling index β as a complexity indicator in Section 5.2.2. Here we limit ourselves to noticing that for $\mu_S > 2$, the diffusion regime is characterized by ordinary scaling $\beta = \frac{1}{2}$, which is a clear manifestation of the fact that for $\mu_S > 2$ the Demon's social life does not produce ostensible deviations from ordinary statistical physics.

5.2.1. Alternative physical interpretation of double subordination

Probably a more attractive interpretation of the results of the previous subsection is obtained by going back to the Demon of Fig. 8. This Demon takes action at every time step of the natural time scale. However not all her actions produce events insofar as not all actions correspond to the drawing of a black ball. We do not make the assumption that $g \ll 1$. We now make the weaker assumption $g \leq 1$ and repeat the earlier calculations to obtain

$$\hat{\Psi}_{SP}(u) = \frac{1}{u + g\hat{\Phi}(u)}, \tag{298}$$

where $\Phi(u)$ is given by (256). Setting $g = 1$, we immediately recover (294), thereby establishing that when each of the Demon's actions generate an event the survival probability $\Psi_{SP}(t)$ coincides with $\Psi^{(S)}(t)$, and consequently with the inverse power law (270).

When $g < 1$, we obtain

$$\hat{\Psi}_{SP}(u) = A_g \hat{E}_\alpha(u), \tag{299}$$

with

$$\hat{E}_\alpha(u) = \frac{1}{u + \lambda_\alpha(g) u^{1-\alpha}}, \tag{300}$$

$$\lambda_\alpha \equiv \left[\frac{g}{(1-g)} \frac{1}{T^\alpha \Gamma(1-\alpha)}\right]^{1/\alpha} \tag{301}$$

and $A_g \equiv \frac{1}{(1-g)}$. Note that the overall factor A_g is an artifact of the approximation done when we moved from the discrete to the continuous time picture. In fact the survival probability up to the occurrence of the first event is $1 - g$, which would cancel with the denominator of A_g. A more revealing way of expressing the result of this subsection is given by

$$\Psi_{SP}(t) = E_\alpha\left(-(\lambda_\alpha(g)t)^\alpha\right), \tag{302}$$

where the survival probability is given by a MLF. This is equivalent to neglecting the regime of transition from the microscopic, discrete-time regime, to the Mittag–Leffler regime. We have to keep in mind that the stretched exponential, $\exp(-(\lambda t)^\alpha)$, although fitting the condition $\Psi_{SP}(0) = 1$ corresponds to a time asymptotic rather than to the microscopic time regime.

We have virtually recovered the same result as that of the previous subsection. This shows that the emergence of a stretched exponential can be interpreted in two different but equivalent ways. The former is based on the concept of double subordination. The first subordination process is based on the adoption of an exponential subordination function, which, as shown in Section 5.1.2, is equivalent to the Demon acting with no rest and a very limited success rate. The second subordination process is determined by the Demon's social life and is characterized by $\mu_S < 2$. Thus, it is evident that this process of double subordination can be interpreted as a single subordination applied to a Demon with a very limited success rate. In fact, as shown here, this second procedure yields essentially the same result as the application of the earlier one.

We stress a significant difference with the Demon of Fig. 8. As we saw earlier, decreasing g has the effect of producing a trivial time dilatation. Here decreasing g does more, insofar as it changes the balance between the time extension of the stretched exponential regime and that of the inverse power-law regime. As a consequence, a mere time re-scaling is not sufficient to connect processes with lower values of g to processes with higher values.

5.2.2. Subordination to an ordinary fluctuation–dissipation (SOFD) process

Let us now address the problem of generalizing the double subordination which was seen to be equivalent to creating a process subordinated to a dichotomous Poisson process with rate g. Here we consider the case where the leading process, in the natural time scale n, is given by the ordinary Langevin equation

$$\frac{\mathrm{d}}{\mathrm{d}n} y = -\gamma y(n) + f(n), \tag{303}$$

where $f(n)$ is noise of intensity

$$\langle f^2\rangle_{\rm eq} = \frac{D}{\tau_c} \tag{304}$$

where the eq subscript refers to the equilibrium thermal bath. According to the Einstein fluctuation–dissipation relation, the mean-square value of y is given by

$$\langle y^2\rangle_{\rm eq} = \frac{D}{\gamma}. \tag{305}$$

We again assume for the elementary time step the condition $\Delta n = 1$ that the noise $f(n)$ has the correlation time $\tau_c = 1$. This is noise with no correlation and the diffusion coefficient D becomes identical to the noise intensity. We note that in this case, the time scale is given by $1/\gamma$, thereby playing the role of $1/g$. As in the case of the process subordinated to dichotomous Poisson fluctuations, the condition $\gamma \ll 1$ makes the time n of the order of $1/\gamma$ virtually continuous.

Applying the same approach as that used to derive (255) from (251), we obtain, see Failla et al. (2004),

$$\frac{\partial}{\partial t}P(y,t) = \int_0^t \Phi(t-t')\left[\gamma\frac{\partial}{\partial y}y + \langle y^2\rangle_{\rm eq}\frac{\partial^2}{\partial y^2}\right]P(y,t')\mathrm{d}t', \tag{306}$$

where the memory kernel in the Laplace domain is defined, through the Laplace transform of the subordination function $\psi^{(S)}(t)$, by (256).

It is important to point out that the regression to equilibrium of the w-moments of the dynamic variable $\langle y^w(t)\rangle$ from an initial out-of-equilibrium state $\langle y(0)\rangle$ can be derived using the same arguments as those adopted to derive (282). Thus we obtain

$$Y_w(t) \equiv \langle y^w(t)\rangle = \sum_{n=0}^{\infty}\int_0^t \mathrm{d}t'\psi_n^{(S)}(t')\Psi^{(S)}(t-t')\exp(-\gamma w n). \tag{307}$$

and, instead of (289) we now have

$$\hat{Y}_w(u) \to \mathrm{e}^{\gamma w}\hat{E}_\alpha(u), \tag{308}$$

with $\hat{E}_\alpha(u)$ given by (300), and λ_α defined by

$$\lambda_\alpha = \left(\frac{\mathrm{e}^{w\gamma}-1}{\Gamma(2-\mu_S)(T_S)^\alpha}\right)^{1/\alpha}. \tag{309}$$

It is evident that increasing the moment index w has the effect of reducing the size of the time interval of the stretched exponential relaxation. Note that these results are obtained by assuming $\langle y^2(0)\rangle \gg \langle y^2\rangle_{\rm eq} = y^2_{\rm rms}$ so as to neglect the influence of the stochastic force. The same results are obtained using (306) with only the friction term on its *rhs*.

The stochastic trajectory $y(t)$ fluctuates within a strip of size $y_{\rm rms}$, thereby making it possible to make predictions based on disregarding the first rather than the second term on the *rhs* of (306). This allows us to evaluate the distribution of the time intervals between two consecutive re-crossings of the origin, $y = 0$.

Note that when we disregard the friction term on the *rhs* of (306), this equation becomes equivalent to the CTRW, see Montroll and Weiss (1965), whose scaling index β for the second moment is known to be

$$\beta = \frac{\mu_S - 1}{2}. \tag{310}$$

This scaling can be proved using (306), in the case where dissipation can be neglected to obtain

$$\frac{\partial}{\partial t}P(y,t) = \int_0^t \Phi(t-t')\langle y^2\rangle_{\rm eq}\frac{\partial^2}{\partial y^2}P(y,t')\mathrm{d}t'. \tag{311}$$

Moving to the Laplace–Fourier domain, we obtain for $P^*(k,u)$

$$P^*(k,u) = \frac{1}{u + k^2\hat{\Phi}(u)}. \tag{312}$$

Using (256) and (210) and considering the limit $u \to 0$ we arrive at

$$P^*(k,u) = \frac{1}{u + \gamma\frac{k^2u^{2-\mu_S}}{\Gamma(2-\mu_S)T^{\mu_S-1}}}. \tag{313}$$

Diffusive scaling implies that $y \propto t^{\beta}$, as we mentioned above, and consequently that the Fourier and Laplace variables are related by

$$k \propto u^{\beta}. \tag{314}$$

Invariance by scaling implies that inserting (314) into (313) so as to make $P^*(k, u)$ depend only on u, has the effect of producing a quantity proportional to $1/u$, which is, in fact, the aged memory of an invariant, namely, time-independent quantity. This is realized by imposing the scaling condition of (310), which is consequently proved. This is equivalent to the diffusion scaling of the fractional diffusion process of Metzler and Klafter (2000a), see, (297). As we pointed out earlier, the stochastic velocity creating, in the absence of friction, the diffusion process $y(t)$ obtained through the subordination to the stochastic velocity responsible for ordinary diffusion.

A further way of characterizing diffusive scaling is given by expressing the solution to (311) in the form (201) with $\delta = \beta$. This is an obvious way to satisfy the space–time scaling condition $y \propto t^{\beta}$, if we take into account that the prefactor $1/t^{\beta}$ only serves the purpose of guaranteeing normalization of $F(y)$ when the integration variable y is replaced by the new integration variable $z = y/t^{\beta}$.

Adopting the scaling form of the probability density (201) allows us to determine the asymptotic properties of the waiting time distribution density $\psi^{(D)}(t)$ which is derived from the origin re-crossing histogram. We record the times t_i defined by

$$y(t_i) = 0 \tag{315}$$

and define the time interval between successive re-crossings $\tau_i = t_{i+1} - t_i$. We note that these are renewal events, insofar as they have been proven, see Cakir et al. (2007), to fit the renewal criterion illustrated in Section 4.2. However, we must emphasize that these renewal events are not as important as the renewal events associated with the subordination function $\psi^{(S)}(t)$. In fact, as we have seen, in the case of the subordination to a coin-tossing process, these events correspond to the choice of either $+1$ or -1. In the case of the double subordination, they correspond to the drawing of a ball, whose color may leave unchanged the sign of ξ_S, if the ball is white, or may also change it, with equal probability, if the ball is black. In the case of the subordination to an ordinary fluctuation–dissipation process, here under discussion, the Demon is creating a fluctuation $y(t(n))$. In other words, the times $t(n)$ are the times at which the fluctuation $y(t)$ may undergo an abrupt change, due to the fact that the stochastic force $f(n)$ is assumed to be white. The effect of subordination can also be interpreted as a way to turn this white noise into correlated noise, insofar as it is kept unchanged for the whole time interval between $t(n)$ and $t(n+1)$.

Consequently, the distribution densities $\psi^{(S)}(t)$ and $\psi^{(D)}(t)$ have different physical meanings, although both become inverse power law in the time asymptotic limit. The inverse power law of $\psi^{(S)}(t)$, with $\mu_S > 2$ would be a choice dictated by the fact that, as we have established with (288), the adoption of a subordination function compatible with ergodicity. This process would not depart, in the macroscopic time regime, from the ordinary forms of exponential relaxation. The inverse power-law nature of $\psi^{(D)}(t)$, with $\mu_D < 2$ is a consequence of (201). In fact,

$$\sum_{n=1}^{\infty} \psi_n^{(D)}(t) = Q(t), \tag{316}$$

where

$$Q(t) \equiv P(0, t) = \frac{1}{t^{\beta}} F(0). \tag{317}$$

The rationale for (316) and (317) is as follows. We locate our diffusing trajectory at $y = 0$ at time $t = 0$ and we wait for this trajectory to come back. In the time asymptotic regime where the scaling condition of (201) applies, the trajectory $y(t)$ can be found in the original position only as a result of the re-crossing process. This property is obvious in the natural time condition. The t time scale is justified by observing that the probability of not leaving the origin is proportional to $1/t^{\mu_S - 1}$ and consequently faster than $1/t^{\frac{\mu_S - 1}{2}}$, which is the probability of finding the particle at $y = 0$ in the scaling regime.

From (316) we derive

$$\frac{\hat{\psi}^{(D)}(u)}{1 - \hat{\psi}^{(D)}(u)} = \hat{Q}(u), \tag{318}$$

which yields

$$\hat{\psi}^{(D)}(u) = \frac{\hat{Q}(u)}{1 - \hat{Q}(u)}. \tag{319}$$

Let us use (317) and the Tauberian theorem, according to which, for $\alpha < 1$, $t^{\alpha - 1} \to \frac{1}{u^{\alpha}}$. We set $1 - \alpha = \beta$, which is a legitimate choice insofar as $\beta < \alpha$ and we obtain

$$\hat{Q}(u) = \frac{\text{const}}{u^{1-\beta}} \tag{320}$$

and consequently

$$\hat{\psi}^{(D)}(u) \approx \left(1 - \frac{u^{1-\beta}}{\text{const}}\right). \tag{321}$$

By inserting (321) into the *rhs* of (319) and using (210) again we find

$$\mu_D = 2 - \beta. \tag{322}$$

This is an interesting result. It means that the re-crossing events are not ergodic since $\mu_D < 2$. However, we have to alert the reader to the fact that these events do not correspond to objective facts. They are a consequence of assigning to the re-crossing of the origin a special physical significance that may not correspond to reality. Here we are making the assumption that, due to the Demon's action, the index μ_S corresponds to a sequence of real physical events. It is interesting to notice that the condition $\mu_S = \mu_D$ is realized when $\beta = \frac{1}{3}$, which is the well known scaling of the Kardar–Parisi–Zhang renormalization theory, see Kardar et al. (1986). Thus, we conclude that the identification of re-crossings with significant renewal events, in the case of the KPZ condition generates a satisfactory scenario. In fact, in this case re-crossings and subordination events are characterized by the same non-ergodic index $\mu = \frac{5}{3}$.

However, adopting the re-crossing technique can establish a distinction between μ_S and μ_D, when a renormalization approach different from the KPZ theory applies. To clarify this last point, let us go back to the natural time scale, and establish the distribution of time intervals between two consecutive re-crossing of the level $R > y_{\text{rms}}$. In this case, the dissipation process cannot be neglected, and it has the effect of establishing a re-crossing distribution that involves μ_S directly. To obtain analytical results we go back to the natural time scale, and let the network evolve until it reaches the equilibrium distribution described by

$$P_{\text{eq}}(y) = \frac{1}{\left(2\pi y_{\text{rms}}^2\right)^{1/2}} \exp\left(-\frac{y^2}{2y_{\text{rms}}^2}\right). \tag{323}$$

We now study the recrossing of the level $R > y_{\text{rms}}$ using (316). In this case $Q(t)$ is time independent. We set the condition

$$Q(t) = g_R \equiv \gamma R P_{\text{eq}}(R), \tag{324}$$

where g_R coincides with the Kramers rate, see Kramers (1940). Thus, we obtain

$$\psi_R(n) = g_R \mathrm{e}^{-g_R n}. \tag{325}$$

The transition from n- to t-time scale is achieved in the usual way, as described by (282) with e^{-gn} replaced by $\mathrm{e}^{-g_R n}$, thereby yielding

$$\Psi_R(t) = \mathrm{e}^{g_R} E_\alpha(t), \tag{326}$$

where $E_\alpha(t)$ is derived from its Laplace transform that is identical to (290) with λ_α given by

$$\lambda_\alpha = \left(\frac{\mathrm{e}^{g_R} - 1}{\Gamma(2 - \mu_S)(T_S)^\alpha}\right)^{1/\alpha}. \tag{327}$$

We note that with increasing R, the rate g_R becomes smaller thereby extending the time interval over which the stretched exponential dominates the inverse power law.

This has the effect of establishing a direct connection with the subordination process. In fact, we can relate the stretched exponential relaxation directly to the subordination process. In practice, the determination of μ_S through this procedure can be difficult, due to the fact that the statistics become poorer with increasing R. For a valuable determination of μ_S we can express this parameter as a function of μ_D. Using (297) and (322) we obtain

$$\mu_S = 5 - 2\mu_D, \tag{328}$$

which, of course, in the KPZ case, yields $\mu_S = \mu_D = 5/3$.

It is convenient to mention that this subordination perspective, in the case of the random growth of surfaces studied by Failla et al. (2004) leads to a remarkably good agreement between theory and numerical simulation. The time series generated by complex networks are finite and their own generators are networks of finite size. It was observed, see Bianco et al. (2007b) and Failla et al. (2004), that the adoption of the subordination function with a non-truncated inverse power-law distribution density is not realistic, because it rests on the idealized condition that the time series under study is infinite. As pointed out by Failla et al. (2004), a convenient way to take truncation effects into account rests on replacing (290) with

$$\hat{E}_\alpha(u) = \frac{1}{u + (\lambda_\alpha)^\alpha (u + \Gamma_{\text{trunc}})^{1-\alpha}}, \tag{329}$$

where the parameter Γ_{trunc} defines the time parameter

$$T_{\text{trunc}} \equiv \frac{1}{\Gamma_{\text{trunc}}}. \tag{330}$$

This choice implies that the subordination function $\psi^{(S)}(t)$ is also truncated. This truncation arises because, according to (329) the real $\Phi(t)$ is related to the ideal by means of the relation

$$\Phi(t) = \Phi_0(t)\exp(-\Gamma_{\text{trunc}}t), \tag{331}$$

which, in turn, thanks to (256) yields

$$\hat{\psi}^{(S)}(u) = \frac{\hat{\Phi}_0(\Gamma_{\text{trunc}}+u)}{u+\hat{\Phi}_0(\Gamma_{\text{trunc}}+u)}. \tag{332}$$

Thus, when $u \ll \Gamma_{\text{trunc}}$, $\hat{\psi}^{(S)}(u)$ becomes the Laplace transform of an exponential subordination function. In the case where Γ_{trunc} is, due to the finite network size, of the order λ_α, the inverse power law of the MLF does not emerge, and the whole process is virtually described by a stretched exponential relaxation. This does not mean that the inverse power-law does not contribute to the process. It does, although within the limits established by the finite size of the networks under study. Excellent agreement between theory and numerical experiment was found, see Failla et al. (2004), by adopting this perspective.

We also point out that when $g_R \ll 1$, (327), yields $T_S \gg \frac{1}{\lambda_\alpha}$. As a consequence, the renewal events of the subordination process keep their inverse power-law nature in the time scale where the survival probability maintains its form as a stretched exponential function. This property is important for the foundation of the CME of Section 6. In fact, as we shall see, this phenomenon of information transport is based on the FDT of the first kind of Section 6.2.1, and this new form of linear response to external perturbations is based on the fact that the times of occurrence of the Demon's action are very slightly modified by the external perturbations. Thus, we see that even if the survival probability does not show any sign of an inverse power law, the key role for this new form of response to emerge, is realized by events with a well defined complexity index μ_S. In other words, even if experimentally we only see the successful actions of the Demon, all her actions are slightly perturbed, even those that remain unseen.

Finally, it is important to explain why the survival probability $Y_1(t)$ (308) can be obtained from the survival probability (289) by replacing g with γ. This can be explained again using the success rate concept. In fact, as we have seen in this subsection, in the natural time scale the time interval between two significant fluctuations of y is under the control of the Kramers prescription that assigns to the corresponding waiting-time distribution density the exponential form (325). This interpretation is not quite satisfactory, due to the dependence on the threshold R, which seems to be arbitrary. A more compelling argument is given by the remark that the regression to equilibrium of a fluctuation y significantly larger than y_{rms} is $e^{-\gamma t}$, thereby leading to $Y_1(t)$ (308). In other words, here the success rate has to do with the attainment of a level much higher than that of the many more numerous fluctuations of small intensity.

5.2.3. What is the most convenient way to generalize the FDT?

In the last few years there has been an increasing interest in the relaxation processes described by the MLF, see, e.g., Metzler and Klafter (2000a) and Mainardi (1996). The reason for this interest is that the MLF interpolates between a stretched exponential relaxation at short times and an inverse power law relaxation at long times. Pottier (2003) derived this form of relaxation from the GLE, see Mori (1965a,b) and Kubo (1966). Other authors have derived the same kind of anomalous regression to equilibrium using the theoretical perspective of CTRW. The two theoretical approaches are quite different, insofar as the former has a Hamiltonian foundation, see, e.g., Mori (1965a,b) and Kubo (1966), whereas the compatibility of the second approach with a Hamiltonian foundation is questionable. In fact, according to Kenkre and Knox (1974) and Budini (2005) the formal equivalence between the non-Markov master equation generated by the CTRW and the one produced by the Zwanzig contraction approach (see Zwanzig (1961)) corresponds to a genuine physical equivalence. Other authors, see, e.g., Cakir et al. (2007), Bologna et al. (2003) and Balescu (2007), studied the time convoluted form shared by CTRW and the Zwanzig projection (see Kenkre and Knox (1974) and Budini (2005)), and reached the conclusion that the formal equivalence does not guarantee physical equivalence.

The discussion of the physical difference between the CTRW and the Zwanzig projection method is not entirely academic. In fact, in the CTRW there are genuine events, while the Zwanzig projection method derives a GME from a Liouville statistical equation, with no evident genuine events. The equivalence between these two pictures, once firmly established, would make the claims of event detection subjective.

In the specific case discussed in this subsection, concerning GLE and CTRW yielding the MLF, there is no formal equivalence between the two prescriptions, and the physical equivalence is limited to only the first moment regression to equilibrium. As far as the second moment is concerned, the two prescriptions are known (see Kubo (1966)) to yield different results. However, as we show, the finite size of the data has the effect of annihilating this important difference, thereby weakening any claim concerning the event renewal character.

The current interest for the adoption of GLE as a proper theoretical tool for the study of physiological processes, see, e.g., Mokshin et al. (2005) and Yulmetyev et al. (2005), and the recent discovery of renewal events in EEG data (see Bianco et al. (2007a,b) and Buiatti et al. (2007), Buiatti et al. (2008)) has motivated looking for criteria to assess which representation is correct.

The main purpose of this subsection is to analyze the intriguing issue of the equivalence between GLE and CTRW from the point of view of time series, having in mind those of a physiological nature. These analyses may guide researchers

in this field towards answering the important question: Are there renewal events in physiological processes? We show that renewal events may emerge from the GLE theory, more as an artifact of the detection method than as a genuinely physiological property. This has the effect of making the search for genuine renewal events more difficult. We shall find however a promising way to assess the renewal character of a process, which can be made compelling by its application to real data and by the numerical treatment of artificial sequences.

It is important to take into account that the physiological networks under study are physical networks of finite size. As a consequence of the finite size, we expect that the time asymptotic limit is affected by truncation effects. As pointed out by Failla et al. (2004) and as shown in an earlier subsection, a convenient way to take truncation effects into account rests on including a truncation by replacing (290) with (329). In other words, at times $t > T_{\text{trunc}}$, namely for $u < \Gamma_{\text{trunc}}$, the relaxation $Y_1(t)$ becomes exponential. In the case $T_{\text{trunc}} \sim \frac{1}{\lambda_\alpha}$ the inverse power law of the MLF is suppressed and the relaxation process is described by a stretched exponential turning into an ordinary exponential for $t > T_{\text{trunc}}$.

We now show that this truncation makes it difficult to assess whether we have to use the subordination perspective or the GLE. As discussed in Section 2.1, the GLE is a well established approach for extending the fluctuation–dissipation relation to the non-Markov case (see Mori (1965a,b)) and Kubo (1966)). The GLE reads

$$\frac{\mathrm{d}}{\mathrm{d}t}y(t) = -\int_0^t \mathrm{d}t'\varphi(t')y(t-t') + F(t), \tag{333}$$

where the memory kernel $\varphi(t)$ is related to the equilibrium autocorrelation function of the fluctuation $F(t)$ by means of

$$\varphi(t-t') = \frac{\langle F(t)F(t')\rangle_{\text{eq}}}{\langle y^2\rangle_{\text{eq}}}. \tag{334}$$

A number of years ago Adelman (1976) noticed that the formal solution to (333) can be expressed in the form

$$y(t) = \int_0^t \mathrm{d}t' E(t-t')F(t') + E(t)y(0), \tag{335}$$

with the function $E(t)$ defined by means of its Laplace transform $\hat{E}(u)$ as

$$\hat{E}(u) = \frac{1}{u+\hat{\varphi}(u)}. \tag{336}$$

In the ordinary case where $F(t)$ is noise with no correlation (white noise), the Laplace transform of the memory kernel is independent of u, $\hat{\varphi}(u) = \gamma$, thereby reducing the Laplace transform (336) to $1/(u+\gamma)$, the Laplace transform of the ordinary exponential $\exp(-\gamma t)$. Thus, (335) becomes the solution of the ordinary Langevin equation.

Adelman (1976) proved that under the assumption that $F(t)$ is a delta correlated Gaussian stochastic process, the equation of motion for the probability density function $P(y,t)$ becomes

$$\frac{\partial}{\partial t}P(y,t) = -\frac{\dot{E}(t)}{E(t)}\left[\frac{\partial}{\partial y}y + \langle y^2\rangle_{\text{eq}}\frac{\partial^2}{\partial y^2}\right]P(y,t). \tag{337}$$

We shall refer to this equation as GFPE2, and we invite the reader to compare it to GFPE1, defined by (306). We note that both equations rest on the ordinary fluctuation–dissipation process described by the Fokker–Planck operator L_{FP}

$$L_{FP} \equiv \frac{\partial}{\partial y}y + \langle y^2\rangle_{\text{eq}}\frac{\partial^2}{\partial y^2}. \tag{338}$$

In the former case, GFPE1, the generalization is done through the time convolution of $L_{FP}P(y,t)$ with $\Phi(t)$, whereas in the latter, the constant dissipation parameter γ is replaced by the time dependent dissipation rate $\lambda(t)$

$$\lambda(t) \equiv -\frac{\dot{E}(t)}{E(t)}. \tag{339}$$

It is interesting to note that there is a case where Adelman's generalized exponential of (336) becomes identical to the Mittag–Leffler generalized exponential. According to Weiss (1999) the memory kernel generated by a non-ohmic bath can be expressed as

$$\varphi(t) = C\int_0^{\omega_D}\rho(\omega)\cos(\omega t)\mathrm{d}\omega, \tag{340}$$

where C is a suitable constant factor, $\rho(\omega)$ the frequency distribution and ω_D the Debye frequency. Weiss discussed the general case

$$\rho(\omega) \propto \omega^{\beta-1}, \tag{341}$$

with β ranging from $\beta = 0$ to $\beta = 2$. The cases $\beta > 1$ and $\beta < 1$ are denoted as super-Ohmic and sub-Ohmic, respectively. It is shown by Pottier (2003) that

$$\hat{\varphi}(u) = ku^{\beta-1}. \tag{342}$$

We see that the super-Ohmic case generates the anomalous relaxation process described by

$$\hat{E}(u) = \frac{1}{u + (\lambda_\alpha)^\alpha u^{1-\alpha}} \tag{343}$$

with $\lambda_\alpha \equiv k^{1/\alpha}$ and $\alpha = 2 - \beta$, yielding $\alpha < 1$, and consequently MLF relaxation. Of course, the ordinary exponential relaxation is generated by the Ohmic bath, with $\beta = 1$.

Let us consider an out-of-equilibrium initial state $\langle y(0)\rangle \neq 0$, under the condition $\phi(t) = \gamma\Phi(t)$, in which case the GLE of (333) yields the same relaxation process for the first moment as does GFPE1, (306), described by

$$\frac{\mathrm{d}}{\mathrm{d}t}\langle y(t)\rangle = -\gamma \int_0^t \mathrm{d}t' \Phi(t - t')\langle y(t')\rangle. \tag{344}$$

The case $\mu < 2$, according to (313) yields the same stretched exponential parameter α as the super-Ohmic bath, prescribed by (343), and consequently a relaxation process described by the MLF. It is straightforward to demonstrate, however that the two pictures yield different results for the higher-order moments. Thus, while both approaches yield

$$\frac{\langle y(t)\rangle}{\langle y(0)\rangle} = E_\alpha\left(-(\gamma_\alpha t)^\alpha\right), \tag{345}$$

GFPE1 generates

$$\left\langle y^2(t)\right\rangle = y_{\mathrm{rms}}^2\left\{1 - \left[E_\alpha\left(-(\gamma_\alpha t)^\alpha\right)\right]^2\right\} \tag{346}$$

and GFPE2 generates the similar but not the same equation

$$\left\langle y^2(t)\right\rangle = y_{\mathrm{rms}}^2\left\{1 - E_\alpha\left(-2(\gamma_\alpha t)^\alpha\right)\right\}. \tag{347}$$

Thus, in principle, it should be possible to assess if a given complex time series is generated by SOFD or by GLE. However, the problem is more difficult than expected. In fact, it has been recently remarked (see Bianco et al. (2007a,b) and Failla et al. (2004)) that a time series of finite length is characterized by the truncation effects described in Section 5.2.2, thereby justifying why the events produced by EEG's dynamics are satisfactorily described by stretched exponential functions. If the truncation time is comparable to $1/\gamma_\alpha$ the MLF inverse power law is not manifest and only the stretched exponential is visible. In this case, there is apparently a complete equivalence between GLE and SOFD.

There are good reasons to believe that EEG time series form a renewal process with $\mu_S < 2$ (see Bianco et al. (2007a,b)). However, this does not rule out the possibility that the GLE approach affords a picture as satisfactory as the SOFD theoretical perspective. Let us consider the case where the two methods yield (345) with $\alpha < 1$. Let us also make the assumption that only the stretched exponential and not the inverse power law of the MLF is visible. The experimental detection of the parameter α of the stretched exponential allows us to determine the power-law index $\mu_S = 1 + \alpha$ only in the case where the SOFD perspective applies. In this case, in fact, as explained in Section 5.2, the parameter α is generated by the renewal Demon's activities. If the EEG theory applies the parameter α does not have anything to do with Demon's social life: it is rather the manifestation of long-time memory produced by the super-Ohmic bath.

Therefore, let us look for a property that is peculiar to the Demon's actions and focus attention on the time series $y(t)$. We fix a threshold R and monitor the times t_i at which

$$|y(t_i)| = R, \tag{348}$$

and evaluate the distribution of the crossing times to this level $\tau_i = t_{i+1} - t_i$. The distribution of crossing times is denoted $d(\tau)$ and the corresponding survival probability is defined

$$D(t) = \int_t^\infty \mathrm{d}\tau \mathrm{d}(\tau). \tag{349}$$

On the basis of earlier arguments and as pointed out by Cakir et al. (2007) we expect that for R^2 of the order of y_{rms}^2, both theories yield

$$D(t) \propto \frac{1}{t^{\mu_D - 1}}, \tag{350}$$

with

$$\mu_D = 2 - \frac{\alpha}{2}, \tag{351}$$

which is in general different from $\mu_S = 1 + \alpha$, although sharing with it the property $\mu_D < 2$. The analysis by Cakir et al. (2006) establishes that the prediction of (351), determined essentially by the origin re-crossing, is characterized by renewal aging, regardless of the source of the scaling $\alpha/2$, either the renewal Demon or the trajectory long-time memory. Therefore this result is not a reliable way to determine the genuine parameter μ, if the complex process is of the SOFD type.

The case $R^2 \gg y_{\rm rms}^2$ is much more promising. In fact in this case, in the natural time scale, according to Kramers (1940) the survival probability $D(n)$ is given by

$$D(n) = g\mathrm{e}^{-gn}, \tag{352}$$

with

$$g = A\exp(-\gamma R^2/B), \tag{353}$$

where $A \sim \gamma$ and $B \sim y_{\rm rms}^2$. By applying the same approach as that used in Section 5.2.2, we conclude that $D(t)$ is a stretched exponential with $(\lambda_\alpha)^\alpha \propto g = A\exp(-\gamma R^2/B)$, a prediction that can be checked experimentally.

In summary, both GLE and SOFD theories generate a stretched exponential relaxation. This equivalence has the effect of weakening the claims that EEG dynamics is characterized by renewal and non-ergodic events as studied by Bianco et al. (2007b). However, the adoption of the threshold method outlined in this subsection may afford a way to establish that the EEG fluctuations are driven by the action of the renewal non-Poisson Demon described herein. The recent work of Bianco et al. (2007b) established that a set of interacting channels is characterized by the presence of non-ergodic renewal events. The discovery of non-ergodic renewal events imbedded in the EEG data of a single electrode would confirm the findings of Buiatti et al. (2007) and consequently would prove that the single electrode inherits the complexity of the whole network. The above arguments may stimulate research in this direction.

5.2.4. Conjectures on EEG data

It is important to note that the relationship between indices given by (322) is based on the scaling assumption of the probability density given by (201). This assumption is legitimate for the calculation of the re-crossing times only for time intervals shorter than the localization time. In fact, at longer times it is not possible to neglect the role of friction in (337). We have to adopt the same kind of calculation that we do with $R > y_{\rm rms}$. In fact, when the time interval between successive re-crossings of the origin becomes very large, the trajectory $y(t)$ becomes of the order of $y_{\rm rms}$, or larger. In this case, we cannot neglect friction. It is therefore convenient to make the same kind of calculation as that adopted for $R > y_{\rm rms}$. The condition that the equilibrium distribution is Gaussian does not conflict with the ideally non-ergodic nature of the process under study. In fact, this condition sets equilibrium in the natural time sale, a condition that is essentially lost when moving from the natural to the experimental time scale. If we impose the Gaussian condition, we are not necessarily forced to assume $R > y_{\rm rms}$. If we select $R = 0$ to observe the origin re-crossings, we must replace (324) with

$$Q(t) = g_{R=0} \equiv \gamma y_{\rm rms} P_{\rm eq}(0) = \frac{\gamma}{(2\pi)^{1/2}}, \tag{354}$$

thereby generating a survival probability with the structure of a stretched exponential function with the parameter λ_α of (327) related to $g_{R=0}$ of (354). We denote the survival probability corresponding to $R = 0$ with the symbol $\Psi_D(t)$ to stress that this is the survival probability corresponding to the waiting time distribution density $\psi_D(t)$ with the inverse power law index μ_D established by (322).

5.2.5. Infinitely aged non-stationary autocorrelation function

At the present time we do not have a formula linking the short-time region where $\psi^{(D)}(\tau)$ shows an inverse power-law form with the index μ_D of (322) to the large-time scale where the survival probability $\Psi_D(\tau)$ shows a stretched exponential structure. Buiatti et al. (2007) examined the single electrode EEGs and used very ingenious arguments to prove, although with a technical language different from that used herein, the central role of renewal events.

According to the arguments of Section 4.4.1 the number of actions per unit time produced by the Demon with $\mu_S < 2$, under the condition that an action occurs at $t = 0$, see (212), should decrease as

$$P(t) \propto \frac{1}{t^{2-\mu_S}}. \tag{355}$$

Note that this time dependence of $P(t)$ makes it impossible to express the aged waiting time distribution $\psi_{t_a}(t)$ in analytical form. However, if $\mu_S = 2 - \eta$, with $1 \gg \eta > 0$, we use the assumption that $P(t)$ is constant, and derive the age-dependent waiting time distribution (219), as shown in Section 4.4.3. In accordance with the results illustrated in Section 4.4.3, we find that keeping t_a fixed and changing t, the subordination function of age t_a moves from the form for $t \ll t_a$

$$\psi_{t_a}^{(S)}(t) \propto \frac{1}{t^{\mu_S - 1}}, \tag{356}$$

to the form for $t \gg t_a$

$$\psi_{t_a}^{(S)}(t) \propto \frac{1}{t^{\mu_S}}. \tag{357}$$

This result indicates a promising road to establish the occurrence of renewal events in the brain, based on the assumption that the picture of Section 5.2.2 is correct. However, we have to distinguish between large and small quakes. Small quakes correspond to fluctuations on the natural time scale that are much smaller than the square root of D/γ, see (305). Large quakes, on the contrary, refer to fluctuations much larger than the square root of D/γ, and the interval between two consecutive large quakes is ruled by Kramers theory, as argued in Section 5.2.3. Consequently, the large quakes, as discussed in Section 5.2.2, correspond to the rare successes of a Demon with a very small success rate. The technique of analysis of single electrode data used by Buiatti et al. (2007) reveals the crucial parameter μ_S through a judicious use of the property (356). In fact, these authors study the diffusion equation corresponding to the diffusive process

$$\frac{\mathrm{d}}{\mathrm{d}t}x = y(t), \tag{358}$$

with a de-trending method allowing them to suppress the systematic trends that have the effect of generating large quakes. The de-trending method that they adopt restricts their considerations to small fluctuations of the order of $f(n)$. They have to convert the de-trended fluctuations into many Gibbs networks, using the standard method of a mobile window of size l. As a consequence we have to apply an approach to the evaluation of the correlation function based on the prescription (204). There are two main problems with the use of this formula: (a) (204) holds true for a dichotomous fluctuation; (b) the aging effect. Problem (a) is solved by noticing that the subordination theory illustrated in Section 5.2.2 does not depend on the specific form of $f(n)$, provided that it is uncorrelated. Let us assume, therefore, that $f(n)$ is dichotomous noise. The de-trending method applied by Buiatti et al. (2007) corresponds to focusing on the weak quakes, and consequently on the continuous time t realization of the fluctuations $y(n)$ of (303) essentially independent of the dissipation term $-\gamma y(n)$. In other words, we can focus on the dichotomous fluctuation generated in the t-time scale by $f(n)$. This allows us to use (204).

What about problem (b)? It is plausible to imagine that the aging parameter t_a cannot become infinite. Adopting a moving window method implies that we aim at determining the autocorrelation function of maximum age, here $t_a \approx 1/\lambda_\alpha$, with λ_α given by (309) with $w = 1$. Adopting the de-trending method yields $t \ll t_a$, and consequently, it involves the use of (356). The autocorrelation function (infinitely aged survival probability) corresponding to this condition consequently has to be determined by

$$\frac{\mathrm{d}}{\mathrm{d}t}\Psi^{(\infty)}(t) \propto t^{1-\mu_S}. \tag{359}$$

We note that this expression for the autocorrelation function is valid for $t \ll t_a$ and that for $t \gg t_a$, namely, for $t \gg 1/\lambda_\alpha$, according to (357), is expected to decay as $1/t^{\mu_S-1}$. We have to stress, however, that when the subordination theory of Section 5.2.2 applies, the long-time regime is no longer described by dichotomous fluctuations and the large quakes must be taken into account.

Summarizing, we see that adopting an autocorrelation function that increases rather than decreases with time, is the price we pay for adopting the prescription of ordinary stationary statistical physics, which assigns to the diffusion equation of (358) the following time-dependent second moment

$$\left\langle x^2(t)\right\rangle = 2y_{\mathrm{rms}}^2 \int_0^t \mathrm{d}t' \int_0^{t'} \mathrm{d}t'' \Psi^{(\infty)}(t''). \tag{360}$$

In the long-time limit the second moment is expected to be proportional to $t^{2\delta}$. By differentiating (360) three times with respect to time and using (359), we obtain the relation between indices

$$\delta = \frac{4-\mu_S}{2}, \tag{361}$$

in complete accordance with the conclusions of Kalashyan et al. (2007) who interpret the theoretical prescription of (361) as the scaling index corresponding to an infinitely aged network.

Using the theoretical prescription of (361) and the values of δ, slightly larger than 1, obtained by Buiatti et al. (2007) from their EEG analysis, we obtain values for μ_S close to 1.9, in remarkable agreement with the minimal spanning tree (MST) analysis (see Kruskal (1956)) adopted by the Bianco et al. (2007a,b). This is strong support for the perspective illustrated herein: The renewal events generated with the subordination function $\psi_S(t)$ mirrors in the dynamics of a single EEG the structured breakdown revealed by the MST method applied to the entire set of electrodes.

5.2.6. Interacting neural networks and EEGs

What is the origin of the subordination theory used in the earlier subsections? There are good reasons to believe that there exists an intimate connection between the stretched exponential form of $\Psi_D(t)$ and the time evolution of the single electrodes monitoring the brain as studied by Buiatti et al. (2007). To establish this connection Bianco et al. (2007a,b) studied a set of EEG channels of a patient with the help of the MST technique (see Kruskal (1956)). We follow their approach and measure the correlation c_{ij} between channels i and j at a generic time t, and define the distance

$$d_{ij} = \sqrt{\frac{1-c_{ij}}{2}}. \tag{362}$$

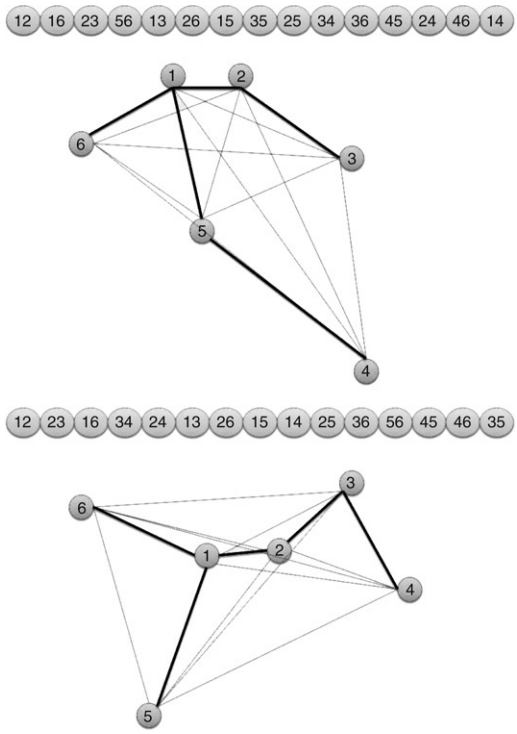

Fig. 10. The two panels show the tree structures corresponding to two different ordering of the distances d_{ij}.

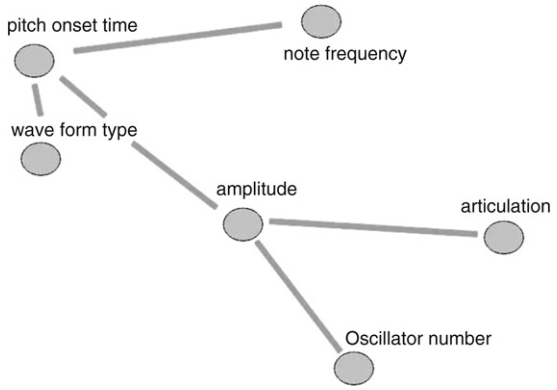

Fig. 11. Music composition as a complex network. The figure shows the six music components of the music stimulus. Note frequency — audio frequency in Hertz of the pitch of a given note event; Waveform type — indicates whether the note event frequency is played by one or several standard waveforms: sine wave, triangle wave, square wave, or sawtooth wave; Amplitude — the loudness of the note event (0.0–1.0); Articulation — the length of time the note event lasts; Oscillator number — the symbol (1–4) that represents which specific oscillator (of four oscillators) in the overall texture is sounding the particular tone; Pitch onset time — the time (in ms) at which each tone begins.

Since c_{ij} ranges from -1 to 1, the distance d_{ij} is smaller for the larger correlation. We order the distances d_{ij} from the shortest to the longest and connect the corresponding sites. We do not establish any connection when such a connection results in a closed loop. The set of sites connected with this method generates a tree structure. We define an event as the abrupt change from one tree configuration to another. The procedure is illustrated by Fig. 10.

The MST method establishes a hierarchy of correlations among the sites, and through them a tree, which from time to time abruptly changes its structure. If these abrupt changes of structure generate a time series $\{t_i\}$ satisfying the renewal condition of (215), illustrated by Fig. 10, then these are the crucial events we are looking for in the EEG data.

Of course, a set of electrodes is not the only example of a network. A music composition, whose musical vector $\mathbf{V}(t)$ is known (see Winsor (1992)) affords another example of a network. The musical vector $\mathbf{V}(t)$ has six components as illustrated in Fig. 11, namely, pitch onset time (in milliseconds), note frequency (in hertz), wave form type, amplitude, articulation, preset number, and oscillation number. These six components are thought of as analogous to the single EEG electrodes on the patient's scalp.

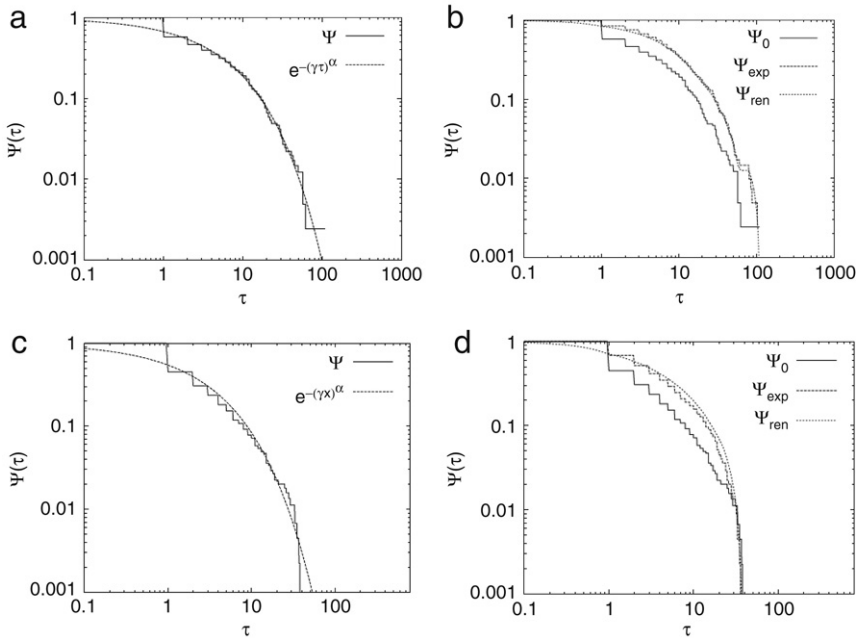

Fig. 12. Panel (a) and (b) refer to the brain and to the music composition, respectively. In both cases the renewal criterion of Eq. (215) is satisfactorily fulfilled.

Bianco et al. (2007a,b) established an exciting similarity in the network structure of music composition and the workings of the human brain. In both cases there are quakes and the time interval between two consecutive quakes generates a survival probability that is well described by a stretched exponential and in both cases the quakes are renewal events. All this is illustrated by Fig. 12, where it is evident from the form of the MST analysis of the EEG time series that this signal is generated by a renewal non-Poisson process. These statistics give rise to the stretched exponential distribution of time intervals between critical events.

Is this similarity essential for the transport of information from the music composition to the brain? The answer to this question appears to be yes and is a consequence of CME. One purpose of this Report is to establish the foundation of the CME and demonstrate how this principle may help to settle this intriguing question regarding the transfer of information from one complex network to another. This is discussed in the following section.

6. Complexity matching effect (CME)

As we discussed, resonant phenomena have been among the most useful mechanisms in extracting weak signals from noisy backgrounds: a linear dynamic process responds strongly to a harmonic perturbation with a frequency matching the natural frequency of the network; effective two-state SR phenomena respond strongly when the period of a harmonic perturbation matches the transition rate of the random fluctuations; and in aperiodic SR, see, e.g., Collins et al. (1996b), where the rate of perturbation (Poisson) matches the transition rate of the two-state process. However, as phenomena become more complex the conditions for resonance become more subtle.

Network complexity increases as interactions become more strongly nonlinear, as the number of degrees of freedom increase and as the counting statistics for events deviate from Poisson. These three properties converge in the synchronization of the dynamical elements in a complex network, whether the isolated elements are modeled as linear or nonlinear oscillators, limit cycles, or chaotic attractors, see, e.g., Kuramoto (1981) and Winfree (1990). Both the mechanisms of synchronization and SR have been used to provide insight into the behavior of complex networks as, for example, into the dynamics of collections of neurons studied by Moss et al. (2004). Even more recently the question of how to transmit information through a complex network in which the simplifying assumptions of traditional statistical physics are no longer valid has been addressed by Goychuck and Hänggi (2003) and Barbi et al. (2005), for example, the assumption that the unperturbed dynamics can be described by an autocorrelation function with a finite correlation time discussed by Kubo (1957). Barbi et al. (2005) conclude that a complex network described by intermittent fluctuations with non-Poisson statistics does not respond to external periodic perturbations. Sokolov (2006) and Sokolov and Klafter (2006) have reached the same conclusion.

Here we review the extension of the investigations of the perturbation of complex networks discussed by Barbi et al. (2005), Sokolov (2006) and Sokolov and Klafter (2006) to a new resonance phenomenon, that is, the determination of how one complex network responds to an excitation by a second complex network as a function of the matching of the measures

of complexity of the two networks. Consider the complex system to be a NPR network and the measure of complexity to be the inverse power-law index. More precisely, we consider a NPR network, with power-law index $\mu_S < 2$, and study, in analogy with the theory of SR by Benzi et al. (1981), the case where the rate of production of jumps, a kind of renewal event, is modulated by an external excitation. Barbi et al. (2005), Sokolov (2006) and Sokolov and Klafter (2006) used a harmonic perturbation, which we do not do here, but instead we use a stochastic signal as the excitation. In the present case the network satisfies the NPR condition with $\mu_S < 2$ and the excitation is another NPR process with power-law index $\mu_P < 2$. We present heuristic arguments that the transport of information attains maximum efficiency at the matching condition $\mu_S = \mu_P$. This matching condition is called the *complexity matching effect* (CME) for the obvious reasons that in our theoretical framework, genuinely complex processes satisfy the NPR condition with $\mu_S < 2$, so that the parameter μ_S becomes a complexity index and two systems with the same $\mu's$ have the same degree of complexity. Although we focus on $\mu_S < 2$, as the most dramatic form of deviation from the conditions of ordinary statistical physics, it is convenient to notice that the whole range $\mu_S < \infty$, implies the existence of diverging moments of the distribution density $\psi^{(S)}(\tau)$ of sufficiently high degree. This is a departure from the normality condition ensured by the exponential condition. We note that the parameter range $2 < \mu_S < 3$, although ensuring the existence of a finite mean waiting time value, generates a divergence of the second moment and with it the breakdown for the application of the central limit theorem, as discussed in Section 6.3.

In this section we substantiate the conjectures suggested by the MST analysis of both the brain's EEG signal and music composition illustrated in Section 5. The reason why a complex network is proved to be most sensitive to perturbations with comparable complexity rests on the observation that each non-ergodic, non-Poisson network can be thought of as emerging from the subordination to a network with a fixed time scale.

6.1. Heuristic approach to CME

In this subsection we concisely review the phenomenon of SR and the underlying notions of ordinary statistical physics in a form suitable for a heuristic derivation of the CME.

6.1.1. Response of a Poisson network to perturbation

It is evident that the unperturbed Demon's actions is equivalent to the ordinary master equation (263). At any drawing of black balls the Demon tosses a coin, and if she tosses a head (tail) she assigns to the fluctuations ξ_S the value 1 (-1). Using a language inspired by the two-state system, we say that at any drawing of black balls the Demon jumps from one state to the other or remains in the same state, with equal probability. Let us imagine that the Demon's action is affected by an external perturbation influencing the number of balls according to whether the Demon is in the state $|1\rangle$ or in the state $|2\rangle$. Thus the rate g, which is time independent, when no external perturbation is applied to the network, becomes time dependent:

$$g_{\pm}(t) = g_0(1 \mp \epsilon\xi_P(t)). \tag{363}$$

Thus the constant matrix $g\mathbf{K}$ of (263) is replaced by the time dependent matrix $\mathbf{T}(t)$ defined by

$$\mathbf{T}(t) \equiv \frac{1}{2}\begin{bmatrix} -g_+(t) & g_-(t) \\ g_+(t) & -g_-(t) \end{bmatrix} \tag{364}$$

and the difference variable $\Pi(t)$ obeys the equation of motion

$$\frac{\mathrm{d}}{\mathrm{d}t}\Pi(t) = -g_0\Pi(t) + \epsilon g_0\xi_P(t). \tag{365}$$

The exact solution to (365), moving from the equilibrium condition $\Pi(0) = 0$, is

$$\Pi(t) = \epsilon g_0 \int_0^t \mathrm{d}t' \exp\left(-g_0(t-t')\right)\xi_P(t'). \tag{366}$$

In the special case of a harmonic perturbation:

$$\xi_P(t) = \cos(\omega t) \tag{367}$$

it is straightforward to prove that for $t \to \infty$ this exact solution (366) yields

$$\Pi(t) = A\cos(\omega t + \phi) \tag{368}$$

with

$$A = \frac{g_0}{\left({g_0}^2 + \omega^2\right)^{1/2}} \tag{369}$$

and

$$\tan\phi = \frac{\omega}{g_0}. \tag{370}$$

As a consequence, the maximum response, with perfect reproduction of the perturbation signal is obtained when $\frac{\omega}{g_0} \to 0$.

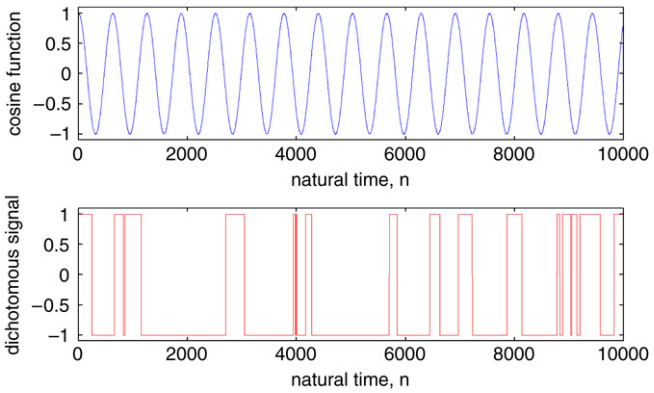

Fig. 13. Panel (a) We plot $\xi_S(t) = \cos(\omega t)$ Panel (b) We plot $\xi_P(t)$ generated by the subordination to the coin tossing prescription with $g = 1$.

In Fig. 13 we have plotted $\xi_S(t)$ and $\xi_P(t)$ in a special situation, namely when for $t \to \infty$ both functions cross the origin the same number of times. We have in fact assumed that $\langle t \rangle = \frac{1}{g} = \frac{\pi}{\omega}$. According to (369) this is not the condition for the response of maximum intensity, in spite of a misinterpretation of the phenomenon of SR. However, $\omega \approx g_0$ signals the condition for the response to obtain significant intensity.

6.1.2. Autocorrelation function

To establish a connection between the result (366) and the current literature on the FDT, let us evaluate the equilibrium autocorrelation function $\langle \xi_S(t)\xi_S(t') \rangle$. In general the cross-correlation function between two generic variables, A and B, is given by

$$\langle A(t)B(t') \rangle = \sum_{\mu,\mu'} A_\mu P(\mu, t|\mu', t') B_{\mu'} P_{\mu'}(t'), \tag{371}$$

where A_μ and $B_{\mu'}$ denote the values of the variables A and B in the states $|\mu\rangle$ and $|\mu'\rangle$, respectively. $P_\mu(t)$ is the probability that the network is in the state $|\mu\rangle$ at time t, and $P(\mu, t|\mu', t')$ is the conditional probability that the network is in the state $|\mu\rangle$ at time t, given that it is in the state $|\mu'\rangle$ at time t'. In the specific case here under discussion, due to the dichotomous nature of $\xi_S(t)$, we have

$$\langle \xi_S(t)\xi_S(t') \rangle = \left[P(+, t|+, t') - P(-, t|+, t')\right] p_1(t') + \left[P(-, t|-, t') - P(+, t|-, t')\right] p_2(t'). \tag{372}$$

Let us consider the ordinary master equation (263) and relax the assumption that, in the absence of perturbation, the rate g remains constant. This serves the purpose of extending the derivation of the autocorrelation function to the case of non-renewal aging. Let us assume that (263) is replaced with

$$\frac{\mathrm{d}}{\mathrm{d}t}\mathbf{p} = g_0(t)\mathbf{K}\mathbf{p}(t). \tag{373}$$

We thus obtain

$$\Pi(t) = \exp\left(-\int_{t'}^{t} g_0(t'')\mathrm{d}t''\right)\Pi(t'). \tag{374}$$

Taking into account the definition of $\Pi(t)$, we rewrite (374) as

$$p_1(t) - p_2(t) = \exp\left(-\int_{t'}^{t} g_0(t'')\mathrm{d}t''\right)\left(p_1(t') - p_2(t')\right), \tag{375}$$

and using (375), we obtain

$$P(+, t|+, t') - P(-, t|+, t') = \exp\left(-\int_{t'}^{t} g_0(t'')\mathrm{d}t''\right) \tag{376}$$

and

$$P(+, t|-, t') - P(-, t|-, t') = -\exp\left(-\int_{t'}^{t} g_0(t'')\mathrm{d}t''\right). \tag{377}$$

By inserting (376) and (377) into (372), and using $p_1(t') + p_2(t') = 1$, we obtain

$$\langle \xi_S(t)\xi_S(t')\rangle = \exp\left(-\int_{t'}^{t} g_0(t'')\right). \tag{378}$$

Using the non-stationary survival probability (277) we rewrite (378) as

$$\langle \xi_S(t)\xi_S(t')\rangle = \Psi(t,t'). \tag{379}$$

Although we have derived (379) in the special case of non-renewal aging, we point out that this equality applies to the case of renewal aging, as well, as previously discussed in detail by Allegrini et al. (2005). This relation is a generalization of the OP (see Onsager (1931)). We create an initial out-of-equilibrium condition by ignoring, for instance, the networks located in state $|2\rangle$, regardless of whether we are in equilibrium or not. If the whole network is in equilibrium, the autocorrelation function is stationary, and, consequently, the survival probability simplifies to $\Psi(t,t') = \Psi_{\rm stat}(t-t')$.

6.1.3. Fluctuation–dissipation theorem (FDT)

We are now in a position to relate the preliminary results obtained, (368)–(370), concerning the response of a network to external perturbation, to general LRT. The FDT of the first kind discussed by Kubo et al. (1985) plays quite an important role in physics, insofar as the response to external perturbation, which can be experimentally detected, exposes information concerning the network's dynamics. The FDT facilitates in developing the foundation of proper models for complex condensed matter processes, see, e.g., Crisanti and Ritort (2003). The most general form of LRT is given by

$$\Pi(t) \equiv \langle A(t)\rangle = \epsilon \int_0^t \chi_{AB}(t,t')\xi_P(t')\mathrm{d}t', \tag{380}$$

where A is the network variable, whose mean value in the absence of perturbation is assumed to vanish. The average $\Pi(t) = \langle A(t)\rangle$ is the response to perturbation $\xi_P(t)$ and is a function describing the perturbation time dependence and ϵ is the perturbation strength. The FDT is a theoretical proposal for the form of the response function $\chi_{AB}(t,t')$. In the recent condensed matter literature by Crisanti and Ritort (2003) the form ordinarily adopted for the response function $\chi_{AB}(t,t')$ is

$$\chi_{AB}(t,t') = \frac{\mathrm{d}}{\mathrm{d}t'}\langle A(t)B(t')\rangle, \tag{381}$$

where B is the variable through which the system is coupled to the external perturbation.

Herein we focus on the case $A = B = \xi_S$. Thus, in the dichotomous case yielding (379), we suppress the subscripts and write (381) as

$$\chi(t,t') = \frac{\mathrm{d}}{\mathrm{d}t'}\Psi(t,t'). \tag{382}$$

Using (378) we note that in the Poisson case, with time-independent rate g, the autocorrelation function $\langle \xi_S(t)\xi_S(t')\rangle$ is stationary

$$\langle \xi_S(t)\xi_S(t')\rangle = \mathrm{e}^{-g_0(t-t')}. \tag{383}$$

Thus, (366) satisfies the conventional FDT. However, (382) does not require stationarity.

In principle, another possible extension of the FDT to the non-stationary case can be obtained by imposing the condition

$$\chi(t,t') = -\frac{\mathrm{d}}{\mathrm{d}t}\Psi(t,t'). \tag{384}$$

In the stationary case the generalization (384) coincides with the generalization (382) and in this case both coincide with the traditional proposal of Kubo.

Are the two generalization of FDT equivalent in the non-stationary case? It is easy to prove that the condition of non-renewal aging yields the generalization (382). To establish this important property, imagine that the box used by our Demon is deteriorating. As a consequence, even in the absence of an external perturbation the rate $g_0(t)$ changes as a function time. In this case the matrix $\mathbf{T}(t)$ is given by

$$\mathbf{T}(t) \equiv \frac{1}{2}\begin{bmatrix} -(1-\epsilon\xi_P(t)) & (1+\epsilon\xi_P(t)) \\ (1-\epsilon\xi_P(t)) & -(1+\epsilon\xi_P(t)) \end{bmatrix} g_0(t). \tag{385}$$

By repeating the same calculations as those leading to (366), we now obtain

$$\Pi(t) = \epsilon \int_0^t \mathrm{d}t' g_0(t') \exp\left(-\int_{t'}^{t} \mathrm{d}t'' g_0(t'')\right) \xi_P(t'), \tag{386}$$

which is an evident realization of (382). We remind the reader that a NPR process can be described by a time dependent $g(t)$, as shown by (276). However, in that case $g(t)$ is ineluctably stochastic, insofar as the occurrence of an event resets it to the original value. The earlier derivation of (382) rests on the assumption that the time dependence of $g(t)$ is independent of the event occurrence. In Section 6.2 we show that the generalization (384) applies to the case of the stochastic rate of (276) and consequently to the case of renewal aging.

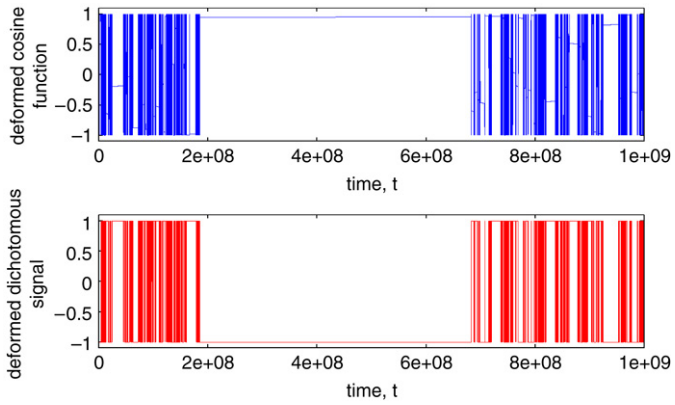

Fig. 14. Panel (a) describes a single realization of the subordination procedure applied to the harmonic signal of panel (a) of Fig. 13. Panel (b) describes a single realization of the subordination procedure applied to the Poisson signal of panel (b) of Fig. 13.

6.1.4. A perturbation created by means of the subordination to a harmonic signal

In this subsection we present an intuitive explanation of why the CME is expected to occur. This is shown in Fig. 14 using the signal depicted in Fig. 13. This latter figure shows that in the time scale t the perturbation $\xi_P(t)$ that in the natural time scale generates resonance effects, in the experimental time scale t generates the same clustering effects as those characterizing the dynamics of the unperturbed non-ergodic renewal fluctuation $\xi_S(t)$. To shed light on this fact, let us study in detail the subordination to the harmonic signal

$$\xi_P(n) = \cos(\omega n). \tag{387}$$

We evaluate the average over infinitely many realizations of the subordination prescription by means of

$$\Xi(t) \equiv \langle \xi_P(t) \rangle. \tag{388}$$

Adopting a calculation of the same kind as that used to evaluate the subordination to stochastic processes, after a little algebra, we obtain

$$\hat{\Xi}(u) = \frac{1}{u + \hat{\Phi}(u)\left[(1-\cos(\omega)) + \frac{\hat{\Phi}(u)\sin^2(\omega)}{u+\hat{\Phi}(u)(1-\cos(\omega))}\right]}. \tag{389}$$

As in the case of a subordination to a stochastic signal $\xi_S(n)$, of a Poisson nature, with rate g, the function $\Xi(t)$ becomes inverse power law in the long time limit, with g replaced by $\omega^2/2$. More precisely, in this case we obtain

$$\lambda_{\alpha,\omega} = \left(\frac{1-\cos(\omega)}{\Gamma(2-\mu_S)(T_S)^\alpha}\right)^{1/\alpha}. \tag{390}$$

The behavior of $\Xi(t)$ in the intermediate time scale is not quite clear. We limit ourselves to noticing that there must be a connection with the fractional oscillator of Stanislavsky (2006). In Fig. 15 we illustrate the time evolution of the fractional oscillator, which looks like the phase–space orbit for a linear dissipative oscillator. Actually, according to the theory developed in the present subsection, this is the average value over many realizations of the subordination approach to the regular motion of a single oscillator. Each realization of the subordination to a harmonic motion is a stochastic process, and the apparent dissipation is an effect of the phase decoherence produced by the superposition of infinitely many stochastic realizations.

The striking similarity between a realization of the subordination to a Poisson process and the realization of the subordination to the harmonic perturbation suggests that to make a non-Poisson network respond to a perturbation we need to adapt the perturbation to the network. In other words, in the same way as the harmonic perturbation of Fig. 13(a) turned out to be a convenient perturbation for the Poisson process $\xi_S(t)$ of Fig. 13(b), it is plausible that the perturbation $\xi_P(t)$, of Fig. 14(a) obtained through subordination to the harmonic perturbation of Fig. 13(a) is the proper perturbation of the non-Poisson network $\xi_S(t)$ of Fig. 14(b), which is obtained via subordination to the Poisson process $\xi_S(n)$ of Fig. 13(b).

Fig. 16 shows that the above conjecture regarding subordination is correct. Here we study the case where the waiting time distribution of the network S is generated by the dynamical model of Section 4.1. We assign to the parameters of this model the subscript S to distinguish them from those of the complex perturbation, whose parameters are labeled with the subscript P. We assume that the parameter T of the inverse power-law distribution density is perturbed by the system P through

$$T_S^{\pm}(t) = T_S(1 \pm \epsilon \xi_P(t)), \tag{391}$$

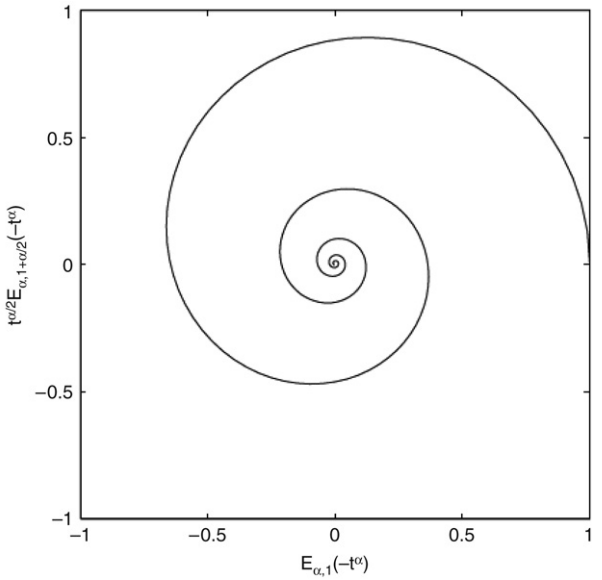

Fig. 15. This figure illustrates the fractional oscillator of Stanislavsky (2006). The dissipative nature of this oscillator is actually the consequence of averaging on infinitely many realizations of the subordination procedure.

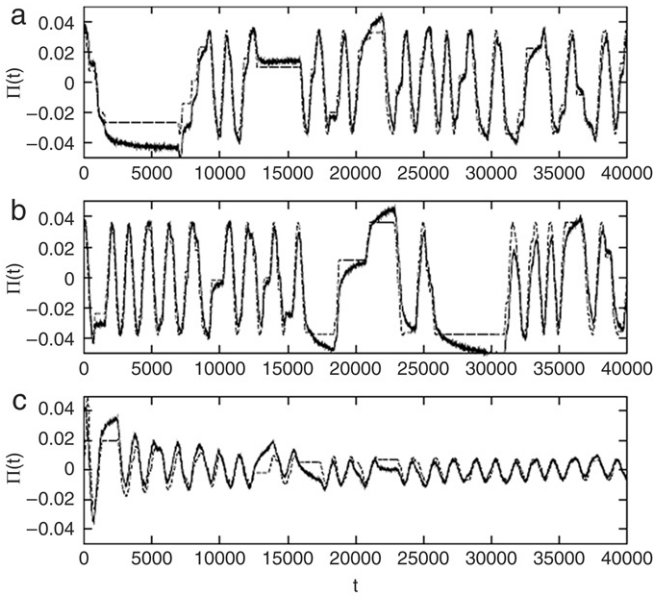

Fig. 16. $\Pi(t)$ as a function of time. $\epsilon = 0.1$. (a) $\mu_P = 1.8$, $\mu_S = 1.9$. The two lines are the numerical response (solid) and, according to prescription (a), the signal $\xi_P(t)$ multiplied by ϵA, with $A = 0.34$ (dashed). (b) The same for $\mu_P = 1.9$, $\mu_S = 1.9$. $A = 0.37$. $\mu_P = 1.9$, $\mu_S = 1.55$. The two lines are the numerical response (solid) and, according to the heuristic prescription of Eq. (392), the signal $\xi_P(t)$ is multiplied by $0.39\epsilon(\omega t)^{\mu_S-\mu_P}$ (dashed), where $\omega = 0.01$ is the frequency of the harmonic signal of Eq. (387). Taken from Allegrini et al. (2006).

where $\xi_P(t)$ is obtained from the subordination to the harmonic signal of (387) with a subordination function whose complexity index is denoted by μ_P. To interpret their numerical results Allegrini et al. (2006) used the following two heuristic prescriptions:

(a) The case $\mu_P < \mu_S$ for which the correspondence between $\Pi(t)$ and the perturbation is emphasized by multiplying $\xi_P(t)$ by ϵA, with A being a fitting parameter.
(b) The case $\mu_P > \mu_S$ where they suggested that

$$\Pi(t) = \epsilon\xi_P(t)k_1(\mu_S, \mu_P)(\omega t)^{\mu_S-\mu_P}. \tag{392}$$

The parameter k_1 is taken from the theory but its functional dependence on the power-law indices is not important here. This fitting function is used to stress that, although the perturbation details are satisfactorily reproduced, there is a decreasing amplitude evident, signaling a decreased efficiency of the process of information transmission when $\mu_P > \mu_S$.

The important information signaled by Fig. 16 is that when the non-Poisson network is coupled to a single realization of the subordination to the harmonic perturbation, the average over infinitely many responses reproduces quite well the details of the perturbing signal.

The next part of this section is devoted to deriving a proper theory to account for this important result.

6.2. New FDT of the first kind

In this subsection we address the problem of deriving a new form of the FDT of the first kind to serve as a foundation for the CME. Figs. 14 and 16 suggest that to maximize the information transfer the perturbing signal $\xi_P(t)$ must have the same complexity as the system S. Furthermore, the results illustrated in Fig. 16 are based on the fact that the renewal events of the signal $\xi_P(t)$ affect the time of occurrence of the renewal events of the system S. Therefore the new FDT should emerge from a physical condition where this key fact is explicitly taken into account.

As discussed in Section 5.2.2 large quakes are rare, and the interval between large quakes is described by a distribution density whose explicit form may significantly depart from the inverse power law. Nevertheless, we have seen that even in this case the subordination function $\psi^{(S)}(t)$ is an inverse power law, and even when the large quakes are rare, the Demon is very active. It is therefore expected that a system P may influence a network S, with apparently a very limited number of S large quakes perturbed by a limited number of P large quakes. Actually, we imagine that the P actions influence the S actions, thereby implying that after a long time, significant effects may occur, in apparent contradiction with the assumption of weak perturbation strength and the rareness of the perturbing events. This is the ostensible manifestation of a very large number of extremely weak quakes that produce virtually invisible effects.

For these reasons we focus attention on the case where the actions correspond to events, and the survival probability of the fluctuation $\xi_S(t)$ coincides with the survival probability of the subordination function $\psi^{(S)}(t)$. Therefore we study how the perturbing signal $\xi_P(t)$ changes the occurrence times of the S events. To illustrate CME, we make the same assumptions for the network P.

6.2.1. How to perturb the subordination function $\psi^{(S)}(t)$

We focus attention on the content of Section 6.1, and on the simplest form of subordination, given by (251). To make it possible for an external perturbation to create a bias so that (251) may describe a transition from the equilibrium $p_1 = p_2$ to an out-of-equilibrium condition $p_1 \neq p_2$, it is necessary to establish a correlation between the drawing of a time τ and $\mathbf{p}(t)$. As a consequence, the renewal properties that led us to derive (251) and the equivalent time-convoluted GME (255) are lost. It is also evident that this way of proceeding leads to an entanglement between the external perturbation and the non-Poisson statistics responsible for the time convoluted structure of (255).

In spite of these difficulties, Allegrini et al. (2007c) have shown that in the limiting case of very weak perturbation the linear response structure of (380) is recovered with the non-ordinary FDT prescription (384). It is convenient to review their approach to this result.

We adopt the stochastic Liouville equation (SLE) of Kubo (1969a,b). Thus, in a discrete time representation, we have

$$\mathbf{f}(t+1) - \mathbf{f}(t) = -\frac{1}{2}\begin{bmatrix} r_+(t) & -r_-(t) \\ -r_+(t) & r_-(t) \end{bmatrix}\mathbf{f}(t), \tag{393}$$

where $\mathbf{f}(t)$ denotes a two-dimension vector, whose components $f_1(t)$ and $f_2(t)$ are the fluctuating probabilities that the system is in the state $|1\rangle$ and $|2\rangle$, respectively, at time t. In the unperturbed case $r_+(t) = r_-(t) = r_0(t)$. The fluctuating rate $r_0(t)$ is a quantity always vanishing except when an event occurs where it achieves the value 1. In this case, we realize the prescription of the subordination theory by assuming that the time interval between two events is described by the waiting time distribution density $\psi^{(S)}(\tau)$, as in CTRW theory, see, e.g., Weiss (1994). We assume that as an effect of an external perturbation the occurrence time of an event is slightly changed according to whether the network is in the state $|1\rangle$ or in the state $|2\rangle$. Thus when an event occurs in $|1\rangle$ no event occurs in $|2\rangle$, and vice-versa, and the stochastic functions $r_+(t)$ and $r_-(t)$ achieve the value 1 at different times. It is evident that this is a way to perturb the subordination function $\psi^{(S)}(t)$.

Let us define

$$\Sigma(t) = f_1(t) - f_2(t), \tag{394}$$

so that from (249) we obtain

$$\Sigma(t) = [1 - S(t-1)]\,\Sigma(t-1) - D(t-1), \tag{395}$$

where the difference variable is $D(t) \equiv \frac{r_+(t)-r_-(t)}{2}$ and the sum variable is $S(t) \equiv \frac{r_+(t)+r_-(t)}{2}$. The solution to (395), with initial condition $\Sigma(0) = 0$, is

$$\Sigma(t) = -\sum_{t'=0}^{t-1} D(t')Q(t,t'), \tag{396}$$

where if $t = t' + 1$, $Q(t, t') \equiv 1$, and if $t > t' + 1$, $Q(t, t') \equiv \left[1 - S(t' + 1)\right] \cdots [1 - S(t - 1)]$. Using the definition of the difference variable, we rewrite (396) as

$$\Sigma(t) = -\frac{1}{2}\sum_{t'=0}^{t-1} r_+(t')Q(t, t') + \frac{1}{2}\sum_{t'=0}^{t-1} r_-(t')Q(t, t'). \tag{397}$$

It is important to point out that we prepare the network such that $r_+(0) = r_-(0) = 1$ and therefore $\Sigma(1) = 0$. We have to determine how to obtain a non-vanishing value as an effect of a perturbation at later times. At time t, there are trajectories with $r_+(t) = 1$, trajectories with $r_-(t) = 1$ and trajectories with no event occurring, $r_+(t) = r_-(t) = 0$. Averaging implies that we multiply $\Sigma(t)$ by 1, which is equivalent to assuming that an event occurs in either $|1\rangle$ or $|2\rangle$. If an event occurs in $|2\rangle$ the earlier event occurred in $|1\rangle$. Consequently, the average over the trajectories where the event occurs in $|2\rangle$ forces us to average the first term on the *rhs* of (397). If an event occurs in $|1\rangle$ the earlier event occurred in $|2\rangle$. In this case we have to use the second term on the *rhs* of (397). Thus, incorporating both possibilities we write

$$\Pi(t) = \langle\Sigma(t)\rangle = -\frac{1}{2}\sum_{t'=0}^{t-1}\left[\langle r_+(t')Q(t, t')\rangle - \langle r_-(t')Q(t, t')\rangle\right], \tag{398}$$

where $\langle r_\pm(t')Q(t, t')\rangle$ is the conditional probability that an event occurs in $|2\rangle$ ($|1\rangle$) at time t, given that an earlier event occurred at time t' in the state $|1\rangle$ ($|2\rangle$). The time t', refers to an event occurring in $|1\rangle$ ($|2\rangle$), is the time at which we start waiting for a successive event in the state $|2\rangle$ ($|1\rangle$), with probability density of occurrence denoted by $\psi^{(\mp)}(t, t')$. Thus, we write

$$\Pi(t) = -\frac{1}{2}\int_0^t dt'[\psi^{(-)}(t, t')\pi^{(+)}(t') - \psi^{(+)}(t, t')\pi^{(-)}(t')]. \tag{399}$$

To derive a linear response we must study the influence of the external perturbation on the generator of non-Poisson statistics. Therefore let us go back to the rate of event production $g(t)$ (276). The perturbation of μ_S leads to a nonlinear response; to produce a linear response we perturb only T_S. Let us consider the case where the events are generated at each time step with the probability

$$g_\pm(t) = \frac{g_0[1 \mp \epsilon\xi_P(t)]}{1 + g_1[1 \mp \epsilon\xi_P(t)]\Delta t}, \tag{400}$$

where $\Delta t \equiv t - t_i$, with t_i denoting the time of occurrence of the last event prior to time t. In the absence of perturbation $\epsilon = 0$, this resetting time properly describes the renewal nature of two-state networks. We note that for $\Delta t \ll 1/r_1$ the transition rate simplifies to

$$g_\pm(t) = g_0[1 \mp \epsilon\xi_P(t)]. \tag{401}$$

and for $\Delta t \gg 1/r_1$

$$g_\pm(t) = \frac{g_0}{1 + r_1\Delta t}. \tag{402}$$

These two forms occur because at large times the external perturbation does not produce first-order effects on the distribution of sojourn times between consecutive events. As made evident by (401) and (402), the perturbed generator of events (400) is a proper representation of a perturbation so weak as to leave the complexity index μ unchanged. We see that this weak perturbation leads to

$$\psi^{(\pm)}(t, t') \to \psi(t, t') \tag{403}$$

as well as to,

$$\pi^{(\pm)}(t') \to \frac{1}{2}[1 \mp \epsilon\xi_P(t')]. \tag{404}$$

By inserting (403) and (404) into (399), we obtain (380) with the linear response defined by (384). In fact, we obtain for the non-stationary density

$$\psi(t, t') = -\frac{d}{dt}\Psi(t, t'), \tag{405}$$

which is the new form of the FDT. We shall refer to this theory as the *dynamical theory* to stress that it emerges from the dynamic influence of perturbation on the time of occurrence of the critical events of the system S.

Note that we are adopting the condition of direct subordination to the coin tossing process. Thus, as shown by (258), the regression to equilibrium is determined by the subordination function $\psi^{(S)}(t)$, and coincides with the corresponding survival probability $\Psi^{(S)}(t)$, as indicated by (259). As a consequence of this fact, the linear response function $\chi(t, t')$ must be expressed through the subordination function of age t', by means of

$$\chi(t, t') = \psi^{(S)}(t, t'). \tag{406}$$

6.2.2. Phenomenological theory

We have seen that the historical FDT can be generalized in two distinct ways, corresponding to (382) and (384). We have also seen that the former way is a natural choice when the anomalous statistics are generated by a time-dependent generator of Poisson events.

This is a delicate issue, which has lead to confusion and misunderstanding in the literature. In fact, we have to distinguish the case where the generator is weakly perturbed from the case where the perturbation is sufficiently intense to create an overall departure from Poisson statistics. In the former case, we can express the network response by means of the traditional FDT. In the latter case we have to consider the resulting statistical process as a form of complexity that is expected to violate the CME illustrated herein. In fact, we advocate a definition of complexity resting on the key role of crucial events, which are non-ergodic renewal (NER) events. We cannot rule out the possibility that even the processes generated by the slow modulation of Poisson processes may host invisible crucial events that in the long-time limit produce deviations from ordinary statistical physics, see, e.g., Allegrini et al. (2007b). However, we caution the reader that the existence of these different forms of complexity may produce an apparent violation of the LRT discussed earlier.

As far as the generalization of the FDT resting on (382) is concerned, it is convenient to point out that it is adopted by some researchers, see, e.g., Sokolov (2006), also in the renewal case. We refer to this treatment of the renewal processes as the *phenomenological theory*, which is derived from the adoption of the response function (382). Taking into account that we are discussing a renewal condition resting on the direct subordination to the coin-tossing process, and using (208), we now express the response function $\chi(t, t')$ as

$$\chi(t, t') = P(t')\Psi^{(S)}(t - t'). \tag{407}$$

The function $P(t)$ denotes the number of events produced per unit time by the non-Poisson generator of events, and its explicit expression in the long-time limit is given by (212).

Let us insert (407) into (380), which allows us to recover a time convoluted expression, provided that the perturbation $\xi_P(t')$ is replaced by the effective perturbation $\xi_{\text{eff}}(t')$:

$$\xi_{\text{eff}}(t') = P(t')\xi_P(t'). \tag{408}$$

It is immediately evident that this effective perturbation corresponds to a weakening intensity as a function of time due to the inverse power-law form of $P(t)$. In the long time limit the response of the network is expected to vanish.

6.2.3. Response to harmonic perturbation

The qualitative prediction of the phenomenological theory is confirmed by the dynamical theory. Barbi et al. (2005) used the FDT (384) to predict the response to the harmonic perturbation

$$\xi_P(t) = \cos(\omega t), \tag{409}$$

and found for $\Pi(t)$ the analytical expression

$$\Pi(t) \approx \epsilon \frac{\cos(\frac{\pi}{2}\mu_S + \omega t)}{\Gamma(\mu_S - 1)\,(\omega t)^{2-\mu_S}}, \tag{410}$$

in the asymptotic time limit

This result (410) for the residual probability confirms that the non-ergodic non-Poisson processes can be thought of as a genuine manifestation of complexity. In fact, we have seen that the analysis of EEG data, for instance, suggests that collective processes with extended memory are created as an effect of self-organization, and that the emerging structures are abruptly destroyed and replaced by new structures, with no memory of the time duration of the earlier structures. As a consequence, the network does not respond to harmonic perturbations. We have seen with (368) that a Poisson network does respond to harmonic perturbations. A complex dynamics corresponding to the mere superposition of many Poisson process would respond to harmonic perturbation, and the weight of a Poisson component with rate g_0 would be given by (369). Of course, the superposition of harmonic modes would also respond to harmonic perturbation. The lack of a response to harmonic perturbation is an indication that the network S cannot be decomposed into a superposition of either linear modes or Poisson processes. This is a consequence of the fact that the spontaneous onset of cooperation is incompatible with the existence of non-interacting units.

6.2.4. Transmission of the statistics of P to S

Let us establish that a complex network S can respond to a perturbation with suitable complexity. Consider the Gibbs ensemble of the network $S + P$, and evaluate the average $\langle \xi_S(t) \rangle_{SP}$. Note that

$$\langle \xi_S(t) \rangle_{SP} = \left\langle \langle \xi_S(t) \rangle_S \right\rangle_P . \tag{411}$$

We select all the responses to the same perturbation, characterized by a given $\xi_P(t)$, evaluate their average, denoted by $\langle\xi_S(t)\rangle_S$ and finally take the average over all possible perturbations denoted by $\langle\cdots\rangle_P$ so as to obtain the final result denoted by $\langle\cdots\rangle_{SP}$. In summary, this procedure leads to

$$\langle\Pi(t)\rangle = \langle\langle\xi_S(t)\rangle\rangle = \epsilon\int_0^t \mathrm{d}t'\chi(t,t')\langle\xi_P(t')\rangle, \tag{412}$$

where we suppressed the bracket subscripts for notational convenience.

Both the S- and P-signals are dichotomous fluctuations with the values 1 and -1. To produce a perturbation effect it is convenient to assume that all the perturbations ξ_P holds 1 at $t = 0$, and that all of them are located at the beginning of their sojourn in state $|1\rangle$. This is an out-of-equilibrium assumption that is plausible for the perturbing network. As a consequence, (412) becomes

$$\langle\Pi(t)\rangle = \langle\langle\xi_S(t)\rangle\rangle = \epsilon\int_0^t \mathrm{d}t'\chi(t,t')\Psi_P(t'), \tag{413}$$

where $\Psi_P(t)$ is the perturbation survival probability for which we assume the following analytical form

$$\Psi_P(t) = \left(\frac{T_P}{t+T_P}\right)^{\mu_P-1}. \tag{414}$$

This slow decay corresponds to the probability that no perturbation event occurs up to time t. The network S evolves in time so as to reach the steady value that would correspond to a constant perturbation abruptly applied at $t = 0$. However, during this process a perturbation event occurs that has the effect of abruptly changing the external field. Thus, $\langle\langle\xi_S(t)\rangle\rangle$ does not reach a steady value, but decays after reaching a maximum value. Using the method of Laplace transforms it is possible to evaluate the time asymptotic behavior of the response.

Here we discuss two different physical conditions for the network S.

6.2.5. Network S at equilibrium

Unfortunately, when $\mu < 2$ an equilibrium condition does not exist. However, the adoption of the dynamic theory and of the results of Aquino et al. (2004) suggest a way of solving the problem that brings us back to the ordinary FDT. Imagine that the system S has been prepared at a time $-t_a$ so large that $t \ll t_a$. In this case, see Aquino et al. (2004),

$$\psi(t,t') \propto \left(\frac{1}{t-t'}\right)^{\mu_S-1}. \tag{415}$$

Consequently, adopting (413) and using the form of the response function given by (406) leads us to conclude that the system S inherits the perturbation statistics from (414) if $\mu_P < \mu_S$. On the other hand, if $\mu_S < \mu_P$ the network S maintains its own statistics from (415).

Note that the same result is obtained if we adopt the phenomenological theory. In fact, in this case

$$P(t') \propto \frac{1}{t_a+t'} \approx \frac{1}{t_a}, \tag{416}$$

as a consequence of $t \ll t_a$, while

$$\Psi(t-t') \propto \left(\frac{1}{t-t'}\right)^{\mu_S-1} \tag{417}$$

so that using the response (407) in (413) yields the expected result.

6.2.6. Network S out-of-equilibrium

Let us make the assumption that, although at time $t = 0$ half of the networks S are in the state $|1\rangle$ and half in the state $|2\rangle$, all them are at the beginning of their sojourn in the corresponding states. This is an out-of-equilibrium condition that yields a totally different result from that of the previous subsection. Using the dynamical theory we obtain

$$\frac{\langle\Pi(t)\rangle}{\epsilon} = \frac{k_1(\mu_S,\mu_P)}{t^{\mu_P-1}} + \frac{k_2(\mu_S,\mu_P)}{t^{\mu_P+1-\mu_S}}, \tag{418}$$

where $k_1(\mu_S,\mu_P)$ and $k_2(\mu_S,\mu_P)$ are analytic functions of the power-law indices whose forms do not contribute to this discussion and are therefore not recorded here. In this case we see that for $\mu_S < 2$ and $\mu_P < 2$ the network S always inherits the perturbation statistics from the first term on the *rhs* of (418).

When we adopt the phenomenological theory, we obtain

$$\frac{\langle\Pi(t)\rangle}{\epsilon} = \frac{k_1(\mu_S,\mu_P)}{t^{\mu_P-1}} + \frac{k_2(\mu_S,\mu_P)}{t^{\mu_S-1}}, \tag{419}$$

with predictions that are qualitatively equivalent to those of the dynamic theory with the assumption that the network S has been prepared in the very distant past.

6.2.7. Direct assessment of the correlation between S and P

Using the same arguments as those adopted to get information from $\langle \Pi(t) \rangle$, we examine the cross-correlation

$$C_{SP}(t) = \langle \xi_S(t)\xi_P(t) \rangle, \tag{420}$$

where $\langle \cdots \rangle$ denotes an average over a Gibbs ensemble of networks $S + P$. We focus our attention on the cross-correlation indicator

$$\Xi_{SP} = \lim_{t \to \infty} C_{SP}(t). \tag{421}$$

Adopting this cross-correlation indicator allows us to resolve some doubts affecting the selection of $\langle \Pi(t) \rangle$ as an autocorrelation indicator. In fact, it is very attractive to interpret the fact that for $t \to \infty$

$$\langle \xi_S(t) \rangle \propto \Psi_P(t) \tag{422}$$

as an indication that S inherits the statistics of P. The question remains as to the generality of this result.

The analytical results that we obtain depend on the preparation condition adopted for the network. When the network S, with $\mu_S < 2$, is prepared at $t_a = \infty$ and the perturbation is prepared and applied to S at $t = 0$, we have for the cross-correlaion indicator

$$\Xi_{SP} \neq 0 \tag{423}$$

if $\mu_P < \mu_S$. This prediction is in qualitative agreement with the arguments resting on the use of (415) and supports the fact that under this condition the system S inherits the statistics of P.

When the network S, with $\mu_S < 2$ is prepared at $t = 0$ and the perturbation is prepared and applied to S at $t = 0$, we again have (423) if $\mu_P < 2$. This last prediction is in qualitative agreement with (418) and supports the fact that when this condition is satisfied the network S inherits the statistics of P.

6.2.8. Towards a new principle

The arguments used so far to illustrate the CME have been based on dichotomous fluctuation $\xi_S(t)$. The same approximation has been made to produce the perturbing signal $\xi_P(t)$, except in the case of the stretched cosine adopted in Fig. 14. However, it is plausible that CME goes beyond the dichotomous approximation, but the role of crucial events is essential. We have a generator of S events and a generator of P events. Implementing both generators we make the network S sensitive to the network P by filling the empty time interval between two consecutive events with a positive or a negative value of $\xi_S(t)$. The same approach is used to define $\xi_P(t)$. This serves the purpose of making $\xi_S(t)$, and the corresponding events as well, sensitive to $\xi_P(t)$ and to the renewal events of P.

In the special case when we adopt the double subordination, the resulting survival probability is a MLF. However, the key subordination function is an inverse power law. The same argument applies to the case of SOFD process. We also note that to fully appreciate the new FDT in action, it is necessary to prepare both network and perturbation at $t = 0$, a property that can be used in the case of non-ergodic renewal networks such as BQDs, but which does not seem to be the proper condition for the EEG analysis. In this latter case it is convenient to imagine the network prepared at $t_a = \infty$.

In summary, we observe that:

(a) The specific choice that we make to fill the time interval between two consecutive events does not seem to be essential for the perturbation events to transfer information to the network events.

(b) The essential ingredient of the subordination process is given by the inverse power-law subordination function (271)

(c) The network is prepared in the infinitely distant past $t_a = \infty$.

On the basis of these remarks we are led to conclude that the OP must be generalized as follows. At equilibrium a macroscopic fluctuation can be realized whose regression to equilibrium is a MLF, of which, due to the finite time effect, only the stretched exponential portion is visible. Let us consider the case when the environment of the network S is another complex network P. Let us assume that the subordination functions of these two networks are inverse power laws with indices μ_S and μ_P, respectively, both of them fitting the non-ergodic condition, $\mu_P < \mu_S < 2$. In this case in the network S a macroscopic fluctuation emerges intermittently, and its regression to equilibrium is determined by the stretched exponential

$$E_\alpha(t) = \exp[-(\lambda_\alpha t)^\alpha], \tag{424}$$

with $\alpha = \mu_P - 1$.

Note that the discussion in Section 5.2.2 lends further support to this conclusion. In fact, the large quakes are rare. It is apparently implausible that the large quakes of the perturbing system, which are rare as well, would influence the occurrence of the large quakes of the network. We are convinced that this apparently incomprehensible phenomenon can be understood using the arguments of Section 5.2.2: the dialogue between S and P rests on the small and virtually invisible effects that the P actions exert on the S actions. The small quakes are not rare.

6.3. Sun-climate

We have to point out that, although the condition $\mu < 2$ is challenging due to the breakdown of the ergodic condition, as we discuss in the next section, the condition $\mu > 2$ can also generate interesting effects. The causes of global warming, the increase in the average global temperature near the Earth's surface of approximately 0.8 ± 0.1 °C since 1900, are not as apparent as some recent scientific publications and the popular media indicate. We show that the changes in the Earth's average surface temperature are directly linked to two distinctly different aspects of the Sun's dynamics: the short-term statistical fluctuations in the Sun's irradiance and the longer-term solar cycles. This argument for the direct linking of the dynamics of the Sun to the response of the Earth's climate is based on the statistical arguments presented herein and augments the interpretation of the causes of global warming presented in the United Nations' 2007 IPCC report Climate Change (2007).

The 'majority opinion' regarding the causes of global warming is based on the analysis done using large-scale computer codes that incorporate all identified physical/chemical mechanisms into global circulation models (GCM) in an attempt to recreate and understand the variability in the Earth's average temperature over time. The IPCC report concludes that the contribution of solar variability to global warming is negligible, to a certainty of 95%. It is reported that the 'scientific majority' believes the average warming observed since the beginning of the industrial era is due to the increase in anthropogenic greenhouse gas concentrations in the atmosphere.

The Earth's atmosphere, landmasses and oceans, absorb and redistribute the total solar irradiance (TSI) by means of coupled nonlinear hydrothermal, geochemical and radiative dynamic processes producing the average global temperature. Versions of these physical mechanisms are included in the GCMs, but what is not addressed in these simulations, over and above the global temperature trend of the last thirty years, are the statistics of the average global temperature anomalies. The statistical variability in the Earth's average temperature is interpreted as noise and as noise these temperature fluctuations are thought to contain no useful information and are consequently smoothed to emphasize the presumably more important long-time changes in the average global temperature. Moreover, according to the Central Limit Theorem the statistics of the fluctuations in such large-dimensional networks ought to be Gaussian and the fact that they are not remains unexplained. This prompted the study of temperature fluctuations as a problem in non-equilibrium statistical physics wherein statistical fluctuations often provide useful information about the transport properties of complex phenomena, for example, through the fluctuation–dissipation theorem.

We use the response of the Earth's air temperature fluctuations to the variability of solar irradiation as an interesting contemporary example. Scafetta and West (2003) and Scafetta et al. (2004) have found the surprising property that the air temperature anomalies, analyzed with the Diffusion Entropy (DE) method (see Scafetta et al. (2001) and Grigolini et al. (2001)), reveal the complexity index for the Earth's temperature anomalies $\mu_E > 2$, which, in turn, suggests a possible connection with the statistics of hard-x-ray solar flares studied by Grigolini et al. (2002). Grigolini et al. (2002) found that the statistics of solar flares generates $\mu_P = 2.138$. The application of the same DE techniques to the average global temperature fluctuations, as discussed (Scafetta and West, 2003), yields $\mu_E = 2.18$ (Northern Hemisphere), $\mu_E = 2.1$ (Southern Hemisphere), $\mu_E = 2.19$ (over land) and $\mu_E = 2.07$ (over ocean). Note that the Earth plays the role of the system S. Thus, we replace S with E. Furthermore, the Sun plays the role of the perturbation. Thus, in this case the symbol P denotes the Sun and is denoted by the intensity suffix I.

How can we explain the connection between the activity on the sun and the temperature anomalies on the earth? In this case the system E generates the time sequence of air temperature fluctuations $\{\Delta T\}$ and the system P generates a sequence of flares, described by the time series $\{t_i\}$. We consider the flares as indicators of sun's dynamic complexity. Although Scafetta and West (2003) did not use the aging technique to ensure the renewal character of the solar flares, they made a careful analysis based on the comparison between the diffusion and second moment scaling that afforded a compelling indication that solar flares are in fact renewal. In other words, they established that the conversion of the time of occurrence of solar flares into a diffusion process is generated by a Lévy walk, see Section 3.2.1, and this is only possible if the solar flares are renewal.

Thus, the sequence of the times of occurrence of solar flares is a sequence of renewal events, characterized by the parameter μ_I fulfilling the condition $2 < \mu_I < 3$. The condition $\mu_I > 2$ makes the solar flare process compatible with equilibrium and ergodicity. However, although the mean interval between two consecutive flares exists and is finite, the mean-square value is divergent, thereby implying fluctuations from the mean value of large intensity, which is responsible for the scaling

$$\delta = \frac{1}{\mu_I - 1}, \tag{425}$$

larger than the ordinary diffusive scaling of $\delta = 1/2$.

The DE method, see, Allegrini et al. (2002b), is characterized by the property of affording the correct scaling, therefore going beyond the evaluation of the distribution variance that, in principle, should diverge, as a result of Lévy statistics.

Let us now discuss the second time series, namely, the sequence of air temperature fluctuations $\{\Delta T\}$. This is a virtually continuous signal, insofar as it is represented by a time scale much larger than the time scale of the former sequence. Scafetta and West (2003) and Scafetta et al. (2004) derived a surrogate sequence qualitatively similar to the real sequences of temperature fluctuations by recording the number of solar flares contained in the unit time scale of temperature fluctuations.

As a result of the fractal and self-similar properties of the time series $\{t_i\}$, the resulting fluctuation has the same clustering structure as the original time series, and the interval between two consecutive clusters is characterized by the same power-law index μ_I as the original time series. Due to the coarse graining adopted the variance of the surrogate fluctuation ΔT is finite, and, as a consequence, as pointed out by Allegrini et al. (2002b), the DE technique is expected to detect the same scaling as that produced by the original time series, namely, the scaling parameter (425).

This argument is attractive, but its weakness is that it implies an energy balance that would suggest an extremely detailed and probably very complicated model. Let us see therefore how adopting the concept of CME developed in this section helps us to bypass these complications. We refer to the air temperature fluctuations in a hypothetical situation in which there are no interactions with the solar flares. Also in this hypothetical case it is plausible to imagine that a surrogate time series exists corresponding to an unknown complexity parameter $\mu_E^{(0)}$, see West and Grigolini (2008) for a complete discussion.

The problem that we have to address now is that of establishing a connection between the Sun's irradiance $\Delta I(t)$ and the Earth's temperature fluctuation $\Delta T(t)$. Let us imagine that both are satisfactorily described by surrogate time series as the one derived by Scafetta and West (2003) from the solar flare theory discussed by Grigolini et al. (2002). In the absence of coupling they are characterized by the complexity parameters $\mu_E^{(0)}$ (air temperature fluctuations) and $\mu_I = 2.138$, see, Grigolini et al. (2002). We do not use the superscript (0) for sunlight, insofar as we assume that the Sun drives the Earth's temperature with no feedback.

In the absence of linking the time series $\Delta I(t)$ and $\Delta T(t)$ are uncorrelated. Let us now discuss how the CME establishes a correlation and why the DE technique enables us to detect it, regardless of its weakness. We imagine an ideal experiment and explain why the application of the DE technique is virtually equivalent to realizing this ideal experiment in practice. Imagine that it is possible, in principle, to record infinitely many time series of the former kind, corresponding to the same time series of the latter kind. According to the FDT of (380) we have

$$\langle \Delta T(t) \rangle = \epsilon \int_0^t \mathrm{d}t' \chi(t, t') \Delta I(t'). \tag{426}$$

Moreover, imagine that this excitation experiment can be done infinitely many times so as to turn (426) into

$$\langle\langle \Delta T(t) \rangle\rangle = \epsilon \int_0^t \mathrm{d}t' \chi(t, t') \left\langle \Delta I(t') \right\rangle. \tag{427}$$

This experiment is impossible in practice, but the application of the DE technique corresponds to its realization. In fact, this technique rests on the use of a mobile window of length l that explores all the possible positions of the time series. The left end of the window corresponds to the beginning of the observation process, the time origin $t = 0$ of (427). The right end of the window corresponds to the evaluation of the response of E after a time l. Among all possible conditions concerning $\Delta I(t)$ we have to select only those fulfilling the condition $\Delta I(t) > 0$. The negative contributions would cancel with the positive, thereby preventing us from estimating the transfer of complexity from the Sun to the Earth's atmosphere. Under these conditions, we obtain the response function

$$\chi(t, t') \propto \frac{1}{(t - t')^{\mu_E^{(0)} - 1}}. \tag{428}$$

In fact, the linear response function is proportional to the time derivative of the equilibrium autocorrelation function, which is proportional to $1/(t - t')^{\mu_E^{(0)} - 2}$, as required by the condition of infinite age. We assume that $\left\langle \Delta I(t') \right\rangle$ is prepared at $t = 0$ to be $\left\langle \Delta I(t') \right\rangle \propto 1/t^{\mu_I}$, and thereby obtain the condition

$$\mu_E^{(0)} > \mu_I. \tag{429}$$

Note that $\mu_I \approx 2.1$ and the unknown average global temperature power-law index is supposed to fit the ergodic condition $\mu_E^{(0)} > 2$. Thus, the earth assumes the anomalous solar flare statistics independently of whatever ergodic value $\mu_E^{(0)} > 2$ it had previously. This explains why the Earth's air temperature fluctuations inherit the solar flare statistics as shown by Scafetta and West (2003) and discussed in the DE context by West and Grigolini (2008).

6.4. Non-ergodic statistics

Over a hundred years ago Gibbs (1928) had the brilliant idea that the two kinds of averages that occur in statistical physics, averages over time and averages over ensembles, are in fact the same. This property has come to be called the ergodic hypothesis, and for all his effort using statistical mechanics, Gibbs was never able to prove the truth of this hypothesis in a mathematically rigorous way. As the mathematician Wiener (1948) pointed out:

> It was not until about 1930 that a group of mathematicians – Koopman, von Neumann, Birkhoff (see Hopf (1937)) – finally established the proper foundations of the Gibbs statistical mechanics . . . as Plancherel and others have shown, there is no significant case where that hypothesis is true. No differentiable path can cover an area in the plane, even if

> it is of infinite length . . . at the end..Gibbs himself . . . replaced this hypothesis by the *quasi-ergodic* hypothesis, which merely asserts that in the course of time a system generally passes indefinitely near to every point in the region of phase space determined by the known invariants.

The ergodic hypothesis as proved today, states that an ensemble average and a time average are asymptotically equal, that is, equal in the limit of infinitely long observation time. In the study of simple physical networks that are at or near equilibrium the ergodic hypothesis is almost invariably made. However, as the networks of interest become more complex and measuring instruments become more refined, the equivalence of these averages is no longer so apparent. As observed by Bel and Barkai (2005) as measurements on single particle trajectories have become possible, ensemble averages, that is, many particle averages, do not yield the same information as do long time single-trajectory averages. This subsection, in part, follows the logic presented by these authors.

The canonical equilibrium distribution function is given by (62) which for a discrete set of energy levels e_j indexed by j, can be written

$$W_j = Z^{-1}\mathrm{e}^{-\beta e_j}, \tag{430}$$

and the partition function (63) is replaced with

$$Z = \sum_j \mathrm{e}^{-\beta e_j}. \tag{431}$$

Consequently, the ensemble average of a physical observable O_j is given by

$$\langle O\rangle = Z^{-1}\sum_j O_j \mathrm{e}^{-\beta e_j}. \tag{432}$$

Now let us turn our attention to the measurement of a single trajectory in which the particle spends an amount of time t_j in the state j and the total observation time is t_T. In this way the relative frequency $\overline{p}_j$ is the total fraction of time spent in the state j, that being,

$$\overline{p}_j = \frac{t_j}{t_T}, \tag{433}$$

and the time average of the physical observable O_j is

$$\overline{O} = \sum_j O_j \overline{p}_j. \tag{434}$$

According to equilibrium statistical mechanics the validity of the ergodic theorem implies the equality of the two kinds of averages

$$\langle O\rangle = \overline{O} \tag{435}$$

and the relative frequency of the sojourn time in the state j is equal to the canonical distribution

$$W_j = \overline{p}_j. \tag{436}$$

Thus, in an ergodic network the fraction of sojourn times is non-random in the thermodynamic limit of long measurement time, see Majumdar and Comtet (2002).

On the other hand, in a general dynamic network the relative frequency of sojourn times within any given state is a random variable for non-ergodic networks, even asymptotically in time. This can be explained by recalling that one of the conditions for ergodicity is that the measurement time is much longer than the characteristic time scales for the network dynamics. However, when the dynamic time scales diverge, as happens when the inverse power-law sojourn time distribution has an index $\mu < 2$, this condition for ergodicity cannot be satisfied. Note that the waiting or sojourn time distribution function $\psi(t)$ with a diverging first moment was introduced into physics by Scher and Montroll (1975) in the CTRW context and has been subsequently found in many areas of physics, see, e.g., Brokmann et al. (2003), Bardou et al. (2002), Metzler and Klafter (2000a) and Hughes (1996).

The analysis of the non-ergodic case can be done by considering a two-state network where the sojourn time is the 'light-on' and 'light-off' positions is inverse power law. We use the inverse power law (170) to select a integer time τ_1 and create the first visible quiescent region $(0, \tau_1)$ filled on the integers with $+$ signs. At time $t = \tau_1$ we draw another integer τ_2 from (170), and put on the integers $-$ signs from $t = \tau_1$ to $t = \tau_1 + \tau_2$. This procedure is continued indefinitely, creating an infinitely large number of quiescent regions with alternate signs. Now we create an ensemble of realizations of sequences of this kind.

Let us consider a window located between times t and $t + l$. Denoting the position of the window filled with $+$ by l_+ and similarly for l_-, we have

$$p_\pm(l, t) = \frac{l_\pm(t)}{l(t)} \tag{437}$$

where the window l moves along the sequence. If we take the limit of the total observation time going to infinity we obtain

$$\overline{p}_{\pm}(l) = \lim_{t_T\to\infty} \frac{1}{t_T}\int_0^{t_T} p_{\pm}(l,t)\mathrm{d}t. \tag{438}$$

We expect

$$\overline{p}_{\pm}(l) = 1/2 \tag{439}$$

since there are only two possible states, which is the correct result for an ergodic network. However, the present network is not ergodic, so (439) is not correct. We find instead that either $\overline{p}_+(l) = 1$ or $\overline{p}_+(l) = 0$, with equal probability. Consequently, a given trajectory gives $\overline{p}_+ = 1$ and another trajectory gives $\overline{p}_+ = 0$, either one or the other.

More precisely, the distribution of the average fraction of time spent sojourning in the + state is

$$P(\overline{p}_+) = \frac{A_+ \sin\pi(\mu-1)}{\pi} F(\overline{p}_+) \tag{440}$$

with

$$F(\overline{p}_+) = \frac{\overline{p}_+^{\mu-2}\left(1-\overline{p}_+\right)^{\mu-2}}{\left(1-\overline{p}_+\right)^{2(\mu-1)} + A_+^2\overline{p}_+^{2(\mu-1)} + 2A_+(1-\overline{p}_+)^{\mu-1}\overline{p}_+^{\mu-1}\cos\pi(\mu-1)}. \tag{441}$$

This expression was first derived by Lamperti (1958) with the coefficient A_+ given in terms of the equilibrium distribution W_+

$$A_+ = \frac{W_+}{1-W_+}. \tag{442}$$

When the power-law index is given by $\mu = 1.5$ and $A_+ = 1$, (440) reduces to the arcsin law

$$P(\overline{p}_+) = \frac{1}{\pi}\frac{1}{\sqrt{\overline{p}_+\left(1-\overline{p}_+\right)}} \tag{443}$$

a result originally due to Lévy, see Feller (1971). These results show that the condition $\mu < 2$ give rise to a non-ergodic process, as is evident from (443). We see that this distribution diverges at both extremes $\overline{p}_+ = 1$ and $\overline{p}_+ = 0$ and clearly indicates that when a single experiment is carried out, yielding a single sequence, we do not obtain the ensemble average 1/2. We obtain the time average of either $\overline{p}_+ = 1$ or $\overline{p}_+ = 0$, as proven by Lamperti as part of the theorem relating to (441).

Eq. (441) was derived by Bel and Barkai (2006a) with $\overline{p}_+$ and A_+ replaced with $\overline{p}_j$ and A_j, rather than proven as a mathematical theorem for the fraction of time occupying a given set as Lamperti did in his doctoral dissertation. These authors also developed the implications of non-ergodicity for complex physical networks. For example, when the local detailed balance condition is satisfied the coefficient is replaced with

$$A_j = \frac{W_j}{1-W_j} \tag{444}$$

and $1 < \mu \leq 2$. When $\mu = 2$ the usual ergodic behavior is obtained and for $\mu < 2$, the non-ergodic case, the exponent is the anomalous diffusion exponent in the relation $\langle x^2\rangle \propto t^{\mu-1}$.

7. Synchronization-induced crucial events

The phenomenon of synchronization was first documented by Huygens in a letter to the Royal Society dated February 27, 1665. As described by Bennett et al. (2002) he elaborated on his findings in a contemporaneous letter to his father in which he described observations made while he was confined to his room by a brief illness. He determined that two pendulum clocks swung in exactly the same frequency and 180 degrees out of phase. Moreover, after perturbing one pendulum the synchronization was restored within thirty minutes and remained indefinitely. An excellent brief history of the phenomenon is given by Bennett et al., as well as a modern treatment of the associated nonlinear mathematical problem of the coupling of two pendula. As they point out the onset of synchronization and unique phase relations is a fundamental problem that arises in phenomena ranging from neurobiology and brain function as discussed by Rodriguez et al. (1999) to animal locomotion shown by Strogatz and Stewart (1993). A much more extended history of this remarkable discovery is given by Strogatz (2003) in his remarkable book on the general phenomenon of synchronization and its far reaching implications.

In previous sections we have seen that non-ergodic renewal processes represent a most attractive form of complexity, requiring a revision and extension of the fundamental tools of non-equilibrium statistical physics, such as the FDT of the first kind. Here we discuss one origin of this form of complexity. In this section we establish that synchronization is a basic property behind the emergence of this form of complexity. The former model sheds light onto the origin of the BQD

complexity, being confined however to the index value $\mu = 1.5$. The latter model is closer to the neuron dynamics and may have a more direct connection with the complexity of the brain. Here we focus on the case $\mu < 2$, implying a diverging average time interval between consecutive events, thereby yielding ergodicity breakdown as shown by Bel and Barkai (2006c). We refer to these processes as NER processes.

The human brain is considered by some to be the most complex network in the universe and attempts to construct formal representations of that complexity have met with only limited success. Consequently, investigators have relied on capturing certain identifiable characteristics within models to understand the possible mechanisms within the brain. One such property is that of synchronization and its potential role in connecting neurophysiological processes to consciousness and higher brain function. The relation between synchronization and the graphical analysis of complex networks for brain science is reviewed by Stam and Reijneveld (2007).

The timing of biological oscillators such as pacemaker cells in the human heart are notoriously poor clocks, which is to say that the firing period varies from cell to cell and from firing to firing. However, collections of such naturally variable entities when allowed to interact become phase locked and lose their individual variability. How natural phenomena accomplish this phase synchronization has been gaining increasing attention since Wiener's (1958) early work on understanding the alpha rhythm in EEG data and Turing's (1952) work on the modeling of collective phenomena. The more recent mathematical investigations into the coupling mechanisms of such collectives was made by Kuramoto (1981) using a network of coupled nonlinear oscillators to mimic natural synchronization in oscillating chemical reactions. A similar strategy was employed by Winfree (1990) in his studies of cardiac oscillations. Glass and Mackey (1988) extended our understanding of biorhythms to include modern nonlinear dynamics and chaos theory. But the phenomenon of synchronization became mature with the excellent book by Strogatz (2003) in which he presents a compelling case for synchronization being a fundamental mechanism for organizing confusion into complexity in natural phenomena, whether it is clapping, fireflies or the brain.

The modern mathematical representations of biological clocks are often chaotic attractors, that are periodic, but not harmonic, for example, the Rössler oscillator has been used to represent the output of a single neuron by Stam (2005). Wood et al. (2006) have shown that coupled stochastic clocks can manifest cooperative, that is to say, synchronized behavior. Varela et al. (2001) postulate that brain function, such as cognition, rests on the cooperative behavior of collections of many neurons. The strategy of Bianco et al. (2007b) is to map brain activity onto networks and consequently study the dynamics of the collections of neurons modeled as such networks. The latter authors find that the changes in the topology of the network describing the brain activity are driven by a NER process.

Moreover, a collection of BQDs appears to have the same dynamical behavior as brain activity, see Nirmal et al. (1996), Kuno et al. (2001), Kuno et al. (2003) and Shimizu et al. (2001), and so Bianco et al. (2007b) postulate that the two complex networks may have a common dynamic model. In this subsection we present a network of coupled two-state stochastic clocks and establish that at the onset of phase synchronization the dynamics of the network has the same properties as collections of BQDs and/or neurons within the brain, that is, they are NER networks as discussed by Bianco et al. (2007b).

7.1. Synchronization and non-ergodic renewal processes

Sun et al. (2008) pointed out that synchronization is not a single concept, but has a variety of subtleties arising in physical, chemical, social and neural networks whose mathematical analyses have provided distinctions between the complete synchronization of Carroll and Pecora (1990), the phase synchronization of Rosa et al. (1998) and Rosenblum et al. (1996), the lag synchronization of Rosenblum et al. (1997), Rim et al. (2002), Shahverdiev et al. (2002) and Zhan et al. (2002), the generalized synchronization of Rulkov et al. (1995), Kocarev and Parlitz (1996), Brown (1998), Boccaletti and Valladares (2000) and Shahverdiev and Shore (2005), the intermittent lag synchronization of Rosenblum et al. (1997) and Boccaletti and Valladares (2000), the imperfect phase synchronization of Zaks et al. (1999), the almost synchronization of Femat and Solis-Perales (1999) and finally the anticipating synchronization of Voss (2000). Consequently, we restrict our discussion to a very small piece of this literature, that piece which most closely relates to the non-ergodic statistics discussed in the previous section, including the influence of age.

7.1.1. Two-state stochastic clocks

Consider an ensemble of networks each with N two-state stochastic clocks and each clock within a given network coupled to N_c other clocks within that network. Using our earlier bra and ket notation the two states of the clock correspond to the phases 0 for $|1\rangle$ and π for $|2\rangle$. The master equation for a single clock of a network in the ensemble is

$$\frac{dP_1}{dt} = -g_{12}P_1 + g_{21}P_2$$
$$\frac{dP_2}{dt} = -g_{21}P_1 + g_{12}P_2 \tag{445}$$

where P_j is the probability of finding the clock in the state $|j\rangle$, $j = 1, 2$ and g_{ij} the rate of transition from the state $|j\rangle$ to the state $|i\rangle$. The transition rates are indexed in this peculiar way in order to be defined by means of the prescription introduced by Wood et al. (2006):

$$g_{ij} = g \exp\left[K\left(\pi_i - \pi_j\right)\right] \tag{446}$$

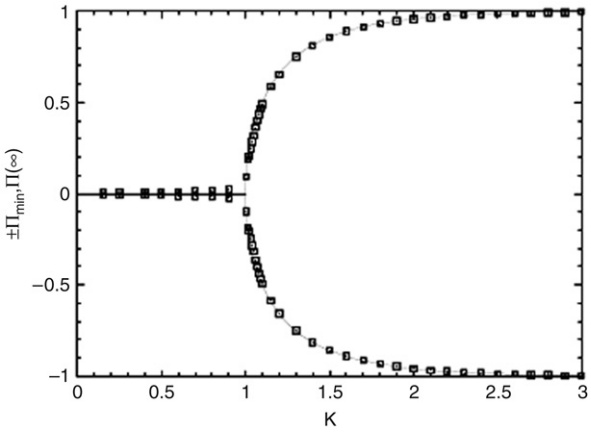

Fig. 17. The minima of the potential and the asymptotic value of the dynamic variable is shown as a function of the coupling constant K. The full line is the theoretical prediction obtained solving the equation for the extrema of the potential. The squares denote the results of numerical evaluation of the asymptotic value of the dynamic variable for an ensemble of networks with 10^5 clocks. [Taken from Bianco et al. (2007a,b)].

where again, the subscripts are restricted to the two values, $i, j = 1, 2$. In (446) the parameter g is the unperturbed transition rate of a single clock, $K > 0$ is the coupling constant and π_j is the fraction of the N_c coupled clocks that are in the state $|j\rangle$. Wood et al. (2006) place their clocks in a d-dimensional lattice where only the nearest neighbors are coupled. Thus, every clock is coupled to $N_c = 2d$ other clocks. Bianco et al. (2007b) adopt, instead, an all-to-all coupling: $N_c = N - 1$. With this latter choice, in the mean field approximation, when $N \to \infty$, the probabilities in the transition rate simplify to

$$\pi_j = P_j \tag{447}$$

which in this limit is exact. Implementing the normalization condition $P_1 + P_2 = 1$, in the mean-field limit, the master equation (445) reduces to

$$\frac{\mathrm{d}\Pi(t)}{\mathrm{d}t} = -2g\Pi\cosh[K\Pi] + 2g\sinh[K\Pi] = -\frac{\partial V(\Pi)}{\partial\Pi} \tag{448}$$

where $\Pi = P_1 - P_2$ and, of course, the difference variable lies in the interval $(-1, 1)$.

Eq. (448) describes the overdamped motion of a particle, whose 'position' is Π within the symmetric potential $V(\Pi)$ and the values of its minima depend only on the coupling constant K. It is straight forward to show that there is a critical value of the coupling parameter K_c given by $K = K_c = 1$, such that: (1) If $K \leq K_c$ the potential has only one minima located at $\Pi = 0$; (2) if $K > K_c$ the potential is symmetric and has two minima located at $\pm\Pi_{\min}$ separated by a barrier with the maximum centered at $\Pi = 0$. The potential has the same form as the quartic potential shown in Fig. 1 and the height of the potential barrier is here a monotonic function of the coupling parameter K.

The time evolution of the dynamic variable Π is determined by the extrema of the potential $V(\Pi)$ and consequently two kinds of dynamic evolution are possible: (1) If $K \leq K_c$, the dynamic variable $\Pi(t)$ will, after a transient, settle to an asymptotic value $\Pi(\infty) = 0$ independently of the initial condition $\Pi(0)$; (2) if $K > K_c$, the dynamic variable $\Pi(t)$ will, after a transient, reach the asymptotic value $\Pi(\infty) = \Pi_{\min} \neq 0$ for an initial condition $\Pi(0) > 0$, $\Pi(\infty) = -\Pi_{\min} \neq 0$ for an initial condition $\Pi(0) < 0$ and finally $\Pi(t) = 0$ for all time given an initial condition $\Pi(0) = 0$. In Fig. 17 we compare the minima $\pm\Pi_{\min}$ and the numerical evaluation of $\Pi(\infty)$ for different values of the coupling constant K.

Fig. 17 shows that a phase transition occurs at $K = K_c = 1$. For a single clock the condition $\Pi(\infty) = \pm\Pi_{\min} = P_1 - P_2 \neq 0$ corresponds to the statistical 'preference' of the particle to be in either state $|1\rangle$ or $|2\rangle$. This is a consequence of the transition rates being different if the coupling parameter is greater than the critical value. Inserting the mean-field value of the probabilities (447) into the expression for the transition rates (446) and allowing the dynamic variable to reach its asymptotic value we obtain

$$g_{12} = g\mathrm{e}^{-K\Pi(\infty)} \neq g_{21} = g\mathrm{e}^{K\Pi(\infty)}. \tag{449}$$

Fig. 18 confirms the prediction of (449) showing that if $\Pi(\infty) = \Pi_{\min}$ the single clock spends on average more time in the state $|1\rangle$ and if $\Pi(\infty) = -\Pi_{\min}$ the single clock spends on average more time in the state $|2\rangle$. The probability density function for the sojourn times in both the preferred and not-preferred state are exponential functions with different mean sojourn times.

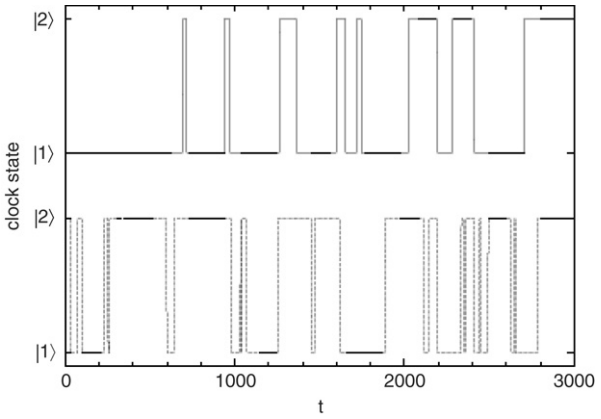

Fig. 18. The typical time series of a single clock of a network in the ensemble. The solid line refers to a positive initial state and the dashed line to a negative initial state. The number of clocks in the single network of the ensemble is 10^5, the unperturbed transition rate is $g = 0.01$ and the coupling parameter is $K = 1.05$. [Taken from Bianco et al. (2007b)].

7.1.2. Collective behavior

Bianco et al. (2007b) also explored the collective behavior of a single network of N clocks under the all-to-all coupling condition and in order to do this they introduced a familiar collective phase variable. The global clock variable is defined as

$$\xi(t) \equiv \frac{1}{N}\sum_{j=1}^{N} e^{i\Phi_j(t)} = \frac{N_1(t) - N_2(t)}{N}. \tag{450}$$

Here Φ_j is the phase of the jth clock and has the value 0 if the clock is in $|1\rangle$ and π is the clock is in $|2\rangle$ and $N_1(t)$ are the number of clocks in the former state at time t and $N_2(t)$ is the number of clocks in the latter state at time t. In the mean field case, when $N \to \infty$, the single network becomes a statistical ensemble of identical clocks. In this case the master equation for the single network is (445) where P_j is the probability that any clock in the ensemble is in the state $|j\rangle$. Consequently, from the definition (450), we obtain in the mean-field limit

$$\xi(t) = P_1(t) - P_2(t) = \Pi(t). \tag{451}$$

Thus, for a network with infinitely many clocks, the time behavior of the global clock variable $\xi(t)$ is identical to that of the dynamic variable $\Pi(t)$. Excluding the unstable initial point $\xi(0) = 0$ for $K > K_c$ we obtain $\xi(\infty) = \pm\Pi_{\min} \neq 0$ thereby establishing that a global phase synchronization occurs in the network at the onset of a phase transition. Moreover, the time evolution of a single clock of the network is the one depicted by Fig. 18, where we see that state $|1\rangle$ is preferred statistically if $\xi(\infty) = \Pi_{\min}$ and state $|2\rangle$ is preferred statistically if $\xi(\infty) = -\Pi_{\min}$.

When the mean-field limit is not taken, there is a finite number of clocks and the dynamical picture stemming from the above master equation is changed. Bianco et al. (2007b) pointed out that in the finite number case the master equation is that for the infinite number situation except that the transition rates fluctuate

$$g_{jk} \to g_{jk} + \epsilon_{jk} \tag{452}$$

where the fluctuations are on the order of $1/\sqrt{N}$. If the number of clocks is very large but still finite we consider the mean-field approximation to be nearly valid and are able to replace (448) with

$$\frac{d\Pi(t)}{dt} = -\frac{\partial V(\Pi)}{\partial \Pi} - \eta(t)\Pi(t) + \varepsilon(t) \tag{453}$$

where the multiplicative fluctuation has the form

$$\eta(t) = \epsilon_{12}(t) + \epsilon_{21}(t) \tag{454}$$

and the additive fluctuation is given by

$$\varepsilon(t) = \epsilon_{12}(t) - \epsilon_{21}(t). \tag{455}$$

The random fluctuations induce transitions between the two state of the potential well. Thus, for a network with a finite number of clocks the phase synchronization of (448) is not stable. The global clock variable fluctuates between the two minima for the coupling parameter greater than the critical value as depicted in Fig. 19. The single clock follows the fluctuations of the global clock variable ξ, switching back and forth from the condition where the state $|1\rangle$ is preferred statistically to that where the state $|2\rangle$ is preferred statistically.

The probability density functions of the sojourn times in the state $\xi > 0$ or $\xi < 0$ as shown in Fig. 19 are identical since the potential is symmetric. Thus, we denote them by $\psi(\tau)$. Let us consider a condition where the coupling constant K is

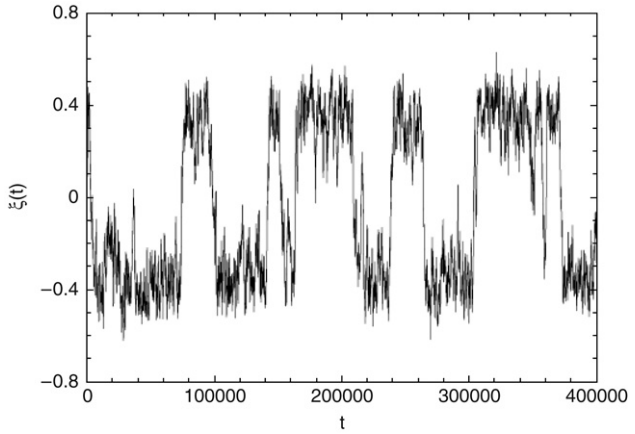

Fig. 19. The global variable $\xi(t)$ as a function of time is graphed for the parameter values $K = 1.05, g = 0.01$ for a network with 10^3 clocks. [Taken from Bianco et al. (2007b)].

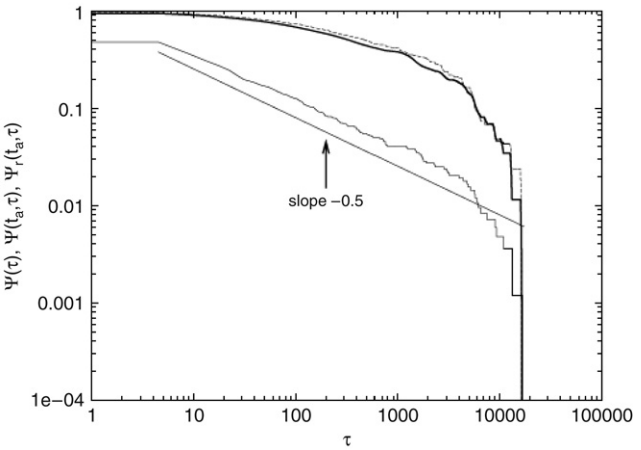

Fig. 20. The survival probability $\Psi(\tau)$ (full line), the survival probability $\Psi(t_a, \tau)$ (dashed line) and the survival probability in the renewal case $\Psi_r(t_a, \tau)$ (full thick line) as a function of sojourn time τ. Here, for clarity, we plot only the survival probability of age $t_a = 500$. [Taken from Bianco et al. (2007b)].

close to the critical value $K - K_c \ll 1$. In this case, the height of the barrier separating the wells of the potential is smaller than or comparable to the intensity of the fluctuations in (453). Under these conditions, we would expect an inverse power law of the form $\psi(\tau) \propto \tau^{-3/2}$ for an extended interval of sojourn times, see Margolin and Barkai (2005). This is exactly what is observed by Bianco et al. (2007b) in Fig. 20, where the full line denotes the survival probability $\Psi(\tau)$, namely, the probability of observing a sojourn time larger than τ, which in this case would be $\tau^{-1/2}$. For any fixed value of the unperturbed rate g, the height of the potential barrier increases as the value of the coupling parameter increases. Eventually, the barrier height becomes much larger than the intensity of the fluctuations, so consequently, the power-law behavior depicted in Fig. 20 vanishes, the theoretical arguments of Margolin and Barkai (2005) lose validity and an exponential behavior emerges, as predicted by Kramers theory (1940).

7.1.3. The effect of age

The influence of age on synchronization is established by showing that the transition between the states in the potential well is a renewal process. We evaluate the survival probability $\Psi(t_a, \tau)$ of age t_a by observing a sojourn time larger than τ when the observation starts at a time t_a after a crossing from $\xi > 0$ to $\xi < 0$ or vice versa. Note that with this definition of an aged survival probability we have $\Psi(t_a = 0, \tau) = \Psi(\tau)$. Now we compare the aged survival probability with the expected survival probability evaluated according to renewal theory $\Psi_r(t_a, \tau)$ as discussed in the previous section and by Bianco et al. (2005). If the two survival probabilities are equal $\Psi(t_a, \tau) = \Psi_r(t_a, \tau)$ for all ages t_a the process described by the survival probability $\Psi(\tau)$ is a renewal process. If $\Psi(\tau)$ is not an exponential function, $\Psi(t_a, \tau)$ yields a slower decay than does $\Psi(\tau)$, a condition that is denoted as 'aging' by Bianco et al. (2005). Fig. 20 shows that the transition between the minima of the potential well is a renewal process, that is the equality $\Psi(t_a, \tau) = \Psi_r(t_a, \tau)$ is established numerically and consequently there is aging.

On the other hand, as the value of the coupling parameter K is increased the aging property is lost because the survival probability $\Psi(\tau)$ becomes an exponential function, see Bianco et al. (2005). Even with this loss of aging the renewal property persists, as is also evident in Fig. 20.

In summary, for an ensemble of networks with an infinite number of two-state clocks, a phase transition occurs at the critical value of the coupling parameter $K_c = 1$. The phase transition mirrors a statistical 'preference' for a single clock and for the ensemble a global phase synchronization as depicted in Fig. 17. If the number of clocks in the network is finite the phase synchronization is not stable. In this case, the variable describing the collective motion of the network is characterized by non-Poisson intermittent behavior, see Fig. 20. At the onset of the phase transition ($K - K_c \ll 1$), the zero crossings of the global variable define a series of events with the properties: (1) The probability density function of inter-event intervals (full line in Fig. 20) has a non-Poisson non-ergodic character ($\psi(t) \propto t^{-3/2} \Rightarrow$ infinite mean inter-event interval). (2) The sequence of inter-event intervals satisfy the renewal aging condition, cf. Fig. 20. These two properties are observed properties of the statistics of BQDs, see Nirmal et al. (1996), Kuno et al. (2001), Kuno et al. (2003) and Shimizu et al. (2001), and brain activity as measured by EEG time series shown by Bianco et al. (2007b), suggesting that a network consisting of a finite number of coupled two-state clocks may be a useful model for the dynamics of both processes.

7.2. Firing synchronization as a source of NER behavior

The origin of complexity is still the subject of intense debate, with significant interest devoted to the study of time series with the times signaling the occurrence of events. The time intervals between events are described by inverse power laws and is a clear manifestation of human activity as discussed by Daly and Porporato (2006) and Barabási (2005). This phenomenon seems to be typical of processes characterized by the interaction among the elementary constituents, which can be neuronal, see, e.g., Plenz and Thiagarajan (2007), as well as human shown by Daly and Porporato (2006), Barabási (2005) and Plenz and Thiagarajan (2007) stressed the role of neuron synchronization as a source of neuronal avalanches and concluded that the theoretical foundation of these processes remains open. We emphasize that complexity can also generate survival probabilities with stretched exponential structure. However, Bianco et al. (2007b) argue that, although the inverse power law with index $\mu < 2$ is not visible, it is the crucial property underlying the neuron social life. According to the theory proposed by Bianco et al. (2007a,b) the search for the social life origin of complexity must not be restricted to phenomena generating inverse power laws. Consequently, the burst effects emerging from the inverse power law, see, e.g., Daly and Porporato (2006) and Barabási (2005), are a special case of a more general condition that requires a more complete investigation.

Here again EEG time series constitute a data base that suggests how to proceed with the modeling. Early in its history EEG time series had been arbitrarily segmented into a number of frequency bands in the mistaken belief that these intervals identified different functions of the brain. One such interval was that of the alpha rhythm centered on 10 Hz. It had been thought to characterize a passive or idling state of the brain, in part, because this frequency component is quite strong for a person sitting quietly with eyes closed and almost always vanishes when the eyes are opened. Başar et al. (1997) emphasize that this early view of EEG alpha has been replaced by a modern one associating alpha rhythm with diverse brain function including *spontaneous* alpha activity indicating a spectral width; *evoked* alpha oscillations that are time-locked to a stimulus; *induced* alpha oscillation that are generated by, but not time-locked to, a stimulus and finally that alpha rhythms do not have unique local generators, but have generators that are spatially distributed. This latter view implies that the dynamics of alpha processes (spontaneous, evoked or induced) involves clusters of neurons which synchronize. Başar, along with his colleagues, has developed an integrative theory of alpha oscillations in brain functioning, see Başar (2006). They suggest that the alpha rhythm may act as a nonlinear clock in the manner suggested by Wiener (1958) to serve as a gating function to facilitate the association mechanisms in the brain.

A well known model of neuron synchronization is that proposed by Mirollo and Strogatz (1990). However, this model cannot be adopted as a prototype of the origin of complexity insofar as, when synchronized, all the neurons fire at the same time thereby realizing a perfectly periodic process. In this subsection we study the case when the individual neurons of the Mirollo and Strogatz model are stochastic and establish that a stretched exponential survival probability emerges from the synchronization process, thereby affording a satisfactory dynamical derivation of the social life origin of the deviations from exponential survival probabilities.

7.2.1. Stochastic version of the Mirollo and Strogatz model

We consider a set of N neurons, each of which obeys the discrete stochastic equation

$$x(t+1) = (1-\gamma)x(t) + S + \sigma\xi(t), \tag{456}$$

where $\xi(t)$ is a random variable with either the value of 1 or of -1, with equal probability, with no memory of earlier values. The quantity σ is the noise intensity. The quantity $S > 0$ serves the purpose of making the variable x essentially increase as a function of time. The neuron variable x moves from the initial condition $x = 0$ and through fluctuations around the deterministic time evolution considered by Mirollo and Strogatz (1990) reaches the threshold value $x = 1$. When the neuron variable reaches the threshold value, it fires and resumes the initial value $x = 0$. It is straightforward to show that

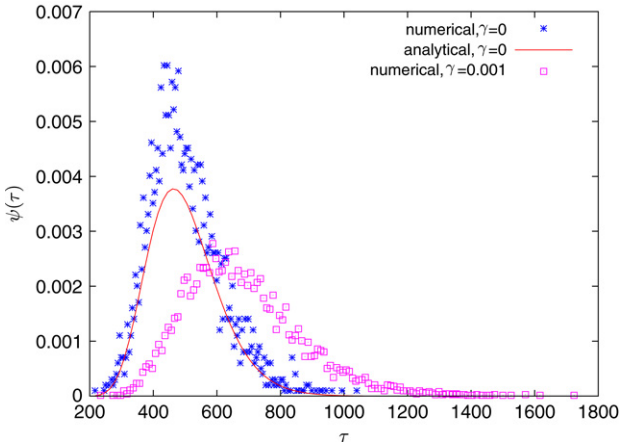

Fig. 21. Waiting time distribution density $\psi(\tau)$ as a function of the interval between two consecutive firings, τ.

the variable x can reach threshold only when the condition $\frac{S}{\gamma} < 1$ applies. In this case the time necessary for the neuron to reach the threshold, called T_{MS}, is given by

$$T_{MS} = \frac{1}{\gamma} \ln\left(\frac{1}{1-\frac{\gamma}{S}}\right). \tag{457}$$

The coupling among the neurons is established according to the rule set by Mirollo and Strogatz (1990): when one neuron fires all the other neurons make a little jump ahead of size $k > 0$. In summary the dynamics of the whole set of N neurons is determined by the parameters S, γ, k and σ.

We define an event as a special occurrence characterized by one neuron firing. We use an additional parameter, w, to give additional information about the event. The parameter w is an integer number and denotes an event where at least w neurons fire. We denote the corresponding waiting-time distribution with the symbol $\psi(w, t)$. It is important to notice that in the case $N = 1$, the only waiting-time distribution available is $\psi(t) \equiv \psi(w = 1, t)$, which has a form that can be evaluated numerically, and is illustrated in Fig. 21. Note that in the case $\gamma = 0$, it is known that with the choice of units adopted in this article

$$\psi(\tau) = \frac{1}{(2\pi\sigma^2\tau^3)^{1/2}} \exp\left[-\frac{(1-S\tau)^2}{2\sigma^2\tau}\right]. \tag{458}$$

The analytic expression (458) was first obtained by Gerstein and Mandelbrot (1964) in their application of a random walk with drift in the presence of an absorbing boundary to the analysis of single neuron spike activity. In their model the interspike interval distribution was identified with the first passage time distribution to the firing potential (location of the absorbing boundary). This model was generalized by Wise (1975) by making the absorbing boundary a fluctuating threshold potential, which enabled him to explain data from cerebral neurons in rabbits and respiratory neurons in cats, in which log–log plots suggested negative powers of time in tails of probability density functions. The same result was obtained for physiological clearance curves, for example, injected radiocalcium that goes into and out of the blood, tissue and bone before being expelled from the body. Wise (1981) emphasizes that what is observed depends on the distribution of many time intervals between successive transitions of the same particle of tracer. The probability density of the occurrence is proportional to $t^{-\mu}$ where μ is not necessarily equal to 1.5 as it is in (458).

We are not aware of any analytical expression for $\psi(\tau)$ when $\gamma > 0$. However, we see from Fig. 21 that $\gamma > 0$ has the effect of shifting to larger times the distribution maximum while leaving almost unchanged the other properties of the distribution. It is important to point out that the mean time $T_{sn} \equiv \langle\tau\rangle$ has a finite value and turns out to be 501.454 in the case illustrated in Fig. 21.

It is important to realize that $\psi(\tau)$ with increasing N undergoes a faster and faster decay. In Fig. 22 we plot distribution densities for different values of N as a function of the dimensionless time $t_{dl} = \frac{Nt}{T_{sn}}$ and we find (Fig. 23) that with N of the order of 10 the waiting time distribution becomes indistinguishable from the Poisson distribution $\psi_P(\tau)$ defined by $\psi_P(\tau) = ge^{-g\tau}$, with $g = \frac{N}{T_{sn}}$. In this sense, we can look at a set of N independent stochastic neurons as a Poisson network. This is a consequence of the fact that the average interval between two consecutive firings of the same neuron is finite.

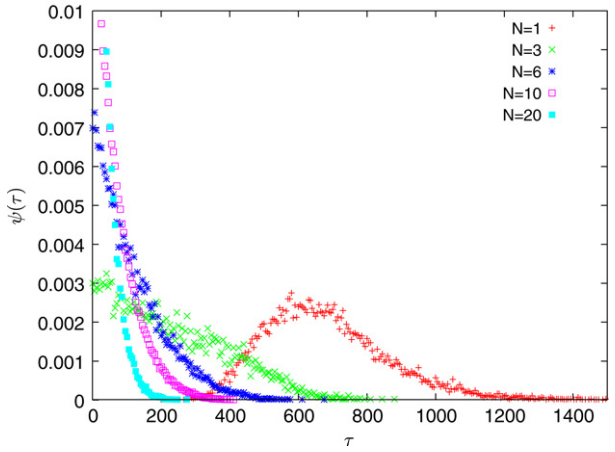

Fig. 22. The waiting time distribution density $\psi(\tau)$ as a function of the time interval between two consecutive firings of at least one neuron. By increasing the number N of non-intracting neurons, the time interval between two consecutive firings becomes shorter, and the function $\psi(\tau)$ becomes closer and closer to an exponential function.

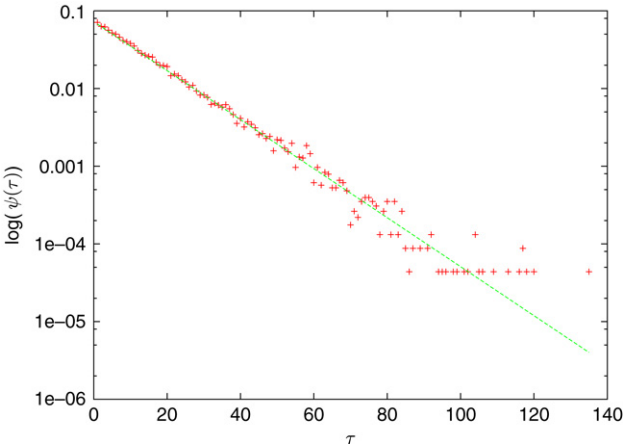

Fig. 23. The numerical result of Fig. 22 with $N = 20$ in a log-linear representation emphasizing the exponential form of that distribution density.

7.2.2. Switching on the coupling

In this subsection we illustrate with the help of Fig. 24 the waiting-time distribution $\psi(w, \tau)$, with $w \geq 1$ with $k = 0.01$. We see that the resulting waiting time distribution is a stretched exponential

$$\Psi(\tau) = \exp\left(-(\lambda t)^{\alpha}\right) \tag{459}$$

with $\alpha = 0.85$.

With Fig. 25 we show the dependence of λ on k. We see that the stretched exponential regime becomes less extended with increasing k. Finally with the help of Fig. 26 we show that $\mu_S = \alpha + 1$ moves from the condition $\mu_S = 2$ corresponding to total randomness to smaller values comparable to those afforded by the MST analysis of the brain shown by Bianco et al. (2007a). It is important to notice that for values of α of the order of 0.6 the synchronization effects become very intense so as to violate the condition of intermediate randomness on which the model of the brain used herein rests.

We have shown that this model provides a satisfactory foundation of the survival probability described by (329). More precisely $\hat{\Psi}(u)$, the Laplace transform of $\Psi(t)$ has the form

$$\hat{\Psi}(u) = \frac{1}{u + \lambda^{\alpha}(u + \Gamma)^{1-\alpha}}. \tag{460}$$

Not only the parameters λ and α are determined by the dynamical model, but also the truncation parameter Γ which is determined by the time T_{MS} rather than by the finite sequence of renewal events. We have also found that the subordination function can be written

$$\psi^{(S)}(\tau) \propto \frac{1}{\tau^{\mu_S}} \exp(-\Gamma\tau), \tag{461}$$

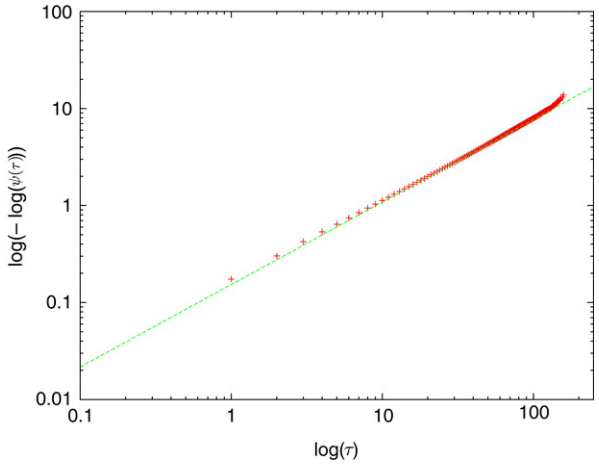

Fig. 24. The waiting time distribution $\psi(w,\tau)$ in the $\log(-\log\psi)$ versus $\log\tau$ representation, clearly indicating that the distribution is a stretched exponential function.

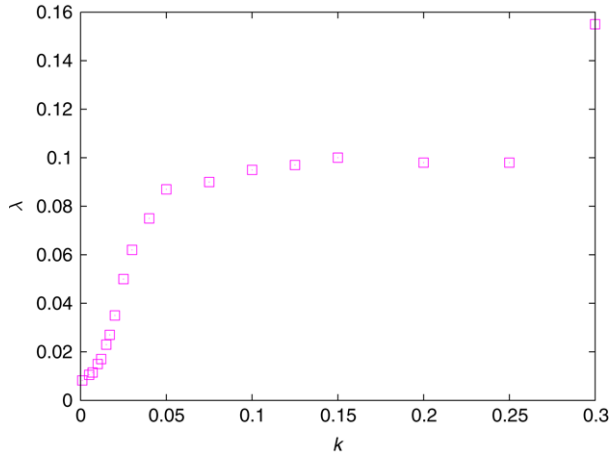

Fig. 25. λ as a function of the coupling k.

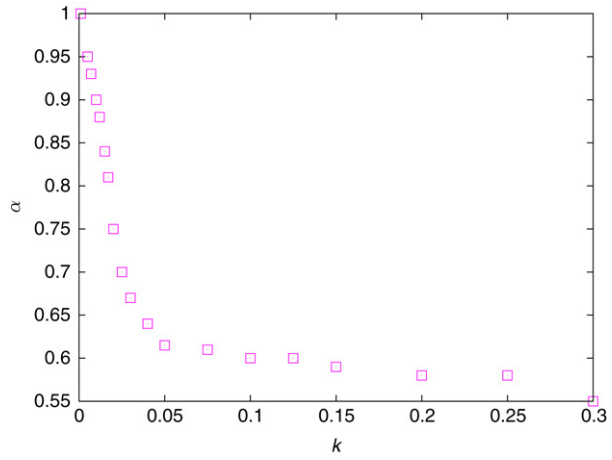

Fig. 26. α as a function of the coupling k.

thereby affording a dynamic foundation of the subordination approach to the brain dynamics illustrated in Section 5.2.2 while at the same time substantiating the arguments of Barabási (2005) on the cooperative origin of the inverse power-law distribution densities.

Preliminary research shows that both the model of Section 7.1.2 and the model of Section 7.2.1 may generate cooperative behavior, from which the non-ergodic renewal events emerge, with no recourse to the all-to-all coupling condition, if the clocks (Section 7.1.2) and the neurons (Section 7.2.1) are distributed on the sites of complex network models in the manner prescribed by Watts and Strogatz (1998), Barabási and Albert (1999) and Holme and Kim (2002). This is a consequence of the fact that clusters of direct connections favor the emergence of local synchronization and the links among different clusters turn the local into global synchronization. In the case of regular networks with a finite number of links between one site and its first L nearest-neighbors, there is no synchronization with couplings of moderate intensity. The adoptions of random networks introduced by Erdös and Rényi (1960) favors the onset of synchronization, and the adoption of complex networks significantly enhances the emergence of the complexity described by (460). Research work is being done to establish the extent the clustering, see, e.g, Watts and Strogatz (1998), or the scale-free, see, e.g., Barabási and Albert (1999) property facilitates the emergence of the complexity described by (460). It is also important to assess the role of complex networks where both properties are present. In fact, recently a new type of network has been proposed by Holme and Kim (2002) with both high clustering and an inverse power-law distribution of edges. It has been noticed that the scaling property of the complex networks is shared by the human brain as noted by Kim (2004).

We conclude this section by remarking that the model of Section 7.2.1 affords a satisfactory foundation for the subordination approach to modeling the brain as done in Section 5.2.2 and shows that the complexity index $\mu_S < 2$ proposed by Bianco et al. (2007a) is an appropriate parameter value to describe the global behavior of the brain and its response to external stimuli such as music.

8. Concluding remarks

This review has demonstrated that there exists a subtle connection between information exchange within and between networks and the complexity of those networks. Here we summarize those aspects of the review that directly support this thesis and discuss some of the implications pertaining to the CME.

We explore some of the implications of the CME by introducing a context that is perhaps more familiar than the non-stationary, non-Poisson, non-ergodic stochastic processes of this review, that being, $1/f$-noise or $1/f$-phenomena. The existence of such phenomena was recognized by Bernoulli (1738), when he introduced the notion of a utility function. He was interested in characterizing the social well being of an individual and the utility function was intended to do that. Bernoulli reasoned that a change in some unspecified quantity f denoted by Δf, elicits different responses from different people depending on how much f they already possess. His conclusion was that people respond to the percentage change $\Delta f/f$ rather than to the magnitude of the change, Δf itself. Over the nearly three centuries since Bernoulli first thought about these things, his idea has been transformed in a number of different ways — each attempting to capture the complexity of the network to which the idea was applied. We use these application areas to record some of these transformations and connect this perspective with that of complexity matching.

The final section briefly ties together some loose ends.

8.1. CME and 1/f-noise

One point we did not previously stress is that power-law autocorrelation functions have inverse power-law spectra as is easily shown using a Tauberian theorem. The importance of this observation is emphasized here because $1/f$-noise is ubiquitous in biological, social and physical networks and analysis suggests that the scaling we have identified in complex networks may be causally related to these familiar phenomena.

There is a widespread conviction that $1/f$-noise is the signature of complexity, where the spectrum of the phenomenon is given by $1/f^{\nu}$. Here we list some complex processes producing $1/f$-noise and discuss how these networks communicate among themselves, which raises the question of what may be the reason for the transfer of information between two complex networks.

8.1.1. The brain

The brain is perhaps the most interesting example of a complex network having complex dynamics. Thus, we first discuss the experimental research work aiming at checking either directly or indirectly the brain's dynamic action. Recent psychological experiments led Kello et al. (2007) to argue that $1/f$-scaling reflects the coordinative basis of cognitive function. This is in keeping with the main conclusions of a recent review by Wagenmakers et al. (2004), that being, that cognitive tasks produce $1/f$-noise in the EEG signal.

We point out that the emergence of $1/f$-noise can be detected by converting the underlying time series, such as the EEG, into a diffusion process. This conversion of data allows us to determine the corresponding Hurst coefficient H. A widely used method to convert a time series into a diffusion process is the detrended fluctuation analysis (DFA) introduced by Peng et al. (1995). The width of the diffusion process w increases with the size l of the exploring window as $w(l) \propto l^H$, with the second moment scaling index H being related to the inverse power-law index μ by $H = (4-\mu)/2$ (see Section 5.2.5 and (361)). Thus, since the autocorrelation function scales as t^{2H-2} we obtain for the scaling index of the spectrum in terms of the Hurst exponent

$$\nu = 2H - 1, \tag{462}$$

or in terms of the inverse power-law index

$$\nu = 3 - \mu. \tag{463}$$

According to the convention adopted in the literature that a phenomenon is $1/f$-noise when the spectral index is in the interval $0.5 < \nu < 1.5$, we obtain that the Hurst exponent is in the interval $0.75 < H < 1.25$ is equally a signature of $1/f$-noise. Note that either index exceeding the value 1 is a sign of aging, as pointed out by Kalashyan et al. (2007) to explain EEG signals.

The work of Buiatti et al. (2007) affords additional evidence that the brain is a source of $1/f$-noise. It is interesting to notice that some interest is also devoted to the condition $H < 0.5$ generating a spectrum that in the low-frequency limit yields $S(f) \propto f^{1-2H}$, see Hoop and Peng (2000). Some authors, see, e.g., Valdez and Amazeen (2008) study how spatial, physical and timing constraints affect planning and control process in aiming at targets. They find that the aiming tasks generate values of H such as 0.75 and 0.80, and consequently $1/f$-noise. A recent analysis conducted by Correll (2008) on reaction time to stimuli seems to indicate that the more challenging the task the less intense the $1/f$-noise produced. This may not conflict with the conviction that cognition generates $1/f$-noise if we take into account that $\nu > 1$ implies $\mu < 2$ and consequently, because of (355), a rate of event generation vanishes asymptotically in time: the more extended the observation time, the less intense the $1/f$-noise becomes. This conjecture, of course, rests on the assumption that a challenge of increasing difficulty increases the time necessary to complete the effort.

The results of these psychophysical tests suggest that $1/f$-noise may also emerge from the analysis of EEG signals. The analysis of the local field potentials of a cat's parietal association cortex conducted by Bédard et al. (2006) confirms the emergence of $1/f$-noise, although the interpretation of this spectrum is that it is due to the filtering properties of extracellular media rather than to the existence of critical states.

Another interesting study, concerning the human brain, indirectly confirms the existence of $1/f$-properties as observed by Gong et al. (2007). These authors investigate patterns of collective phase synchronization in brain activity in awake, resting humans with eyes closed. They find that the alpha range of the human EEG activity is characterized by changing patterns and that these fluctuations generate renewal events. The time interval between two consecutive EEG events is described by an inverse power-law distribution density $p(\tau)$, with power index $\mu = 1.61$. We have seen that $1/f$-noise yields $S(f) \propto 1/f^{\nu}$ with $\nu = 3 - \mu$. Thus, the work of Gong et al. (2007) generates $\nu = 1.39$, well within the widely accepted range for $1/f$-noise. We consider these experimental observation as additional evidence that multiple activities of the brain generate $1/f$-noise.

Musha (1981) reported that $1/f$-noise plays a role in the relief of chronic, intractable pain for which transcutaneous electrical nerve stimulation is beneficial. This treatment has a history dating back to 46 AD and was used clinically as early as 1855. In recent experiments the uses of various random stimulation spectra in such treatments were compared. The electrical signal was applied in order to disrupt pain messages to the brain and the spectrum of frequencies in the signal determined the success of the disruption. In the majority of cases, a $1/f$-spectrum for the applied signal was preferred and reduced pain levels caused by trauma, cancer, lumbago and back pain for significant periods after the stimulation was stopped, see Musha (1981).

8.1.2. Body movements

Deligniéres et al. (2004) and Deligniéres et al. (2008) stimulate the regular tapping or the regular oscillation of a joystick by means of a metronome. Then, after switching off the metronome, they monitor the fluctuating departures from the induced periodicity, and find that the spectrum has the property $S(f) \propto 1/f^{\nu}$, with $\nu = 0.97$ and 1.19, respectively. Other scientists, such as Kadota et al. (2004) studied the human movements in synchronization with external events and found ν values fluctuating in the vicinity of 1, with measurement errors compatible with the emergence of perfect $1/f$-noise.

It is worth noting that some authors analyze the movements produced by physical activity, see, e.g., Paraschiv-Ionescu et al. (2008) by using the Hurst coefficient H determined by DFA, see Peng et al. (1995), and the above relation between the indices (462). The typical value found by Paraschiv-Ionescu et al. (2008) are $\nu = 0.7$ and 0.6 for healthy subjects and 0.5 and 0.47 for patients with chronic pain. Note that the pathological patients are on the lower boundary for $1/f$-noise. In this field, as well, the convention has been adopted by researchers that $1/f$-noise represents a healthy physiological condition.

Perhaps the most familiar body movement is that of walking, but the regular gate of everyday experience is actually not very regular. The variability in the stride interval, the time interval between successive heel strikes, was first discovered by Vierordt (1881) in the 19th century, with the follow-up experiments to quantify the degree of irregularity in walking done by Hausdorff et al. (1995), nearly 120 years later. The scaling behavior of the inter-stride interval time series was determined using a number of different methods of data analysis leading to consistent results. The average fractal dimension for normal healthy adults is determined to be approximately 1.25, see, Hausdorff et al. (1999) and West (2006) yielding $\nu = 0.5$. Moreover, people basically use the same control network when they are standing still, maintaining balance, as when they are walking. This leads one to suspect that the body's slight movements around the center of mass of the body, postural sway, would have the same statistical behavior as that observed during walking and this is found to be the case as discussed by Collins and De Luca (1994) and Lauk et al. (1998).

8.1.3. Heart beat variability

Kaplan and Talajic (1991) among many others, see, e.g., the review by West (2006), show that the time interval between two consecutive heart beats (the time interval between consecutive R peaks in an electrocardiogram) is not constant and that its fluctuations generate $1/f$-noise. The more recent work of Hennig et al. (2006) confirms the $1/f$-noise nature of RR interval distribution. In fact, it has been known for some time that 'normal sinus rhythm' is not strictly periodic, but is characterized by a broad-band, inverse power-law spectrum as first quantified by Kobayashi and Musha (1982) and Goldberger et al. (1985). The heart rate is modulated by a complicated control network consisting of respiratory, sympathetic and parasympathetic regulators. Akselrod et al. (1981) showed that individual suppression of these regulators considerably alters the interbeat interval power spectrum in healthy individuals, but a broad-band spectrum persists. The importance of heart beat variability was finally established by a task force formed by the *North American Society of Pacing and Electophysiology* and the *Board of the European Society of Cardiology* in their published report (Heart rate variability (1996)).

There are at least 16 different methods that have been developed to assess heart rate variability, a few of which have been touched on in this review, but most of which do not concern us here. The number of techniques is mentioned only to indicate that the scaling nature of the beat-to-beat interval time series has an extensive literature and has been established from a number of different analytic perspectives. The scaling nature of the RR-interval distribution was first recognized by Peng et al. (1993), along with the fact that the increments in the human heartbeat time series possess the limit distribution of Lévy and not that of Gauss. Using the DFA on the differences between successive time intervals, they find that $H \approx 0$ for healthy individuals, whereas for those with severe heart failure $H \approx 0.5$, but the statistical distribution for the two groups is the same. They conclude that the difference in the observed scaling is a consequence of the ordering of the heartbeat intervals differences and not their statistics, that is, the pathology appears in the autocorrelation of the underlying time series.

8.1.4. Music and noise

As we show subsequently, there is experimental evidence that one complex network, the brain, with $1/f$-complexity, is sensitive to the stimulus exerted on it by another $1/f$-network. The conjecture that the matching of the exponents in the separate $1/f$-networks facilitates the transport of information seems to afford scientific support for the observation that music can cast a spell on the brain. Given that the brain is a $1/f$-noise network (see Bédard et al. (2006)), as discussed above, it is expected to be especially sensitive to $1/f$-noise. We may explain the fascination exerted on the brain by music given that music is a source of $1/f$-noise, as established in the pioneer work of Voss and Clarke (1975). There is general agreement on the $1/f$-nature of music, see Hsu and Hsu (1991), although the research work of Boon and Decroly (1995), resting on a dynamical approach to music, suggests that ν may be significantly larger than 1.

The work of Jennings et al. (2004) is based on the use of the DFA method applied to the loudness of music. We use again the relation (462) to discuss the connection between the deviation from ordinary diffusion and $1/f$-noise. These authors find that H fluctuates in the vicinity of 1 with excursions at both short and long times into the non-ergodic region $\nu > 1$.

According to Su and Wu (2007) the scaling indices have the new relation $\psi = 2H + 1$. This relation among the indices is due to the fact that if the fluctuations of ξ, with a stationary and extremely slow correlation function generates $S(f) \propto 1/f^{\nu}$, with $\nu = 2H - 1$, the integrated signal $x = \int \xi(t)\mathrm{d}t$ generates the spectrum $S(f) \propto 1/f^{\eta}$ with $\eta = \nu + 2 = 2H + 1$. Replacing the symbol η with the symbol ν we obtain

$$\nu = 2H + 1, \tag{464}$$

which has to be compared to (462). It is important to stress that this simple rule is another way to emphasize the non-stationary character of the corresponding music composition. Thus, with H slightly smaller than 1, ξ generates stationary music composition with $\nu < 1$ and with H slightly larger than 0; on the other hand, x generates a non-stationary music composition with $\nu > 1$.

It is worth mentioning that according to Bigerelle and Iost (2000) the fractal dimension ($D = 2 - H$) of music can be evaluated with such great precision as to make this a reliable way to classify music. Music is a familiar example of an external stimulus generating emotion, which Hachinski and Hachinski (1994) expressed as:

> In every culture music is used to communicate, entertain, express and elicit emotion. Yet underlying questions remain. Why do people respond to music? Why are we overcome with melancholy when hearing one tune and overjoyed when hearing another? Why do some melodies cause chills up and down one's spine and others evoke calm, peace and well-being? How can combinations of sounds produce such diverse emotional and physical reactions?

According to Hachinski and Hachinski (1994) music triggers a hierarchical cooperation between the two hemispheres of the brain, and this cooperation is very close to the phase transition condition realized by the synchronization of many elements, the condition behind the picture advocated by Gong et al. (2007).

It is interesting to note that Lewis (2005) advocates a theoretical approach to emotions based on the bridge between emotion and neurobiology through the concept of appraisal. Appraisal is more general than decision making: it includes perception, attention, evaluation, memory, and so on, as well as decision making. According to Lewis appraisal denotes an evaluative or interpretative function that is critical for eliciting emotion, and has to do with cognitive processes that are directed toward what is important for the self.

Appraisal, according to Lewis (2005) is the expression of a process of self-organization, which is the spontaneous emergence of order from nonlinear interactions among the components of a complex dynamic network. In fact, Lewis suggests a bridge between emotion theory and neurobiology based on a Dynamic System (DS) principle, where appraisal takes place through phase transition processes. Self-organizing DS (see Lewis (2005)):

> . . . move across the threshold of instability and jump abruptly to new stabilities. These jumps, sometimes called phase transitions or bifurcations, occur when system orderliness breaks down as the result of some perturbation and new patterns of organization rapidly self-amplify.

Appraisal involves abrupt changes in time that are reminiscent of the abrupt configuration changes revealed by the statistical analysis of the human EEG conducted by Gong et al. (2007). The important role of DS is also stressed by Ward (2001) who proposes the concept of human behavior *unfolding in time* as the unifying theme to understand perception, memory, psychophysics, judgment, decision making and consciousness. This leads to a view very close to that of appraisal, see Lewis (2005), with abrupt transitions explained in terms of *unfolding in time* networks. The ideal continuous time of physics is replaced by a discrete and stochastic time that seems to be related to the CTRW time discussed herein.

How is it possible for music to trigger emotions, if emotions have this complex origin? If we make the assumption that a kind of resonance exists between networks sharing the same complexity, the $1/f$-noise complexity, it may become possible to understand why music triggers emotions.

On the basis of the correspondence between music and the $1/f$-nature of the main physiological processes, one may be tempted to interpret music as an expression of an evolutionary homeostatic feedback-mechanism more than as a social function, see Wallin (2000). However, we notice that the principle of "emotion transfer" is not confined to the influence of music on the brain. Rather, as we show subsequently, the same $1/f$-noise principle leads to social networks with the self-organizing elements being human beings and the brain's EEG with the neurons being the self-organizing elements.

8.1.5. The visual arts and variability

It is not only about the distribution concerning the regularity in music that we as humans make judgements. We similiarly discriminate in examining photographs and paintings. Nyikos et al. (1994) reported a study of the distribution of the breakup of space in a number of the great artists and found $1/f$-phenomena in the paintings by Durer, Munch, Rembrandt and Picasso.

More recently, the method of scaling analysis has been applied to the paintings of Pollock, see Alvarez-Ramirez et al. (2008), Taylor et al. (1999, 2002). Analysis of Alvarez-Ramirez et al. (2008) establishes a connection with the $1/f$-noise issue and also suggests how the visual inspection of a painting can be converted into an 'equivalent' time-dependent stimulus, of a nature comparable to the musical stimulus. In fact, these authors imagine an observer looking at a painting from left to the right at a fixed level. This corresponds to exerting on the eye a time-dependent stimulus that is an effective one-dimensional stochastic trajectory. They evaluate the dimension D of this stochastic trajectory, thereby yielding information on ν through the well known formula $D = 2 - H$. Using the earlier relation $\nu = 2H - 1$, we obtain $\nu = 3 - 2D$. Alvarez-Ramirez et al. (2008) find typical values of the fractal dimension $D = 1.1$ and $D = 0.9$, corresponding to $\nu = 0.8$ and $\nu = 1.2$, respectively, again suggesting an excursion of $1/f$-noise into the non-ergodic regime.

Here we see two contrasting ways $1/f$-phenomena enter our lives. First through the aesthetic judgements we make regarding music and art and second through the perception of pain in our bodies, see West and Deering (1995):

> Apparently, the same $1/f$-signal that can soothe the savage beast, can in another way also relieve the beast of his pain. Perhaps in a way we do not yet understand, a pain-free life and a joyfully aesthetic one may be related in some biologically fundamental way.

8.1.6. Linguistics

There exists a surprising connection between music and sociology established by a well known linguistic principle, Zipf's law as discussed by Manaris et al. (2005). Zipf law establishes that the relative frequency of occurrence of a written word is proportional to $1/r^{\nu}$, where r is the rank of that word in the given language. According to Zipf the index should have unit value, $\nu \approx 1$. The connection with $1/f$-noise is obtained by identifying the rank r with the frequency f. Manaris et al. (2005) find that the $1/f$-noise properties of music can be interpreted as a manifestation of Zipf's law in music. They find, for instance, that the *chromatic-tone distance*, namely, the time interval between consecutive repetitions of chromatic tones, obeys Zipf's law. At the same time, Zipf's law is closely connected to Pareto's law (see Seuront and Mitchell (2008)), which establishes that the probability of a randomly chosen individual within a society having an income larger than a given income level x, no matter how large, is proportional to $1/x^k$. Seuront and Mitchell (2008) and Adamic and Huberman (2002) as well, state that Zip's law and Pareto's law, are equivalent.

If we denote by ν the power index of Zipf's $(1/f)$ law, it is straightforward to prove that $\nu = 1/k$. It is remarkable that the distribution density $p(\tau)$, where τ now denotes the chromatic tone distance is of the form

$$p(\tau) \propto \frac{1}{\tau^{\mu}}, \tag{465}$$

with

$$\mu = 1 + k = 1 + \frac{1}{\nu}. \tag{466}$$

We point out that ν must be very close to 1, so as to fit the condition pointed out by Manaris et al. (2005) of realizing the $1/f$- condition. In this case, we set

$$\nu = 1 - \epsilon, \tag{467}$$

with $\epsilon \ll 1$, thereby turning (466) into

$$\mu = 2 + \epsilon, \tag{468}$$

which is identical to (463), established by the renewal theory reviewed in this report.

The equivalence between linguistic laws and sociological laws suggests that a process of interaction exists for the transfer of this property, reflecting at the same time the cooperation of the brain's neurons and the cooperation among the individuals within society. According to Jäger and van Rooij (2007) language structure reflects both psychological and social constraints. We can state that language, as music, may be considered to satisfy both neurobiological and sociological constraints, if we accept the complexity matching principle, according to which the communication between complex networks rests on them sharing the same $1/f$-noise property.

8.1.7. Genome

The phenomenon of $1/f$-noise is also exhibited by DNA sequences as determined using a modified random walk argument by Voss (1992, 1994) and Peng et al. (1992). Li and Holste (2005) using updated and human sequence data found the presence of $1/f$-noise in the DNA sequences of all human chromosomes. The values of ν in this case are usually smaller than 1 with some excursions to values slightly larger than 1, such as 1.03, 1.05 and 1.12. According to the renewal theory illustrated herein, see (463), these values correspond to $\mu = 1.97$, $\mu = 1.95$ and $\mu = 1.88$, respectively. One may infer that genomes also find a convenient niche as a $1/f$-phenomenon.

How can we interpret this property? We think that this observation may help the development of an ambitious research approach that according to Ward (2001) is needed to allow biology and cognitive sciences to realize accomplishment as impressive as those of physics. Ward noticed that the DNA dogma is widely accepted: the genetic code informs the variety of life on this planet. However, there is no theory explaining how this occurs, and Ward expresses the view concerning scientific progress (see Ward (2001)):

> If we are to more closely approach the impressive accomplishments of physics, we must incorporate a dynamical component into cognitive theory, and into psychological theory as a whole and because of the complex systemic nature of cognitive and psychological phenomena, the dynamical component will have to be in the form of dynamical systems theory.

At the end of this subsection we shall see that $1/f$-noise has the effect of spreading from one network to another. Therefore, we conjecture that the adoption of the $1/f$-property may serve the purpose of introducing the needed dynamics into the description of genomes. However, to establish the truth of this conjecture requires the theoretical development desired by Ward.

8.1.8. Sociology

The cooperation among neurons within the human brain is intrinsically a problem of general interest, but in addition the behavior of the brain has become a paradigm for any form of cooperative behavior within complex networks including those of sociological interest, see, e.g., Sumpter (2006) and Gross and Blasius (2008). Neuroeconomics, as described by Kenning et al. (2005) is a new discipline based on this paradigm. Frederick et al. (2002) outline that decisions involving tradeoffs among costs and benefits occurring at different times are important and ubiquitous in economics. The influence of neuroeconomics on decision making rests on an interdisciplinary research activity, involving the intervention of behavioral psychologists such as Rachlin and Jones (2008) as well as that of neurophysiologists, e.g., Wittmann et al. (2007a), and health-care providers. The psychological experiments on how individuals discount delayed rewards, which is to say individuals prefer smaller rewards immediately after a decision rather than larger rewards delayed for some time, are used as a way to evaluate the influence of drugs and other addictions on the brain, as found by Wittmann et al. (2007b).

For this reason, the research work of a neurophysiological nature done by Plenz and Thiagarajan (2007), Beggs (2007) and Levina et al. (2007), plays a central role in the field of complexity and is expected to shed light on the origin of complexity itself (Bak et al., 1987). For example, the new concept of an avalanche is a set of elements showing simultaneous enhanced activity. In the experimental work of Beggs (2007) and Plenz and Thiagarajan (2007) the elements are electrodes, monitoring the global activity of a local set of neurons, and in the numerical work of Geisel et al. (1985) the elements are integrate-and-fire model neurons. The avalanche size is the number of elements in the avalanche and is distributed according to a power law with exponent $-3/2$ for Beggs and Plenz (2003, 2004), Plenz and Thiagarajan (2007) and Beggs (2007) and between $-3/2$ and -2 for Levina et al. (2007).

There seems to be general agreement on the power-law distribution of the avalanche size, which fits the theoretical prediction of Bak (1996) Self-Organized Criticality (SOC) theory. The adoption of the SOC perspective led da Silva et al. (1998) to conclude that the time interval between two consecutive avalanches is also distributed as an inverse power law. The inverse power-law distribution of the time intervals between two consecutive events is a property shared by some

theoretical models for decision making processes, see Barabási (2005), thereby yielding the same time statistics as the results of psychological experiments by Takahashi et al. (2007), which Wittmann and Paulus (2007) have shown to mirror brain activity.

However, the stable recurrence over time of an avalanche's spatiotemporal patterns remains an elusive issue requiring clarification, see Plenz and Thiagarajan (2007). This required clarification is of importance not only for neurophysiological processes but for the foundation of non-equilibrium statistical physics. The recent discovery of the statistical aging and non-ergodicity in the fluorescence of single nanocrystals by Brokmann et al. (2003), named BQD, triggered the interest of many researchers adopting the CTRW perspective such as Bouchaud and Georges (1990), Metzler and Klafter (2000b) and Sokolov et al. (1996), from which an important approach to the study of non-ergodic processes has emerged from Rebenshtok and Barkai (2007). Bianco et al. (2007a) discovered quakes in the brain that seem to share the same non-ergodic properties as the BQD, thereby making it even harder to account for the stable time recurrence, see Plenz and Thiagarajan (2007). Notice that earlier numerical results indicate that the emergence of an inverse power law is produced by strong cooperation, which generates values of μ significantly smaller than 2, and consequently very far from the $1/f$-noise condition. This is in keeping with the fact that the accomplishment of a difficult task may produce a significant deviation from the $1/f$-noise condition.

The model of cooperating neurons described in Section 7.2.1 seems to be a convenient way to settle these controversial aspects. In fact, when the coupling k among neurons is weak, and the randomness parameter σ is conveniently large, the time interval between two consecutive quakes generates a survival probability with the stretched exponential form $\Psi(t) = \exp(-(\lambda t)^{\alpha})$, with $\alpha < 1$. Apparently, the connection with $1/f$-noise is lost. However, $\mu = 1 + \alpha$ indicates that, although invisible, a $1/f$-noise generator is present. When the coupling K is large enough, the inverse-power law of the Mittag–Leffler function becomes visible, and a direct connection with the results of the psychophysical tests emerges.

8.1.9. 1/f-networks perturbed by 1/f-networks

In summary, $1/f$-noise is an ubiquitous property of self-organized networks, whose origin is still the object of debate and controversy. However, there seems to be no doubt that $1/f$-noise spreads upwards from molecules to mindfulness as argued by Anderson (2000). But how does one explain this surprising spreading? There exists another property of $1/f$-noise networks that may help in understanding this spreading process. The $1/f$-networks seem to communicate among themselves more easily than with networks not having $1/f$-complexity.

Soma et al. (2003) have shown that the brain is more sensitive to $1/f$-noise than to white noise. Along the same lines Yu et al. (2005) have recently shown that the neurons in the primary visual cortex exhibit higher coding efficiency and information transmission rate for $1/f$-signals than for white noise.

Billock and Tsou (2006) have shown that $1/f$-noise has also been used to produce hallucinations. Takakura et al. (1979) found that the pain-relief efficiency of subcutaneous electrical stimulation is doubled by synchronizing the electrical pulses with $1/f$-noise.

There is also indirect proof that a $1/f$-noise network is sensitive to $1/f$-fluctuations generated by another $1/f$-noise network. Mutch (2005) developed a new kind of mechanical ventilator, called a biologically variable ventilator, that incorporates $1/f$-noise into the variability of the ventilator. Mutch has established that this new kind of ventilator is of vital use in critical care units because it provides enhanced oxygenation of the blood as well as other indicators of post operative recuperation over and above the values produced by traditional ventilators.

Kawashima (2006) has designed a comfortable swing according to the cardiac condition of each individual person. The basic principle is that this device feeds back the heartbeat fluctuation of the individual to the motion of the swing. The power spectrum of the envelope of the waveform of swinging evaluated by the participants to the experiments is a $1/f$-noise spectrum with $\nu \approx 0.98$.

Tsuruoka et al. (2007) have shown that listening to the music of Mozart has the effect of inducing $1/f$-noise on heart beating. This result may become comprehensible if we make the assumption that there is a special matching between Mozart's music ($1/f$-composition), the brain's organization ($1/f$-complex network) and the heartbeat (another $1/f$-noise process), all of which is consistent with CME.

8.1.10. Plausible conjecture

Watanabe et al. (2008) have assessed the physiological influence of music on the brain by MRI techniques. This important technique however leaves unanswered the question of what the fractal nature of music has to do with the efficiency of the music stimulus. We are led to conjecture that the $1/f$-property optimizes the effectiveness of the music, taking into account that this would explain the universal aesthetic appeal of fractals found by Spehar et al. (2003). In fact, the aesthetic appeal of music is matched by that of beautiful pictures characterized by space fractals. According to Ward (2001) the movement of the observer's eye who is enjoying the picture, inherits the fractal, $1/f$-noise, properties of the picture, in accordance with the view of Alvarez-Ramirez et al. (2008). This is an attractive example of a process unfolding in time. Thus, the brain is efficiently stimulated by $1/f$-noise, as in the experiment of Soma et al. (2003).

All these results suggest that the communication between complex networks is facilitated by these networks sharing the $1/f$-noise property. It is appealing to imagine that the brain is the source of $1/f$-noise fluctuations, and that the brain may easily exchange information with the heart through the $1/f$–$1/f$ interaction and that psychological tests mirror the $1/f$-nature of the brain. As we have seen, there is a significant amount of experimental evidence that $1/f$-noise favors

the exchange of information between complex networks. The renewal theory illustrated herein and the related CME is an attempt at setting all this on a quantitative basis, with the discovery that $\mu < 2$ ($\nu > 1$) may represent the condition of maximum efficiency for this information transfer.

8.2. CME and some loose ends

8.2.1. Beyond ordinary SR

Ordinary SR rests on the response of a stochastic network to a harmonic perturbation given by (368) and (369). The maximum response intensity is obtained when $g_0 \gg \omega$. In the absence of perturbation the network spends on average the same amount of time, $1/g_0$, in each of its two states. Thus, in practice to observe this condition of maximum response, we should monitor the time τ spent by the Poisson network in each of its two states in a short time interval $[t - \Delta t/2, t + \Delta/2]$ around t, where the perturbation is harmonic $\epsilon cos(\omega t)$. We should adopt the Gibbs perspective and average over infinitely many realizations of the response to the same perturbation, and as a result of this averaging process obtain a mean time $\langle\tau\rangle = (1 \pm \frac{\epsilon}{2})/g_0$. The measurement is sufficiently precise to establish with high accuracy the time difference ϵ/g_0. This measurement becomes increasingly difficult, eventually becoming impossible as $g_0 \to \infty$ and $\epsilon \to 0$. This information limitation is similar to the one we encounter in assessing the departure from the Poisson condition of the individual clocks, whose collective behavior is illustrated by Fig. 19. The failure to notice the non-Poisson nature of interacting clocks and the failure to recognize the close correlation between a high-rate Poisson network and the perturbing signal have a common origin, namely, the finite information capacity of the observation process. For this reason it is more appropriate to replace the concept of SR with the notion of *information resonance* (IR) (see Section 2.3.2).

There is an intimate relation among response, information transmission and the experimental detection of the cooperative behavior enhanced by complex networks, where the concept of IR may turn out to be beneficial to understanding the role of complex networks. As an interesting example we quote the recent work of Acebrón et al. (2007) who connected many two-state signaling device of the same type as that illustrated by (30) so as to form a scale-free network. In an earlier section we found that a complex network has the effect of mimicking in some way the effect of increasing dimensions in a nearest-neighbor interaction model. As a consequence, synchronization is enhanced. Acebrón et al. (2007) found the surprising effect that a complex network sustains the typical SR response. With no coupling, there is no response and when the coupling is turned on a finite response of increasing intensity with increasing coupling emerges. This response reaches a maximum and for further coupling intensity increase beyond this maximum, the response decreases to zero with couplings of sufficiently high intensity. If the average number of interactions increases the regression to the no-response condition occurs with coupling strength of smaller intensity. In the case of all-to-all coupling there is no sign of response. This may lead to the mistaken impression that the topology of complex networks is more efficient than the all-to-all interaction condition for generating cooperation. Of course, this is not true.

The cooperation generated by the all-to-all coupling condition generates a condition comparable to $g_0 = \infty$ and, consequently, according to (368) and (369), it should generate the greatest possible response. If we take into account the condition of IR, we may better approximate the real reasons for the failure of the all-to-all coupling topology to produce a finite response. The all-to-all coupling regime produces an infinite amount of information that cannot be stored within the network.

The theory for the CME is still in its infancy, and we expect that in the near future it will be refined by a large number of investigators. We are, however, in a position to stress another key aspect of this new phenomenon. This is that the non-ergodic events of the perturbation affect the times of occurrence of events by a very small amount, ensuring the validity of LRT. In other words, the CME rests on the linking of the perturbation and network. This aspect has been overlooked in the crucial events of the earlier investigation on SR. We think that this review affords a plausible explanation of why the earlier theoretical investigations have missed this important mechanism. We invite the reader to compare (384) with (382). The former linear response function applies when the times of occurrence of the network's crucial events are perturbed by the external stimulus, and the latter one refers to the case when the time of occurrence of the crucial events of the network are assumed to be unperturbed by the external stimulus. The latter is not a proper assumption in the case of two interacting complex networks, if the renewal condition applies. However, this assumption is implicitly made, for instance, by some authors. In the ergodic case, the two prescriptions coincide, and this explains why from within ordinary SR it becomes difficult to appreciate the dialogue between crucial events. It is interesting that in the Poisson case the CME should be more properly called *rate matching*. In this case, the dialogue between the S and the P events does not have any manifestation at the Gibbs ensemble level, and the S networks does not change its statistics since it is Poisson before and after switching on the coupling with the network P. However, if the observation is made at the level of single trajectories, Luković et al. (2008) have shown that the rate matching, $g_S = g_P$ corresponds to a transition from the condition where the P-events attract the S-events to that where the P-events repel the S-events.

8.2.2. Complex processes are dominated by the action of crucial events

The importance of making a neurophysiological model robust against changes in model details was advocated more than 20 years ago by such notables as Hopfield (1982):

> The bridge between simple circuits and the complex computational properties of higher nervous systems may be the spontaneous emergence of new computational capabilities from the collective behavior of large numbers of simple processing elements.

Renormalization group theory introduced by Wilson (1975) affords a solid theoretical foundation for this property of emergence. Thus, it should not come as a surprise that this review advocates the crucial role of non-ergodic events for the transmission of information. The dynamic model of Section 7.2.1 shows how the interaction among many neurons induces the emergence of non-ergodic events.

However, this review shows that crucial events are not limited to the large quakes that the MST reveal to be present in the brain's EEG records, see Section 5.2.6. The theory of Section 5.2.2 explains that the large quakes are the result of an accumulation effect produced by many small quakes, or actions, which in some cases may remain invisible. The adoption of special techniques of analysis, for instance, the DE technique of Section 6.3, may reveal the presence of these crucial events. One application leads to a reasonable explanation as to why the Earth's air temperature anomalies bear the signature of solar flare intermittency. This is an example of application of the CME to geophysical phenomenon.

8.2.3. GLE and SOFD processes

In Section 2.1.1 we have seen that many authors focus on the GLE as a source of complexity, pointing out that the earlier work by the founders of this theory did not consider the role of anomalous diffusion in their original treatment. The fact that the GLE yields dynamics intermediate between Newton and Langevin was already pointed out many years ago, but the discovery that non-ohmic baths may produce an extremely slow regression to equilibrium, based on inverse power laws rather than exponential relaxation is the main reason why these properties are judged to be a form of complexity. In this review we advocate a more general form of complexity, based on renewal non-Poisson events. In Section 5.2.3 we discussed how to establish whether EEG time series, for example, are an expression of the GLE complexity or of renewal complexity.

We cannot rule out, however, that when people are sleeping, both forms of complexity may be present and that a satisfactory approach to understanding brain dynamics may require the subordination to the GLE rather than the ordinary Langevin equation.

As far as subordination is concerned, we notice that the physical arguments yielding (126) can be interpreted as a subordination to a Lévy process. This is a form of complexity where the cooperative properties yielding deviation from ordinary statistical physics might act twice, at the level of determining the social life waiting time distribution of (271) and at the level of creating space jumps within space jumps, whose second moment is divergent.

8.2.4. Memory and renewal

We hope that this review contributes to clarifying the difference between trajectory and probability memory. If we consider the diffusion regime occurring prior to localization, namely the long transient corresponding in the natural time scale to the time interval $[0,\ 1/\gamma]$ (see Section 5.2.2) we obtain, using (306),

$$\frac{\mathrm{d}}{\mathrm{d}t}\left\langle y^2(t)\right\rangle = 2y_{\mathrm{rms}}^2\int_0^t \mathrm{d}t'\Phi(t'). \tag{469}$$

On the other hand, if we assume that in this regime

$$\frac{\mathrm{d}}{\mathrm{d}}y = \xi(t), \tag{470}$$

where $\xi(t)$ is assumed to be a correlated but stationary fluctuation, using standard methods of statistical physics, see, for instance Trefan et al. (1994), we obtain

$$\frac{\mathrm{d}}{\mathrm{d}t}\left\langle y^2(t)\right\rangle = 2\xi_{\mathrm{rms}}^2\int_0^t \mathrm{d}t'\Phi_\xi(t'), \tag{471}$$

where $\Phi_\xi(t)$ is the normalized autocorrelation function of the fluctuation $\xi(t)$. On the basis of this equivalence one is led to set $\Phi(t) = \Phi_\xi(t)$. This is mathematically correct. However, whether renewal complexity or complexity resting on the trajectory memory applies can be settled experimentally, by recording the differences between two consecutive values of the time series $\{y(t)\}$, so as to define the fluctuation $\xi(t)$. It is expected that the numerical evaluation of $\Phi_\xi(t)$ will encounter extraordinary technical difficulties and that eventually this dynamical derivation of anomalous diffusion will remain unsettled, if the renewal complexity applies. In fact, in this case the process is correctly described by the memory kernel $\Phi(t)$, but this memory kernel is not an autocorrelation function. This memory kernel is defined through the subordination function $\psi^{(S)}(t)$, see (256), and, in the case $\mu_S < 2$, it is strongly dependent on preparation and on t_a, as discussed in Section 4.4.2.

Acknowledgments

The authors acknowledge financial support from ARO and E.G. and P.G. additional support from Welch through grants W911NF-05-1-0205 and B-1577, respectively.

References

Acebrón, J.A., Lozano, S., Arenas, A., 2007. Phys. Rev. Lett. 999, 128701.
Adamic, L.A., Huberman, B.A., 2002. Glottometrics 3, 143.
Adelman, S.A., 1976. J. Chem. Phys. 64, 124.
Akin, O.C., Paradisi, P., Grigolini, P., 2006. Physica A 371, 157–170.
Akselrod, S., Gordon, D., Ubel, F.A., Shannon, P.C., Borger, A.L., Cohen, R.J., 1981. Science 213, 220.
Albert, R., Barabási, A.-L., 2002. Rev. Modern. Phys. 74, 48.
Allegrini, P., Grigolini, P., West, B.J., 1996. Phys. Rev. E 54, 4760.
Allegrini, P., Grigolini, P., Rocco, A., 1997. Phys. Rev. E 233, 309.
Allegrini, P., Grigolini, P., Hamilton, P., Palatella, L., Raffaelli, G., 2002a. Phys. Rev. E 65.
Allegrini, P., Bellazzini, J., Bramanti, G., Ignaccolo, M., Grigolini, P., Yang, J., 2002b. Phys. Rev. E 66, 015101(R).
Allegrini, P., Balocchi, R., Chillemi, S., Grigolini, P., Hamilton, P., Maestri, R., Palatella, L., Raffaelli, G., 2003a. Phys. Rev. E 67, 062901.
Allegrini, P., Aquino, G., Grigolini, P., Palatella, L., Rosa, A., 2003b. Phys. Rev. E 68, 056123.
Allegrini, P., Benci, V., Grigolini, P., Hamilton, P., Ignaccolo, M., Menconi, G., Palatella, L., Raffaelli, G., Scafetta, N., Virgilio, M., Yang, J., 2003c. Chaos Solitons Fractals 15, 517.
Allegrini, P., Grigolini, P., Palatella, L., West, B.J., 2004. Phys. Rev. E 70, 046118.
Allegrini, P., Aquino, G., Grigolini, P., Palatella, L., Rosa, A., West, B.J., 2005. Phys. Rev. E 71, 066109.
Allegrini, P., Barbi, F., Grigolini, P., Paradisi, P., 2006. Phys. Rev. E 73, 046136.
Allegrini, P., Grigolini, P., West, B.J., 2007a. Phys. Rev. Lett. 99, 010603.
Allegrini, P., Barbi, F., Grigolini, P., Paradisi, P., 2007b. Chaos Solitons Fractals 34, 11–18.
Allegrini, P., Bologna, M., Grigolini, P., West, B.J., 2007c. Phys. Rev. Lett. 999, 010603.
Allegrini, P., Bologna, M., Grigolino, P., Lukovic, M., 2006, arXiv:cond-mat/0608341v1 [cond-mat.stat-mech].
Alvarez-Ramirez, J., Ibarra-Valdez, C., Rodriguez, E., Dagdug, L., 2008. Physica A 387, 281.
Anderson, C.M., 2000. Conscious. Emot. 1, 193.
Arecchi, F.T., Lisi, F., 1982. Phys. Rev. Lett. 49, 34.
Aquino, G., Bologna, M., Grigolini, P., West, B.J., 2004. Phys. Rev. E 70, 036105.
Aquino, G., Grigolini, P., West, B.J., 2007. Europhys. Lett. 80, 10002.
Babloyantz, A., 1986. In: Mayer-Kress, G. (Ed.), Dimensions and Entropies in Chaotic Systems. Spring Verlag, Berlin.
Babloyantz, A., Destexhe, A., In: Proceed. Int Conf. on Neural Networks, San Diego, 1987.
Baddeley, R., Abbott, L.F., Booth, M.C.A., Sengpiel, F., Freeman, T., Wakeman, E.A., Rolls, E.T., 1997. Proc. R. Soc. Lond. 264, 1775.
Bak, P., Tang, C., Wiesenfeld, K., 1987. Phys. Rev. Lett 59, 381.
Bak, P., 1996. How Nature Works: The Science of Self-organized Criticality. Copernicus, Springer-Verlag.
Baiesi, M., Paczusky, M., Stella, A.L., 2006. Phys. Rev. Lett. 96, 05103.
Balescu, R., 2007. Chaos Solitons Fractals 34, 62.
Ball, D.A., 1956. Information Theory, 2nd ed. Pitman, New York.
Balucani, U., Lee, M.H., Tognetti, V., 2003. Phys. Rep. 373, 409.
Bao, J.-D., Zhuo, Y.-Z., 2003. Phys. Rev. Lett. 91, 138104.
Bao, J.-D., Song, Y.-L., Zhuo, Y.-Z., 2005. Phys. Rev. E 72, 011113.
Bao, J.-D., Zhuo, Y.-Z., Oliveira, F.A., Haänggi, P., 2006. Phys. Rev. E 74, 061111.
Barabási, A.-L., Albert, R., 1999. Science 286, 509.
Barabási, A.-L., 2003. Linked. Plume, New York.
Barabási, A.-L., 2005. Nature 435, 207.
Barbi, F., Bologna, M., Grigolini, P., 2005. Phys. Rev. Lett. 95, 220601.
Bardou, F., Bouchaud, J.-P., Aspect, A., Cohen-Tannoudji, C., 2002. Lévy Statistics and Laser Cooling. Cambridge University Press, Cambridge, UK.
Barkai, E., Silbey, R.J., 2000. J. Phys. Chem. B 104, 3866.
Barkai, E., 2003. Phys. Rev. Lett. 90, 104101.
Başar, E., Schürmann, M., Başar-Eroglu, C., Karakaş, S., 1997. Int. J. Psychophysiol. 26, 5.
Başar, E., 2006. Int. J. Psychophysiol. 60, 133.
Beck, C., Cohen, E.G.D., 2003. Physica A 322, 267.
Beck, C., 2001. Phys. Rev. Lett. 87, 180601.
Bédard, C., Kröger, H., Destexhe, A., 2006. Phys. Rev. Lett. 97, 118102.
Bedeaux, D., Lakatos, K., Shuler, K., 1971. J. Math. Phys. 12, 2116.
Beggs, J.M., Plenz, D., 2003. J. Neurosci. 23, 11167.
Beggs, J.M., Plenz, D., 2004. J. Neurosci. 24, 5216.
Beggs, J.M., 2007. Nature Phys. 3, 834.
Bel, G., Barkai, E., 2005. Phys. Rev. Lett. 94, 240602.
Bel, G., Barkai, E., 2006a. Europhys. Lett. 74, 15.
Bel, G., Barkai, E., 2006b. J. Phys. C 17, S4287.
Bel, G., Barkai, E., 2006c. Phys. Rev. E 73, 016125.
Bennett, M., Schatz, M.F., Rockwood, H., Wiesenfeld, K., 2002. Proc. Roy. Soc. London Ser. A 458, 563.
Bennett, C.H., 1982. Int. J. Theoret. Phys. 21, 905; 1987. Sci. Amer. 257, 108.
Benzi, R., Sutera, A., Vulpiani, A., 1981. J. Phys. A 14, L453.
Bernoulli, D., 1954. Econometrica 22, Translated from Latin to English by L. Sommer from Comm. Acad. Sca. Imp. Pet. V 175 (1738).
Berry, M.V., 1979. J. Phys. A 12, 781.
Bianco, S., Grigolini, P., Paradisi, P., 2005. J. Chem. Phys. 123, 174704.
Bianco, S., Grigolini, P., 2005. Chaos Solitons Fractals 34, 41.
Bianco, S., Ignaccolo, M., Rider, M.S., Ross, M., Winsor, P., Grigolini, P., 2007a. Phys. Rev. E 75, 061911.
Bianco, S., Geneston, E., Grigolini, P., Ignaccolo, M., 2007b. Physica A 387, 1387–1392.
Bigerelle, M., Iost, A., 2000. Chaos Solitons Fractals 11, 2179.
Billock, V.A., Tsou, B.H., 2006. Proc. Natl. Acad. Sci. 104, 8490.
Boccaletti, S., Valladares, D.L., 2000. Phys. Rev. E 62, 7497.
Bologna, M., Grigolini, P., Riccardi, J., 1999. Phys. Rev. E 60, 6435.
Bologna, M., Grigolini, P., West, B.J., 2002. Chem. Phys. 284, 115.
Bologna, M., Grigolini, P., Pala, M., Palatella, L., 2003. Chaos Solitons Fractals 17, 601.
Boon, J.P., Decroly, O., 1995. Chaos 5, 501.
Bouchaud, J.P., Georges, A., 1990. Phys. Rep. 195, 127.
Bouchaud, J., 1992. J. Phys. 12, 1705.
Brillouin, L., 1962. Science and Information Theory. Academic Press, New York.
Brokmann, X., Hermier, J.-P., Messin, G., Desbiolles, P., Bouchaud, J.-P., Dahan, M., 2003. Phys. Rev. Lett. 90, 120601.
Brown, R., 1829. Philos. Mag. 6, 161.

Brown, R., 1998. Phys. Rev. Lett. 81, 4835.
Budini, A.A., 2005. Phys. Rev. E 72, 056106.
Buiatti, M., Grigolini, P., Palatella, L., 1999. Physica A 268, 214.
Buiatti, M., Papo, D., Baudonniére, P.-M., van Vreeswijk, C., 2007. Neuroscience 146, 1400.
Cakir, R., Grigolini, P., Krokhin, A.A., 2006. Phys. Rev. E 74, 021108.
Cakir, R., Krockin, A., Grigolini, P., 2007. Chaos Solitons Fractals 34, 19–32.
Calabrese, P., Gambassi, A., 2005. J. Phys. A 38, R 133.
Calder III, W.A., 1984. Size, Function and Life History. Harvard University Press, Cambridge, MA.
Câteau, H., Reyes, A.D., 2006. Phys. Rev. Lett. 96, 058101.
Carroll, T.L., Pecora, L.M., 1990. Phys. Rev. Lett. 64, 821.
Cohen, D., 1997. Phys. Rev. E 55, 1422.
Cohen, E.G.D., 2004. Physica D 193, 35.
Collins, J.J., De Luca, C.J., 1994. Phys. Rev. Lett 73, 764.
Collins, J.J., Chow, C.C., Imhoff, T.T., 1995. Nature 376, 236.
Collins, J.J., Chow, C.C., Capela, A.C., Imhoff, T.T., 1996a. Phys. Rev. E 54, 5575.
Collins, J.J., Imhoff, T.T., Grigg, P., 1996b. J. Neurophysiol. 76, 642.
Compiani, M., Fonseca, T., Grigolini, P., Serra, R., 1985. Chem. Phys. Lett. 114, 503.
Compte, A., 1996. Phys. Rev. E 53, 4191.
Correll, J., 2008. J. Person. Social Psychol. 94, 48.
Cortes, E., West, B.J., Lindenberg, K., 1985. J. Chem. Phys. 82, 2708.
Costa, I.V.L., Vainstein, M.H., Lapas, L.C., Batista, A.A., Oliveira, F.A., 2006. Physica A 371, 130.
Costa, L., Da, F., Rodrigues, F.A., Travieso, G., Villas Boas, P.R., 2007. Adv. Phys. 56, 167.
Cox, D.R., 1967. Renewal Theory. Metheun & Co., London.
Crisanti, A., Ritort, F., 2003. J. Phys. A R-181.
Daly, E., Porporato, A., 2006. Phys. Rev. E 74, 041112.
da Silva, L., Papa, A.R.R., de Souza, A.M.C., 1998. Phys. Lett. A 242, 343.
de Sola Price, D., 1963. Little Science, Big Science. Columbia University Press, NY.
Deligniéres, D., Lemoine, L., Torre, K., 2004. Human Move. Sci. 23, 87.
Deligniéres, D., Torre, K., Lemaine, L., 2008. Acta Psychoogica 127, 382.
Dutta, P., Horn, P.M., 1981. Rev. Modern. Phys. 53, 497.
Einstein, A., 1905. Ann. Phys. 17, 549.
Erdös, P., Rényi, A., 1960. Random Graphs. In: Publication of the Mathematical Institute of the Hungarian Academy of Science, vol. 5. pp. 17–61.
Failla, R., Grigolini, P., Ignaccolo, M., Schwettmann, A., 2004. Phys. Rev. E 70, 010101 (R).
Feldmann, A., Gilbert, A.C., Willenger, W., Kurtz, T.G., 1998. Comput. Commun. Rev. 28, 1.
Femat, R., Solis-Perales, G., 1999. Phys. Lett. A 262, 50.
Ferrario, M., Grigolini, P., 1979. J. Math. Phys. 20, 2567.
Fechner, G.T., 1860. Elemente der Psychophysik. Breitkopf and Hartel, Leipzig.
Feller, W., 1971. An Introduction to Probability Theory and Its Applications, vol. 2. J. Wiley & Sons, New York.
Feng, J., Zhang, P., 2001. Phys. Rev. E 63, 051902.
Ford, G.W., Kac, M., Mazur, P., 1965. J. Math. Phys. 6, 504.
Fowler, H., Leland, W.E., 1991. IEEE J. Selected Areas Commun. 9, 1139.
Fox, R., 1977. J. Math. Phys. 18, 2331.
Freeman, W.J., 1975. Mass Action in the Nervous System. Academic Press, New York, p. 489 (Chapter 7).
Freeman, W.J., 1987. Biol. Cybern. 56, 139–150.
Frederick, S., Loewenstein, G., O'Donoghue, T., 2002. J. Econom. Lit. 40, 351.
Fronzoni, L., Grigolini, P., Mannella, R., Zambon, B., 1985. J. Stat. Phys. 41, 553.
Gammaitoni, L., Hänggi, P., Jung, P., Marchesoni, F., 1998. Rev. Modern. Phys. 70, 223.
Gibbs, J.W., 1928. Collected Works. Longmans, Green.
Geisel, T., Nierwetberg, J., Zacherl, A., 1985. Phys. Rev. Lett. 54, 616.
Gerstein, G.L., Mandelbrot, B., 1964. Biophys. J. 4, 41.
Glass, L., Mackey, M.C., 1988. From Clocks to Chaos; The Rhythms of Life. Princeton University Press, Princeton, NJ.
Glöckle, W.G., Nonnenmacher, T., 1993a. J. Stat. Phys. 71, 741.
Glöckle, W.G., Nonnenmacher, T., 1993b. Rheol. Acta 33, 337.
Glöckle, W.G., Nonnenmacher, T.F., 1991. Macromolecules 24, 6426.
Godréche, G., Luck, J.M., 2001. J. Stat. Phys. 104, 489.
Goldberger, A.L., Bhargava, V., West, B.J., Mandell, A.J., 1985. Biophys. J. 48, 525.
Gong, P., Nikolaev, A.R., van Leeuwen, C., 2007. Phys. Rev. E 76, 011904.
Goychuck, I., Hänggi, P., 2003. Phys. Rev. Lett. 91, 070601.
Grigolini, P., 1979. Chem. Phys. 38, 389.
Grigolini, P., 1985. Adv. Chem. Phys. 62, 1.
Grigolini, P., Rocco, A., West, B.J., 1999. Phys. Rev. E 59, 2603.
Grigolini, P., Palatella, L., Raffaelli, G., 2001. Fractals 9, 439.
Grigolini, P., Leddon, D., Scafetta, N., 2002. Phys. Rev. E 65, 046203.
Grigolini, P., Allegrini, P., West, B.J., 2007. Chaos Solitons Fractals 34, 3–10.
Gross, D., Harris, C.M., 1998. Fundamentals of Queueing Theory, 3rd ed. Wiley-Interscience, New York, NY.
Gross, T., Blasius, B., 2008. J. R. Soc. Interface 5, 259.
Hachinski, K.V., Hachinski, V., 1994. Can. Med. Assoc. J. 151, 293.
Haldeman, C., Beggs, J.M., 2005. Phys. Rev. Lett. 94, 058101.
Hausdorff, J.M., Peng, C.K., Ladin, Z., Ladin, J.Y., Wei, J.Y., Goldberger, A.L., 1995. J. Appl. Physiol. 78, 349.
Hausdorff, J.M., Zemany, L., Peng, C.K., Goldberger, A.L., 1999. J. Appl. Physiol. 86, 1040.
Heart rate variability, 1996. European Heart J. 17, 354.
Heinsalu, E., Patriarca, M., Goychuk, I., Hänggi, P., 2007. Phys. Rev. Lett. 999, 120602.
D. Helbing, S. Lämmer, Supply and production networks: From the bullwhip effect to business cycles. cond-mat/0411486v1, 2004.
Hennig, T., Maass, P., Hayano, J., Heinrichs, S., 2006. J. Biol. Phys. 32, 383.
Hilfer, R. (Ed.), 2002. Applications of Fractional Calculus in Physics. World Scientific Publishing, Singapore.
Hinomoto, S., Shima, K., Tanji, T., 2003. Neural Comput. 15, 2803.
Holme, P., Kim, B.-J., 2002. Phys. Rev. E 65, 026107.
Hoop, B., Peng, C.-H., 2000. J. Membrane Biol. 177, 177.
Hoover, W.G., 1985. Phys. Rev. A 31, 1695.
Hopf, E., 1937. Ergeb. Math., vol. 5. Springer, Berlin.
Hopfield, J.J., 1982. Proc. Natl. Acad. Sci. USA 79, 2554.

Hsu, K.J., Hsu, A., 1991. Proc. Natl. Acad. Sci. 88, 3507.
Hughes, B.D., 1996. Random Walks and Random Environments. Calderon Press, Oxford.
Infeld, E., Rowlands, G., 1990. Nonlinear Waves, Solitons and Chaos. Cambridge University Press, Cambridge.
Ingen-Housz, J., 1973. In: Gillispie, C.C. (Ed.), Dictionary of Scientific Biology. Scribners, NY, p. 11.
Jäger, G., van Rooij, R., 2007. Synthese 159, 99.
Jensen, H.J., 2000. Self-Organized Criticality. In: Cambridge Lecture Notes in Physics, Cambridge University Press, Cambridge UK.
Jennings, H.D., Ivanov, P.Ch., Martins, A.de M., da Silva, P.C., Viswanathan, G.M., 2004. Physica A 336, 585.
Kadota, H., Kudo, K., Ohtsuki, T., 2004. Neuroscience Lett. 370, 97.
Kalashyan, A.K., Buiatti, M., Grigolini, P., 2007. Chaos Solitons Fractals. doi:10.1016/j.chaos.2007.01.062.
Kaplan, D.T., Talajic, M., 1991. Chaos 1, 251.
Kardar, M., Parisi, G., Zhang, Y.-C., 1986. Phys. Rev. Lett. 56, 889.
Kawashima, T., 2006. JSME Internat. J. 49, 814.
Kello, C.T., Beltz, B.C., Holden, J.G., Van Orden, G.C., 2007. J. Exp. Psychol. 136, 551.
Kenkre, V.M., Montroll, E.W., Shlesinger, M.F., 1973. J. Stat. Phys. 9, 45.
Kenkre, V.M., Knox, R.S., 1974. Phys. Rev. B 9, 5279.
Kenning, P., Plassmann, H., Deppe, M., Kugel, H., Schwindt, W., 2005. Editorial of a special issue devoted to neuroeconomics, Münster, May 25–27 (2004). Brain Res. Bull. 67, 341.
Kim, B.J., 2004. Phys. Rev. Lett. 93, 168701.
Kinouchi, O., Copelli, M., 2006. Nature Phys. 2, 348.
Kish, L.B., Harmer, G.P., Abbott, D., 2001. Fluc. Noise Lett. 1, L13–L19.
Klafter, J., Zumofen, G., 1994. Phys. Rev. Lett. 49, 4873.
Kobayashi, M., Musha, T., 1982. IEEE Trans. Biomed. Eng. 29, 456.
Kocarev, L., Parlitz, U., 1996. Phys. Rev. Lett. 76, 1816.
Kramers, H.A., 1940. Physica 7, 284.
Kruskal, J.B., 1956. Proc. Amer. Math. Soc. 7, 48.
Kubo, R., 1957. J. Phys. Soc. Japan 12, 570.
Kubo, R., 1966. Rep. Prog. Theoret. Phys. 29, 255.
Kubo, R., 1969a. Adv. Chem. Phys. 16, 101.
Kubo, R., 1969b. J. Phys. Soc. Japan 26 (Suppl.), 1.
Kubo, R., Toda, M., Hashitusume, N., 1985. Statistical Physics. Springer, Berlin.
Kuno, M., Fromm, D.P., Hamann, H.F., Gallagher, A., Nesbitt, D.J., 2001. J. Chem. Phys. 115, 1028.
Kuno, M., Fromim, D.P., Hohmson, S.R., Gallagher, A., Nesbitt, D.J., 2003. Phys. Rev. B 67, 125304.
Kuramoto, Y., 1981. Physica A 126, 128.
Laloux, L., Le Doussal, P., 1998. Phys. Rev. E 57, 6296.
Lamperti, J., 1958. Trans. Math. Soc. 88, 380.
Landauer, R., 1993. Physica A 194, 551.
Landauer, R., 1996a. Science 272, 1914–1918.
Landauer, R., 1996b. Phys. Lett. Section A 217, 188–193.
Langevin, P., 1908. C. R. Acad. Sci. Paris 146, 530.
Lapas, L.C., Costa, I.V.L., Vainstein, M.H., Oliveira, F.A., 2007. Europhys. Lett. 77, 3704.
Laskin, N., Lambadaris, I., Harmantzis, F.C., Devetsikiotis, M., 2002. Comp. Netw. 40, 363–375.
Lauk, M., Chow, C.C., Pavlik, A.E., Collins, J.J., 1998. Phys. Rev. Lett. 80, 413.
Layne, S.P., Mayer-Kress, G., Holzfuss, J., 1986. In: Mayer-Kress, G. (Ed.), Dimensions and Entropies in Chaotic Systems. Spring Verlag, Berlin, pp. 246–256.
Levina, A., Herrmann, J.M., Geisel, T., 2007. Nature Phys. 3, 857.
Lee, M.H., 1982a. Phys. Rev. B 26, 2547.
Lee, M.H., 1982b. Phys. Rev. Lett. 49, 1072.
Lee, M.H., 1983a. J. Math. Phys. 24, 2512.
Lee, M.H., 1983b. Phys. Rev. Lett. 51, 1227.
Lee, M.H., 2006. J. Phys. A 39, 4651.
Lee, M.H., 2007. Phys. Rev. Lett. 98, 190601.
Legoll, F., Luskin, M., Moeckel, R., 2007. Arch. Ration. Mech. Anal. 184, 449.
Leland, W.E., Taqqu, M.S., Willinger, W., Wilson, D.V., 1994. IEEE/ACM Trans. Netw. 2, 1.
Lewis, M.D., 2005. Behav. Brain Sci. 28, 169.
Li, M., Vitányi, P., 1997. An Introduction to Kolmogorov Complexity and Its Applications. Springer, NY.
Li, W., Holste, D., 2005. Phys. Rev. E 71, 041910.
Lindenberg, K., West, B.J., 1990. The Nonequilibrium Statistical Mechanics of Open and Closed Systems. VCH Publishers, New York, NY.
Lowen, S.B., Teich, M.C., 1993. Phys. Rev. E 47, 992.
Lowen, S.B., Teich, M.C., 2005. Fractal-Based Point Processes. John Wiley, New York.
Lotka, A.J., 1926. J. Wash. Sci. 16, 317.
Lotka, A.J., 1924. Elements of Mathematical Biology. Dover, NY, 1956; first published by the Williams and Wilkins Co.
Lukovic, M., Ignaccolo, M., Fronzoni, L., Grigolini, P., 2008. Phys. Lett. A 372, 2608.
Lutz, E., 2004. Phys. Rev. Lett. 93, 190602.
Machlup, S., 1977. Sixth Int. Symp. on Noise in Physical Systems. National Bureau of Standards, pp. 157–160.
Mainardi, F., 1996. Chaos Solitons Fractals 7, 1461.
Majumdar, S.N., Comtet, A., 2002. Phys. Rev. Lett. 89, 060601.
Manaris, B., Romero, J., Machado, P., Krehbiel, D., Hirzel, T., Pharr, W., Davis, R.B., 2005. Comput. Music J. 29, 55.
Mandelbrot, B.B., van Ness, J.W., 1968. SIAM Rev. 10, 422.
Mandelbrot, B.B., 1977. Fractals, Form and Chance. W.F. Freeman, San Francisco, CA.
Margolin, G., Barkai, E., 2005. Phys. Rev. Lett. 94, 1.
Margolin, G., Barkai, E., 2006. J. Stat. Phys. 122, 137.
Maxwell, J.C., 2001. Theory of Heat. Dover, New York, originally published in 1888.
MacDonald, N., 1983. Trees and Networks in Biological Models. John Wiley & Sons, NY.
McNamara, B., Wiesenfeld, K., Roy, R., 1988. Phys. Rev. Lett. 60, 2626.
Meakin, P., 1998. Fractals, Scaling and Growth far from Equilibrium. In: Cambridge Nonlinear Science Series, vol. 5. Cambridge University Press, New York, NY.
Mega, M.S., Allegrini, P., Grigolini, P., Latora, V., Palatella, L., Rapisarda, A., Vinciguerra, S., 2003. Phys. Rev. Lett. 90, 188501.
Metzler, R., Barkai, E., Klafter, J., 1999a. Europhys. Lett. 46, 431.
Metzler, R., Barkai, E., Klafter, J., 1999b. Phys. Rev. Lett. 82, 3563.
Metzler, R., Barkai, E., Klafter, J., 1999c. Physica A 266, 343.
Metzler, R., 2000. Phys. Rev. E 62, 6233.
Metzler, R., Klafter, J., 2000a. Phys. Rep. 339, 1.

Metzler, R., Klafter, J., 2000b. J. Phys. Chem. B 104, 3851.
Mikosch, T., Resnick, S., Rootzén, H., Stegeman, A., 2002. Ann. Appl. Probab. 12, 23.
Min, W., Luo, G., Cherayil, B.J., Kou, S.C., Xie, X.S., 2005. Phys. Rev. Lett. 94, 198302.
Mirollo, R.E., Strogatz, S.H., 1990. SIAM J. Appl. Math 50, 1645.
Mohanty, A.K., Narayana Rao, A.V., 2000. Phys. Rev. Lett. 84, 1832.
Mokshin, A.V., Yulmetyev, R.M., Hänggi, P., 2005. Phys. Rev. Lett. 95, 200601.
Montroll, E.W., Weiss, G., 1965. J. Math. Phys. 6, 178.
Montroll, E.W., West, B.J., 1979. In: Montroll, E.W., Lebowitz, J. (Eds.), Fluctuation Phenomena. North-Holland.
Montroll, E.W., Shlesinger, M.F., 1983. J. Stat. Phys. 32, 209.
Monthus, C., Bouchaud, J.-P., 1996. J. Phys. A 29, 3847.
Mori, H., 1965a. Prog. Theoret. Phys. 33, 423.
Mori, H., 1965b. Prog. Theoret. Phys. 34, 399.
Moss, F., Ward, L.M., Sannita, W.G., 2004. Clinical Neurophysiol. 115, 267–281.
Musha, T., 1981. In: Meijer, P.H.E., Mountain, R.D., Soulen, R.J. (Eds.), Sixth Int. Sym. on Noise in Physical Systems. Nat. Bureau of Standards, p. 142.
Mutch, W.A.C., 2005. In: Stocks, Nigel G., Abbott, Derek, Morse, Robert P. (Eds.), Fluctuations and Noise in Biological, Biophysical, and Biomedical Systems III. In: Proc. of SPIE, vol. 5841. p. 1.
Network Science, National Research Council of the National Academies, Washington, DC, 2005. www.nap.edu.
Newman, M.E.J., 2003. SIAM Rev. 45, 167.
Nicolis, C., Nicolis, G., 1981. Tellus 33, 225.
Nirmal, M., Dabbousi, B.O., Bawendi, M.G., Macklin, J.J., Trautman, J.K., Harris, R.D., Brus, L.E., 1996. Nature 383, 802.
Nordseick, A., Lamb, W.W., Uhlenbeck, G.E., 1940. Physica 7, 344.
Nosé, S., 1985. J. Chem. Phys. 81, 511.
Nyikos, L., Balazs, L., Schiller, R., 1994. Fractals 2, 143.
Onsager, L., 1931. Phys. Rev. 38, 2265; 1931. Phys. Rev. 37, 405.
Oppenheim, I., Shuler, K.E., Weiss, G.H., 1977. Stochastic Processes in Chemical Physics: The Master Equation. MT Press, Cambridge.
Paraschiv-Ionescu, A., Buchser, E., Rutschmann, B., Aminian, K., 2008. Phys. Rev. E 77, 021913.
V. Pareto, Cours d'Economie Politique, Lausanne, 1897.
W. Pauli, S. Hirzel (Ed.), Festschrift zum 60 geburtstag A. Sommerfeld, Leipzig, 1928.
Paxson, V., Floyd, S., 1995. IEEE/ACM Trans. Netw. 3, 226–244.
Pelton, M., Grier, D.G., Guyot-Sionnest, P., 2004. Appl. Phys. Lett. 85, 819.
Peng, C.K., Buldyrev, S., Goldberger, A.L., Havlin, S., Simons, M., Stanley, J.E., 1992. Nature 356, 168.
Peng, C.K., Mietus, J., Hausdorff, J.M., Havlin, S., Stanley, H.G., Goldberger, A.L., 1993. Phys. Rev. Lett. 70, 1343.
Peng, C.-K., Havlin, S., Stanley, H.E., Goldberger, A.L., 1995. Chaos 5, 1.
Plenz, D., Thiagarajan, T.C., 2007. Trends Neurosci. 30, 101.
Pottier, N., 2003. Physica A 317, 371.
Rachlin, H., Jones, B.A., 2008. J. Behav. Dec. Making 21, 29.
Rabotnov, Y.N., 1980. Elements of Hereditary Solid Mechanics (M. Konyaeva Trans.). MIR Publishers, Moscow, trans. from Russian.
Rebenshtok, A., Barkai, E., 2007. Phys. Rev. Lett. 999, 210601.
Resnick, S., Rootzén, H., 2000. Ann. Appl. Probab. 10, 753.
Rim, S., Kim, I., Kang, P., Park, Y.J., Kim, C.M., 2002. Phys. Rev. E 66, 015205.
Rodríguez-Iturbe, I., Rinaldo, A., 1997. Fractal River Basins: Chance and Self-Organization. Cambridge University Press, Cambridge, UK.
Rodriguez, E.G., Geoge, N., Lachaux, J.P., Martinerie, J., Renault, B., Varela, F., 1999. Nature 397, 430.
Rosa, E.R., Ott, E., Hess, M.H., 1998. Phys. Rev. Lett. 80, 1642.
Rosenblum, M.G., Pikovsky, A.S., Kurths, J., 1996. Phys. Rev. Lett. 76, 1804.
Rosenblum, M.G., Pikovsky, A.S., Kurths, J., 1997. Phys. Rev. Lett. 78, 4193.
Rulkov, N.F., Sushehik, M.M., Tsimring, L.S., Abarbanel, H.D.I., 1995. Phys. Rev. E 51, 980.
Sakai, Y., Funahashi, S., Shinomoto, S., 1999. Neural Netw. 12, 1181.
Sakai, Y., 2001. Neural Netw. 14, 1145.
Salinas, E., Seinowski, T.J., 2002. Neural Comput. 14, 2111.
Samko, S.G., Kilbas, A.A., Marichev, O.I., 1993. Fractional Integrals and Derivatives. Gordon and Breach Science Publishers, Switzerland.
Scalas, E., 2007. Chaos Solitons Fractals 34, 33–40.
Scafetta, N., West, B.J., 2003. Phys. Rev. Lett. 90, 248701.
Scafetta, N., Grigolini, P., Imholt, T., Roberts, J., West, B.J., 2004. Phys. Rev. E 69, 026303.
Scafetta, N., Hamilton, P., Grigolini, P., 2001. Fractals 9, 193.
Scher, H., Montroll, E., 1975. Phys. Rev. B 12, 2455.
Schneider, W.R., Wyss, W., 1989. J. Math. Phys. 30, 134.
Scott, J., 2000. Social Network Analysis: A Handbook, 2nd ed. Sage, London.
Sen, S., Sinkovits, R.S., Chakravarti, S., 1996. Phys. Rev. Lett. 77, 4855.
Sen, S., Philips, J.C., 1995. Physica A 216, 271.
Sen, S., 2002. Physica A 315, 150.
Sen, S., 2006. Physica A 360, 304.
Seuront, L., Mitchell, J.G., 2008. J. Marine Syst. 69, 310.
Shadlen, M.N., Newsame, W.T., 1998. J. Neurosci. 18, 3870.
Shahverdiev, E.M., Sivaprakasam, S., Shore, K.A., 2002. Phys. Lett. A 292, 320.
Shahverdiev, E.M., Shore, K.A., 2005. Phys. Rev. E 71, 016201.
Shannon, C.E., Bell Syst. Tech. J. 27, 379–423;
Shannon, C.E., Bell Syst. Tech. J. 27 (1948) 623–656.
Shannon, C.E., Weaver, W., 1959. The Mathematical Theory of Communication. University of Illinois Press, Urbana, IL.
Shimizu, K.T., Neuhauser, R.G., Leatherdale, C.A., Empedocles, S.A., Woo, W.K., Bawendi, M.G., 2001. Phys. Rev. B 63, 205316.
Shinomoto, S., Tsubo, Y., 2001. Phys. Rev. E 64, 041910.
Shlesinger, M.F., Hughes, B.D., 1981. Physica A 109, 597.
Shlesinger, M.F., West, B.J., Klafter, J., 1987. Phys. Rev. Lett. 58, 1100.
Skagerstam, B.-S.K., Hansen, A., 2005. Europhys. Lett. 72, 513.
Sokolov, I.M., Klafter, J., Blumen, A., 1996. Phys. Today 49 (2), 33.
Sokolov, I.M., 2000. Phys. Rev. A 63, 011104.
Sokolov, I.M., Metzler, R., 2003. Phys. Rev. E 67, 010101 (R).
Sokolov, I.M., 2006. Phys. Rev. E 73, 067102.
Sokolov, I.M., Klafter, J., 2006. Phys. Rev. Lett. 97, 140602.
Soma, R., Nozaki, D., Kwak, S., Yamamoto, Y., 2003. Phys. Rev. Lett. 91, 078101.
Spehar, B., Clifford, C.W.G., Newell, B.R., Taylor, R.P., 2003. Comput. Graph. 27, 813.
Stanislavsky, A.A., 2006. Eur. Phys. J. B 49, 93.

Stam, C.J., 2005. Clinical Neurophysiol. 116, 2266.
Stam, C.J., Reijneveld, J.C., 2007. Nonlinear Biomed. Phys. 1, 3.
Stevens, C.F., Zador, A.M., 1998. Nat. Neurosci. 1, 210.
Strogatz, S.H., Stewart, I., 1993. Sci. Amer. 269, 102.
Strogatz, S., 2003. SYNC. Hyperion Books, New York.
Struick, L.C.E., 1978. Physical Aging in Amorphous Polymers and Other Materials. Elsevier, Houston.
Su, Z.-Y., Wu, T., 2007. Physica A 380, 418.
Sumpter, D.J.T., 2006. Phil. Trans. R. Soc. B 361, 5.
Sun, Z., Xu, W., Yang, X., 2008. Math. Comput. Modeling.
Szeto, H.H., Chang, P.Y., Decena, J.A., Chang, Y., Wu, D., Dwyer, G., 1992. Am. J. Physiol. 262, R141.
Szilard, L., 1929. Z. Phys. 53, 840.
Takahashi, T., Ikeda, K., Hasegawa, T., 2007. Behav. Brain Funct. 3, 52.
Takakura, K., Sano, K., Kosugy, Y., Ikebe, J., 1979. Appl. Neurophysiol. 42, 314.
Taylor, R.P., Micolich, A.P., Jonas, D., 2002. Leonardo 35, 203.
Taylor, R.P., Micolich, A.P., Jonas, D., 1999. Nature 399, 422.
Trefan, G., Floriani, E., West, B.J., Grigolini, P., 1994. Phys. Rev. E 50, 2564.
Tsuruoka, M., Tsuruoka, Y., Shibasaki, R., Yasuoka, Y., in: Proceedings of the 29th Annual International Conference of the IEE EMBS Cité Internationale, Lyon, France, 2007.
Turing, A.M., 1952. Philos. Trans. R. Soc. London Ser. B 327, 37.
Vainstein, M.H., Costa, I.V.L., Morgado, R., Oliveira, F.L., 2006. Europhys. Lett. 73, 726.
Valdez, A.B., Amazeen, E.R., 2008, Exp. Brain Res. doi:10.1007/s00221-0088-1305-0.
Van Hove, L., 1955. Physica (Amsterdam) 21, 517.
van Vreewijk, C., 2001. Neurocomputing 38, 417.
Varela, F., Lachauz, J.P., Rodriguez, E., Martinerie, J., 2001. Nature Rev. Neurosci. 2, 229.
Vazques, A., Rácz, B., Lukács, A., Barabási, A.-L., 2007. Phys. Rev. Lett. 98, 158702.
Vierordt, 1881. Uber das Gehen des Menchen in Gesunden und kranken Zustaenden nach Selbstregistrirender Methoden. Tuebigen, Germany.
Vlad, M.O., 1992a. Physica A 184, 290.
Vlad, M.O., 1992b. Internat. J. Modern. Phys. B 6, 419.
Vlad, M.O., Ross, J., Schneider, F.W., 2000. Phys. Rev. E 62, 1743.
Voss, R.F., Clarke, J., 1975. Nature (London) 258, 317.
Voss, R.F., Clarke, J., 1976. Phys. Rev. 13, 556.
Voss, R.F., 1992. Phys. Rev. Lett. 68, 3805.
Voss, R.F., 1994. Fractals 2, 1.
Voss, R.F., 2000. Phys. Rev. E 61, 5115.
Wagenmakers, E.-J., Farrell, S., Ratcliff, R., 2004. Psychonomic Bull. Rev. 11, 579.
Wallin, N.L., 2000. Human Evol. 15, 199.
Wallace, R., 2000. Internat. J. Bifur. Chaos 10, 493–502.
Ward, L.M., 2001. Dynamical cognitive science. In: A Bradford Book. The MIT Press, Cambridge, MA.
Watanabe, T., Yagishita, S., Kikyo, H., 2008. NeuroImage 39, 483.
Watts, D.J., Strogatz, S.H., 1998. Nature (London) 393, 440.
Watts, D.J., 1999. Small Worlds. Princeton University Press, Princeton, NJ.
Weibel, E.R., 2000. Symmorphosis. Harvard University Press, Cambridge, MA.
Weishaupt, D., Köchli, V.D., Marincek, B., 2003. How does MRI Work? An Introduction to the Physics and Function of Magnetic Resonance Imaging. Springer-Verlag, Berlin, Heidelberg.
Weiss, G.H., 1994. Aspects and Applications of the Random Walk. North-Holland, Amsterdam.
Weiss, U., 1999. Quantum Dissipative Systems, 2nd ed. World Scientific, Singapore.
West, B.J., Seshadri, V., 1982. Physica A 113, 203.
West, B.J., 1990. Fractal Physiology and Chaos in Medicine. In: Studies in Nonlinear Phenomena in Life Science, vol. 11. World Scientific, Singapore.
West, B.J., Grigolini, P., Metzler, R., Nonnenmacher, T.F., 1997. Phys. Rev. E 55, 99.
West, B.J., 1999. Physiology, Promiscuity and Prophecy at the Millennium: A Tale of Tails. In: Studies in Nonlinear Phenomena in Life Science, vol. 11. World Scientific, Singapore.
West, B.J., Deering, W., 1994. Phys. Rep. 246, 1.
West, B.J., Deering, W., 1995. The Lure of Modern Science. In: Studies in Nonlinear Phenomena in Life Science, vol. 11. World Scientific, Singapore.
West, B.J., Nonnenmacher, T., 2001. Phys. Lett. A 278, 255–259.
West, B.J., Bologna, M., Grigolini, P., 2003. Physics of Fractal Operators. Springer, New York.
West, B.J., 2006. Where Medicine Went Wrong. In: Studies in Nonlinear Phenomena in Life Science, vol. 11. World Scientific, New Jersey.
West, B.J., Grigolini, P., 2008. Phys. Rev. Lett. 100, 088501.
Wiener, N., 1948. Cybernetics. MIT Press, Cambridge, MA.
Wiener, N., 1958. Nonlinear Problems in Random Theory. MIT Press and John Wiley, New York.
Willinger, W., Paxson, V., 1998. Notices Amer. Math. Soc. 45, 961–970.
Willis, J.C., 1922. Age and Area; A Study in Geographical Distribution and Origin of Species. Cambridge University Press.
Wilson, K.G., 1975. Rev. Modern. Phys. 55, 583.
Winfree, A.T., 1990. The Geometry of Biological Time. Springer-Verlag, Berlin.
Winsor, P., 1992. Automated Music Compoition. University of North TX Press, Denton, TX.
Wise, M.E., 1975. In: Patil, G.P., et al. (Eds.), Statistical Distributions in Scientific Work, vol. 2. D. Reidel, Dordrecht, Holland, pp. 241–262.
Wise, M.E., 1981. In: Taillie, C., et al. (Eds.), Statistical Distributions in Scientific Work, vol. 6. D. Reidel, Dordrecht, Holland, pp. 211–231.
Wittmann, M., Paulus, M.P., 2007. Trends Cognitive Sci. 12, 7.
Wittmann, M., Leland, D.S., Paulus, M.P., 2007a. Exp. Brain Res. 179, 1.
Wittmann, M., Leland, D.S., Churan, J., Paulus, M.P., 2007b. Drug Alcohol Dependence 98, 183.
Wood, K., Van den Broeck, C., Kawai, R., Lindenberg, K., 2006. Phys. Rev. Lett. 96, 145701.
Yu, Y., Romero, R., Lee, T.S., 2005. Phys. Rev. Lett. 94, 108103.
Yule, G.U., 1924. Proc. Roy. Soc. London 213, 403.
Yulmetyev, R.M., Yulmetyevaa, D., Gafarova, F.M., 2005. Physica A 354, 404.
Zaks, M.A., Park, E.J., Rosenblum, M.G., Kurths, J., 1999. Phys. Rev. Lett. 82, 4228.
Zeng, F.G., Fu, Q., Morse, R., 2000. Braun Res. Interact. 869, 251.
Zhan, M., Wei, G.W., Lai, C.H., 2002. Phys. Rev. E 65, 036202.
Zipf, G.K., 1949. Human Behavior and the Principle of Least Effort. Addison-Wesley.
Zumofen, G., Klafter, J., 1994. Europhys. Lett. 25, 565.
Zwanzig, R., 1961. Phys. Rev. 124, 983.
Intergovernmental Panel on Climate Change, Climate Change 2007, The Physical Science Basis, 2007.